Functional analysis of kinases in the malaria parasite *Plasmodium falciparum*

Inauguraldissertation

zur

Erlangung der Würde eines Doktors der Philosophie

vorgelegt der

Philosophisch-Naturwissenschaftlichen Fakultät

der Universität Basel

von

Eva Hitz

Basel, 2021

Genehmigt von der Philosophisch-Naturwissenschaftlichen Fakultät
auf Antrag von
Prof. Dr. Till Voss, Prof. Dr. Hans-Peter Beck und Dr. Moritz Treeck

Basel, den 15.09.2020

Prof. Dr. Martin Spiess
Dekan der Philosophisch-Naturwissenschaftlichen Fakultät

Table of contents

Acknowledgements

First of all, I thank Till Voss very much for giving me the opportunity to pursue my PhD in the Gene Regulation Unit at Swiss TPH. Till, I am very grateful for all the support I got from you and all the ideas and discussions we shared – it was a very interesting, demanding and instructive journey and I highly appreciate you giving me the possibility and support to become an independent scientist. Furthermore, you also always took my personal struggles seriously and had an open ear whenever needed – thank you for that!
A big thank you goes to Hans-Peter Beck and Moritz Treeck for their constant support and help – I am extremely glad for all the input and directions you gave me, which definitely helped to get all projects on the right track and not to get lost in the jungle of possibilities! Special thanks goes to Hans-Peter Beck and his former lab members for sharing their passion for science with me, which led me to pursue my PhD.
I also want to thank all my collaborators for your great work and the good experiences I had working with all of you, both personally and professionally. Special thanks goes to Mathieu Brochet for arranging a stay at his lab – I could both share my knowledge and learn a lot from you and Aurélia, thanks for that!
A big thank you goes to former and current members of the GR lab especially to Niggi, Eilidh, Michael, Elvira and Travis, but also to Armin, Maria, Anna, Nadja and many other Swiss TPH colleagues – I loved talking about science (and maybe more so about non-scientific subjects) with you and laughing together over lunch, coffee and a beer – this sometimes really made my day and surely kept me from going “academia nuts”. You are not only great colleagues but became dear friends!
I want to thank Jürg, Karin and Anna and my “fascht e familie” – you were always understanding when I had to work on weekends, left early or showed up late for an event, if lab work didn’t go (or actually did go) as planned. Thanks to all of you sincerely for making this hard work so much easier by being supportive and always understanding! I also thank you for keeping my mind far away from science and work if there was need for that.
I want to thank Zeno for being the most supportive person I could ever have imagined. I highly appreciate how much cooking and housekeeping you did while I was still in the lab – this made everything so much easier for me and your good food always kept my spirits high! You made me feel better if something at work did not go as hoped and planed and you always believed that I could do it. Finally yet importantly, you never made me feel bad about missing things but you were just happy when I was there – thanks for that!

Summary

Despite massive control efforts and extensive successes in reducing the malaria burden in the past decades, malaria still causes more than 400'000 deaths worldwide each year with the highest toll on African children under the age of five. The protozoan parasite *Plasmodium falciparum* is responsible for the majority of disease burden and deaths and its complex life cycle represents a challenge in disease control and treatment. During the intraerythrocytic asexual cycle, a subset of parasites undergoes sexual commitment and their progeny develop into gametocytes, the parasite form transmissible from humans to *Anopheles* vectors. Extensive research has identified that a drop in the level of the host lipid lysophosphatidylcholine is perceived by the parasite and induces sexual commitment by activating the expression of the transcription factor PfAP2-G, the master regulator of sexual conversion.

In this PhD project, I aimed at elucidating a potential upstream molecular pathway that induces expression of PfAP2-G. In more detail, using a PfAP2-G reporter cell line and other techniques to study sexual commitment, we investigated the involvement of nine *P. falciparum* kinases in this putative signalling pathway. We therefore generated a variety of transgenic parasite lines including kinase knockout as well as conditional knockdown, overexpression and inducible knockout mutants. However, investigating the effect of increased and decreased kinase expression levels did not conclusively identify any of these kinases as pathway component involved in sexual commitment signalling.

Nevertheless, having generated a variety of transgenic cell lines, I further studied the effect of changes in kinase expression levels on asexual and sexual intraerythrocytic parasite development. Interestingly, I identified that while the mitogen-activated protein kinase (MAPK) PfMAP-2 is dispensable for asexual parasite development, it is essential for male gametogenesis. Furthermore, we confirmed the essential role of the casein kinase 2 catalytic subunit PfCK2α in erythrocyte invasion by merozoites and likely also asexual parasite development. In addition, we discovered that PfCK2α is indispensable for sexual development and to my knowledge, this is the first kinase identified as being essential for gametocyte maturation. Finally, I studied the function of PfPKAc, the catalytic subunit of the cAMP-dependent protein kinase A. I confirmed that PfPKAc is required for asexual parasite growth due to its importance in erythrocyte invasion. I further showed that conditional overexpression of PfPKAc is lethal for intraerythrocytic asexual parasite development. Interestingly, however, selection of parasites tolerant to PfPKAc overexpression was possible. All six independently obtained survivor populations, but none of the unselected overexpression-sensitive mother clones, carried mutations in the putative serine/threonine kinase Pf3D7_1121900. We identified

Pf3D7_1121900 as the *P. falciparum* orthologue of the 3-phosphoinositide-dependent protein kinase-1 (PfPDK1). In model eukaryotes, the PDK1 kinase is known to phosphorylate and activate various AGC kinases including PKA. Using targeted mutagenesis, I was able to show the essential role for PfPDK1-dependent phosphorylation of PfPKAc. This phosphorylation seems to be crucial for PfPKAc activity in *P. falciparum*.

The present PhD thesis describes new insights into the function of three essential kinases in asexual and sexual development of *P. falciparum.* Hence, this work broadens our knowledge on kinase function and regulation in malaria parasites in general and provides new potential antimalarial drug targets. Finally, the tools developed during this work will provide important resources for future research on sexual commitment und protein function in *P. falciparum*.

Abbreviations

aPK	atypical protein kinases
bp	base pair
BSD	blasticidin-S-deaminase
cKD	conditional knockdown
cOE	conditional overexpression
DD	FKBP/destabilization domain
DIC	differential interference contrast
DTT	dithiothreitol
ePK	eukaryotic protein kinases
gDNA	genomic DNA
GOI	gene of interest
hDHFR	human dihydrofolate reductase
HR	homology region
HRP	horseradish peroxidase
IDC	intraerythrocytic developmental cycle
IFA	immunofluorescence assays
iKO	inducible knockout
IMC	inner membrane complex
iRBC	infected red blood cell
kb	kilobase
kDa	kilodalton
KO	knockout
SLI	selection-linked integration
NPP	new permeability pathways
OE	overexpression
OPK	other protein kinases
PCR	polymerase chain reaction
RAPA	rapamycin
RBC	red blood cell
sgRNA	single guide RNA
uRBC	uninfected red blood cell
WT	wild type
XA	xanthurenic acid
yDHODH	yeast dihydroorotate dehydrogenase

Chapter 1

General Introduction and Background

Chapter 1

General Introduction and Background

Malaria

Malaria is an infectious disease caused by protozoan parasites of the *Plasmodium* genus. Six *Plasmodium* species regularly infect humans, including *Plasmodium falciparum*, which accounts for the majority of cases and the most severe form of human malaria [1-3]. *Plasmodium vivax* represents the most widespread species worldwide; however, it is less distributed in Africa [2,4]. Although the malaria burden has decreased over the last decades, still 228 million cases were detected and 405'000 people died of the disease in 2018, with the majority of deaths occurring in African children under the age of five [3].

The life cycle of *Plasmodium falciparum*

P. falciparum has a complex life cycle during which sporozoites are transmitted to humans by the bite of a female *Anopheles* mosquito (Fig. 1) [5]. Sporozoites are injected into the skin from where they make their way via the bloodstream to the liver to eventually infect hepatocytes. Inside the liver cells, asexual proliferation leads to the production of

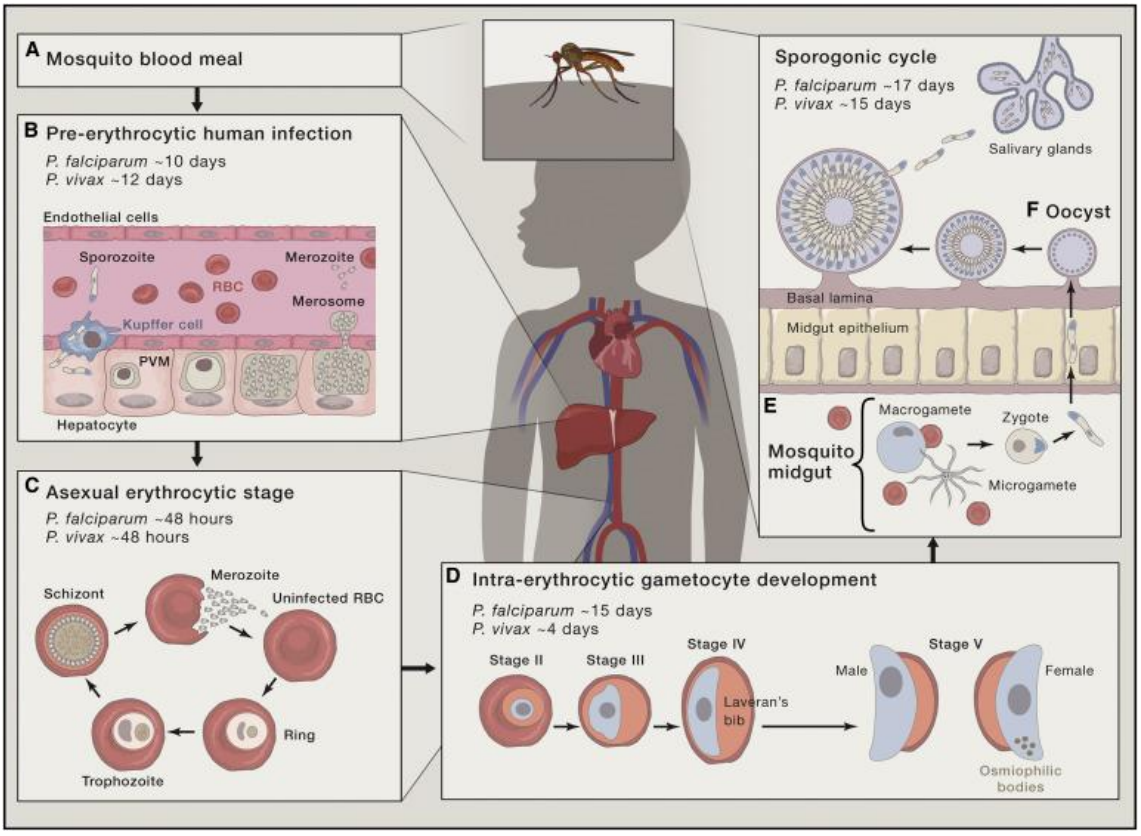

Figure 1: The *Plasmodium* life cycle from Cowman et al., 2016 [5].

thousands of merozoites, which are subsequently released into the blood circulation. Once in the blood, they infect red blood cells (RBCs) and thereby start the intraerythrocytic developmental cycle (IDC). Upon invasion of the RBCs, merozoites develop inside the RBC into ring stage parasites followed by trophozoites and finally schizonts that release up to 32 new merozoites into the bloodstream. A fraction of trophozoites undergoes sexual commitment and - upon schizont rupture - their daughter cells differentiate into mature male or female gametocytes instead of re-entering the IDC. A female *Anopheles* mosquito feeding on an infected human potentially takes up these sexual stages, which further develop in the mosquito vector. Here, they exit the erythrocyte in the mosquito midgut and develop into male and female gametes, which fuse and produce a zygote. Subsequently, the zygote develops into a motile ookinete, which passages through the peritrophic and midgut membrane of the mosquito. Underneath the basal lamina, the parasite forms an oocyst containing thousands of sporozoites. After egress, sporozoites enter the salivary glands of the mosquito and in the saliva are transmitted to a new human host during a blood meal (Fig. 1) [5].

Sexual commitment, gametocytogenesis and AP2-G

Besides the asexual IDC, a small subset of intraerythrocytic parasites undergoes sexual commitment and generates gametocytes. *P. falciparum* gametocytes develop within the erythrocyte through five distinct morphological stages (I-V) and only mature stage V gametocytes are infectious to the mosquito vector [6,7]. The entry into the sexual cycle and thus the generation of gametocytes is the only branching point in the entire life cycle of the parasite and thus an important cell fate decision event. This process, known as sexual commitment, occurs in trophozoites during the IDC preceding gametocyte differentiation [8]. Brancucci and colleagues have further narrowed down this time point and found that between 34 ± 2 hours post invasion (hpi), the cell fate decision is irreversibly determined [8]. Upon schizont rupture, sexually committed merozoites invade RBCs but instead of entering schizogony they undergo sexual differentiation and develop into gametocytes [7,9]. Another recent study demonstrated that ring stage parasites can undergo “same cycle commitment”, resulting in rings directly differentiating into gametocytes [10].

Experiments performed *in vitro* revealed that the sexual commitment rate is influenced by diverse environmental signals thus varying from the background conversion rate observed in routine culturing. For instance, an increased commitment rate was observed in cultures treated with different inhibitors of nucleic acid synthesis or antimalarial drugs such as chloroquine [11,12]. Other researchers identified conditioned medium [13] as well as host hormones [14] or cAMP/PKA-signalling [15,16] as modulators of sexual commitment.

However, only in 2017 Brancucci and colleagues have conclusively identified lysophosphatidylcholine (LysoPC), a host serum lipid, as an environmental regulator of sexual conversion [8]. Whereas the presence of physiological levels of LysoPC in culture medium was shown to keep sexual commitment rates down to background levels in different *P. falciparum* strains, the absence of LysoPC induces sexual commitment by a factor of about 5-10 [8] (Brancucci et al., manuscript in preparation). A recent study has further identified a correlation of high plasma LysoPC levels with low gametocyte to asexual ratios in malaria patients [17].

Recent research revealed the first molecular mechanisms and genes involved in the sexual cell fate decision process of *Plasmodium* parasites. First, two independent studies showed that AP2-G, a member of the apicomplexan-specific ApiAP2 family of transcription factors [18,19], is the key regulator of sexual commitment in *P. falciparum* and the rodent malaria parasite *P. berghei* [20,21]. AP2-G null mutants generated in these *Plasmodium* species are unable to commit to sexual differentiation [20,21], as is the *P. falciparum* F12 parasite line carrying a loss-of-function mutation in the *pfap2-g* coding region [20,22]. Second, the *pfap2-g* locus is enriched in trimethylated lysine 9 on histone 3 (H3K9me3) [23,24], which is a conserved histone mark of heterochromatin [25]. Heterochromatin typically represents the highly condensed and transcriptionally inaccessible form of chromatin in contrast to the transcriptionally accessible euchromatin [25]. Heterochromatin protein 1 (HP1), a conserved regulator of heterochromatin formation and epigenetic gene silencing, binds to H3K9me3 [26,27]. Indeed, it was found that *P. falciparum* HP1 (PfHP1) binds to the H3K9me3-enriched *pfap2-g* locus [28]. Brancucci et al. further showed that conditional depletion of PfHP1 leads to upregulation of PfAP2-G expression and a concomitant 25-fold increased rate of sexual commitment [29]. In addition, Filarsky and colleagues identified the *P. falciparum* gametocyte development 1 (GDV1) protein as regulator of sexual commitment acting upstream of PfHP1 and PfAP2-G. GDV1 was shown to target heterochromatin and mediate the eviction of PfHP1 from the *pfap2-g* locus thereby inducing sexual commitment [30]. Interestingly, a positive correlation of levels of GDV1-dependent genes, PfAP2-G and other factors with the ratio of gametocyte to asexual rings in *P. falciparum*-infected humans further supports the identified regulation of this process *in vivo* [17].

These and additional research findings have defined our current working model regarding the activation and regulation of the *pfap2-g* locus and the function of the PfAP2-G transcription factor in *P. falciparum* (Fig. 2) [31]. The *pfap2-g* locus is epigenetically silenced in asexual parasites in a PfHP1-dependent manner [28,29]. Upon sensing of low LysoPC levels by the parasite, the expression of GDV1 is induced, which itself leads to the eviction of PfHP1 from the *pfap2-g* locus [8,29,30]. Once the *pfap2-g* locus

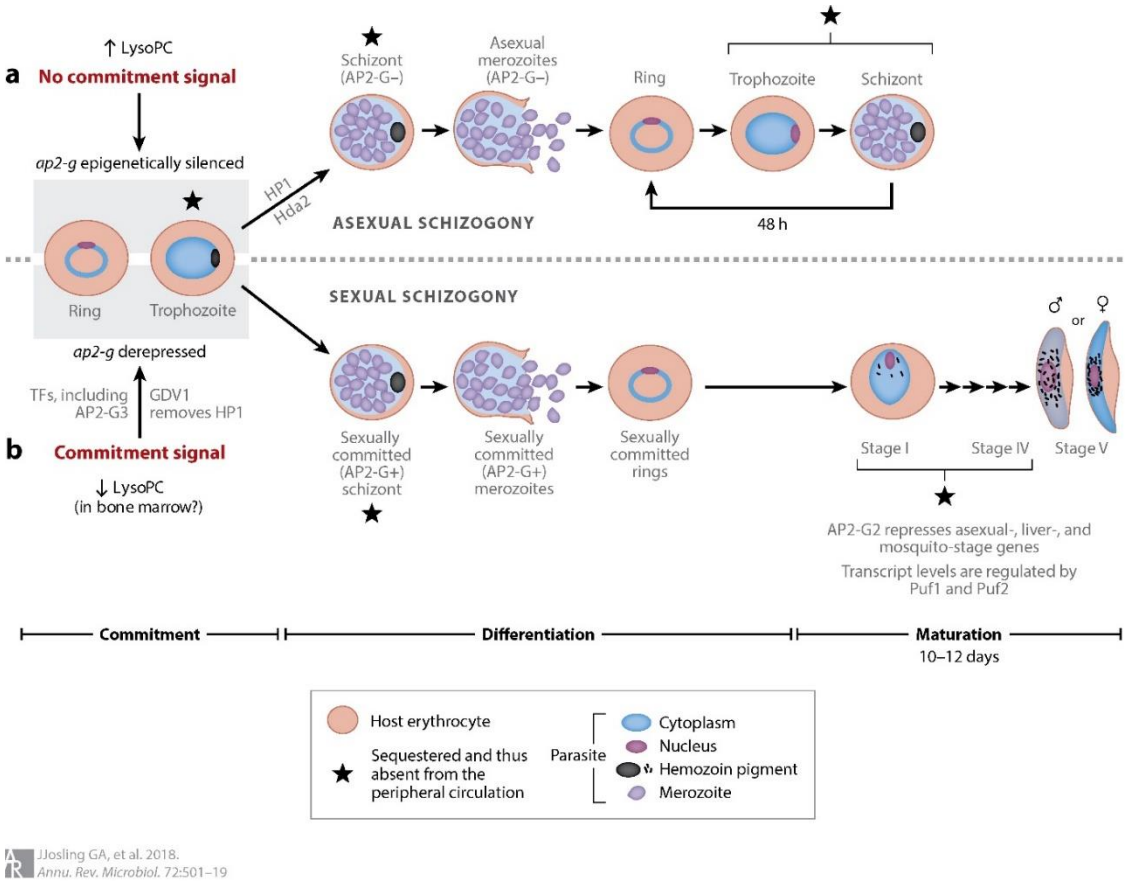

Figure 2: Proposed model for the regulation of sexual commitment in *P. falciparum* from Josling et al., 2018 [31].

is activated, the protein is expressed and as a transcription factor PfAP2-G activates downstream commitment- and gametocyte-specific genes [32].

As outlined above, several external stimuli were reported to modulate the sexual commitment rate and the work of Brancucci and colleagues finally conclusively identified the host factor LysoPC as an important environmental trigger of sexual commitment [8]. Hence, the parasite senses and finally reacts to low levels of LysoPC with the expression of the transcription factor PfAP2-G. It is therefore likely that *Plasmodium* parasites promote perceived external signals internally via signalling pathways as seen in many different model eukaryotes [33].

Kinase signalling

Signalling is a common feature of all biological domains of life and various signalling pathways have been described and identified in a variety of organisms [34,35]. In brief, signalling pathways promoting extracellular signals usually start with a receptor perceiving an environmental stimulus or trigger, generally in form of a small molecule, known as ligand. Upon binding, the receptor changes its conformation and triggers downstream events. Such a receptor either possesses an intracellular domain able to

promote the signal or is associated with an enzyme fulfilling this function. In the cell, a signal can be promoted by a series of molecular events based on several signal pathway components such as enzymes and second messengers. This signalling cascade or pathway results in a cellular change induced for instance by activation of a transcription factor influencing downstream genes [34]. Hence, such cascades allow promoting signals in a complex, compartmentalized cell and can trigger reactions and adaptations to environmental stimuli. In addition, the involvement of several pathway components allows the control and tight regulation of signal promotion and amplification [36,37].

Signalling in eukaryotes is well studied in general and research has also been conducted on signalling in unicellular eukaryotes and their reaction to environmental stimuli. Brewer's yeast *Saccharomyces cerevisiae* can sense nutrients in its environment and promote signals by a variety of signalling pathways, which allows it to react and adapt to environmental changes [38]. *S. cerevisiae* preferentially uses glucose as carbon and energy source. However, in case glucose levels in the environment are low, yeast cells can respond for instance by stimulating gluconeogenesis and autophagy [38]. In fission yeast *Schizosaccharomyces pombe*, the stress-activated protein kinase (SAPK) pathway was shown to promote transcription initiation and hence the adaptation of fission yeast to environmental stress [39].

The pathways described are dependent on the action of kinases, which are essential components of most signalling cascades [40]. Kinases are enzymes phosphorylating their substrate by transferring the γ phosphate group of adenosine triphosphate (ATP) to the hydroxyl group of different targets such as lipids and amino acids. Dephosphorylation of targets occurs through the action of phosphatases [41]. The eukaryotic protein kinases are divided into two main groups, the conventional or eukaryotic protein kinases (ePK) and the atypical protein kinases (aPK) that have no sequence similarity to known ePKs [35]. The ePKs represent one of the largest protein superfamilies identified to date and its kinase families are conserved across species [35]. The kinase domain of ePKs consists of 12 subdomains, which allow the enzyme to fold a conserved catalytic core necessary for its functional activity [42]. Along with the subdomains, several motifs and single amino acids are conserved and important for kinase function such as binding to ATP. Based on accessory domains, the sequence similarity between catalytic domains and the mode of action, the ePKs are grouped into seven families and an additional group of so-called “other protein kinases” (OPK) (Table 1) [35,42,43].

Table 1: Classification of ePKs into seven main groups and the OPK.

Kinase group	Description/Name origin
AGC	Cyclic-nucleotide-dependent kinases (PKA, PKG, PKC)
CAMK	Calcium/Calmodulin-dependent protein kinases
CK1	Casein kinases
CMGC	CDK (cyclin-dependent kinases), MAPK (mitogen-activated protein kinases), GSK3 (glycogen synthase kinase 3) and CLKs (CDK-like kinases)
STE	Serine/Threonine kinases
TK	Tyrosine kinases
TKL	Tyrosine kinase-like kinases (serine-threonine protein kinases)
OPK	Other protein kinases

Depending on the kinase and its substrate, phosphorylation can have different outcomes such as substrate activation or deactivation as well as modification of its function [44]. Activating phosphorylation can be observed in the mitogen-activated protein kinase (MAPK) pathway wherein kinases activate their downstream targets, mostly other kinases, by phosphorylation. The MAPK pathway is a very common and important signalling pathway in eukaryotes and is able to promote externally received signals within a cell [45,46]. For instance, once *S. cerevisiae* senses pheromones, it undergoes several physiological changes in preparation to mate with another yeast cell; the pheromone signal is intracellularly transmitted via the MAPK cascade [47].

Kinase signalling in *P. falciparum*

In *Plasmodium*, no complete signalling pathway has been revealed so far. Nevertheless, conserved pathway components including kinases, phosphatases and second messengers have been identified in the malaria parasite and potential pathways are suggested [48-51].

Of the seven ePK groups classified in eukaryotes, only six have been identified in *P. falciparum* since the tyrosine kinases (TK) are absent in the malaria parasite [52]. In addition, in *P. falciparum* the STE kinase group is drastically reduced and completely lacks the MAPKK family [52]. The malaria kinome consists of 84-99 members depending on the stringency of the inclusion criteria applied [53-55]. In addition to the six ePK groups, *P. falciparum* possesses “orphan kinases”, which do not cluster within one of the described ePK groups. Some of these orphan kinases represent so-called composite kinases, combining features of different ePK groups [49]. Interestingly, *P. falciparum* also

owns several calcium-dependent protein kinases (CDPKs) belonging to the CAMK group, which are absent in metazoans but found in plants and other alveolates [49]. Several different parasite kinases including members of the PfCDPK, PfCDK and AGC group (and many others) have already been analysed and partially characterized on the functional level and they were shown to regulate important processes such as merozoites egress, host cell invasion and intraerythrocytic development [49,50,56]. More information on *P. falciparum* kinase signalling in general and the function of nine selected kinases is given in Chapter 2.

Rationale

Despite a considerable body of literature on parasite kinases, our understanding of *P. falciparum* signalling is still very limited and we are far away from completely resolving a signalling cascade in the malaria parasite. We therefore lack crucial knowledge on how external signals are perceived and promoted by the parasite.

In humans, the function and regulation of kinases is extensively studied and kinases have recently gained a lot of attention as promising drug targets especially in cancer treatment [57,58]. Also for antimalarial treatment, several *P. falciparum* kinases were proposed as drug targets including for instance the cAMP-dependent protein kinase A (PfPKA) [59-62] as well as the casein kinase 2 (PfCK2) [63-66]. New promising drug targets are urgently needed in anti-malarial compound development, since resistance of parasites against all currently used drugs has been reported [67-69].

Importantly, to date not a single kinase involved in regulating the sexual commitment pathway has been identified. The discovery of kinases triggering the activation of the *pfap2-g* locus would generate important new insights into the parasites' molecular strategy underlying the production of malaria transmission stages. Importantly, drugs interfering with sexual commitment could block transmission of the parasite and thus promote malaria elimination [3,70].

Hence, new knowledge on *Plasmodium* signalling and kinase function in general will not only deepen our knowledge on parasite biology but might promote anti-malarial compound development in the future.

Main aims and objectives

The main aim of this PhD thesis was the identification and characterization of a kinase involved in sexual commitment signalling and hence activating expression of the transcription factor PfAP2-G.

For this purpose, four specific objectives were developed:

Objective 1: Generation of a transgenic *pfap2-g* reporter mother cell line.

Objective 2: Generation of conditional kinase over-expression and loss-of-function parasite lines (in the *pfap2-g* reporter mother cell line).

Objective 3: Phenotypic screening of the transgenic parasite lines using high-content imaging, flow cytometry and immunofluorescence assays (IFA) to identify kinases affecting the rate of sexual commitment.

Objective 4: Further functional analysis of priority candidate kinases.

In the scope of this work, nine parasite kinases were investigated for their involvement in *P. falciparum* sexual commitment signalling. A summary of the data resulting from studying these nine kinases is presented in Chapter 2. Since this work has not conclusively identified a kinase involved in sexual commitment signalling, the generated transgenic cell lines were further studied to identify a potential role for these kinases in asexual and sexual intraerythrocytic development. Three main projects that resulted from studying three of these kinases (PfMAP-2, PfCK2α and PfPKAc) in more detail are presented in manuscript format (published, under review or in preparation) in Chapters 3-5 and form the main part of this PhD thesis.

Chapter 2

Kinases and Sexual Commitment

Chapter 2

Kinases and Sexual Commitment

Introduction and Rationale

Several environmental stimuli have been reported to modulate the sexual commitment rate of *P. falciparum* parasites [1-6]. However only in 2017, Brancucci and colleagues conclusively identified the host lipid LysoPC as regulator of sexual conversion [7]. Depletion of LysoPC was shown to trigger expression of the master regulator of sexual commitment, PfAP2-G [7]. In this project, we hypothesized that a signalling pathway must act in perceiving and transmitting this environmental signal, finally leading to expression of the transcription factor PfAP2-G in the parasite nucleus. Kinases have indispensable functions in eukaryotic signalling and are integral components of various signalling pathways. Therefore, kinases represent a reasonable starting point for the identification of signal pathway components involved in activating the *pfap2-g* locus and triggering sexual commitment in *P. falciparum*.

Although about 90 kinases have been identified and several of them partially characterized in *P. falciparum*, our knowledge on kinase function and regulation in different parasite stages is still scarce. Solyakov and colleagues investigated the effect of kinase knockouts (KOs) on the viability of intraerythrocytic *P. falciparum* parasites [8]. Of 65 ePK addressed in this study, 32 are dispensable during the IDC since the authors successfully generated KO cell lines. However, these dispensable kinases might have important functions *in vivo* and/or during other developmental stages of the complex life cycle [9]. Similarly, 23 ePK of the rodent malaria parasite *P. berghei* were found to be dispensable for asexual parasite growth in the mouse [10]. Importantly, none of the studied KO lines both in *P. falciparum* and *P. berghei* showed obvious alterations in sexual commitment rates or a defect in gametocytogenesis [8,10]. Consequently, kinases important for sexual commitment and development might also be essential during the IDC. However, to my knowledge, no studies have been conducted to systematically investigate the ability of transgenic kinase KO cell lines to undergo sexual conversion and to determine their sexual commitment rates.

In this study, eight parasite kinases were initially chosen to investigate their potential involvement in sexual commitment signalling upstream of PfAP2-G. Selection of these candidates was based on existing knowledge of their proposed function or interaction partners in *Plasmodium* spp. or the function of their homologues in other eukaryotes. The kinases of interest studied within the scope of this project are listed in Table 1. The

following paragraphs contain the rationale for choosing these kinases based on knowledge available in 2017, when the candidates were selected.

P. falciparum possesses two mitogen-activated protein kinase (MAPK) homologues, PfMAP-1 and PfMAP-2, which belong to the group of CMGC kinases [11]. The exact function of PfMAP-1 in *P. falciparum* still needs to be determined. However, Dorin-Semblat and colleagues were able to generate a *pfmap-1* KO parasite line, which was still able to produce gametocytes [11]. Considering the importance of MAPK in signalling and adaptive responses in different eukaryotes, PfMAP-1 could nevertheless have a regulatory function in the upstream pathway of *pfap2-g* activation. Furthermore, PfMAP-2 protein levels were elevated in the *pfmap-1* KO parasite line, which might be an indication for functional compensation by PfMAP-2 [11]. In contrast to PfMAP-1, PfMAP-2 seems to be essential for completion of the asexual parasite cycle as a KO line could only be achieved in case the KO plasmid was co-transfected with a PfMAP-2 complementation construct [11]. Curiously, its orthologous *pbmap-2* gene in *P. berghei* was successfully knocked out without any apparent developmental or multiplication defect observed in blood stage parasites. However, male PbMAP-2 KO gametocytes showed a massive decrease in exflagellation suggesting a role for this kinase in male gametogenesis [12-14].

The *P. falciparum* casein kinase 2 (PfCK2) also belongs to the group of CMGC kinases. Dastidar and colleagues suggested a role of PfCK2 in chromatin dynamics [15]. Co-immunoprecipitation using the two regulatory kinase subunits found in *P. falciparum* led to the recovery of proteins belonging to the nucleosome assembly and regulation pathway as well as chromatin-associated substrates such as histones [15]. In addition, work performed in our lab (published in the meantime) showed that PfHP1 is a target of PfCK2-dependent phosphorylation *in vitro* [16].

The MO15-related protein kinase (PfMRK) is the fourth kinase of interest belonging to the group of CMGC kinases. PfMRK activity is stimulated by its effector protein PfMAT1 and both were found to co-localize to the nucleus [17]. PfMRK phosphorylates components of the DNA synthesis machinery, which implicates a role for this kinase DNA replication [17]. Furthermore, PfMRK was shown to phosphorylate the C-terminal domain of RNA polymerase II and shows similarities to metazoan CDK7, suggesting a role for PfMRK in cell cycle and gene expression regulation [18-20].

The *P. falciparum* cAMP-dependent protein kinase A (PfPKA) belongs to the AGC kinases and is essential for erythrocyte invasion by merozoites [21-24]. Furthermore, PfPKA seems to be involved in the modulation of anion channel conductance in infected RBCs as well as in the regulation of cytosolic calcium levels in the parasite. In the apicomplexan parasite *Toxoplasma gondii*, one catalytic subunit of the PKA kinase, TgPKAc3, is

involved in the tachyzoite to bradyzoite switch and is therefore an important cell fate decision factor of the parasite [25].

Two NIMA-related kinases belonging to the orphan kinases, PfNEK-1 and PfNEK-4, were also studied as candidate kinases. PfNEK-1 is likely essential for asexual parasite growth and possesses a mitogen-activated protein kinase kinase (MAPKK)–like activation motif [8,26,27]. Indeed, PfNEK-1 was found to phosphorylate PfMAP-2 *in vitro* leading to the hypothesis that PfNEK-1 might function as a surrogate MAPKK, which are absent in *Plasmodium* species [27]. Reiniger and colleagues have shown that PfNEK-4 is expressed in a subset of schizonts that may represent sexually committed parasites [28]. However, the protein seems to be dispensable for both schizogony and gametocytogenesis [28]. In *P. berghei* PbNEK-4 is essential for zygote to ookinete transition in the mosquito vector [29].

FIKK8 belongs to the unique group of *Plasmodium* FIKK kinases. The FIKK serine/threonine protein kinases represent a multigene family of the *Laverania* and are exported to the host cell [30-32]. Whereas these kinases lack the typical glycine-rich ATP binding motif, they all harbour a FIKK motif of unknown function giving the kinase family its name [32]. Interestingly, among the FIKK kinase family, FIKK8 is the only non-exported kinase and the only member of the family that is conserved in all *Plasmodium* species and other Apicomplexans such as *Toxoplasma*, *Cryptosporidium*, *Neospora* and *Eimeria* [33,34].

Experiments performed in our lab have revealed additional candidates putatively involved in sexual commitment signalling, of which the SNF1-related serine/threonine protein kinase PfKIN was studied as the ninth candidate within the scope of this work. The KIN kinase was identified as sensor of nutrient depletion in both *P. berghei* and *P. falciparum* parasites [35]. Upon caloric restriction of parasite-infected mice, *P. berghei* parasites reacted with a reduced parasite multiplication rate based on a decrease in the number of merozoites per schizont. However, knocking out PbKIN resulted in parasites unable to react to this caloric restriction since they multiplied normally [35].

The function of several of the above-mentioned candidate kinases and their involvement in sexual commitment signalling has been investigated in close collaboration with three MSc students. Therefore, a more in-depth analysis of the function of PfFIKK8, PfNEK-1 (MSc thesis Sarah Höhn), PfCK2α (MSc thesis Olivia Grüninger) as well as PfMRK, PfNEK-4 and PfKIN (MSc thesis Lito Zambounis) can be found in the MSc theses of these students.

Table 1: Kinases of interest investigated in this study. Except for PfMAP-1 and PfNEK-4, all listed kinases are considered essential for the asexual IDC of *P. falciparum* or important for normal asexual growth (FIKK8) [8,36]. This table summarizes knowledge on the kinases of interest available in 2017, when candidates were selected.

Kinase	Kinase group	Proposed functions/characteristics (selection)	Publications (selection)
MAP-1	CMGC	Non-essential (*P. berghei* and *P. falciparum*); PfMAP-2 upregulated in PfMAP-1 KO parasites	11,37
MAP-2	CMGC	Male gamete formation in *P. berghei*; likely essential in *P. falciparum*; male gametocyte-specific expression	11-14,38,39
CK2	CMGC	Chromatin dynamics; invasion of RBCs by merozoites; phosphorylation of PfHP1 *in vitro*	15,16,40
MRK	CMGC	Phosphorylation of DNA replication proteins and RNA polymerase II; PfCyc1/PfMAT1/PfMRK complex likely regulator of schizogony and cytokinesis	17-20,41
PKA	AGC	Invasion of RBCs by merozoites (phosphorylation of AMA-1); anion channel conductance; gametocyte deformability	21,23,24,42
NEK-1	Orphan kinase (NIMA-related)	Phosphorylation of PfMAP-2; male gametocyte-specific expression	26,27
NEK-4	Orphan kinase (NIMA-related)	Early commitment marker; essential for transmission from zygote to ookinete (*P. berghei*); KO with reduced multiplication in *P. berghei*	28,29,35
FIKK8	Orphan kinase (FIKK)	Unknown function; the only conserved and non-exported FIKK	33,34,43
KIN	Orphan kinase	Sensing of nutrient depletion in *P. berghei* (KO and chemical approach) and likely *P. falciparum* (only chemical approach)	35

Results

To investigate the involvement of the candidate kinases in sexual commitment signalling, we generated a variety of transgenic cell lines using CRISPR/Cas9- [44-46] and selection-linked integration (SLI)-based [47] gene editing approaches. For each of the candidate kinases, we aimed at generating straight knockout (KO), conditional knockdown (cKD) and/or inducible knockout (iKO) cell lines as well as conditional overexpression (cOE) parasite lines. All successfully generated transgenic cell lines are listed in Table 2. Several of these transgenic lines were generated in the genetic background of a PfAP2-G reporter cell line. This NF54/AP2-G-mScarlet reporter cell line allows for the detection and quantification of sexually committed parasites (based on mScarlet-positivity) using high content imaging and automated image analysis (Brancucci et al., manuscript in preparation). In case parasites were not generated in the genetic background of this reporter cell line, sexual commitment rates were quantified using N-acetylglucosamine

(GlcNac) assays [48] or detection of the gametocyte-specific marker Pfs16 by IFA. Hence, using high content imaging (PfAP2-G-mScarlet positivity measurement), Pfs16 quantifications and GlcNac assays, we investigated the effect of changes in kinase expression levels in all transgenic cell lines (cKD, iKO, KO and cOE) on the ability of parasites to undergo sexual commitment.

Unfortunately, and to our surprise, we could not conclusively identify a role for any of the nine studied candidate kinases in sexual commitment signalling (Table 2). Interestingly, however, two independently generated PfMRK cKD parasite lines showed an extremely low background sexual commitment rate and were essentially insensitive to the induction of sexual commitment using serum-free medium (–SerM) [7]. Hence, –SerM induction only resulted in a small increase in the commitment rate in one of the parasite lines (from 1.2%±0.1 to 4.6%±1.4), whereas the second PfMRK cKD parasite population showed essentially no increase in sexual commitment upon induction (from 1.7%±0.6 to 2.1%±1.1) (MSc thesis Lito Zambounis, unpublished). In contrast, the NF54/AP2-G-mScarlet control cell line shows a background commitment rate of about 6% (6.4%±2.5) and upon induction of sexual commitment using –SerM medium, this rate increases to about 40% (40.6%±7.2) (Brancucci et al., manuscript in preparation). These preliminary observations suggest that PfMRK may indeed be involved in sexual commitment signalling and further experiments to validate these findings are planned (PhD project, Matthias Wyss).

In addition to studying sexual commitment, all generated transgenic cell lines were subjected to further phenotypic and functional analyses. Interestingly, depletion and/or overexpression of three candidate kinases (PfMAP-2, PfCK2α and PfPKAc) revealed profound effects on asexual and/or sexual parasite development (Table 2). An in-depth analysis of the PfMAP-2, PfCK2α and PfPKAc mutant cell lines are presented in manuscript format in Chapters 3-5.

Table 2: Phenotypic screening of transgenic parasite lines. Genetic engineering approaches and systems used for the generation of transgenic cell lines are described in the Approach section. All cOE parasite lines were generated using the *glmS* ribozyme system [49,50], whereas the systems used to generate the cKD cell lines are indicated in brackets (*dd* or *glmS* or a combination). The iKO cell lines are based on the DiCre/loxP system [51-55]. "No effect" in the "phenotype asexuals" column refers to the absence of any obvious effects on asexual parasite morphology, development and multiplication. "No effect" in the "phenotype sexuals" column refers to the absence of any obvious effects on gametocyte morphology, development and male gametogenesis. KO, knockout; iKO, inducible knockout; cKD, conditional knockdown; cOE, conditional overexpression; *dd*, FKBP destabilization domain system [56,57]; *glmS*, *glmS* self-cleaving ribozyme system [49,50].

Kinase/ Kinase subunit	PlasmoDB identifier	Transgenic lines generated	Sexual commitment	Phenotype asexuals	Phenotype sexuals
PfMAP-1	PF3D7_1431500	KO, cOE	no effect	no effect	no effect
PfMAP-2	PF3D7_1113900	KO, cKD (*dd*), cOE	no effect	no effect	KO and cKD exflagellation defect
PfCK2α	PF3D7_1108400	iKO, cKD (*dd*), cOE	no effect	iKO lethal	iKO lethal, cKD no mature stage V gametocytes
PfMRK	PF3D7_1014400	cKD (*dd*), cOE	potential effect	no effect	no effect
PfPKAc	PF3D7_0934800	cKD (*dd_glmS)*, cOE	no effect	cKD and cOE lethal	cKD gametocyte deformability increase (stage III and V)
PfNEK-1	PF3D7_1228300	cKD (*glmS*), cOE	no effect	no effect	no effect
PfNEK-4	PF3D7_0719200	KO, cKD (*glmS*), cOE	no effect	no effect	no effect
PfFIKK8	PF3D7_0805700	KO, cKD (*dd*)	no effect	KO minor growth defect	no effect
PfKIN	PF3D7_1454300	iKO	no effect	no effect	no effect

Approach

General methods describing *P. falciparum* culturing, transfection, fluorescence microscopy, GlcNac assays and all additional methods used to study *P. falciparum* parasites in this work are described in the Methods section of Chapters 3-5. Here, a brief overview of the approach taken to investigate the involvement of the candidate kinases in sexual commitment signalling is given.

CRISPR/Cas9 and SLI engineering of transgenic parasite lines

All but one transgenic parasite lines described in this work were generated using the CRISPR/Cas9 system [58,59]. This system consists of three major components: A Cas9 endonuclease, a single guide RNA (sgRNA) and a donor sequence. The sgRNA promotes target specificity and guides the Cas9 enzyme to the target site, where it induces a double strand break (DSB). Homology regions (HRs) incorporated into the donor sequence and equivalent to the sequences up- and downstream of the DSB are sufficient to initiate double-crossover homologous recombination. The CRISPR/Cas9 system allows editing of the gene of interest (GOI) between the HRs leading to sequence insertion, deletion, or mutagenesis [58,59].

CRISPR/Cas9 has only been introduced in *P. falciparum* recently [45,46] and in our lab we have generated a set of CRISPR/Cas9 plasmids, which were successfully applied in several cases [7,16,44,60,61]. For gene taggings and alterations (such as point mutations), a two-plasmid approach was applied, consisting of a suicide and a donor plasmid [44]. The suicide plasmid encodes the Cas9 enzyme, the sgRNA and a selectable marker whereas the donor plasmid contains the HRs and additional sequences needed for DSB repair and DNA sequence alteration [44]. To generate straight KOs, a single-plasmid approach was applied, in which all described CRISPR/Cas9 elements are contained on one construct. In this approach, editing leads to the replacement of the coding sequence of the GOI with a selectable marker [44].

One transgenic cell line (PfPKAc cKD, Chapter 5) that could not be successfully generated using the CRISPR/Cas9 system was instead produced using a SLI-based approach [47]. The SLI system is based on modification of the GOI using single crossover homologous recombination (only one HR), which results in integration of the whole plasmid backbone into the genome. Furthermore, two selectable markers were used allowing first for the selection of the episomal plasmid followed, upon successful integration, by selection of parasites harbouring the correctly edited GOI. See the other Chapters for more details on our SLI (5) and CRISPR/Cas9 (3-5) approaches.

AP2-G reporter cell line

To detect and quantify sexually committed parasites, we aimed at generating a reporter cell line expressing fluorescently tagged PfAP2-G. Previous studies have shown the successful generation and application of such a reporter cell line (NF54/AP2-G-GFP) in detecting and quantifying sexually committed parasites [7,61]. Here, we wanted to generate a cell line expressing PfAP2-G tagged with a red fluorescent marker allowing us to re-transfect this line and express kinases of interest as GFP fusions. After several unsuccessful attempts using tdTomato and mCherry as fluorescent tags (data not

shown), we were finally able to generate the NF54/AP2-G-mScarlet parasite line using a CRISPR/Cas9-based two-plasmid approach [7,44] (Brancucci et al., manuscript in preparation). I. Niederwieser and D. Ballmer generated the pD_ap2-g-mScarlet donor plasmid and I transfected this construct together with the pH-gC-ap2g-3' suicide plasmid [7] into NF54 wild type parasites. I confirmed successful editing of the *pfap2-g* locus by PCR and N. Brancucci and I verified expression of PfAP2-G-mScarlet in the subset of sexually committed parasites (Brancucci et al., manuscript in preparation).

Conditional expression systems

Three conditional expression systems were used in this project, the FKBP destabilization domain (*dd*) technique [56,57], the *glmS* self-cleaving ribozyme [49,50] and the DiCre/loxP system [51-55]. The FKBP/DD technique is a conditional expression system based on protein stability controlled by the small ligand Shield-1 [56,57]. The *dd* coding sequence was fused to the kinase GOI, which leads to expression of the protein tagged with the DD domain. Shield-1 stabilizes the fusion protein by binding to this domain. Upon removal of Shield-1, the protein is destabilized leading to degradation of the fusion protein in the proteasome [57]. The *glmS* self-cleaving ribozyme was inserted downstream of the coding sequence of the GOI such that it is contained within the 3' untranslated region (UTR) of the corresponding mRNA. Glucosamine (GlcN) activates the *glmS* ribozyme, which subsequently cleaves itself, thus destabilizing the mRNA resulting in RNA degradation. In absence of GlcN, the mRNA remains intact and the protein is expressed [49,50]. Finally, the DiCre/loxP system is based on the action of the Cre recombinase that recombines loxP sites previously inserted into the parasite genome. Depending on the orientation of the loxP sites to each other, the recombination can have different outcomes including gene deletion or conversion [51-55]. In the DiCre system, the Cre recombinase is split into two inactive enzyme domains that can only interact and form a functional recombinase in presence of rapamycin, thus rendering the system inducible [51-55].
In this project, we generated a variety of transgenic cell lines using these conditional expression systems by tagging the candidate kinases of interest using the fluorescent marker *gfp* followed by *dd*, *glmS* (or a combination of both) or flanked by loxP and/or loxPint sites (see below; Table 2 and Chapters 3-5).

Generation and phenotypic screening of transgenic parasite lines

Here, we used both straight KOs and conditional expression system approaches to study the function of kinases of interest in sexual commitment signalling.

Straight KOs were generated using a single plasmid CRISPR/Cas9 approach as described [44]. All cOE kinase parasite lines generated in this work are based on insertion of an additional, exogenous copy of the kinase GOI into the non-essential *glp3* (*cg6,* Pf3D7_0709200) locus [62]. The constitutively active *calmodulin* (PF3D7_1434200) promoter drives expression of the GOI and the kinase gene is tagged with *gfp* followed by the *glmS* ribozyme sequence and the *hrp2* (Pf3D7_0831800) 3' sequence acting as terminator. cKD parasite lines were generated by tagging the endogenous gene with *gfp* followed by either the *dd* or the *glmS* sequence or a *dd-glmS* combination. The systems used to generate the different candidate kinase cKD lines are indicated in Table 2.

Finally, the iKO parasite lines are based on the DiCre/loxP system described above. Briefly, a *gfp* sequence is fused to the candidate kinase coding sequence followed by a loxP site. Additionally, towards the 5' end of the coding sequence a loxPint [63], i.e. a loxP site incorporated into a *sera2* (Pf3D7_0207900) intron, is inserted allowing excision of the majority of the coding sequence after DiCre-mediated recombination. The iKO candidate kinase constructs were transfected into the NF54::DiCre parasite line encoding the DiCre expression cassette [51].

Detailed engineering strategies of all cell lines can be found in Chapters 3-5 and in the MSc theses of Sarah Höhn, Olivia Grüninger and Lito Zambounis. Although we were not successful in producing cKD, iKO (and/or KO) and cOE cell lines for all kinases of interest, we generated at least one transgenic parasite line per candidate kinase (Table 2).

To identify a potential involvement of the kinases of interest in sexual commitment signalling, we investigated the effect of conditional changes in kinase expression levels and kinase KOs on commitment rates and the capacity to induce sexual commitment using –SerM medium [7]. Parasites cultured in –SerM medium supplemented with choline chloride (CC), which was shown to block sexual commitment [7], served as control. As mentioned above, in case the transgenic cell lines were generated in the genetic background of the NF54/AP2-G-mScarlet reporter cell line, sexual commitment rates were determined by quantifying mScarlet-positive parasites among all parasites (Hoechst-positive) using high content imaging and automated image analysis (Brancucci et al., manuscript in preparation). In case the transgenic lines were generated in parasites that do not express PfAP2-G-mScarlet, sexual commitment rates were determined by quantifying sexual parasites using Pfs16 as a marker or by GlcNac assays as described [64].

Discussion and Conclusion

Among the nine kinases investigated, we could not conclusively identify a single kinase involved in the upstream signalling pathway triggering PfAP2-G expression and sexual commitment. However, in collaboration with N. Brancucci, we developed a high content imaging-based pipeline for studying the function of kinases and other factors in sexual commitment signalling. This assay allows us to identify candidate proteins involved in sexual commitment signalling using medium-scale inhibitor or activator screens (Brancucci et al., manuscript in preparation) and to investigate their function using transgenic parasite lines as described in this work.

Since two independently generated PfMRK cKD parasite lines were found essentially unable to react to induction of sexual commitment (–SerM medium), we hypothesize that PfMRK might be part of the signalling cascade regulating PfAP2-G expression and thus sexual commitment. Insufficient stabilization of PfMRK-GFPDD in the cKD parasite lines by Shield-1 could result in the low sexual commitment rates and irresponsiveness to –SerM medium we observed for these cell lines. However, mutations in *gdv1* or *pfap2-g* in these populations could similarly result in the inability of the majority of parasites to undergo sexual commitment and form gametocytes. Establishing PfMRK cKD clones followed by sequencing of *gdv1* and *pfap2-g* coding sequences to identify putative mutations will clarify this hypothesis. In addition, the planned generation of a PfMRK iKO parasite line might further help identify PfMRK as the first known kinase involved in sexual commitment signalling (PhD project, Matthias Wyss).

Furthermore, kinase inhibitor screens performed in our lab have identified additional candidate kinases potentially involved in sexual commitment, which promotes elucidation of the putative signalling pathway acting upstream of PfAP2-G (Brancucci et al., manuscript in preparation). Once candidates are determined, their further functional investigation might reveal additional pathway components and finally clarify the perception and promotion of the LysoPC signal and/or the pathway subsequently resulting in expression of PfAP2-G. Resolving this signalling pathway would not only promote our understanding of *P. falciparum* environmental sensing and signalling but may also provide us with new drug targets for the development of transmission-blocking interventions.

References

1 Ono, T., Ohnishi, Y., Nagamune, K. & Kano, M. Gametocytogenesis Induction by Berenil in Cultured Plasmodium falciparum. *Experimental Parasitology* **77**, 74-78, doi:https://doi.org/10.1006/expr.1993.1062 (1993).

2 Buckling, A. G., Taylor, L. H., Carlton, J. M. & Read, A. F. Adaptive changes in Plasmodium transmission strategies following chloroquine chemotherapy. *Proc Biol Sci* **264**, 553-559, doi:10.1098/rspb.1997.0079 (1997).

3 Williams, J. L. Stimulation of Plasmodium falciparum gametocytogenesis by conditioned medium from parasite cultures. *The American journal of tropical medicine and hygiene* **60**, 7-13, doi:10.4269/ajtmh.1999.60.7 (1999).

4 Lingnau, A., Margos, G., Maier, W. A. & Seitz, H. M. The effects of hormones on the gametocytogenesis of Plasmodium falciparum in vitro. *Applied parasitology* **34**, 153-160 (1993).

5 Kaushal, D. C., Carter, R., Miller, L. H. & Krishna, G. Gametocytogenesis by malaria parasites in continuous culture. *Nature* **286**, 490-492, doi:10.1038/286490a0 (1980).

6 Read, L. K. & Mikkelsen, R. B. Comparison of adenylate cyclase and cAMP-dependent protein kinase in gametocytogenic and nongametocytogenic clones of Plasmodium falciparum. *The Journal of parasitology* **77**, 346-352 (1991).

7 Brancucci, N. M. B. *et al.* Lysophosphatidylcholine Regulates Sexual Stage Differentiation in the Human Malaria Parasite Plasmodium falciparum. *Cell* **171**, 1532-1544.e1515, doi:10.1016/j.cell.2017.10.020 (2017).

8 Solyakov, L. *et al.* Global kinomic and phospho-proteomic analyses of the human malaria parasite Plasmodium falciparum. *Nat Commun* **2**, 565, doi:10.1038/ncomms1558 (2011).

9 Dorin-Semblat, D., Sicard, A., Doerig, C., Ranford-Cartwright, L. & Doerig, C. Disruption of the PfPK7 gene impairs schizogony and sporogony in the human malaria parasite Plasmodium falciparum. *Eukaryotic cell* **7**, 279-285, doi:10.1128/EC.00245-07 (2008).

10 Tewari, R. *et al.* The systematic functional analysis of Plasmodium protein kinases identifies essential regulators of mosquito transmission. *Cell Host Microbe* **8**, 377-387, doi:10.1016/j.chom.2010.09.006 (2010).

11 Dorin-Semblat, D. *et al.* Functional characterization of both MAP kinases of the human malaria parasite Plasmodium falciparum by reverse genetics. *Mol Microbiol* **65**, 1170-1180, doi:10.1111/j.1365-2958.2007.05859.x (2007).

12 Khan, S. M. *et al.* Proteome analysis of separated male and female gametocytes reveals novel sex-specific Plasmodium biology. *Cell* **121**, 675-687, doi:10.1016/j.cell.2005.03.027 (2005).

13 Rangarajan, R. *et al.* A mitogen-activated protein kinase regulates male gametogenesis and transmission of the malaria parasite Plasmodium berghei. *EMBO Rep* **6**, 464-469, doi:10.1038/sj.embor.7400404 (2005).

14 Tewari, R., Dorin, D., Moon, R., Doerig, C. & Billker, O. An atypical mitogen-activated protein kinase controls cytokinesis and flagellar motility during male gamete formation in a malaria parasite. *Mol Microbiol* **58**, 1253-1263, doi:10.1111/j.1365-2958.2005.04793.x (2005).

15 Dastidar, E. G. *et al.* Involvement of Plasmodium falciparum protein kinase CK2 in the chromatin assembly pathway. *BMC biology* **10**, 5, doi:10.1186/1741-7007-10-5 (2012).

16 Bui, H. T. N. *et al.* Mapping and functional analysis of heterochromatin protein 1 phosphorylation in the malaria parasite Plasmodium falciparum. *Scientific Reports* **9**, 16720, doi:10.1038/s41598-019-53325-9 (2019).

17 Jirage, D. *et al.* The malarial CDK Pfmrk and its effector PfMAT1 phosphorylate DNA replication proteins and co-localize in the nucleus. *Mol Biochem Parasitol* **172**, 9-18, doi:10.1016/j.molbiopara.2010.03.009 (2010).

18 Waters, N. C., Woodard, C. L. & Prigge, S. T. Cyclin H activation and drug susceptibility of the Pfmrk cyclin dependent protein kinase from Plasmodium falciparum. *Mol Biochem Parasitol* **107**, 45-55, doi:10.1016/s0166-6851(99)00229-7 (2000).
19 Li, J. L., Robson, K. J., Chen, J. L., Targett, G. A. & Baker, D. A. Pfmrk, a MO15-related protein kinase from Plasmodium falciparum. Gene cloning, sequence, stage-specific expression and chromosome localization. *European journal of biochemistry* **241**, 805-813, doi:10.1111/j.1432-1033.1996.00805.x (1996).
20 Le Roch, K. *et al.* Activation of a Plasmodium falciparum cdc2-related kinase by heterologous p25 and cyclin H. Functional characterization of a P. falciparum cyclin homologue. *J Biol Chem* **275**, 8952-8958, doi:10.1074/jbc.275.12.8952 (2000).
21 Merckx, A. *et al.* Plasmodium falciparum regulatory subunit of cAMP-dependent PKA and anion channel conductance. *PLoS Pathog* **4**, e19, doi:10.1371/journal.ppat.0040019 (2008).
22 Beraldo, F. H., Almeida, F. M., da Silva, A. M. & Garcia, C. R. Cyclic AMP and calcium interplay as second messengers in melatonin-dependent regulation of Plasmodium falciparum cell cycle. *The Journal of cell biology* **170**, 551-557, doi:10.1083/jcb.200505117 (2005).
23 Prinz, B. *et al.* Hierarchical phosphorylation of apical membrane antigen 1 is required for efficient red blood cell invasion by malaria parasites. *Sci Rep* **6**, 34479, doi:10.1038/srep34479 (2016).
24 Leykauf, K. *et al.* Protein kinase a dependent phosphorylation of apical membrane antigen 1 plays an important role in erythrocyte invasion by the malaria parasite. *PLoS Pathog* **6**, e1000941, doi:10.1371/journal.ppat.1000941 (2010).
25 Sugi, T. *et al.* Toxoplasma gondii Cyclic AMP-Dependent Protein Kinase Subunit 3 Is Involved in the Switch from Tachyzoite to Bradyzoite Development. *MBio* **7**, doi:10.1128/mBio.00755-16 (2016).
26 Dorin-Semblat, D. *et al.* Plasmodium falciparum NIMA-related kinase Pfnek-1: sex specificity and assessment of essentiality for the erythrocytic asexual cycle. *Microbiology* **157**, 2785-2794, doi:10.1099/mic.0.049023-0 (2011).
27 Dorin, D. *et al.* Pfnek-1, a NIMA-related kinase from the human malaria parasite Plasmodium falciparum Biochemical properties and possible involvement in MAPK regulation. *European journal of biochemistry* **268**, 2600-2608, doi:10.1046/j.1432-1327.2001.02151.x (2001).
28 Reininger, L., Garcia, M., Tomlins, A., Müller, S. & Doerig, C. The Plasmodium falciparum, Nima-related kinase Pfnek-4: a marker for asexual parasites committed to sexual differentiation. *Malar J* **11**, 250, doi:10.1186/1475-2875-11-250 (2012).
29 Reininger, L. *et al.* A NIMA-related protein kinase is essential for completion of the sexual cycle of malaria parasites. *J Biol Chem* **280**, 31957-31964, doi:10.1074/jbc.M504523200 (2005).
30 Schneider, A. G. & Mercereau-Puijalon, O. A new Apicomplexa-specific protein kinase family: multiple members in Plasmodium falciparum, all with an export signature. *BMC Genomics* **6**, 30, doi:10.1186/1471-2164-6-30 (2005).
31 Sundararaman, S. A. *et al.* Genomes of cryptic chimpanzee Plasmodium species reveal key evolutionary events leading to human malaria. *Nat Commun* **7**, 11078, doi:10.1038/ncomms11078 (2016).
32 Ward, P., Equinet, L., Packer, J. & Doerig, C. Protein kinases of the human malaria parasite Plasmodium falciparum: the kinome of a divergent eukaryote. *BMC Genomics* **5**, 79, doi:10.1186/1471-2164-5-79 (2004).
33 Osman, K. T. *et al.* Biochemical characterization of FIKK8--A unique protein kinase from the malaria parasite Plasmodium falciparum and other apicomplexans. *Mol Biochem Parasitol* **201**, 85-89, doi:10.1016/j.molbiopara.2015.06.002 (2015).

34 Kooij, T. W. *et al.* A Plasmodium whole-genome synteny map: indels and synteny breakpoints as foci for species-specific genes. *PLoS Pathog* **1**, e44, doi:10.1371/journal.ppat.0010044 (2005).
35 Mancio-Silva, L. *et al.* Nutrient sensing modulates malaria parasite virulence. *Nature* **547**, 213-216, doi:10.1038/nature23009 (2017).
36 Davies, H. *et al.* An exported kinase family mediates species-specific erythrocyte remodelling and virulence in human malaria. *Nature microbiology* **5**, 848-863, doi:10.1038/s41564-020-0702-4 (2020).
37 Fang, H. *et al.* Epistasis studies reveal redundancy among calcium-dependent protein kinases in motility and invasion of malaria parasites. *Nat Commun* **9**, 4248, doi:10.1038/s41467-018-06733-w (2018).
38 Dorin, D. *et al.* An atypical mitogen-activated protein kinase (MAPK) homologue expressed in gametocytes of the human malaria parasite Plasmodium falciparum. Identification of a MAPK signature. *J Biol Chem* **274**, 29912-29920, doi:10.1074/jbc.274.42.29912 (1999).
39 Lasonder, E. *et al.* Integrated transcriptomic and proteomic analyses of P. falciparum gametocytes: molecular insight into sex-specific processes and translational repression. *Nucleic Acids Res* **44**, 6087-6101, doi:10.1093/nar/gkw536 (2016).
40 Tham, W. H. *et al.* Plasmodium falciparum Adhesins Play an Essential Role in Signalling and Activation of Invasion into Human Erythrocytes. *PLoS Pathog* **11**, e1005343, doi:10.1371/journal.ppat.1005343 (2015).
41 Robbins, J. A., Absalon, S., Streva, V. A. & Dvorin, J. D. The Malaria Parasite Cyclin H Homolog PfCyc1 Is Required for Efficient Cytokinesis in Blood-Stage Plasmodium falciparum. *mBio* **8**, doi:10.1128/mBio.00605-17 (2017).
42 Ramdani, G. *et al.* cAMP-Signalling Regulates Gametocyte-Infected Erythrocyte Deformability Required for Malaria Parasite Transmission. *PLoS Pathog* **11**, e1004815, doi:10.1371/journal.ppat.1004815 (2015).
43 Lin, B. C. *et al.* The anthraquinone emodin inhibits the non-exported FIKK kinase from Plasmodium falciparum. *Bioorganic chemistry* **75**, 217-223, doi:10.1016/j.bioorg.2017.09.011 (2017).
44 Filarsky, M. *et al.* GDV1 induces sexual commitment of malaria parasites by antagonizing HP1-dependent gene silencing. *Science (New York, N.Y.)* **359**, 1259-1263, doi:10.1126/science.aan6042 (2018).
45 Ghorbal, M. *et al.* Genome editing in the human malaria parasite Plasmodium falciparum using the CRISPR-Cas9 system. *Nature biotechnology* **32**, 819-821, doi:10.1038/nbt.2925 (2014).
46 Wagner, J. C., Platt, R. J., Goldfless, S. J., Zhang, F. & Niles, J. C. Efficient CRISPR-Cas9-mediated genome editing in Plasmodium falciparum. *Nat Methods* **11**, 915-918, doi:10.1038/nmeth.3063 (2014).
47 Birnbaum, J. *et al.* A genetic system to study Plasmodium falciparum protein function. *Nat Methods* **14**, 450-456, doi:10.1038/nmeth.4223 (2017).
48 Fivelman, Q. L. *et al.* Improved synchronous production of Plasmodium falciparum gametocytes in vitro. *Mol. Biochem. Parasitol* **154**, 119-123 (2007).
49 Prommana, P. *et al.* Inducible knockdown of Plasmodium gene expression using the glmS ribozyme. *PLoS One* **8**, e73783, doi:10.1371/journal.pone.0073783 (2013).
50 Winkler, W. C., Nahvi, A., Roth, A., Collins, J. A. & Breaker, R. R. Control of gene expression by a natural metabolite-responsive ribozyme. *Nature* **428**, 281-286, doi:10.1038/nature02362 (2004).
51 Tiburcio, M. *et al.* A Novel Tool for the Generation of Conditional Knockouts To Study Gene Function across the Plasmodium falciparum Life Cycle. *MBio* **10**, doi:10.1128/mBio.01170-19 (2019).
52 Jones, M. L. *et al.* A versatile strategy for rapid conditional genome engineering using loxP sites in a small synthetic intron in Plasmodium falciparum. *Sci. Rep* **6**, 21800, doi:srep21800 [pii];10.1038/srep21800 [doi] (2016).

53 Collins, C. R. *et al.* Robust inducible Cre recombinase activity in the human malaria parasite Plasmodium falciparum enables efficient gene deletion within a single asexual erythrocytic growth cycle. *Mol Microbiol* **88**, 687-701, doi:10.1111/mmi.12206 (2013).
54 Jullien, N. *et al.* Conditional transgenesis using Dimerizable Cre (DiCre). *PLoS One* **2**, e1355, doi:10.1371/journal.pone.0001355 (2007).
55 Jullien, N., Sampieri, F., Enjalbert, A. & Herman, J. P. Regulation of Cre recombinase by ligand-induced complementation of inactive fragments. *Nucleic Acids Res* **31**, e131, doi:10.1093/nar/gng131 (2003).
56 Armstrong, C. M. & Goldberg, D. E. An FKBP destabilization domain modulates protein levels in Plasmodium falciparum. *Nat Methods* **4**, 1007-1009, doi:10.1038/nmeth1132 (2007).
57 Banaszynski, L. A., Chen, L. C., Maynard-Smith, L. A., Ooi, A. G. & Wandless, T. J. A rapid, reversible, and tunable method to regulate protein function in living cells using synthetic small molecules. *Cell* **126**, 995-1004, doi:10.1016/j.cell.2006.07.025 (2006).
58 Lee, M. C. S., Lindner, S. E., Lopez-Rubio, J.-J. & Llinás, M. Cutting back malaria: CRISPR/Cas9 genome editing of Plasmodium. *Briefings in Functional Genomics* **18**, 281-289, doi:10.1093/bfgp/elz012 %J Briefings in Functional Genomics (2019).
59 Wang, H., Russa, M. L. & Qi, L. S. CRISPR/Cas9 in Genome Editing and Beyond. **85**, 227-264, doi:10.1146/annurev-biochem-060815-014607 (2016).
60 Hitz, E., Balestra, A. C., Brochet, M. & Voss, T. S. PfMAP-2 is essential for male gametogenesis in the malaria parasite Plasmodium falciparum. *Scientific Reports* **10**, 11930, doi:10.1038/s41598-020-68717-5 (2020).
61 Brancucci, N. M. B. *et al.* Probing Plasmodium falciparum sexual commitment at the single-cell level. *Wellcome open research* **3**, 70, doi:10.12688/wellcomeopenres.14645.4 (2018).
62 Nkrumah, L. J. *et al.* Efficient site-specific integration in Plasmodium falciparum chromosomes mediated by mycobacteriophage Bxb1 integrase. *Nat Methods* **3**, 615-621, doi:10.1038/nmeth904 (2006).
63 Jones, M. L. *et al.* A versatile strategy for rapid conditional genome engineering using loxP sites in a small synthetic intron in Plasmodium falciparum. *Sci Rep* **6**, 21800, doi:10.1038/srep21800 (2016).
64 Fivelman, Q. L. *et al.* Improved synchronous production of Plasmodium falciparum gametocytes in vitro. *Mol Biochem Parasitol* **154**, 119-123, doi:10.1016/j.molbiopara.2007.04.008 (2007).

Chapter 3

Mitogen-activated protein kinases (MAPK)

This chapter contains the manuscript “PfMAP-2 is essential for male gametogenesis in the malaria parasite *Plasmodium falciparum*” published in *Scientific Reports* (17. July 2020) and available under the following link: https://www.nature.com/articles/s41598-020-68717-5. The Supplementary Dataset 1 and the Supplementary Spreadsheet 1 are not included in this version but are available upon request and are included in the published manuscript version. I am first author of this manuscript and detailed information on the author contribution is given in the according manuscript section.

Chapter 3

PfMAP-2 is essential for male gametogenesis in the malaria parasite *Plasmodium falciparum*

Eva Hitz[1,2], Aurélia C. Balestra[3], Mathieu Brochet[3], Till S. Voss[1,2,*]

[1]Department of Medical Parasitology and Infection Biology, Swiss Tropical and Public Health Institute, 4051 Basel, Switzerland.

[2]University of Basel, 4001 Basel, Switzerland.

[3]Department of Microbiology and Molecular Medicine, Faculty of Medicine, University of Geneva, 1211 Geneva 4, Switzerland.

[*]Corresponding author: till.voss@swisstph.ch.

Summary

In malaria parasites, male gametogenesis is a proliferative stage essential for parasite transmission to the mosquito vector. It is a rapid process involving three rounds of genome replication alternating with closed endomitoses, and assembly of axonemes to produce eight flagellated motile microgametes. Studies in *Plasmodium berghei* have highlighted tight regulation of gametogenesis by a network of kinases. The *P. berghei* MAPK homologue PbMAP-2 is dispensable for asexual development but important at the induction of axoneme motility. However, in *P. falciparum*, causing the most severe form of human malaria, PfMAP-2 was suggested to be essential for asexual proliferation indicating distinct functions for MAP-2 in these two *Plasmodium* species. We here show that PfMAP-2 is dispensable for asexual growth but important for male gametogenesis *in vitro.* Similar to PbMAP-2, PfMAP-2 is required for initiating axonemal beating but not for prior DNA replication or axoneme formation. In addition, single and double null mutants of PfMAP-2 and the second *P. falciparum* MAPK homologue PfMAP-1 show no defect in asexual proliferation, sexual commitment or gametocytogenesis. Our results

suggest that MAPK activity plays no major role in the biology of both asexual and sexual blood stage parasites up until the point of male gametogenesis.

Introduction

In the human host, *Plasmodium* spp. parasites undergo repeated rounds of asexual replication within human red blood cells (RBCs) thereby causing malaria symptoms. A small subset of parasites, however, undergo sexual commitment and differentiate into gametocytes, which are the human-to-mosquito transmissible parasite forms. Previous studies on *P. falciparum* sexual commitment and development have shown that a single intra-erythrocytic schizont gives rise to either only asexual or only sexual progeny [1,2]. However, recent research demonstrated that schizonts can also generate mixed asexual and sexual progeny thus promoting the idea of same cycle sexual conversion in ring stage parasites [3]. Following commitment to sexual development, gametocytes mature over 10 to 12 days and five distinct morphological stages into mature stage V gametocytes. Male-specific marker genes can be detected as early as in stage I/II gametocytes [4], whereas morphological differentiation of male and female gametocytes using Giemsa-stained blood smears is only evident in later stages IV and V. *In vivo*, stage I-IV gametocytes sequester in tissues including the bone marrow and are thus absent from blood circulation [5-9]. In contrast, mature stage V gametocytes re-enter the bloodstream from where they can eventually be taken up by a female *Anopheles* mosquito during a blood meal [10]. Upon ingestion by an *Anopheles* vector, gametocytes encounter major environmental changes in the mosquito midgut. A drop in temperature, a rise in pH and the presence of the mosquito factor xanthurenic acid (XA) trigger the egress of gametocytes from the infected RBC (iRBC) and gamete development [11-15]. Whereas one female gametocyte develops into a single macrogamete, one male gametocyte gives rise to eight flagellated motile microgametes. Gametogenesis is linked to intracellular mobilisation of Ca^{2+}, which in male gametocytes activates three rounds of rapid replication of DNA followed by endomitosis [16]. During this process, parasites also

egress from the RBC and start axoneme biosynthesis. In the last phase of male gametogenesis, axoneme mobility is initiated and male gametes exit into the environment in a process termed exflagellation. At this point, the motile male gametes are still attached to the residual body and bind neighbouring erythrocytes, thus generating so-called exflagellation centres that are visible by bright-field microscopy [17-19]. Subsequently, in the mosquito midgut, one female macrogamete fuses with one male microgamete to generate a zygote. Further development results in a motile ookinete that traverses the mosquito midgut epithelium to form a sessile oocyst. The oocyst undergoes sporogony resulting in the generation of thousands of sporozoites that, upon release from the oocyst, infect the mosquito salivary glands from where they are injected into a new host during a next blood meal.

Studies mainly performed in *P. berghei*, a malaria parasite infecting rodents, have identified several kinases as important components in different steps of male gametogenesis. For instance, the cGMP-dependent protein kinase G (PKG) was shown to be essential for Ca^{2+} mobilisation upon gametocyte activation by environmental triggers [20,21]. Following Ca^{2+} mobilisation, the action of the calcium-dependent protein kinase 4 (CDPK4) is essential for microgamete development at three different steps including the initiation of axoneme motility [18,22,23]. In addition, other calcium-dependent protein kinases (CDPK1 and CDPK2) play important roles at different steps of male gametogenesis [24-26].

In 2005, three different studies identified the atypical *P. berghei* mitogen-activated protein kinase (MAPK) PbMAP-2 as an important component in male gametogenesis [27-29]. MAP-2 together with MAP-1 represent the only two homologues of eukaryotic MAPKs identified in *Plasmodium* spp. [30-33]. In various eukaryotes ranging from yeast to humans, the MAPK signalling pathway was shown to be involved in essential cellular processes including cell differentiation, proliferation as well as survival [34,35]. In *P. berghei*, PbMAP-2 is dispensable for asexual proliferation of blood stage parasites. However, in PbMAP-2 knockout (KO) parasites, a dramatic decrease in the number of exflagellating male

gametocytes was observed when compared to wild type (WT) parasites [27-29]. Tewari and colleagues further scrutinized the PbMAP-2-dependent exflagellation defect and identified an important role for PbMAP-2 late in gametogenesis at the stage of DNA condensation, initiation of axoneme motility and cytokinesis [29]. As expected, due to these defects PbMAP-2 KO parasites were essentially unable to infect *Anopheles* mosquitoes [28,29].

In contrast to *P. berghei*, the role of PfMAP-2 in *P. falciparum* parasites remains elusive as the *pfmap-2* gene was found resistant to KO attempts. It was therefore speculated that PfMAP-2 is essential for *P. falciparum* asexual proliferation and thus may have roles distinct from its function in *P. berghei* parasites [36]. Dorin-Semblat and colleagues could further show that the second *P. falciparum* MAPK, PfMAP-1, is neither essential for asexual development and gametocytogenesis *in vitro* nor for gametogenesis and sporogony in the mosquito vector [36]. However, the authors observed upregulation of PfMAP-2 protein expression in PfMAP-1 KO parasites and therefore suggested a mechanism through which increased PfMAP-2 kinase levels may compensate for the loss of PfMAP-1 function [36]. Such functional compensation would imply that PfMAP-1 still has an important function in asexual *P. falciparum* development *in vitro*. However, in *P. berghei* both MAPKs are dispensable for asexual growth and PbMAP-1/PbMAP-2 double KO parasites show no obvious phenotype in blood stage proliferation [37]. Whereas recent research has shed light into signalling pathways and kinases involved in *P. berghei* male gamete production, knowledge on the molecular players in *P. falciparum* gametogenesis is still scarce. Here, we used CRISPR/Cas9-based gene editing to re-assess MAPK function in *P. falciparum*. We demonstrate that similar to the situation in *P. berghei*, PfMAP-1 and PfMAP-2 are dispensable for asexual proliferation, sexual commitment and gametocyte development and that PfMAP-2 shows male-specific expression and is essential for male gametogenesis.

Results

MAPKs are not essential for *P. falciparum* asexual development

Using reverse genetics, our first aim was to identify the function of PfMAP-2 in *P. falciparum* asexual and sexual development. Therefore, using a single plasmid CRISPR/Cas9 system [38], we aimed at generating a PfMAP-2 KO parasite line, although previous research reported unsuccessful KO attempts [36]. Using this approach, correct editing of the locus would result in the replacement of the *pfmap-2* gene with a blasticidin-S-deaminase (BSD)-expressing resistance cassette. In multiple independent transfections of strain NF54, we obtained drug-resistant parasites 10-14 days after transfection. PCR on genomic DNA (gDNA) confirmed the disruption of the *pfmap-2* gene and the correct integration of the BSD resistance cassette and thus the successful generation of a NF54/MAP-2 KO line (Supplementary Fig. 1). Hence, contrary to previous research, we conclude that PfMAP-2 is not essential for asexual proliferation.

In addition, using the same approach, we also generated a PfMAP-1 KO parasite line (NF54/MAP-1 KO) serving as a control for further experiments. NF54/MAP-1 KO parasites could be readily obtained as previously described [36] (Supplementary Fig. 1). To test if both PfMAPKs are dispensable for asexual growth, we tried to generate a PfMAP-1/PfMAP-2 double KO (dKO) parasite line. We therefore re-transfected the NF54/MAP-2 KO line using a plasmid targeting the *pfmap-1* locus for disruption, this time replacing the *pfmap-1* coding sequence with an expression cassette encoding the drug resistance marker human dihydrofolate reductase (hDHFR) (Fig. 1a). NF54/MAP-1_MAP-2 dKO parasites could be readily obtained and disruption of both *mapk* loci was confirmed by PCR on gDNA (Fig. 1a). To identify whether the absence of both *P. falciparum* MAPKs causes a defect in parasite growth, we performed parasite multiplication assays comparing NF54 WT and NF54/MAP-1_MAP-2 dKO parasites. As shown in Fig. 1b, parasite growth was not affected in the MAPK dKO parasites. Taken together, our data demonstrate that both *P. falciparum* MAPKs are dispensable for

asexual proliferation of blood stage *P. falciparum* parasites *in vitro* and that PfMAP-2 is not required to compensate for the loss of PfMAP-1 function.

MAPKs are not essential for sexual commitment and gametocytogenesis

PfMAP-1 was shown to be dispensable for gametocytogenesis *in vitro* as well as for gametogenesis and sporogony in the mosquito vector [36]. To investigate the effect of the absence of both MAPKs on gametocyte development, we induced sexual commitment in synchronous NF54/MAP-1_MAP-2 dKO parasite cultures at 18-24 hours post invasion (hpi) using serum-free medium (-SerM) as previously described [39]. Parasites cultured on -SerM supplemented with 2 mM choline chloride (a metabolite supressing sexual commitment) (-SerM/CC) served as control [39]. As a proxy for the sexual commitment rate, the percentage of parasites expressing the gametocyte-specific marker Pfs16 in the progeny was quantified by immunofluorescence assays (IFA) (Fig. 2a). Comparison of NF54 WT with the NF54/MAP-1_MAP-2 dKO parasite line did not reveal a significant difference in the sexual commitment rates under both commitment-inducing (-SerM) and control (-SerM/CC) conditions (Fig. 2a). Using Giemsa-stained thin blood smears, gametocyte development was monitored over 10 days and we could not identify any apparent morphological differences between WT and MAPK dKO gametocytes in all five stages (Fig. 2b). In summary, our results demonstrate the dispensability of both MAPKs in regulating *P. falciparum* sexual commitment and development *in vitro*.

PfMAP-2 is essential for male gametogenesis

In *P. berghei* parasites, PbMAP-2 was previously reported to be essential for male gametogenesis and further sexual development in the mosquito vector [27-29]. In light of this function in *P. berghei*, we investigated whether PfMAP-2 KO gametocytes also show a defect in male gametogenesis by assessing exflagellation rates (ERs). Gametogenesis was activated in mature stage V gametocytes using a drop in temperature (from 37°C to room temperature/22°C) and supplementation of the culture medium with XA [40].

Exflagellation centres formed by male gametes were observed and quantified using bright-field microscopy (Fig. 2c). Using total RBC and gametocytemia counts, the ER was calculated as the number of exflagellating parasites per total number of gametocytes. Our experiments revealed that compared to WT gametocytes (100% ±37.6), parasites devoid of the PfMAP-2 kinase displayed a dramatic decrease in the relative number of exflagellation centres formed (4.9% ±3.3) (p=0.0002; unpaired two-tailed Student's t test) (Fig. 2c). Despite this striking exflagellation defect, a minority of male PfMAP-2 KO gametocytes was still able to exflagellate. Similarly, this residual exflagellation capacity was also observed in *P. berghei* PbMAP-2 KO parasites [28,29]. It was speculated that these rare exflagellation events might be attributed to the action of PbMAP-1 partially compensating the loss of PbMAP-2 function [28,29]. To investigate this hypothesis, we performed exflagellation assays on both the PfMAP-1 KO and the MAPK dKO parasite lines. As previously reported, PfMAP-1 KO parasites showed no major exflagellation defect when compared to WT parasites (58% ±23) (mean of two biological replicate experiments) (Fig. 2c). Parasites lacking both *P. falciparum* MAPKs had a similarly pronounced exflagellation defect as the PfMAP-2 KO line and again a small proportion of male gametocytes was still able to exflagellate (3% ±1.6 compared to WT parasites) (p=0.0002; unpaired two-tailed Student's t test). Hence, the residual exflagellation observed in male PfMAP-2 KO gametocytes cannot be explained by partial functional compensation through PfMAP-1. Together, these results demonstrate that PfMAP-2, but not PfMAP-1, has an important role in male gametogenesis *in vitro*, in accord with previous findings in *P. berghei* PbMAP-2 KO parasites [27-29].

PfMAP-2 is specifically expressed in male gametocytes

Transcriptomic and proteomic data suggest that the MAP-2 kinase is specifically expressed in male gametocytes both in *P. berghei* and *P. falciparum* parasites [27,41-43]. However, *in vivo* expression of the protein in sexual stages has neither been assessed in *P. berghei* nor in *P. falciparum* and other studies proposed expression of PfMAP-2

also in asexual blood stage parasites [36,44]. To monitor PfMAP-2 kinase expression, we used a two-plasmid CRISPR/Cas9 gene editing approach [38] to generate a parasite line expressing PfMAP-2 C-terminally tagged with the fluorescent marker GFP fused to a FKBP destabilization domain (DD) that facilitates modulating protein expression levels using the small molecule ligand Shield-1 [45,46] (NF54/MAP-2GFPDD) (Supplementary Fig. 2). PCR on gDNA of the NF54/MAP-2GFPDD conditional knockdown (cKD) parasite line confirmed correct editing of the locus (Supplementary Fig. 2). This PfMAP-2 cKD parasite line allows for protein visualization under DD-stabilizing conditions (+Shield-1) by fluorescence microscopy and further provides the opportunity to investigate the effect of conditional PfMAP-2 depletion (-Shield-1) on parasite biology in comparison to the isogenic control population (+Shield-1). To determine the stage-specific expression of PfMAP-2GFPDD, we performed live cell fluorescence imaging and Western blot analysis on both asexual parasites and gametocytes under protein-stabilizing (+Shield-1) conditions. Western blot analysis revealed expression of PfMAP-2 in stage V gametocytes. In contrast, we did not observe PfMAP-2 expression in trophozoite and schizont stage parasites (Fig. 3a and Supplementary Figs. 2 and 5). Live cell fluorescence imaging of PfMAP-2GFPDD confirmed these findings (Fig. 3a and Supplementary Fig. 2).

To further specify the expression of PfMAP-2 during sexual stage development, we performed both Western blot analysis and live cell fluorescence imaging at all five stages of gametocytogenesis. Both techniques consistently showed peak expression of PfMAP-2 in stage IV and V gametocytes (Fig. 3b and Supplementary Fig. 5). Whereas a weak PfMAP-2GFPDD signal was detected in stage III gametocytes, the PfMAP-2 protein was not identified in gametocyte stages I and II (Fig. 3b). With regard to subcellular localization, the PfMAP-2 protein was detected in the parasite cytoplasm and nucleus in both stage IV and V gametocytes (Fig. 3b).

Interestingly, our live cell fluorescence imaging experiments detected expression of PfMAP-2 only in a subset (approx. 50%) of stage IV and V gametocytes. Since previous

studies indicated that PfMAP-2 is specifically expressed in male gametocytes [27,41-43], we investigated whether the PfMAP-2GFPDD-positive parasites indeed represented male gametocytes. To this end, we performed IFAs using antibodies against GFP and the female gametocyte-specific protein PfG377 [47]. Notably, all gametocytes positively labelled for PfMAP-2GFPDD expression were identified as PfG377-negative and similarly PfG377-positive gametocytes were found to be GFP-negative (Fig. 3c, Supplementary Fig. 2). Quantification of the GFP- and the PfG377-positive cells in biological triplicates revealed a 1:1 ratio of male/female gametocytes (male: 49.7% ±4.2; female: 50.3% ±4.2).

Together, our data demonstrate that the PfMAP-2 kinase is predominantly expressed in late stage (IV and V) gametocytes but not, or only at low levels, in asexual stages and early stage gametocytes. In addition, we confirm at the single cell level that PfMAP-2 is indeed expressed in a male gametocyte-specific manner.

PfMAP-2 is not essential for male gametocytogenesis

Next, we tested the functionality and efficiency of the conditional expression system by comparing NF54/MAP-2GFPDD parasites cultured under protein-stabilizing (+Shield-1) and protein-degrading (-Shield-1) conditions. For this purpose, stage V gametocytes constantly cultured on Shield-1 were split and Shield-1 was removed from one of the paired cultures. 24 hours later, we detected the expression of the PfMAP-2GFPDD protein by live cell fluorescence imaging and Western blot analysis. Efficient degradation of PfMAP-2GFPDD was observed in stage V gametocytes cultured in absence of Shield-1 (-Shield-1) compared to the control population (+Shield-1) using both techniques (Fig. 4a and Supplementary Fig. 6). To confirm the essential role for PfMAP-2 in male gametogenesis, we performed exflagellation assays comparing stage V gametocytes constantly cultured on Shield-1 (+Shield-1) with the paired population from which Shield-1 was removed 24 hours earlier (-Shield-1) (i.e. one day before exflagellation; -1DBE). We identified a dramatic exflagellation defect in -1DBE gametocytes (6.8% ±3.2),

compared to gametocytes cultured in presence of Shield-1 (100% ±33.9) (p=0.0008; unpaired two-tailed Student's t test) (Fig. 4b). The low exflagellation rate found in -1DBE gametocytes is comparable to that observation for PfMAP-2 KO parasites (4.9% ±3.3) (Fig. 2c). Since removal of Shield-1 for only 24 hours causes a dramatic exflagellation defect, we assume that this phenotype is linked to a direct requirement for PfMAP-2 during gametogenesis rather than a prior cryptic role for PfMAP-2 during gametocytogenesis that cannot be detected by microscopic observations (Fig. 2b). To further confirm this hypothesis, we triggered PfMAP-2GFPDD depletion in asexual ring stage parasites before induction of sexual commitment and constantly cultured the resulting gametocytes in absence of Shield-1 (-Shield-1) until mature stage V gametocytes were observed. One day (24 hours) before performing exflagellation assays, we split these PfMAP-2GFPDD-depleted stage V gametocyte cultures and rescued PfMAP-2GFPDD expression in one of the paired populations by addition of Shield-1 (+Shield-1 1DBE). Indeed, stage V gametocytes allowed to re-express PfMAP-2GFPDD for 24 hours (+Shield-1 1DBE) showed a significantly increased exflagellation rate (20.8% ±6.9) compared to gametocytes cultured constantly in absence of Shield-1 (-Shield-1) (1% ±1.2) (p=0.04, unpaired two-tailed Student's t test) (Fig. 4b). However, the +Shield-1 1DBE gametocytes only reached about 20% of the exflagellation rate observed for gametocytes constantly cultured in presence of Shield-1 (+Shield-1) (100% ±32.1) (Fig. 4b). Interestingly, when PfMAP-2GFPDD-depleted stage V gametocytes were allowed to re-express PfMAP-2 for 48 hours prior to performing exflagellation assays (+Shield-1 2DBE), exflagellation rates reached values similar to those determined in control gametocytes (+Shield-1) (92.6% ±20) (Fig. 4b).

Hence, by analysing the PfMAP-2GFPDD cKD mutant we could confirm the essential role of PfMAP-2 in male gametogenesis, since conditional depletion of PfMAP-2 yielded an exflagellation defect comparable to the one observed in PfMAP-2 KO parasites. In addition, our results suggest that the requirement for PfMAP-2 function for successful exflagellation of male gametocytes is based on the action of this kinase during

gametogenesis rather than any prior preparatory processes during male gametocytogenesis.

PfMAP-2 is required to initiate axoneme beating

The defect in exflagellation observed in the absence of PfMAP-2 confirmed the essential function of PbMAP-2 during male gametogenesis in *P. berghei*. We therefore carried out a more detailed phenotypic analysis of the PfMAP-2GFPDD cKD line by removing Shield-1 in stage V gametocytes 24 hours prior to phenotyping assays.

Mature *P. falciparum* gametocytes are crescent-shaped but rapidly become spherical upon stimulation by XA, a process known as “rounding up” [48]. Microscopic observation and quantification of activated gametocytes demonstrated that PfMAP-2GFPDD gametocytes cultured in presence (+Shield-1, 99.7%±0.6) and absence (-Shield-1, 98%±1) of Shield-1 showed no difference in rounding up when activated with XA-containing medium (values represent the means ±SD of three biological replicates, 100 cells were counted per experiment, paired two-tailed Student’s t test).

We then asked whether PfMAP-2 is required to replicate the genome of microgametocytes three times. To do so, cells were stained with the Vybrant DyeCycle Violet DNA dye and fluorescence intensity of non-activated gametocytes and gametocytes activated for 10 min was determined by flow cytometry. Note that due to residual GFP-fluorescence detectable by flow cytometry in gametocytes cultured in absence of Shield-1, those microgametocytes depleted for PfMAP-2GFPDD expression could still be quantified based on fluorescence by gating of GFP-positive cells (Supplementary Fig. 3). No difference in DNA content was detected between microgametocytes cultured in presence and absence of Shield-1, indicating that PfMAP-2 is not required for genome replication in male gametocytes (Fig. 5a and Supplementary Fig. 3). Immunofluorescence labelling with an α-tubulin antibody indicated that axoneme formation is also not affected in PfMAP-2GFPDD-depleted male gametocytes 15 min post-activation (Fig. 5b and 5c). However, in PfMAP-2GFPDD-depleted cells the

axonemes remained bundled around the nucleus, nuclear DNA is not incorporated into the forming microgametes and no exflagellation is observed (Fig. 5c, Supplementary Fig. 3). In contrast, male gametocytes cultured in the presence of Shield-1 began to release motile microgametes into which DNA was incorporated (Fig. 5c, Supplementary Fig. 3).

PfMAP-2 depletion does not affect gene transcription in stage V gametocyte bulk populations

Our results demonstrate the dispensability of PfMAP-2 in male gametocytogenesis but its strict requirement for male gametogenesis. MAPKs were previously shown to indirectly or directly regulate gene expression in other eukaryotes [34,49]. Using a comparative transcriptome analysis, we tested whether PfMAP-2 depletion has an effect on gene expression in mature stage V gametocytes prior to or 10 min after activation using XA. Using the same approach, we also asked if gene expression differs between non-activated gametocytes and gametocytes 10 min post-XA treatment. Note that a previous study reported up to two-fold differential expression of several genes between non-activated gametocytes and gametes 30 min after activation by XA using quantitative real time PCR [50]. To our knowledge, however, potential transcriptional changes occurring during the first 10 min of the exflagellation process have not yet been assessed. To this end, we split NF54/MAP-2GFPDD stage V gametocytes and removed Shield-1 from one of the two paired populations. 24 hours later each of the paired +Shield-1/-Shield-1 populations (stage V ON and stage V OFF) was split again and one half each was triggered for gamete activation by incubation in XA-containing medium for 10 min (stage V act. ON and stage V act. OFF) (Supplementary Fig. 4). Total RNA was then harvested from these four populations in two biological replicate experiments and relative gene expression values were quantified by two-colour microarray analysis [51,52] (Supplementary Dataset 1). As shown in Supplementary Fig. 4, all eight transcriptomes showed almost perfect correlation in pairwise comparisons of their relative mRNA abundances (Perason's $r > 0.98$). Furthermore, by comparison to a published reference

dataset of gametocyte-specific transcripts [53] we show that the transcriptomes determined here display a typical gametocyte-specific gene expression profile (Supplementary Fig. 4). To identify genes potentially regulated in a PfMAP-2-dependent manner, we compared the mean relative gene expression values calculated from the four control samples (+Shield-1; stage V ON and stage V act. ON; two biological replicates each) with those calculated from the four PfMAP-2-depleted samples (-Shield-1; stage V OFF and stage V act. OFF; two biological replicates each). This analysis failed to reveal any genes displaying significant differential expression (mean fold change > 2; $p<0.01$) in PfMAP-2-depleted gametocytes (-Shield-1) versus control gametocytes (+Shield-1) (Supplementary Fig. 4). Similarly, after stratifying the data according to non-activated (pre-XA treatment) and activated (post-XA treatment) gametocytes we didn't identify a single gene consistently up- or down-regulated > 2-fold in both biological replicates when comparing PfMAP-2-depleted gametocytes (-Shield-1) to control gametocytes (+Shield-1) in either of the two conditions (Supplementary Dataset 1). We therefore conclude that (i) PfMAP-2 likely plays no major role in regulating gene expression during exflagellation but rather in phosphorylating crucial cell cycle regulators; and (ii) the process of exflagellation likely occurs in absence of any major changes in gene expression.

Discussion

The complex life cycle of *P. falciparum* includes the asexual proliferation of parasites inside RBCs and the generation of gametocytes necessary for onward parasite transmission. Our study aimed at identifying the function of MAPKs in *P. falciparum* asexual blood stage parasites and sexual development. Using CRISPR/Cas9-based gene editing, we generated PfMAP-2 KO, PfMAP-1 KO and PfMAP-1_MAP-2 dKO parasite lines as well as a PfMAP-2 cKD cell line allowing for conditional PfMAP-2 depletion.

The *Plasmodium* MAPKs cluster with the extracellular signal-regulated kinases 1 and 2 (ERK1/ERK2) family of MAPKs, which integrate extracellular signals into cellular

responses and thus have essential functions in cell proliferation and differentiation in model eukaryotes [35,54]. Hence, it is rather surprising that both *P. falciparum* MAPKs are dispensable for asexual parasite survival. However, in many aspects the *Plasmodium* kinome, including MAPK signalling, seems to diverge from that of other eukaryotes [54]. For instance, the kinome of *Plasmodium* lacks the STE group of eukaryotic protein kinases that includes the classical MAPK-activating kinases MAPKK or MEK [55]. Furthermore, whereas PfMAP-1 contains the classical TXY activation site found in eukaryotic MAPKs, PfMAP-2 lacks this motif and instead contains an atypical TSH activation motif essential for its function [30,56]. Interestingly, the NIMA-related kinase PfNEK-1 might represent an atypical functional homologue of MAPKK/MEK. PfNEK-1 phosphorylates PfMAP-2 *in vitro* and is expressed in a male gametocyte-specific manner in sexual parasite stages [57,58]. Although there is a clear divergence of MAPKs between *Plasmodium* spp. and model organisms, PfMAP-2 as well as its rodent orthologue PbMAP-2 directly or indirectly react to environmental stimuli (e.g. XA, drop in temperature), a feature they share with other eukaryotic members of the ERK1/ERK2 kinase family.

The two MAPKs studied here show peak expression in gametocytes [27,30,33,41,59], and in the *P. berghei* model parasite it was previously shown that both MAPKs are dispensable for asexual parasite proliferation in mice [37]. In addition, PbMAP-2 was found to be essential for male gametogenesis and further parasite development in the mosquito [27-29].

Unlike previously suggested [36], and similar to the situation in *P. berghei*, our results demonstrate that PfMAP-2 is fully dispensable for asexual proliferation of *P. falciparum* parasites. The previous unsuccessful attempt to obtain a PfMAP-2 KO line in 3D7 parasites, a clone of the NF54 strain used here, was based on a single crossover recombination approach that didn't allow for direct selection of PfMAP-2 KO mutants [36]. We therefore believe that our success in creating PfMAP-2 KO parasites was facilitated by the highly efficient CRISPR/Cas9 system and possibility for direct selection of KO

mutants. In addition, *P. falciparum* parasites lacking expression of both MAPKs show no obvious defects in asexual proliferation, sexual commitment and gametocytogenesis, thus revealing the dispensability of both *P. falciparum* MAPKs in these life cycle stages and developmental processes. We can further conclude that the dispensability of PfMAP-1 is not based on upregulation and functional compensation by PfMAP-2 (or *vice versa*). However, PfMAP-2-depleted parasites show a dramatic reduction in exflagellation similar to what has been observed in *P. berghei* parasites [27-29]. Also, we observed specific expression of PfMAP-2 in late stage male gametocytes, which is in line with previously published proteomics and transcriptomics data [27,41-43]. Moreover, we detected PfMAP-2-GFPDD expression only in late stage gametocytes but not in earlier gametocyte stages and asexual parasites. While Dorin and colleagues also observed PfMAP-2 expression specifically in gametocytes [30], two other studies detected PfMAP-2 expression in asexual parasites albeit without providing a comparison with gametocyte samples [36,44]. Since we analysed PfMAP-2 expression in a cKD line, where the expression levels of PfMAP-2GFPDD may be lower compared to PfMAP-2 in WT parasites, we might have missed to detect low level PfMAP-2 expression in asexual blood stages, early gametocyte stages and/or female gametocytes. However, our results clearly demonstrate that PfMAP-2 expression is substantially higher and peaks in stage IV and V gametocytes. Our data further show that PfMAP-2 is not essential for gametocytogenesis, especially as in the PfMAP-2-depleted gametocytes protein re-stabilization as late as in mature stage V gametocytes was sufficient to rescue the exflagellation-negative phenotype. Whether PfMAP-2 has important functions in male gametocytes prior to gametogenesis and exflagellation *in vivo* remains unknown. We also further scrutinized the exflagellation defect and show that upon activation of gametocytes using XA and other stimuli, PfMAP-2-depleted male gametocytes replicate DNA normally, generate octoploid cells and form axonemes. However, upon depletion of PfMAP-2 the replicated nuclear DNA fails to be incorporated into newly forming gametes and microgametocytes do not exflagellate. We therefore conclude that, in

accord with the observations on PbMAP-2 function in *P. berghei* parasites, PfMAP-2 is essential for the initiation and/or the process of genome condensation, axoneme beating and cytokinesis. How exactly PfMAP-2 and its putative substrates are involved in these processes needs to be determined in future experiments.

Furthermore, we could show that there is no additive exflagellation defect when both MAPKs are depleted. PfMAP-1_MAP-2 dKO parasites still showed some residual exflagellation comparable to what was observed in PfMAP-2 KO parasites. Hence, during male gametogenesis, PfMAP-1 does not seem to functionally compensate for the loss of PfMAP-2 expression, suggesting clearly distinct functions of the two parasite MAPKs. Hence, the residual exflagellation rates we observed here in *P. falciparum* and others have reported in *P. berghei* PbMAP-2 KO parasites [28,29] might be explained through partial compensation by a kinase distinct from MAP-1. This putative kinase could either have a substrate specificity overlapping with that of MAP-2 or stochastically phosphorylate substrates essential for the termination of male gametogenesis and exflagellation.

MAPKs phosphorylate a variety of substrates in eukaryotes including the MAPK-activated protein kinases. Amongst other functions, those kinases are involved in gene expression, mRNA stability as well as cell differentiation [49]. Furthermore, in mammals MAPK were shown to directly control gene expression for instance by phosphorylation of transcription factors [34]. In order to identify potential PfMAP-2-dependent regulation of gene expression in male stage V gametocytes as well as gametogenesis, we performed microarray experiments comparing PfMAP-2-stabilizing and -degrading (±Shield-1) as well as gametogenesis activating and non-activating (±XA) conditions. However, we could not identify any transcriptional changes that could be attributed to the function of PfMAP-2 in these stages. We therefore conclude that the role of PfMAP-2 in male gametogenesis is rather based on phosphorylating and changing the activity of target substrates involved in the process of gametogenesis rather than regulating gene expression. In the future, whole cell phosphoproteomics on activated and non-activated

stage V gametocytes will hopefully reveal PfMAP-2 substrates and thus provide further details on the molecular processes acting in male gametogenesis.

In summary, we have shown that both *P. falciparum* MAPKs, PfMAP-1 and PfMAP-2, are dispensable for the asexual proliferation of blood stage parasites and for gametocytogenesis. While PfMAP-1 also plays no obvious role in male gametogenesis, PfMAP-2 is specifically expressed in male gametocytes and essential for the crucial process of gametogenesis and exflagellation. Using mosquito feeding assays, the real impact of the exflagellation defect observed in PfMAP-2-depleted parasites in reducing gametocyte transmission could be determined. Such assays would also help clarifying whether the residual exflagellation observed for a small number of PfMAP-2-depleted microgametocytes produces functional microgametes. Furthermore, future work on the transmission potential of PfMAP-1 KO, PfMAP-2 KO and PfMAP-1_MAP-2 dKO parasites might reveal additional functions for the two MAPKs in sexual development and sporogony in the mosquito vector as well as in sporozoites and intra-hepatic schizogony. In *P. berghei*, both MAPKs were shown to be expressed in liver stages suggesting a potential role for MAPK signalling during hepatocyte infection [60]. Obtaining a better understanding of kinase signalling in various parasite stages during the life cycle will broaden our understanding of signalling pathways in these important pathogens and the evolution of kinases in eukaryotes in general. Finally, detailed insight into the function of kinases regulating essential parasite processes may uncover new targets for drug-based malaria interventions that are urgently needed.

Materials and Methods

Parasite culture

Culturing of *P. falciparum* parasites and synchronization of asexual growth were performed as previously described [61,62]. NF54 asexual parasites were cultured in AB+ or B+ human RBC (Blood Donation Center, Zurich, Switzerland) in RPMI-1640 (10.44 g/liter), 25 mM HEPES, 100 µM hypoxanthine medium, 24 mM sodium bicarbonate and

0.5% Albumax II (Gibco). 2 mM choline chloride (CC) was added to the culture medium to prevent unwanted induction of sexual commitment [39]. Cultures were kept at 37°C and gassed with a mixture of 4% CO_2, 3% O_2 and 93% N_2.

Transfection constructs

Transgenic parasite lines were generated using the CRISPR/Cas9-based genome editing system. The NF54/MAP-2 KO, NF54/MAP-1 KO and the NF54/MAP-1_MAP-2 dKO cell lines were created using a single plasmid approach. The p_gC plasmid [38] used for this purpose encodes the Cas9 enzyme and the U6 single gRNA (sgRNA) expression cassette, and the donor sequences for DNA double strand break repair. The PfMAP-1 and PfMAP-2-specific p_gC plasmids (p_gC_*map-1-ko-bsd* and p_gC_*map-2-ko-bsd*) were generated by performing a Gibson assembly reaction using four fragments (1) the *BamHI*- and *EcoRI*-digested p_gC plasmid [38], (2,3) the *pfmap-1*- or *pfmap-2*-specific 5' and 3' homology regions (HRs) amplified from NF54 WT gDNA (primers HR1_M1_F, HR1_M1_R and HR2_M1_F, HR2_M1_R were used to amplify the *pfmap-1*-specific HRs, whereas primers HR1_M2_F, HR1_M2_R and HR2_M2_F, HR2_M2_R were used to amplify the *pfmap-2*-specific HRs) and (4) a resistance cassette (blasticidin S deaminase, BSD), conferring resistance to blasticidin-S-hydrochloride, flanked by the two HRs. The BSD resistance cassette was amplified from pBcam [63] using primers M1_BSD_F, M1_BSD_R and M2_BSD_F, M2_BSD_R, respectively. These assembled plasmids were subsequently digested with *BsaI* to allow for T4 DNA ligase-dependent insertion of gene-specific sgRNA sequence elements. To generate PfMAP-1 and PfMAP-2 sequence-specific sgRNA elements, complementary oligonucleotides (sgRNA_M1KO_F, sgRNA_M1KO_R and sgRNA_M2KO_F, sgRNA_M2KO_R) were annealed. The resulting double-stranded oligonucleotides carried single-stranded overhangs complementary to the *BsaI*-digested plasmids.

The p_gC_*map-1-ko-hdhfr* plasmid was used to generate the NF54/MAP-1_MAP-2 KO parasite line by transfecting NF54/MAP-2 KO parasites a second time. This plasmid was

generated by assembling three Gibson fragments: (1) The *XbaI*- and *BamHI*-digested p_gC_*map-1-ko-bsd* plasmid retaining the 3' HR, (2) the *pfmap-1*-specific 5' HR amplified from NF54 WT gDNA using primers HR1_M1_F and HR1_M1hDHFR_R, and (3) the human dihydrofolate reductase (hDHFR) resistance cassette amplified from pH-gC [38] using primers hDHFR_F and hDHFR_R.

The NF54/MAP-2GFPDD parasite line was generated using a CRISPR/Cas9-based two-plasmid approach as previously described [38]. The pFdon_*map-2gfpdd* donor plasmid was produced by assembling four fragments in a Gibson reaction using (1) the *HindIII*- and *BamHI*-digested pFdon plasmid [38], (2,3) the 5' and 3' HRs amplified from NF54 WT gDNA using primers HR1_M2KD_F, HR1_M2KD_R and HR2_M2KD_F, HR2_M2KD_R, respectively, and (4) the *gfpdd* sequence amplified from plasmid pHcamGDV1-GFP-DD [38] using primers GFP_F and GFP_R. The corresponding suicide plasmid pHF_gC_*map-2gfpdd* was generated by annealing the complementary oligonucleotides sgRNA_M2KD_F and sgRNA_M2KD_R and subsequently inserting the resulting double-stranded fragment into the *BsaI*-digested pHF_gC plasmid [38] by ligation using T4 DNA ligase. Vector maps and gene editing schemes are provided in Fig. 1 and in Supplementary Figs. 1 and 2. Oligonucleotide sequences used for cloning are provided in the Supplementary Table 1.

Transfection and transgenic cell lines

Transfection of *P. falciparum* parasites with CRISPR/Cas9-based constructs was performed as described previously [38]. NF54 WT parasites were transfected with a total of 100 µg of plasmid DNA (100 µg of p_gC-derived constructs and 50 µg each of pHF_*map-2gfpdd* and pFdon-*map-2gfpdd*). 24 hours after transfection, transfected cultures were treated with 2.5 µg/mL blasticidin-S-hydrochloride (for 10 subsequent days) or 4 nM WR99210 (for six subsequent days) according to the resistance cassette transfected (BSD and hDHFR, respectively). After transfection, NF54/MAP-2GFPDD parasites were constantly cultured on 625 nM Shield-1 (+Shield-1) to stabilize the

PfMAP-2GFPDD protein. Stably growing parasite populations were readily obtained 11-21 days post transfection and correct gene editing was confirmed by PCR on gDNA. PCR results are shown in Fig. 1 and in Supplementary Figs. 1 and 2. Primers used to check for correct gene editing are listed in Supplementary Table 2.

Flow cytometry growth assay

To quantify multiplication of NF54/MAP-1_MAP-2 KO and NF54 WT parasites, flow cytometry measurements of fluorescence intensity were performed. For this purpose, synchronous ring stage (18-24 hpi) parasites were stained using SYBR Green DNA stain (Invitrogen, 1:10,000) for 30 min at 37°C. Parasites were subsequently washed twice in pre-warmed PBS and measured using the MACS Quant Analyzer 10. Per sample 200,000 cells (unifected RBCs+iRBCs) were analysed. The measurement was repeated at 18-24 hpi in the two subsequent generations. Flow cytometry data were analysed using FlowJo_v10.6.1 and parasitemia was determined by gating of SYBR-positive parasites and determining their proportion among all RBCs.

Fluorescence microscopy

In order to determine the expression, localisation and depletion of PfMAP-2GFPDD in asexual and sexual parasite stages of the NF54/MAP-2GFPDD parasite line, live cell fluorescence imaging and IFAs were performed as previously described with some minor adaptations [64]. Live cell fluorescence imaging was used to follow PfMAP-2GFPDD expression during gametocytogenesis (stage I-V) and in asexual stages. Nuclei were stained using Hoechst (Merck) at a final concentration of 5 µg/ml and Vectashield (Vector Laboratories) was used as mounting medium.

For IFAs, thin blood smears were fixed in ice-cold methanol or ice-cold methanol/acetone (60:40) for 2 min. To determine the sexual commitment rate of NF54 WT and NF54/MAP-1_MAP-2 dKO parasites, methanol-fixed slides were probed with the primary antibody mouse IgG1 mAb α-Pfs16 (1:100) (kind gift from Robert W. Sauerwein), and the secondary antibody Alexa Fluor 488-conjugated α-mouse (1:250) (Invitrogen #A-11001).

To determine the sex-specific expression of PfMAP-2GFPDD and to quantify the male/female ratio, methanol/acetone-fixed cells were probed with primary antibody mAb α-GFP (1:100) (Roche Diagnostics #11814460001), and the rabbit-α-PfG377 serum (1:1,000) (kind gift from Pietro Alano) [47], and secondary antibodies Alexa Fluor 488-conjugated α-mouse and 564-conjugated α-rabbit IgG (both 1:250) (Invitrogen #A-11001 and A-11011), respectively. Staining of DNA and mounting of IFA slides was performed using Vectashield with DAPI (Vector Laboratories).

All live cell fluorescence imaging and imaging of methanol and methanol/acetone IFA slides was performed using a Leica DM5000 B fluorescence microscope (20x, 40x and 63x objectives) and images were taken using a Leica DFC345 FX camera and the Leica application suite (LAS) software.

IFAs to stain α-tubulin were performed as described [18]. Briefly, RBCs were fixed with 4% paraformaldehyde/0.05% glutaraldehyde in PBS for one hour followed by permeabilisation with 0.1% Triton X-100/PBS for 10 min and blocking with 2% BSA/PBS for two hours. Permeabilised iRBCs were probed with primary mouse anti-α-tubulin (1:1,000) (clone DM1A, Sigma-Aldrich #T9026) and secondary anti-mouse Alexa-488 (1:1,000) (Thermo Fisher Scientific #A28175) antibodies. Nuclei were stained with DAPI (Life Technologies) during incubation with the secondary antibody. Images were acquired with an Axiocam Fluo microscope (Zeiss).

Western blot

Parasites were obtained by lysis of the RBC membrane using 0.15% saponin/PBS and incubation on ice for 10 min. The obtained parasite pellet was washed 2-3 times in ice-cold PBS. The whole cell protein extract was generated by lysing the parasite pellet in an equal volume of UREA/SDS buffer (8 M Urea, 5% SDS, 50 mM Bis-Tris, 2 mM EDTA, 25 mM HCl, pH 6.5) supplemented with 1 mM DTT and 1x protease inhibitor cocktail (Merck). For each sample, protein lysate derived from equal parasite numbers were separated on a 3-8% NuPage Tris-Acetate gel using NuPage MES buffer (Novex,

Qiagen). The membrane was blocked in 5% milk powder dissolved in 1xPBS/0.1% Tween (PBS-Tween) for 30 min. Proteins were detected using the primary antibodies mouse mAb α-GFP (1:1,000) (Roche Diagnostics #11814460001), or the mouse mAb α-PfGAPDH (1:20,000) [65], diluted in blocking buffer. The membrane was incubated at 4°C over night and subsequently washed 3-4 times using PBS-Tween. The secondary antibody α-mouse IgG (H&L)-HRP (GE healthcare #NXA931) was diluted 1:10,000 in blocking buffer and the membrane was incubated for 1-2 hours and subsequently washed again 3-4 times using PBS-Tween.

Induction of sexual commitment and gametocytogenesis

Sexual commitment was induced in synchronized *P. falciparum* parasites (1-1.5% parasitemia) at 18-24 hpi using -SerM medium as described [39]. The -SerM medium was produced by complementing the described RPMI/HEPES culture medium with 24 mM sodium bicarbonate, 0.39% fatty acid-free BSA (Sigma #A6003) and 30 µM each of the two essential fatty acids oleic and palmitic acid (Sigma #O1008 and #P0500, respectively). Parasites cultured on -SerM medium containing 2 mM choline chloride (-SerM/CC), which blocks sexual commitment, were used as a negative control [39].

To quantify sexual commitment rates, Pfs16 positivity counts were determined for parasites induced for sexual commitment and their matching controls (Fig. 2a). For this purpose, -SerM and -SerM/CC media were removed 30 hours after induction (0-6 hpi; generation 2) and replaced with culture medium containing 10% human serum (Blood Donation Centre, Basel, Switzerland) instead of 0.5% Albumax II (+SerM). Parasites were cultured for another 42 hours before thin blood smears were generated at 42-48 hpi and fixed in ice-cold methanol for subsequent α-Pfs16 IFAs. To follow gametocytogenesis, parasites induced for sexual commitment (-SerM medium) were analysed by inspection of Giemsa-stained blood smears, fluorescence live cell imaging and Western blots. -SerM was replaced with +SerM medium 30 hours after induction (0-6 hpi, generation 2). Another 24 hours later (24-30 hpi; trophozoites and stage I

gametocytes), parasites were cultured on +SerM medium supplemented with 50 mM N-acetylglucosamine (+SerM/GlcNAc) for seven consecutive days to eliminate asexual parasites [66]. Thereafter, gametocytes were cultured using +SerM medium lacking GlcNAc on a heating plate (37°C) to prevent gametocyte activation.

Exflagellation assays

Exflagellation assays were performed on day 13 or 14 of gametocytogenesis using mature stage V gametocytes as described [40]. Briefly, gametocyte cultures were pelleted at 400 g for 3 min and the RBC pellet was resuspended in activation medium (+SerM medium, 100 µM XA) at room temperature/22°C. After 15 min, the number of exflagellation centres and RBCs per mL of culture were quantified in a Neubauer chamber using bright-field microscopy (40x objective). Gametocytemia was determined on Giemsa-stained blood smears.

Flow cytometry analysis of gametocyte DNA content

The DNA content of NF54/MAP-2GFPDD microgametocytes was determined by flow cytometry measurements of fluorescence intensity as described previously [18]. In brief, gametocytes were stained with Vybrant DyeCycle Violet DNA (Thermo Fisher Scientific #V35003) and resuspended in 100 µl of suspended animation medium (RPMI1640 medium containing 25 mM HEPES, 5% fetal calf serum (FCS), 4 mM sodium bicarbonate, pH 7.2). Gamete activation was induced by addition of 100 µl modified exflagellation medium (RPMI 1640 containing 25 mM HEPES, 4 mM sodium bicarbonate, 5% FCS, 200 µM XA, pH 7.8). To rapidly block gametogenesis, 800 µl ice-cold PBS was added at 0 min and 10 min after adding exflagellation medium. Cells were then stained for 30 min at 4ºC with Vybrant DyeCycle Violet DNA (Thermo Fisher Scientific #V35003) and detected using a Beckman Coulter Gallios 4 flow cytometer. Microgametocytes were selected on fluorescence by gating of GFP-positive cells (both ±Shield-1-cultured microgametocytes detectable) (Supplementary Fig. 3). Ploidy was

expressed as a percentage of GFP-positive cells and 5,000 cells were analysed per sample.

Microarray experiments and data analysis

NF54/MAP-2GFPDD stage V gametocytes cultured in presence of Shield-1 were split on day 12 of gametocytogenesis and Shield-1 was removed from one of the paired populations, resulting in samples “stage V ON” and “stage V OFF”. 24 hours later (day 13), the paired populations were split again and in one half each gametogenesis was activated by incubation with XA-containing activation medium for 10 min. These samples are termed “stage V act. ON” and “stage V act. OFF”. All cultures (30 mL, 5% haematocrit, approx. 2% gametocytemia) were subsequently spun for 5 min at 2,000 g and the resulting RBC pellet was resuspended in 9 mL Trizol pre-warmed to 37°C. RNA extraction and cDNA synthesis were performed as described previously [51]. Cy5-labelled sample cDNAs were hybridised against a Cy3-labelled cDNA reference pool prepared from 3D7 WT parasites [67]. Equal amounts of Cy5- and Cy3-labelled cDNA were hybridised for 16 hours at 65°C in an Agilent hybridisation oven (G2545A) on a *P. falciparum* 8×15K Agilent gene expression microarray (GEO platform ID GPL28317), a slightly modified version of the microarray previously published by the Llinas laboratory (GEO platform ID GPL15130) [52] (one probe removed, 19 probes added) (Supplementary Spreadsheet 1). Slides were scanned using the GenePix scanner 4000B and GenePix pro 6.0 software (Molecular Devices). Microarray data have been deposited in the NCBI Gene Expression Omnibus [68] and are accessible through GEO Series accession no. GSE147643. The raw microarray data representing relative transcript abundance ratios between each sample and the reference pool (Cy5/Cy3 log2 ratios) were subjected to lowess normalization and background filtering as implemented by the Acuity 4.0 program (Molecular Devices). Flagged features and features with either Cy3 or Cy5 intensities lower than two-fold the background were discarded. Log2 ratios for multiple probes per gene were averaged. Transcripts showing expression values in at least seven of the

eight samples were included for downstream analysis to identify genes differentially expressed between control (+Shield-1) and PfMAP-2-depleted (-Shield-1) gametocytes. The heat map shown in Supplementary Fig. 4 was generated using Java Treeview [69]. The Volcano plot shown in Supplementary Fig. 4 was generated using Microsoft Excel. The processed microarray dataset is listed in Supplementary Dataset 1.

Data availability

The accession number for the microarray data reported in this paper is GEO: GSE147643. Additional data that support the findings of this study are available in Supplementary Dataset 1.

References

1 Inselburg, J. Gametocyte formation by the progeny of single Plasmodium falciparum schizonts. *J. Parasitol* **69**, 584-591 (1983).

2 Bruce, M. C., Alano, P., Duthie, S. & Carter, R. Commitment of the malaria parasite Plasmodium falciparum to sexual and asexual development. *Parasitology* **100 Pt 2**, 191-200 (1990).

3 Bancells, C. *et al.* Revisiting the initial steps of sexual development in the malaria parasite Plasmodium falciparum. *Nat Microbiol* **4**, 144-154, doi:10.1038/s41564-018-0291-7 (2019).

4 van Biljon, R. *et al.* Hierarchical transcriptional control regulates Plasmodium falciparum sexual differentiation. *BMC Genomics* **20**, 920, doi:10.1186/s12864-019-6322-9 (2019).

5 Smalley, M. E., Brown, J. & Bassett, N. M. The rate of production of Plasmodium falciparum gametocytes during natural infections. *Trans. R. Soc. Trop. Med. Hyg* **75**, 318-319 (1981).

6 Joice, R. *et al.* Plasmodium falciparum transmission stages accumulate in the human bone marrow. *Sci. Transl. Med* **6**, 244re245, doi:6/244/244re5 [pii];10.1126/scitranslmed.3008882 [doi] (2014).

7 Aguilar, R. *et al.* Molecular evidence for the localization of Plasmodium falciparum immature gametocytes in bone marrow. *Blood* **123**, 959-966, doi:blood-2013-08-520767 [pii];10.1182/blood-2013-08-520767 [doi] (2014).

8 Farfour, E., Charlotte, F., Settegrana, C., Miyara, M. & Buffet, P. The extravascular compartment of the bone marrow: a niche for Plasmodium falciparum gametocyte maturation? *Malar. J* **11**, 285, doi:1475-2875-11-285 [pii];10.1186/1475-2875-11-285 [doi] (2012).

9 De Niz, M. *et al.* Plasmodium gametocytes display homing and vascular transmigration in the host bone marrow. *Sci Adv* **4**, eaat3775, doi:10.1126/sciadv.aat3775 (2018).

10 Tiburcio, M. *et al.* A switch in infected erythrocyte deformability at the maturation and blood circulation of Plasmodium falciparum transmission stages. *Blood* **119**, e172-e180, doi:blood-2012-03-414557 [pii];10.1182/blood-2012-03-414557 [doi] (2012).

11 Billker, O., Shaw, M. K., Margos, G. & Sinden, R. E. The roles of temperature, pH and mosquito factors as triggers of male and female gametogenesis of Plasmodium berghei in vitro. *Parasitology* **115 (Pt 1)**, 1-7 (1997).

12 Garcia, G. E., Wirtz, R. A., Barr, J. R., Woolfitt, A. & Rosenberg, R. Xanthurenic Acid Induces Gametogenesis in Plasmodium, the Malaria Parasite. **273**, 12003-12005, doi:10.1074/jbc.273.20.12003 (1998).

13 Nijhout, M. M. Plasmodium gallinaceum: exflagellation stimulated by a mosquito factor. *Exp Parasitol* **48**, 75-80, doi:10.1016/0014-4894(79)90056-0 (1979).

14 Nijhout, M. M. & Carter, R. Gamete development in malaria parasites: bicarbonate-dependent stimulation by pH in vitro. *Parasitology* **76**, 39-53, doi:10.1017/s0031182000047375 (1978).

15 Yamamoto, D. S., Sumitani, M., Hatakeyama, M. & Matsuoka, H. Malaria infectivity of xanthurenic acid-deficient anopheline mosquitoes produced by TALEN-mediated targeted mutagenesis. *Transgenic research* **27**, 51-60, doi:10.1007/s11248-018-0057-2 (2018).

16 Billker, O. *et al.* Calcium and a calcium-dependent protein kinase regulate gamete formation and mosquito transmission in a malaria parasite. *Cell* **117**, 503-514, doi:S0092867404004490 [pii] (2004).

17 Kuehn, A. & Pradel, G. The coming-out of malaria gametocytes. *J Biomed Biotechnol* **2010**, 976827, doi:10.1155/2010/976827 (2010).

18 Fang, H. *et al.* Multiple short windows of calcium-dependent protein kinase 4 activity coordinate distinct cell cycle events during Plasmodium gametogenesis. *Elife* **6**, doi:10.7554/eLife.26524 (2017).
19 Templeton, T. J., Keister, D. B., Muratova, O., Procter, J. L. & Kaslow, D. C. Adherence of erythrocytes during exflagellation of Plasmodium falciparum microgametes is dependent on erythrocyte surface sialic acid and glycophorins. *J. Exp. Med* **187**, 1599-1609 (1998).
20 McRobert, L. *et al.* Gametogenesis in malaria parasites is mediated by the cGMP-dependent protein kinase. *PLoS Biol* **6**, e139 (2008).
21 Brochet, M. *et al.* Phosphoinositide metabolism links cGMP-dependent protein kinase G to essential Ca(2)(+) signals at key decision points in the life cycle of malaria parasites. *PLoS. Biol* **12**, e1001806, doi:10.1371/journal.pbio.1001806 [doi];PBIOLOGY-D-13-03698 [pii] (2014).
22 Brochet, M. & Billker, O. Calcium signalling in malaria parasites. *Mol. Microbiol* **100**, 397-408, doi:10.1111/mmi.13324 [doi] (2016).
23 Ojo, K. K. *et al.* A specific inhibitor of PfCDPK4 blocks malaria transmission: chemical-genetic validation. *J Infect Dis* **209**, 275-284, doi:10.1093/infdis/jit522 (2014).
24 Bansal, A., Molina-Cruz, A., Brzostowski, J., Mu, J. & Miller, L. H. Plasmodium falciparum Calcium-Dependent Protein Kinase 2 Is Critical for Male Gametocyte Exflagellation but Not Essential for Asexual Proliferation. *MBio* **8**, doi:10.1128/mBio.01656-17 (2017).
25 Bansal, A. *et al.* PfCDPK1 is critical for malaria parasite gametogenesis and mosquito infection. *Proc Natl Acad Sci U S A* **115**, 774-779, doi:10.1073/pnas.1715443115 (2018).
26 Sebastian, S. *et al.* A Plasmodium calcium-dependent protein kinase controls zygote development and transmission by translationally activating repressed mRNAs. *Cell Host. Microbe* **12**, 9-19, doi:S1931-3128(12)00200-4 [pii];10.1016/j.chom.2012.05.014 [doi] (2012).
27 Khan, S. M. *et al.* Proteome analysis of separated male and female gametocytes reveals novel sex-specific Plasmodium biology. *Cell* **121**, 675-687, doi:10.1016/j.cell.2005.03.027 (2005).
28 Rangarajan, R. *et al.* A mitogen-activated protein kinase regulates male gametogenesis and transmission of the malaria parasite Plasmodium berghei. *EMBO Rep* **6**, 464-469 (2005).
29 Tewari, R., Dorin, D., Moon, R., Doerig, C. & Billker, O. An atypical mitogen-activated protein kinase controls cytokinesis and flagellar motility during male gamete formation in a malaria parasite. *Mol Microbiol* **58**, 1253-1263 (2005).
30 Dorin, D. *et al.* An atypical mitogen-activated protein kinase (MAPK) homologue expressed in gametocytes of the human malaria parasite Plasmodium falciparum. Identification of a MAPK signature. *J Biol Chem* **274**, 29912-29920 (1999).
31 Doerig, C. M. *et al.* A MAP kinase homologue from the human malaria parasite, Plasmodium falciparum. *Gene* **177**, 1-6 (1996).
32 Graeser, R., Kury, P., Franklin, R. M. & Kappes, B. Characterization of a mitogen-activated protein (MAP) kinase from Plasmodium falciparum. *Mol Microbiol* **23**, 151-159, doi:10.1046/j.1365-2958.1997.2071571.x (1997).
33 Lin, D. T., Goldman, N. D. & Syin, C. Stage-specific expression of a Plasmodium falciparum protein related to the eukaryotic mitogen-activated protein kinases. *Mol Biochem Parasitol* **78**, 67-77, doi:10.1016/s0166-6851(96)02608-4 (1996).
34 Morrison, D. K. MAP kinase pathways. *Cold Spring Harbor perspectives in biology* **4**, doi:10.1101/cshperspect.a011254 (2012).
35 Raman, M., Chen, W. & Cobb, M. H. Differential regulation and properties of MAPKs. *Oncogene* **26**, 3100-3112, doi:10.1038/sj.onc.1210392 (2007).

36 Dorin-Semblat, D. *et al.* Functional characterization of both MAP kinases of the human malaria parasite Plasmodium falciparum by reverse genetics. *Mol. Microbiol* **65**, 1170-1180 (2007).
37 Fang, H. *et al.* Epistasis studies reveal redundancy among calcium-dependent protein kinases in motility and invasion of malaria parasites. *Nat Commun* **9**, 4248, doi:10.1038/s41467-018-06733-w (2018).
38 Filarsky, M. *et al.* GDV1 induces sexual commitment of malaria parasites by antagonizing HP1-dependent gene silencing. *Science* **359**, 1259-1263, doi:359/6381/1259 [pii];10.1126/science.aan6042 [doi] (2018).
39 Brancucci, N. M. B. *et al.* Lysophosphatidylcholine Regulates Sexual Stage Differentiation in the Human Malaria Parasite Plasmodium falciparum. *Cell* **171**, 1532-1544 e1515, doi:10.1016/j.cell.2017.10.020 (2017).
40 Delves, M. J. *et al.* Routine in vitro culture of P. falciparum gametocytes to evaluate novel transmission-blocking interventions. *Nat. Protoc* **11**, 1668-1680, doi:nprot.2016.096 [pii];10.1038/nprot.2016.096 [doi] (2016).
41 Lasonder, E. *et al.* Integrated transcriptomic and proteomic analyses of P. falciparum gametocytes: molecular insight into sex-specific processes and translational repression. *Nucleic Acids Res* **44**, 6087-6101, doi:gkw536 [pii];10.1093/nar/gkw536 [doi] (2016).
42 Miao, J. *et al.* Sex-Specific Biology of the Human Malaria Parasite Revealed from the Proteomes of Mature Male and Female Gametocytes. *Mol Cell Proteomics* **16**, 537-551, doi:10.1074/mcp.M116.061804 (2017).
43 Tao, D. *et al.* Sex-partitioning of the Plasmodium falciparum stage V gametocyte proteome provides insight into falciparum-specific cell biology. *Mol. Cell Proteomics* **13**, 2705-2724, doi:M114.040956 [pii];10.1074/mcp.M114.040956 [doi] (2014).
44 Dahalan, F. A. *et al.* Phosphorylated and Nonphosphorylated PfMAP2 Are Localized in the Nucleus, Dependent on the Stage of Plasmodium falciparum Asexual Maturation. *BioMed research international* **2016**, 1645097, doi:10.1155/2016/1645097 (2016).
45 Armstrong, C. M. & Goldberg, D. E. An FKBP destabilization domain modulates protein levels in Plasmodium falciparum. *Nat. Methods* **4**, 1007-1009 (2007).
46 Banaszynski, L. A., Chen, L. C., Maynard-Smith, L. A., Ooi, A. G. & Wandless, T. J. A rapid, reversible, and tunable method to regulate protein function in living cells using synthetic small molecules. *Cell* **126**, 995-1004 (2006).
47 Alano, P. *et al.* COS cell expression cloning of Pfg377, a Plasmodium falciparum gametocyte antigen associated with osmiophilic bodies. *Mol. Biochem. Parasitol* **74**, 143-156, doi:0166685195024913 [pii] (1995).
48 Sinden, R. E., Canning, E. U., Bray, R. S. & Smalley, M. E. Gametocyte and gamete development in Plasmodium falciparum. *Proc. R. Soc. Lond B Biol. Sci* **201**, 375-399 (1978).
49 Cargnello, M. & Roux, P. P. Activation and function of the MAPKs and their substrates, the MAPK-activated protein kinases. *Microbiol Mol Biol Rev* **75**, 50-83, doi:10.1128/MMBR.00031-10 (2011).
50 Ngwa, C. J. *et al.* Changes in the transcriptome of the malaria parasite Plasmodium falciparum during the initial phase of transmission from the human to the mosquito. *BMC. Genomics* **14**, 256, doi:1471-2164-14-256 [pii];10.1186/1471-2164-14-256 [doi] (2013).
51 Bozdech, Z. *et al.* The transcriptome of the intraerythrocytic developmental cycle of Plasmodium falciparum. *PLoS. Biol* **1**, E5 (2003).
52 Painter, H. J., Altenhofen, L. M., Kafsack, B. F. & Llinas, M. Whole-genome analysis of Plasmodium spp. Utilizing a new agilent technologies DNA microarray platform. *Methods Mol. Biol* **923**, 213-219, doi:10.1007/978-1-62703-026-7_14 [doi] (2013).

53 Young, J. A. *et al.* The Plasmodium falciparum sexual development transcriptome: a microarray analysis using ontology-based pattern identification. *Mol. Biochem. Parasitol* **143**, 67-79 (2005).
54 Talevich, E., Tobin, A. B., Kannan, N. & Doerig, C. An evolutionary perspective on the kinome of malaria parasites. *Philosophical transactions of the Royal Society of London. Series B, Biological sciences* **367**, 2607-2618, doi:10.1098/rstb.2012.0014 (2012).
55 Ward, P., Equinet, L., Packer, J. & Doerig, C. Protein kinases of the human malaria parasite Plasmodium falciparum: the kinome of a divergent eukaryote. *BMC Genomics* **5**, 79 (2004).
56 Treeck, M., Sanders, J. L., Elias, J. E. & Boothroyd, J. C. The phosphoproteomes of Plasmodium falciparum and Toxoplasma gondii reveal unusual adaptations within and beyond the parasites' boundaries. *Cell Host. Microbe* **10**, 410-419 (2011).
57 Dorin, D. *et al.* Pfnek-1, a NIMA-related kinase from the human malaria parasite Plasmodium falciparum Biochemical properties and possible involvement in MAPK regulation. *European journal of biochemistry* **268**, 2600-2608, doi:10.1046/j.1432-1327.2001.02151.x (2001).
58 Dorin-Semblat, D. *et al.* Plasmodium falciparum NIMA-related kinase Pfnek-1: sex specificity and assessment of essentiality for the erythrocytic asexual cycle. *Microbiology* **157**, 2785-2794, doi:10.1099/mic.0.049023-0 (2011).
59 Silvestrini, F. *et al.* Protein export marks the early phase of gametocytogenesis of the human malaria parasite Plasmodium falciparum. *Mol Cell Proteomics* **9**, 1437-1448 (2010).
60 Wierk, J. K. *et al.* Plasmodium berghei MAPK1 displays differential and dynamic subcellular localizations during liver stage development. *PLoS. ONE* **8**, e59755, doi:10.1371/journal.pone.0059755 [doi];PONE-D-12-26551 [pii] (2013).
61 Lambros, C. & Vanderberg, J. P. Synchronization of Plasmodium falciparum erythrocytic stages in culture. *J. Parasitol* **65**, 418-420 (1979).
62 Jensen, J. B. & Trager, W. Plasmodium falciparum in culture: establishment of additional strains. *Am J Trop Med Hyg* **27**, 743-746, doi:10.4269/ajtmh.1978.27.743 (1978).
63 Spycher, C. *et al.* The Maurer's cleft protein MAHRP1 is essential for trafficking of PfEMP1 to the surface of Plasmodium falciparum-infected erythrocytes. *Mol Microbiol* **68**, 1300-1314, doi:10.1111/j.1365-2958.2008.06235.x (2008).
64 Witmer, K. *et al.* Analysis of subtelomeric virulence gene families in Plasmodium falciparum by comparative transcriptional profiling. *Mol. Microbiol* **84**, 243-259, doi:10.1111/j.1365-2958.2012.08019.x [doi] (2012).
65 Daubenberger, C. A. *et al.* The N'-terminal domain of glyceraldehyde-3-phosphate dehydrogenase of the apicomplexan Plasmodium falciparum mediates GTPase Rab2-dependent recruitment to membranes. *Biol Chem* **384**, 1227-1237, doi:10.1515/bc.2003.135 (2003).
66 Fivelman, Q. L. *et al.* Improved synchronous production of Plasmodium falciparum gametocytes in vitro. *Mol. Biochem. Parasitol* **154**, 119-123 (2007).
67 Brancucci, N. M. B. *et al.* Heterochromatin protein 1 secures survival and transmission of malaria parasites. *Cell Host. Microbe* **16**, 165-176, doi:S1931-3128(14)00258-3 [pii];10.1016/j.chom.2014.07.004 [doi] (2014).
68 Edgar, R., Domrachev, M. & Lash, A. E. Gene Expression Omnibus: NCBI gene expression and hybridization array data repository. *Nucleic Acids Res* **30**, 207-210 (2002).
69 Saldanha, A. J. Java Treeview--extensible visualization of microarray data. *Bioinformatics* **20**, 3246-3248 (2004).

Acknowledgements

We are grateful to Robert W. Sauerwein and Pietro Alano for providing primary antibodies against Pfs16 and PfG377, respectively. This work was supported by funding from the Swiss National Science Foundation (BSCGI0_157729) to T.S.V., the Rudolf Geigy Foundation to E.H. and T.S.V. and the Swiss National Science Foundation (BSSGI0_155852 and 31003A_179321) to M.B. M.B. is an INSERM and EMBO young investigator.

Author Contributions

E.H. generated all transgenic parasite lines, designed and performed experiments, analysed and interpreted data, prepared illustrations and wrote the manuscript. A.C.B. performed experiments, analysed and interpreted data and prepared illustrations related to the analysis of male gametocyte exflagellation, and M.B. designed and supervised these experiments, provided resources and wrote the corresponding parts of the manuscript. T.S.V. conceived of the study, designed and supervised experiments, provided resources and wrote the manuscript. All authors contributed to editing of the manuscript.

Competing interests

The authors declare no competing interests.

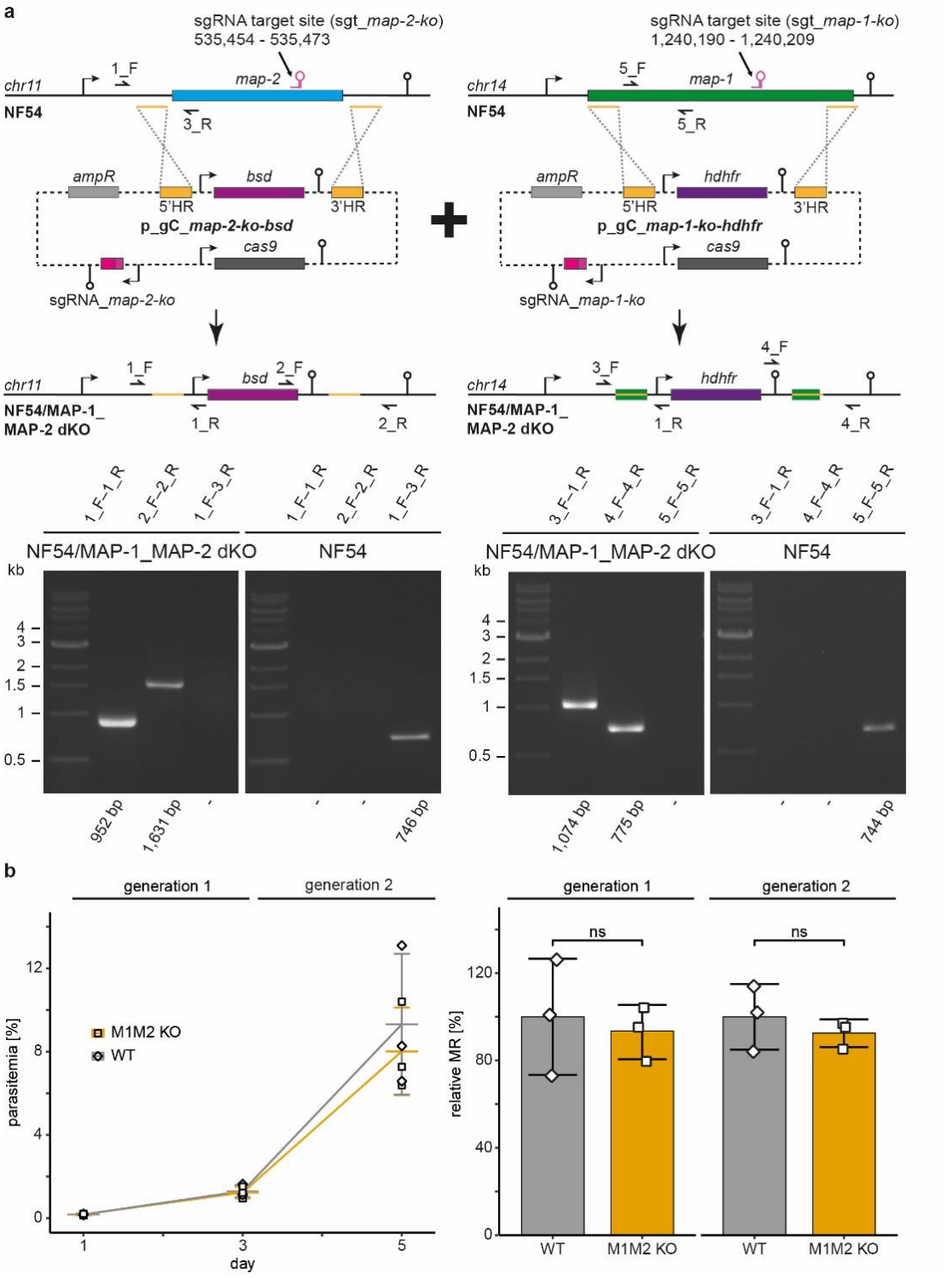

Figure 1. Engineering and growth assay of the MAPK double KO parasite line. **(a)** Top: Scheme depicting the CRISPR/Cas9-based gene editing approach used to generate the NF54/MAP-1_MAP-2 dKO parasite line. Schematic maps of the *pfmap-2* locus and the CRISPR/Cas9 p_gC_*map-2-ko-bsd* plasmid used to generate the NF54/MAP-2 KO line (left), that was re-transfected using the p_gC_*map-1-ko-hdhfr* plasmid to generate the

NF54/MAP-1_MAP-2 dKO parasite line (right). Bottom: PCRs performed on gDNA of NF54/MAP-1_MAP-2 dKO parasites show correct editing of both *mapk* loci. PCRs performed on NF54 WT gDNA serve as controls. **(b)** Left: Flow cytometry data showing the increase in parasitemia of NF54 WT and NF54/MAP-1_MAP-2 dKO parasites over two generations. Right: Multiplication rates quantified from flow cytometry data in NF54 WT and the NF54/MAP-1_MAP-2 dKO parasites in both generations. Values show the means ±SD of three biological replicates with individual data points represented by open squares. ns, not significant (unpaired two-tailed Student's t test). MR, multiplication rate; WT, NF54 WT; M1M2 KO, NF54/MAP-1_MAP-2 dKO.

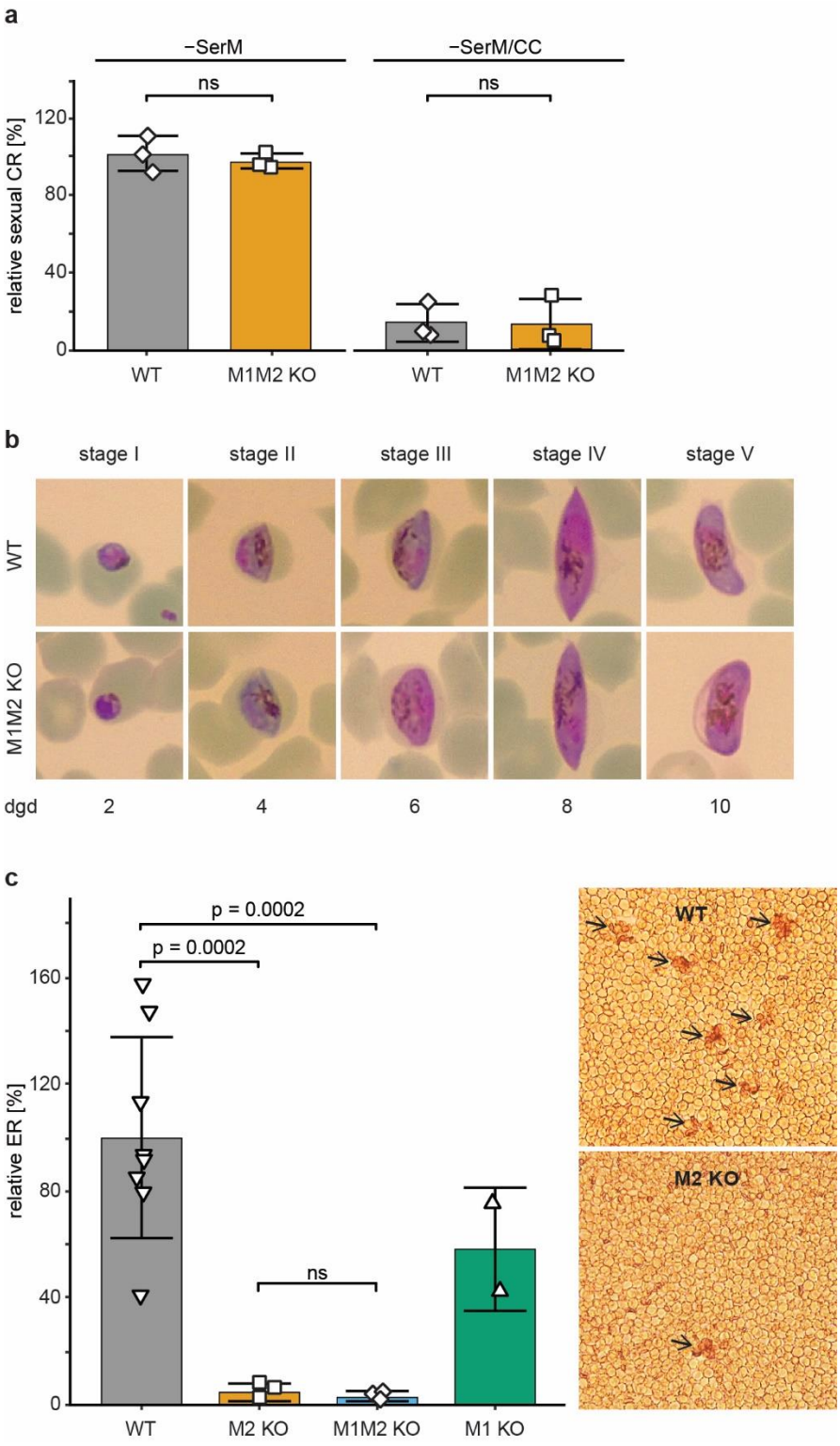

Figure 2. Sexual commitment, sexual development and exflagellation of MAPK double KO parasites. **(a)** Relative sexual commitment rates of NF54 WT and NF54/MAP-1_MAP-2 dKO parasites cultured in serum-depleted medium either in presence (-SerM/CC) or absence (-SerM) of choline chloride quantified using Pfs16-positivity counts from α-Pfs16 IFA (>200 iRBCs counted per experiment). Values show the means ±SD

of three biological replicates with individual data points represented by open squares. ns, not significant; (unpaired two-tailed Student's t test). CR, commitment rate; WT, NF54 WT; M1M2 KO, NF54/MAP-1_MAP-2 dKO. **(b)** Representative images of Giemsa-stained parasites in thin blood smears showing development of NF54 WT and NF54/MAP-1_MAP-2 dKO gametocytes over 10 days and the five (I-V) distinct morphological stages. 1,000x magnification. dgd, day of gametocyte development; WT, NF54 WT; M1M2 KO, NF54/MAP-1_MAP-2 dKO. **(c)** Left: Relative exflagellation rates of NF54/MAP-2 KO, NF54/MAP-1_MAP-2 dKO and NF54/MAP-1 KO gametocytes compared to NF54 WT control parasites. Values show the means ±SD of two (NF54/MAP-1 KO), eight (NF54 WT) or three (NF54/MAP-2 KO and NF54/MAP-1_MAP-2 dKO) biological replicates with individual data points represented by open symbols. Significant differences are indicated (p-value, unpaired two-tailed Student's t test). ns, not significant. Right: Representative images of the number of exflagellation centres (indicated by black arrows) observed in NF54 WT and NF54/MAP-2 KO parasites with comparable gametocytemia (NF54 WT: 2.2%; NF54/MAP-2 KO: 1.8%) by live microscopy (200x magnification). WT, NF54 WT; M1 KO, NF54/MAP-1 KO; M2 KO, NF54/MAP-2 KO; M1M2 KO, NF54/MAP-1_MAP-2 dKO; ER, exflagellation rate.

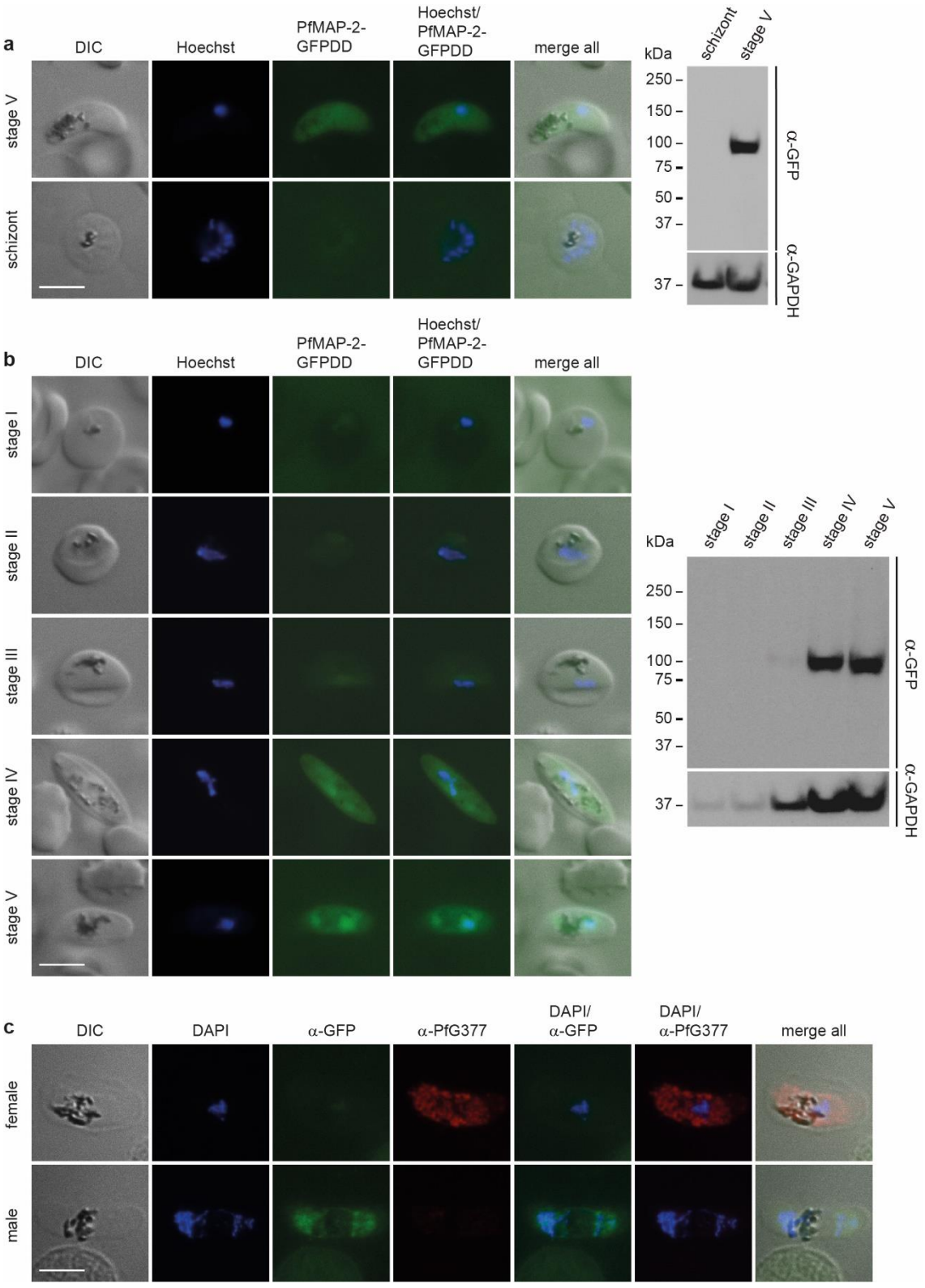

Figure 3. Expression and localisation of PfMAP-2 in NF54/MAP-2GFPDD parasites. **(a)** Expression and localisation of PfMAP-2 in late schizonts (40-48 hpi) and stage V gametocytes assessed by live cell fluorescence imaging and Western blot. Representative live cell fluorescence images are shown. Scale bar = 5 µm. For the

Western blot, parasitemia/gametocytemia was determined by inspection of Giemsa-stained blood smears to ensure loading of equal parasite numbers per lane. MW PfMAP-2GFPDD = 97.9 kDa. MW PfGAPDH = 36.6 kDa (control). **(b)** Expression and localisation of PfMAP-2 in stage I to stage V gametocytes by live cell fluorescence imaging and Western blot. Representative live cell fluorescence images are shown. Scale bar = 5 µm. For the Western blot, gametocytemia was determined by inspection of Giemsa-stained blood smears to ensure loading of equal parasite numbers per lane. MW PfMAP-2GFPDD = 97.9 kDa. MW PfGAPDH = 36.6 kDa (control). **(c)** Representative images of the expression of PfMAP-2GFPDD and PfG377 in stage V male and female gametocytes assessed by IFA. Scale bar = 5 µm. See also Supplementary Fig. 2.

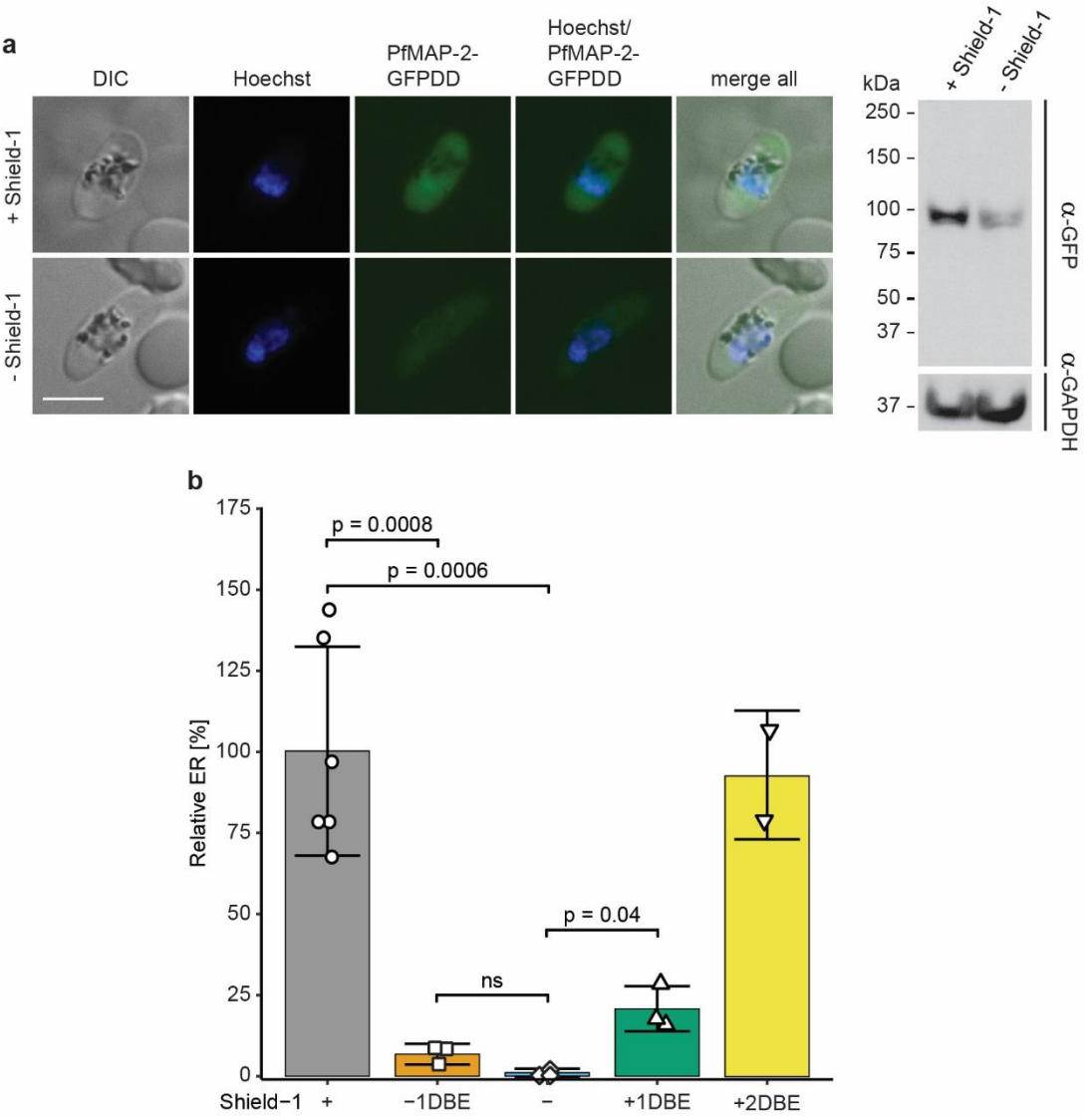

Figure 4. PfMAP-2 depletion in NF54/MAP-2GFPDD parasites prevents exflagellation. **(a)** Expression of PfMAP-2 in stage V gametocytes cultured in presence or absence of Shield-1 by live cell fluorescence imaging and Western blot. Parasites were split (±Shield-1) 24 hours prior to the analysis. Representative live cell fluorescence images are shown. Scale bar = 5 µm. For the Western blot, gametocytemia was determined by inspection of Giemsa-stained blood smears to ensure loading of equal parasite numbers per lane. MW PfMAP-2GFPDD = 97.9 kDa. MW PfGAPDH = 36.6 kDa (control). **(b)** Relative exflagellation rates of NF54/MAP-2GFPDD gametocytes cultured constantly in presence (+) or absence (-) of Shield-1, or where Shield-1 has been removed one day (24 hours) before assessing exflagellation rates (-1DBE) or replenished two days (48 hours) and one day (24 hours) before assessing exflagellation rates (+2DBE and +1DBE,

respectively). Values show the means ±SD of two (+2DBE), three (-; -1DBE; +1DBE) or six (+) biological replicates with individual data points represented by open symbols. Significant differences are indicated (p-value, unpaired two-tailed Student's t test). ns, not significant. ER, exflagellation rate.

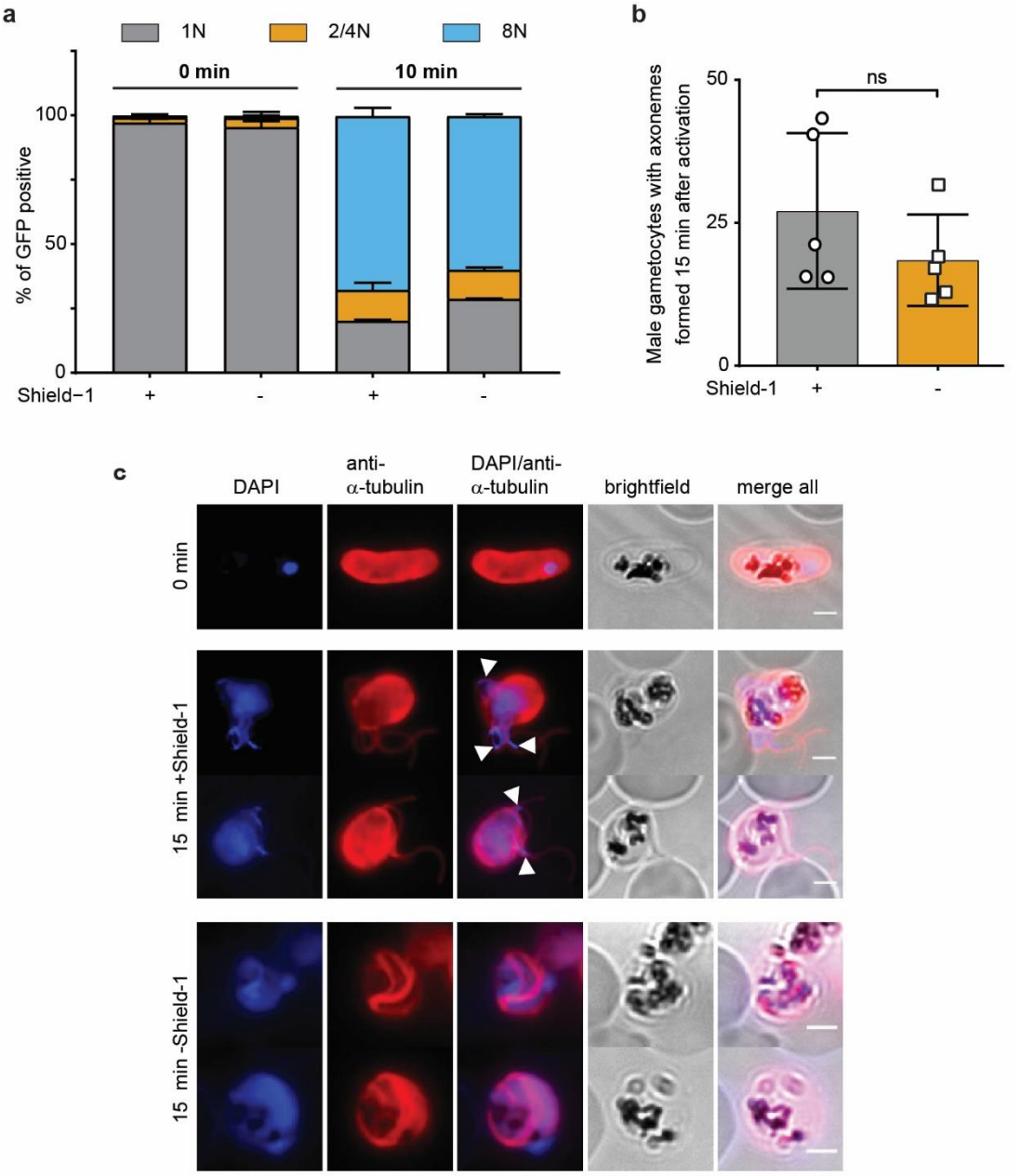

Figure 5. Detailed phenotyping of the exflagellation defect in NF54/MAP-2GFPDD parasites. **(a)** Ploidy of GFP-positive microgametocytes 0 and 10 min after activation of gametogenesis under protein-stabilizing (+Shield-1) and -degrading (-Shield-1) conditions assessed by flow cytometry. Parasites were split (±Shield-1) 24 hours before analysis. Values show the means ±SD of three biological replicates. **(b)** Number of male gametocytes that form axonemes 15 min after activation of gametogenesis, determined from anti-α-tubulin IFAs. Protein-stabilizing (+Shield-1) and -degrading (-Shield-1) culturing conditions are compared. Parasites were split (±Shield-1) 24 hours before analysis. Values show the means ±SD of five biological replicates with individual data

points represented by open symbols. ns, not significant (paired two-tailed Student's t test). **(c)** Representative images of anti-α-tubulin IFAs showing axoneme formation 15 min after activation of gametogenesis. Protein-stabilizing (+Shield-1) and -degrading (-Shield-1) culturing conditions are compared. White arrowheads indicate incorporation of DNA into newly forming microgametes exclusively in parasites cultured under protein-stabilizing (+Shield-1) conditions. Parasites were split (±Shield-1) 24 hours before probing. Scale bar = 2 µm.

Supplementary Information

PfMAP-2 is essential for male gametogenesis in the malaria parasite *Plasmodium falciparum*

Eva Hitz[1,2], Aurélia C. Balestra[3], Mathieu Brochet[3], Till S. Voss[1,2,*]

[1]Department of Medical Parasitology and Infection Biology, Swiss Tropical and Public Health Institute, 4051 Basel, Switzerland.

[2]University of Basel, 4001 Basel, Switzerland.

[3]Department of Microbiology and Molecular Medicine, Faculty of Medicine, University of Geneva, 1211 Geneva 4, Switzerland.

[*]Corresponding author: till.voss@swisstph.ch.

This Supplementary Information file includes:

- Supplementary Figures 1-6
- Supplementary Tables 1-2
- Supplementary Dataset 1
- Supplementary Spreadsheet 1

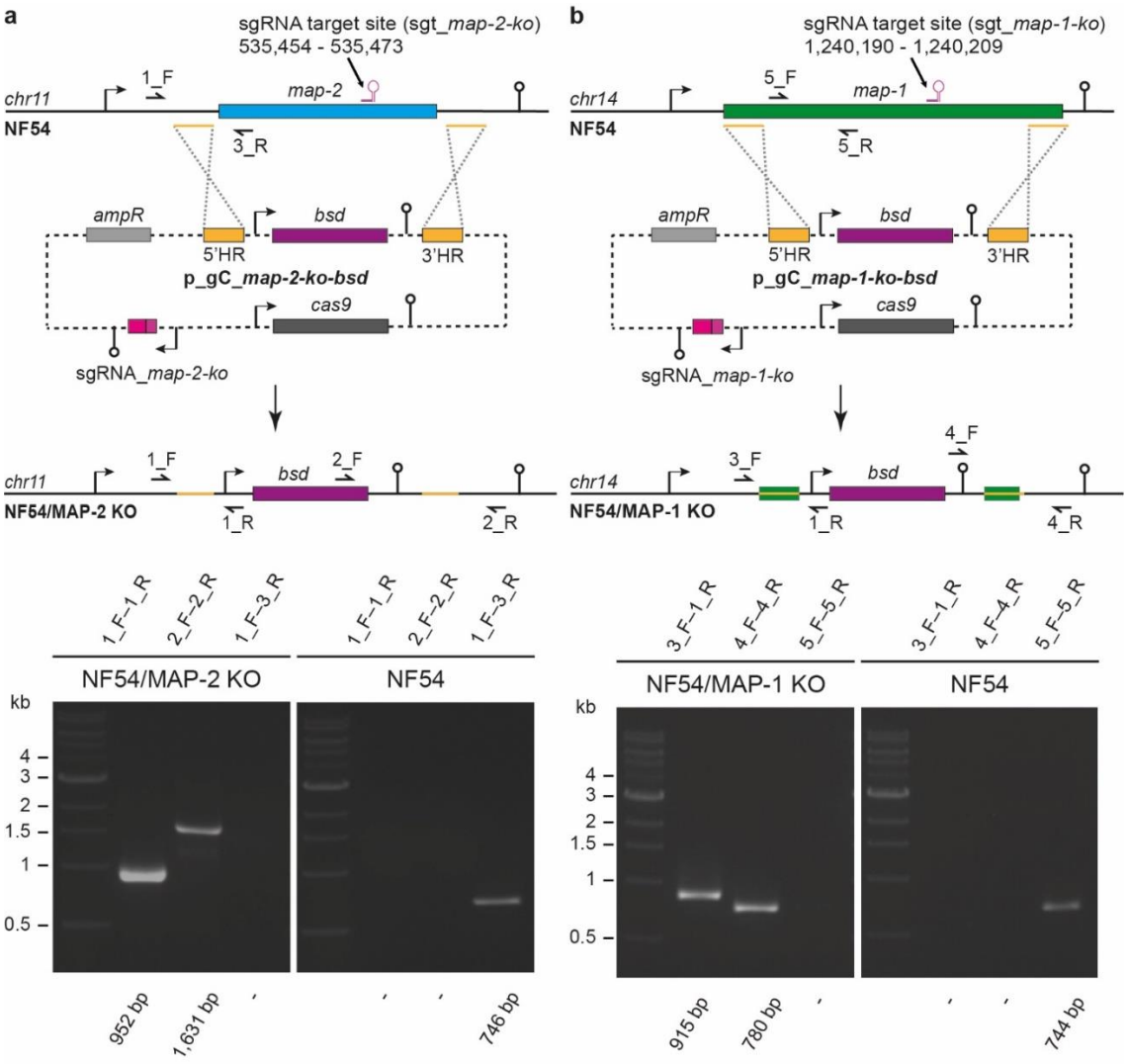

Supplementary Figure 1. Engineering of the PfMAP-1 and PfMAP-2 KO parasite lines. **(a)** Top: Schematic maps of the *pfmap-2* locus, the CRISPR/Cas9 p_gC_*map-2-ko-bsd* plasmid used to generate the NF54/MAP-2 KO parasite line and the disrupted *pfmap-2* locus. Bottom: PCR results on gDNA of NF54/MAP-2 KO parasites show correct editing of the *pfmap-2* locus. PCRs performed on NF54 WT gDNA serve as controls. **(b)** Top: Schematic maps of the *pfmap-1* locus, the CRISPR/Cas9 p_gC_*map-1-ko-bsd* plasmid used to generate the NF54/MAP-1 KO parasite line and the disrupted *pfmap-1* locus. Bottom: PCR results on gDNA of NF54/MAP-1 KO parasites show correct editing of the *pfmap-1* locus. PCRs performed on NF54 WT gDNA serve as controls. NF54, NF54 WT.

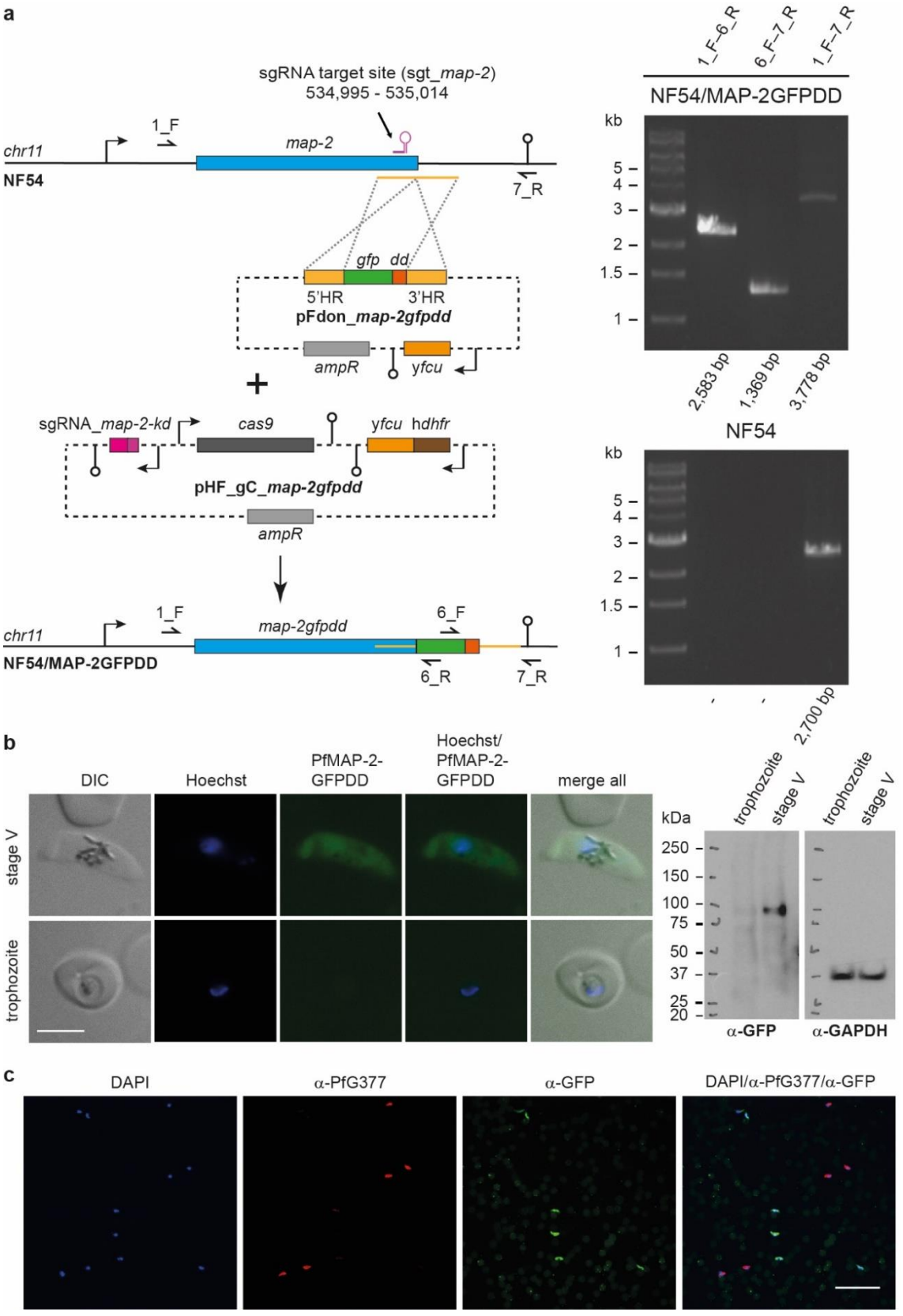

Supplementary Figure 2. Engineering of the NF54/MAP-2GFPDD conditional knockdown parasite line and PfMAP-2 expression. **(a)** Left: Schematic maps of the *pfmap-2* locus, the CRISPR/Cas9 pFdon*_map-2gfpdd* and the pHF*_map-2gfpdd*

plasmids used to generate the NF54/MAP-2GFPDD parasite line and the edited *pfmap-2* locus. Right: PCRs performed on gDNA of NF54/MAP-2GFPDD parasites show correct editing of the *pfmap-2* locus. PCRs performed on NF54 WT (NF54) gDNA serve as controls. **(b)** Expression and localisation of PfMAP-2 in asexual trophozoites (24-30 hpi) and stage V gametocytes assessed by live cell fluorescence imaging and Western blot. Representative live cell fluorescence images are shown. Scale bar = 5 µm. For the Western blot, parasitemia/gametocytemia was determined by inspection of Giemsa-stained blood smears to ensure loading of equal parasite numbers per lane. MW PfMAP-2GFPDD = 97.9 kDa. MW PfGAPDH = 36.6 kDa (control). **(c)** Representative overview images of an α-PfG377/α-GFP IFA experiment on NF54/MAP-2GFPDD stage V gametocytes cultured under protein-stabilizing (+Shield-1) conditions. 200x magnification. Scale bar = 50 µm.

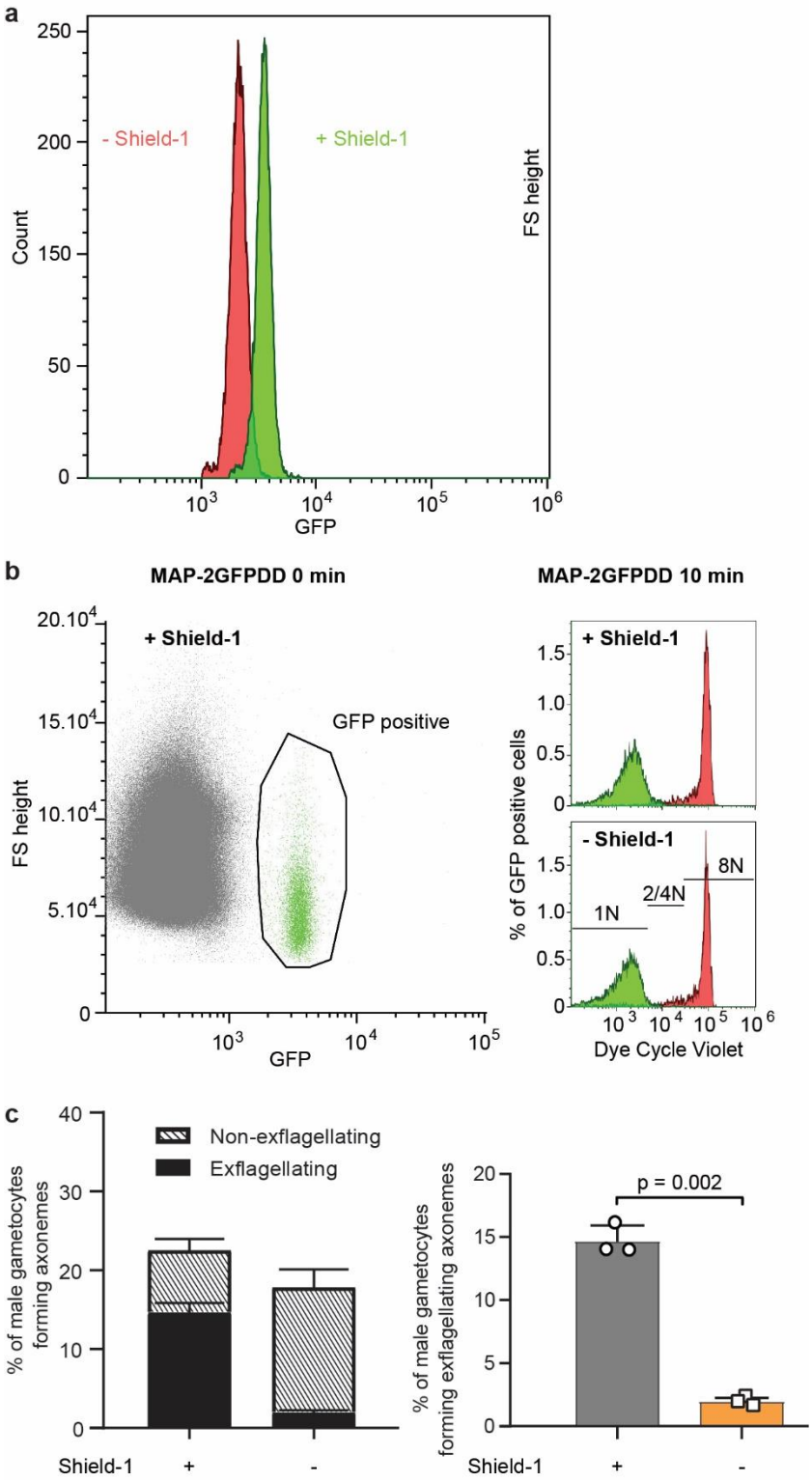

Supplementary Figure 3. Detailed phenotyping of the exflagellation defect in NF54/MAP-2GFPDD parasites. **(a)** Flow cytometry plot showing the differential GFP-fluorescence intensity of NF54/MAP-2GFPDD microgametocytes under protein-degrading (-Shield-1) and protein-stabilizing (+Shield-1) conditions. **(b)** Left: Representative flow cytometry plot showing the fluorescence intensity of individual

microgametocytes cultured under protein-stabilizing (+Shield-1) conditions before activation of gametogenesis (0 min). Vybrant DyeCycle Violet intensity is analysed in the parasite population gated positive for GFP fluorescence. Right: Plots showing the Vybrant DyeCycle Violet intensity and respective ploidy of GFP-positive microgametocytes after (10 min) activation of gametogenesis both under protein-stabilizing (+Shield-1) and protein-degrading (-Shield-1) conditions. **(c)** Left: Plot showing the percentage of microgametocytes forming axonemes and whether or not they exflagellated, determined from anti-α-tubulin IFAs. Right: Percentage of male gametocytes forming exflagellating axonemes after activation of gametogenesis, determined from anti-α-tubulin IFAs. Exflagellating axonemes are defined as axonemes that do not remain around the nucleus. Protein-stabilizing (+Shield-1) and -degrading (-Shield-1) culturing conditions are compared. Parasites were split (±Shield-1) 24 hours before analysis. Values show the mean ±SD of three biological replicates with individual data points represented by open symbols. Significant difference is indicated with the according p-value (paired two-tailed Student's t test).

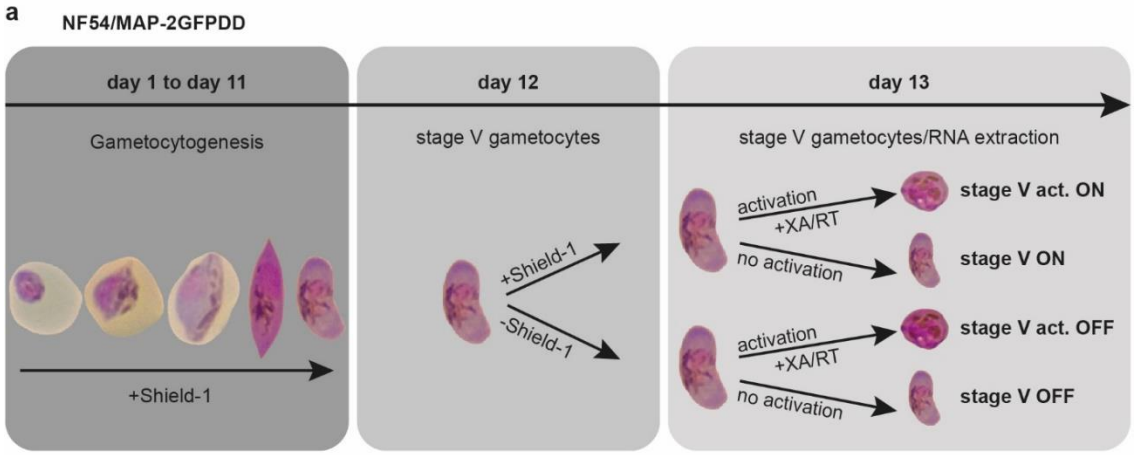

b

		replicate 1				replicate 2			
		stage V ON	stage V act. ON	stage V OFF	stage V act. OFF	stage V ON	stage V act. ON	stage V OFF	stage V act. OFF
replicate 1	stage V ON	1	0.996	0.996	0.995	0.991	0.984	0.988	0.984
	stage V act. ON	0.996	1	0.996	0.997	0.991	0.985	0.989	0.984
	stage V OFF	0.996	0.996	1	0.996	0.990	0.983	0.988	0.983
	stage V act. OFF	0.995	0.997	0.996	1	0.992	0.987	0.990	0.987
replicate 2	stage V ON	0.991	0.991	0.990	0.992	1	0.994	0.997	0.994
	stage V act. ON	0.984	0.985	0.983	0.987	0.994	1	0.994	0.994
	stage V OFF	0.988	0.989	0.988	0.990	0.997	0.994	1	0.995
	stage V act. OFF	0.984	0.984	0.983	0.987	0.994	0.994	0.995	1

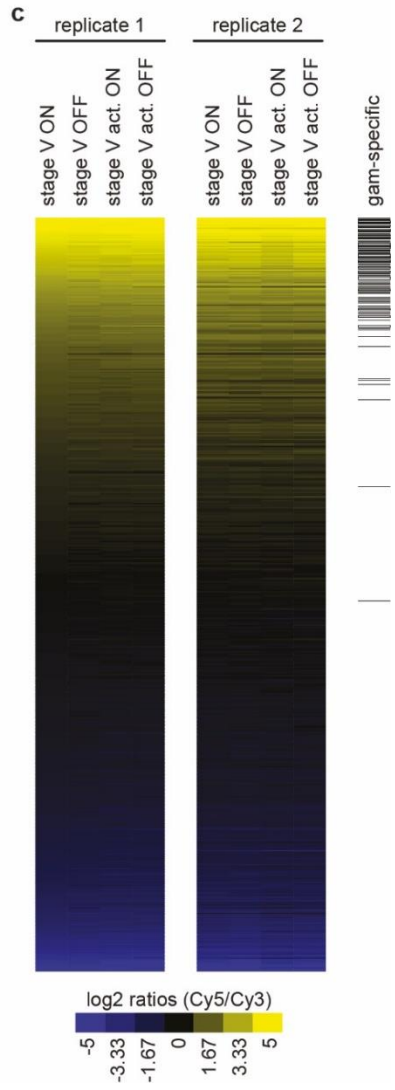

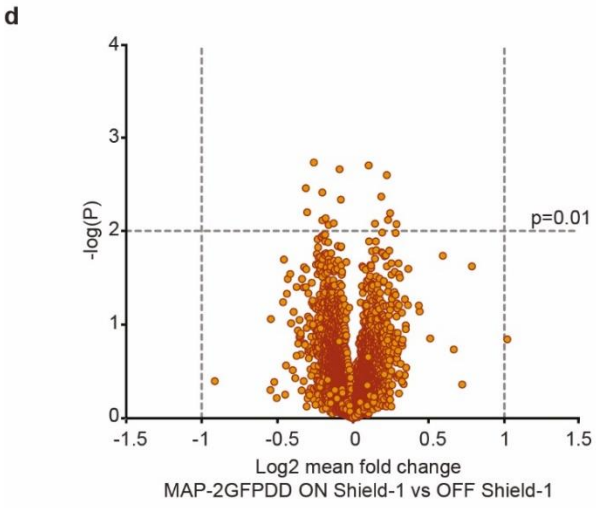

Supplementary Figure 4. Microarray experiments performed using NF54/MAP-2GFPDD stage V gametocytes. **(a)** Schematic of the experimental setup used to generate the non-activated (stage V ON and stage V OFF) and activated (stage V act. ON and stage V act. OFF) stage V gametocyte samples harvested for microarray

experiments. ON, cultured in presence of Shield-1; OFF, cultured in absence of Shield-1; act., XA-induced activation. **(b)** Perason's correlation coefficients for pairwise comparisons of relative mRNA abundances of eight NF54/MAP-2GFPDD microarray samples from two biological replicates. Samples were generated from stage V gametocytes cultured under protein-stabilizing (+Shield-1; ON) and -degrading (-Shield-1; OFF) conditions and before and after XA-induced activation (stage V ON, stage V OFF, stage V act. ON, stage V act. OFF). **(c)** Heat map showing Cy5/Cy3 log2 ratios of all transcripts from the eight NF54/MAP-2GFPDD microarray samples harvested from two biological replicates. Samples were generated from stage V gametocytes cultured under protein-stabilizing (+Shield-1; ON) and -degrading (-Shield-1; OFF) conditions and before and after XA-induced activation (stage V ON, stage V OFF, stage V act. ON, stage V act. OFF). Gametocyte-specific transcripts from a previously published reference dataset[1] are indicated on the right by black horizontal lines. Genes are sorted in descending order according to the Cy5/Cy3 log2 ratio in the stage V ON sample. **(d)** Volcano plot showing the mean fold change in gene expression (log2) between NF54/MAP-2GFPDD gametocytes cultured under protein-stabilizing (+Shield-1; ON) and -degrading (-Shield-1; OFF) conditions and the respective p-values (-log) (unpaired two-tailed Student's t test, equal variance).

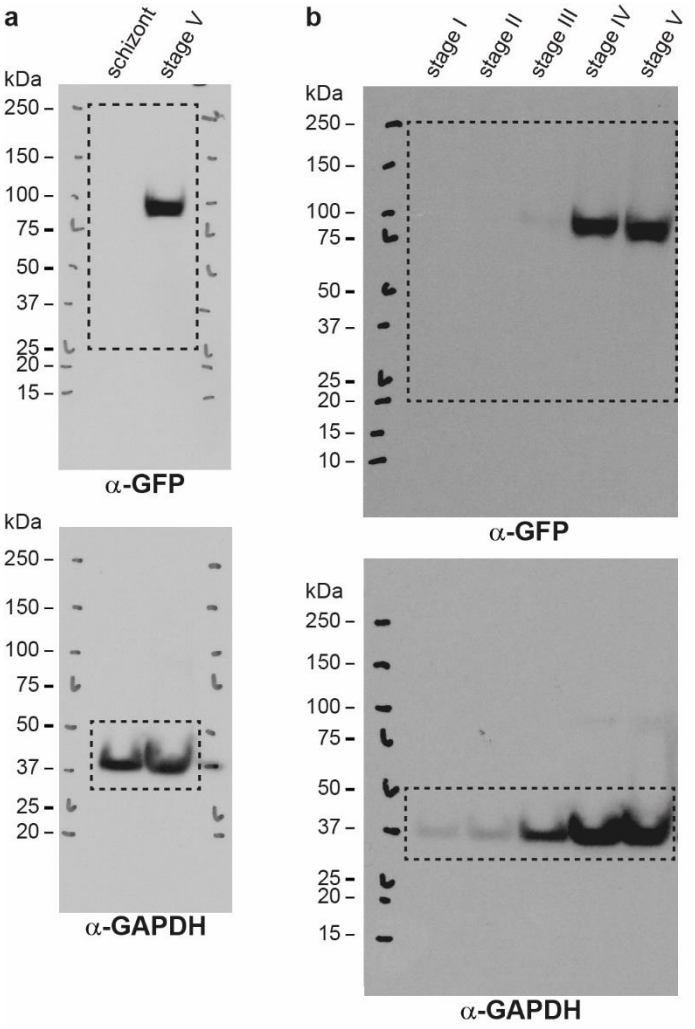

Supplementary Figure 5. Full size Western blots of sections shown in Figure 3. **(a)** Full size Western blots showing the expression of PfMAP-2 in late schizonts (40-48 hpi) and stage V gametocytes. Parasitemia/gametocytemia was determined by inspection of Giemsa-stained blood smears to ensure loading of equal parasite numbers per lane. Dashed lines mark the cropped sections of the blots shown in Figure 3a. MW PfMAP-2GFPDD = 97.9 kDa. MW PfGAPDH = 36.6 kDa (control). **(b)** Full size Western blots showing the expression PfMAP-2 in stage I to stage V gametocytes. Gametocytemia was determined by inspection of Giemsa-stained blood smears to ensure loading of equal parasite numbers per lane. Dashed frames mark the cropped sections of the blots shown in Figure 3b. MW PfMAP-2GFPDD = 97.9 kDa. MW PfGAPDH = 36.6 kDa (control).

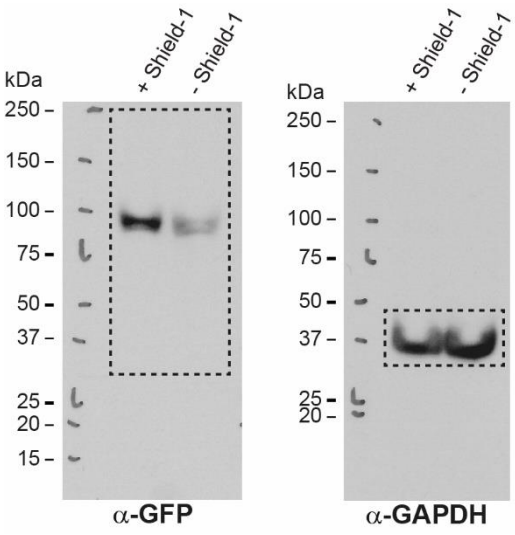

Supplementary Figure 6. Full size Western blot of section shown in Figure 4. Full size Western Blot showing the expression of PfMAP-2 in stage V gametocytes cultured in presence or absence of Shield-1. Parasites were split (±Shield-1) 24 hours prior to the analysis. Dashed frames mark the cropped sections of the blots shown in Figure 4a. MW PfMAP-2GFPDD = 97.9 kDa. MW PfGAPDH = 36.6 kDa (control).

Supplementary Tables

Table 1. Primers used for cloning of CRISPR/Cas9 transfection plasmids. Oligonucleotide names and sequences as well as names of the plasmids and cell lines generated are indicated. Oligonucleotide sequences used to generate PCR fragments for Gibson assembly reactions (Gibson overhangs) and for insertion of gRNA-encoding annealed double-stranded oligonucleotides via T4 DNA ligase-dependent cloning (5' and 3' overhangs) are highlighted with regular and italicized capital letters, respectively.

Oligonucleotide name	**Oligonucleotide sequence 5' → 3'**	**Plasmid name**	**Cell line name**
HR1_M1_F	CAGGGTAGCTGATATCGG ATCCatgcctaaagaagattgcaa gac	p_gC_*map-1-ko-bsd,* p_gC_*map-1-ko-hdhfr*	NF54/MAP-1 KO, NF54/MAP-1_MAP-2 dKO
HR1_M1_R	TTCTATAAATTGAtgctcttaat aattgatatatta	p_gC_*map-1-ko-bsd*	NF54/MAP-1 KO, NF54/MAP-1_MAP-2 dKO
HR1_M1hDHFR_R	CCTTTTCTCTTGTgctcttaata attgatatatta	p_gC_*map-1-ko-hdhfr*	NF54/MAP-1 KO, NF54/MAP-1_MAP-2 dKO
HR2_M1_F	TTATTAAATCTAGAggctctttg aaaagcgtaaac	p_gC_*map-1-ko-bsd*	NF54/MAP-1 KO
HR2_M1_R	CAGTGAGCGAGGAAGCG GAAGCTTgtggaaatagtataatg atttg	p_gC_*map-1-ko-bsd,* p_gC_*map-1-ko-hdhfr*	NF54/MAP-1 KO
M1_BSD_F	ATTATTAAGAGCatcaatttata gaaacaaaatatatac	p_gC_*map-1-ko-bsd*	NF54/MAP-1 KO
M1_BSD_R	TTCAAAGAGCCtctagatttaat aaatatgttcttata	p_gC_*map-1-ko-bsd*	NF54/MAP-1 KO
hDHFR_F	TTAAGAGCacaagagaaaagg cagaaac	p_gC_*map-1-ko-hdhfr*	NF54/MAP-1_MAP-2 dKO
hDHFR_R	ACGCTTTTCAAAGAGCCTtt taataaatatgttcttatatataatg	p_gC_*map-1-ko-hdhfr*	NF54/MAP-1_MAP-2 dKO
sgRNA_M1KO_F	*AAAC*ctttccttgtatactggttc	p_gC_*map-1-ko-bsd,* p_gC_*map-1-ko-hdhfr*	NF54/MAP-1 KO, NF54/MAP-1_MAP-2 dKO
sgRNA_M1KO R	*TATT*gaaccagtatacaaggaaag	p_gC_*map-1-ko-bsd,* p_gC_*map-1-ko-hdhfr*	NF54/MAP-1 KO, NF54/MAP-1_MAP-2 dKO
HR1_M2_F	CAGGGTAGCTGATATCGc atattgaaccttcctattttc	p_gC_*map-2-ko-bsd*	NF54/MAP-2 KO

HR1_M2_R	GTTTCTATAAATTGATgatttt actgagaggttaac	p_gC_*map-2-ko-bsd*	NF54/MAP-2 KO
HR2_M2_F	TTATTAAATCTAGAgaagga atgaaggaatatttc	p_gC_*map-2-ko-bsd*	NF54/MAP-2 KO
HR2_M2_R	CAGTGAGCGAGGAAGCG GAatttattcaagcgggacac	p_gC_*map-2-ko-bsd*	NF54/MAP-2 KO
M2_BSD_F	CTCAGTAAAATCatcaatttata gaaacaaaatatatac	p_gC_*map-2-ko-bsd*	NF54/MAP-2 KO
M2_BSD_R	CCTTCATTCCTTCtctagattta ataaatatgttcttata	p_gC_*map-2-ko-bsd*	NF54/MAP-2 KO
sgRNA_M2KO_F	*AAAC*ttatttcctggatcttcttg	p_gC_*map-2-ko-bsd*	NF54/MAP-2 KO
sgRNA_M2KO_R	*TATT*caagaagatccaggaaataa	p_gC_*map-2-ko-bsd*	NF54/MAP-2 KO
HR1_M2KD_F	CGAGTCAGTGAGCGAGGA ttatcacctgatcataattc	pFdon_*map-2-gfpdd*	NF54/MAP-2GFPDD
HR1_M2KD_R	CTTTTCTGGTGGATGTTGA Gtttcgctggtataattaaatcagcatg aaatg	pFdon_*map-2-gfpdd*	NF54/MAP-2GFPDD
HR2_M2KD_F	ACTGGAATGAgcataatttttatct atac	pFdon_*map-2-gfpdd*	NF54/MAP-2GFPDD
HR2_M2KD_R	AGGCCCTTTTCTCTTGTGt aatttattcaagcgggacac	pFdon_*map-2-gfpdd*	NF54/MAP-2GFPDD
GFP_F	CTCAACATCCACCAGAAA AGtttctacaatatgggatccagtgga atgagtaaag	pFdon_*map-2-gfpdd*	NF54/MAP-2GFPDD
GFP_R	GATAAAAATTATGCtcattcca gttttagaagctc	pFdon_*map-2-gfpdd*	NF54/MAP-2GFPDD
sgRNA_M2KD_F	*AAAC*gcaaagttaaatatacatca	pHF_*map-2-gfpdd*	NF54/MAP-2GFPDD
sgRNA_M2KD_R	*TATT*tgatgtatatttaactttgc	pHF_*map-2-gfpdd*	NF54/MAP-2GFPDD

Table 2. Primers used for PCRs on gDNA of transgenic parasite lines. Oligonucleotide names and sequences as well as the names of the cell lines from which gDNA was extracted to perform integration PCRs are indicated.

Primer name	Primer sequence 5' → 3'	Cell line name
1_F	atatctactgtctccatatac	NF54/ MAP-2 KO; NF54/MAP-1_MAP-2 dKO; NF54/MAP-2GFPDD
1_R	cattgtttaatactactacatg	NF54/ MAP-2 KO; NF54/ MAP-1 KO; NF54/MAP-1_MAP-2 dKO
2_F	gtatattttaaactagaaaagg	NF54/ MAP-2 KO; NF54/MAP-1_MAP-2 dKO
2_R	tgactaagacatgcataagag	NF54/ MAP-2 KO; NF54/MAP-1_MAP-2 dKO
3_F	ccacaacaacatttatcatt	NF54/ MAP-2 KO; NF54/MAP-1_MAP-2 dKO
3_R	tcatccctactactagactc	NF54/ MAP-1 KO; NF54/MAP-1_MAP-2 dKO
4_F	catgttttgtaatttatgggatagcg	NF54/ MAP-1 KO; NF54/MAP-1_MAP-2 dKO
4_R	gatagttttacaacggttcag	NF54/ MAP-1 KO; NF54/MAP-1_MAP-2 dKO
5_F	gttgggtagtacgcattatac	NF54/ MAP-1 KO; NF54/MAP-1_MAP-2 dKO
5_R	agaactacatgctctaggttg	NF54/ MAP-1 KO; NF54/MAP-1_MAP-2 dKO
6_F	ggttatgtacaggaaagaac	NF54/MAP-2GFPDD
6_R	gtgtgagttatagttgtattcc	NF54/MAP-2GFPDD
7_R	tcatccctactactagactc	NF54/MAP-2GFPDD

Dataset 1. Processed microarray data obtained from NF54/MAP-2GFPDD stage V gametocytes. Columns A-B: Gene ID and gene annotation (www.plasmodb.org; v41). Column C: gametocyte-specific genes[1]. Columns D-K: Cy5/Cy3 log2 ratios for all transcripts in the eight samples harvested from two biological replicates from NF54/MAP-2GFPDD stage V gametocytes cultured in presence (columns D-G) or absence (columns H-K) of Shield-1 before (columns D, E, H, I) and after (columns F, G, J, K) XA-induced activation. Column L: mean fold change in gene expression (log2) between NF54/MAP-2GFPDD gametocytes cultured in presence and absence of Shield-1. Column M: p-value (unpaired two-tailed Student's t test, equal variance). Columns N-Q: fold change in gene expression (log2) between NF54/MAP-2GFPDD gametocytes cultured in presence and absence of Shield-1 for each replicate experiment performed before and after XA-induced activation. ON, cultured in presence of Shield-1; OFF, cultured in absence of Shield-1; act., XA-induced activation.

Spreadsheet 1. Comparison of the GEO microarray platforms GPL15130 and GPL28317. Worksheet 1: Comparison of the overall design and probe content of the *P. falciparum* Agilent microarray platforms GPL15130 (Agilent-037237) [2] and GPL28317 (Agilent-085039) (this study). Worksheet 2: Names (column 1), IDs (column 2) and sequences (column 3) of the oligonucleotide probes that differ between the *P. falciparum* Agilent microarray platforms GPL15130 (Agilent-037237) [2] and GPL28317 (Agilent-085039) (this study). *P. falciparum* codon-optimised marker gene sequences for which probes have been included in the GPL28317 (Agilent-085039) microarray (column D).

References

1 Young, J. A. *et al.* The Plasmodium falciparum sexual development transcriptome: a microarray analysis using ontology-based pattern identification. *Mol Biochem Parasitol* **143**, 67-79, doi:10.1016/j.molbiopara.2005.05.007 (2005).

2 Painter, H. J., Altenhofen, L. M., Kafsack, B. F. & Llinas, M. Whole-genome analysis of Plasmodium spp. Utilizing a new agilent technologies DNA microarray platform. *Methods Mol. Biol* **923**, 213-219, doi:10.1007/978-1-62703-026-7_14 (2013).

Chapter 4

Casein kinase 2 (CK2)

This chapter contains the manuscript “The catalytic subunit of *Plasmodium falciparum* casein kinase 2 is essential for gametocytogenesis” published in *Communications Biology* (12. March 2021) and available under the following link:. https://www.nature.com/articles/s42003-021-01873-0. I am first author of this manuscript and detailed information on the author contribution is given in the according manuscript section.

Chapter 4

The catalytic subunit of *Plasmodium falciparum* casein kinase 2 is essential for gametocytogenesis

Eva Hitz[1,2], Olivia Grüninger[1,2], Armin Passecker[1,2], Matthias Wyss[1,2], Christian Scheurer[1,2], Sergio Wittlin[1,2], Hans-Peter Beck[1,2], Nicolas M. B. Brancucci[1,2], Till S. Voss[1,2,*]

[1]Department of Medical Parasitology and Infection Biology, Swiss Tropical and Public Health Institute, 4051 Basel, Switzerland.

[2]University of Basel, 4001 Basel, Switzerland.

[*]Corresponding author: till.voss@swisstph.ch.

Summary

Casein kinase 2 (CK2) is a pleiotropic kinase phosphorylating substrates in different cellular compartments in eukaryotes. In the malaria parasite *Plasmodium falciparum*, PfCK2 is vital for asexual proliferation of blood stage parasites. Here, we applied CRISPR/Cas9-based gene editing to investigate the function of the PfCK2α catalytic subunit in gametocytes, the sexual forms of the parasite that are essential for malaria transmission. We show that PfCK2α localizes to the nucleus and cytoplasm in asexual and sexual parasites alike. Conditional knockdown of PfCK2α expression prevented the transition of stage IV into transmission-competent stage V gametocytes, whereas the conditional knockout of *pfck2a* completely blocked gametocyte maturation already at an earlier stage of sexual differentiation. In summary, our results demonstrate that PfCK2α is not only essential for asexual but also sexual development of *P. falciparum* blood stage parasites and encourage studies exploring PfCK2α as a potential target for dual-active antimalarial drugs.

Introduction

Malaria is responsible for more than 400,000 deaths worldwide each year, of which most are caused by *Plasmodium falciparum* [1]. Malaria parasites have a complex life cycle during which sporozoites are transmitted to humans by the bite of an infected female *Anopheles* mosquito. Sporozoites reach the liver and multiply inside hepatocytes over several days to release tens of thousands of merozoites back into the blood stream, where they invade red blood cells (RBCs) and start the intraerythrocytic developmental cycle (IDC). Once inside a RBC, the merozoite develops into a ring stage parasite, then into a trophozoite and finally into a schizont that eventually releases up to 32 merozoites to invade new RBCs. Continuous rounds of these IDCs are responsible for all malaria-related morbidity and mortality. During each IDC, a small fraction of trophozoites undergoes sexual commitment and – after completing schizogony – their ring stage progeny differentiate within 10 to 12 days into either male or female gametocytes instead of entering another round of intraerythrocytic multiplication. When taken up by a female *Anopheles* mosquito feeding on an infected human, mature gametocytes undergo sexual reproduction in the mosquito midgut and ultimately generate sporozoites rendering the vector infectious to the next human host.

In the past two decades, immense control efforts have led to a global reduction in malaria cases and malaria-related deaths [1]. However, this success has stagnated in many regions of the world in the past five years and in some areas the number of cases even increased [1]. Furthermore, it has become evident that resistance to the frontline drug Artemisinin used in combination therapies can arise, resulting in delayed parasite clearance and thus an increased transmission potential [2]. Further drawbacks include resistance of the *Anopheles* vector to insecticides as well as behavioral changes of the mosquitoes resulting in increased numbers of infectious bites [3]. It is therefore evident that new interventions and treatments are needed to further decrease the global malaria burden in the future. In recent years, kinases have gained more attention as potential drug targets and with Glivec (Imatinib Mesylate), the first kinase inhibitor for cancer

treatment has been approved by the FDA in 2001 [4]. Several *P. falciparum* kinases have also been proposed as potential drug targets and MMV390048, targeting the phosphatidylinositol 4-kinase, is currently tested in clinical phase 2 trials [5-9]. Another kinase that has repeatedly been referred to as an attractive potential antimalarial drug target is the *P. falciparum* casein kinase 2 (PfCK2) [10-13].

In most eukaryotes, the CK2 protein kinase is a tetramer consisting of two catalytic alpha subunits (α and α') and a dimer of regulatory beta (β) subunits [14]. CK2 has been described as a pleiotropic and constitutively active kinase shown to be associated with the phosphorylation of hundreds of substrates in different eukaryotes including yeast and humans [15-18]. CK2 substrates are found in various cellular compartments such as the nucleus, the Golgi apparatus, the endoplasmic reticulum and the cytoplasm [14,19]. For instance, transcription factors and other nuclear proteins were identified as CK2 substrates or interactors in yeast [20,21]. The diversity of substrates and their numerous subcellular localisations explain the essentiality of CK2 in cell differentiation, proliferation and apoptosis as well as in the processes of gene expression and protein synthesis [14,17,19]. Gene disruption experiments further confirmed the essentiality of CK2 in different model eukaryotes including mice and yeast [22-24].

Intriguingly, in contrast to other eukaryotic CK2 kinases *P. falciparum* PfCK2 is composed of only one catalytic alpha subunit (PfCK2α) and two regulatory beta subunits (PfCK2β1 and PfCK2β2) [25,26]. All PfCK2 subunits are expressed throughout the IDC and localise to the parasite cytoplasm and nucleus [10,27-29]. Both PfCK2 subunits were found resistant to knockout attempts suggesting they are essential for parasite viability [10,12]. Furthermore, pull-down experiments performed in two different studies revealed that PfCK2α interacts with both β subunits [10,12] and the β subunits are able to regulate PfCK2α activity *in vitro* [12]. The catalytic PfCK2α subunit potentially undergoes auto-phosphorylation at several sites (e.g. Thr^{63}, Tyr^{20}) to regulate kinase activity [11-13]. The importance of Thr^{63} auto-phosphorylation has been confirmed since mutation of this site prevented auto-phosphorylation and reduced kinase activity [11].

PfCK2 is likely involved in chromatin dynamics since chromatin-related proteins such as nucleosome assembly proteins, histones and members of the ALBA protein family are likely substrates of PfCK2α [10]. Nuclear proteins involved in mitosis and DNA replication as well as proteins associated with merozoite invasion, motility and post-translational modification were also identified as potential interactors and substrates of PfCK2 [10]. Furthermore, *P. falciparum* merozoite invasion ligands of the reticulocyte binding-like homolog (Rh) and erythrocyte binding-like antigen (EBA) families are phosphorylated at their cytoplasmic domain by PfCK2 *in vitro* and these modifications seem to play an important role during the RBC invasion process [30,31]. Conditional knockdown (cKD) of PfCK2α expression in 3D7 parasites caused a lethal phenotype related to a defect in merozoite invasion, highlighting that PfCK2α is essential for the propagation of asexual blood stage parasites [31]. Hence, PfCK2 clearly has a variety of substrates and vital roles also in *P. falciparum*, which is in line with the wide range of functions attributed to CK2 in other eukaryotes. Interestingly, PfCK2α can be chemically inhibited by confirmed CK2 inhibitors including CX4945, 3,4,5,6-tetrabromobenzotriazole (TBB) and Quinalizarin in *in vitro* kinase assays with fifty percent inhibitory concentrations (IC_{50}) in the low µM to nM range [11-13]. A kinase-directed inhibitor library screen identified the kinase inhibitor Rottlerin as differentially active against PfCK2 (IC_{50} = 7 µM) compared to human CK2 (IC_{50} > 20 µM), suggesting the possibility of selectively targeting PfCK2 [12]. However, whether CK2 kinase inhibitors block parasite growth in *in vitro* cultures and *in vivo* remains to be determined.

Here, we performed an in-depth functional analysis of PfCK2α in asexual blood stage parasites and during sexual commitment and gametocytogenesis. Our data confirm the importance of PfCK2α in merozoite invasion and intra-erythrocytic dvelopment. Furthermore, we demonstrate its essentiality for gametocyte maturation. In addition, we show that out of four validated CK2 inhibitors tested in *in vitro* kinase inhibition assays, none shows potent activity against parasite multiplication.

Results

CRISPR/Cas9-mediated engineering of transgenic parasite lines to study PfCK2α expression and function

We initially engineered two parasite lines to study PfCK2α. The first line expresses PfCK2α-GFP to investigate the subcellular localisation of PfCK2α expressed at wild type (WT) levels. The second line expresses PfCK2α tagged with a GFP-FKBP/DD destabilization domain fusion, which allows knocking down PfCK2α expression levels by removal of the stabilizing ligand Shield-1 from the culture medium [32,33]. Because one of our aims was to test if PfCK2α has a role in regulating sexual commitment, the PfCK2α-GFP and PfCK2α-GFPDD transgenic lines were generated in NF54 parasites expressing a mScarlet-tagged version of PfAP2-G (NF54/AP2-G-mScarlet) (Brancucci et al., manuscript in preparation). The transcription factor PfAP2-G is known as the master regulator of sexual commitment [34,35] and we previously used parasites expressing GFP-tagged PfAP2-G to mark and distinguish sexually committed from asexual parasites by live cell fluorescence microscopy [36]. Here, we used a two-plasmid CRISPR/Cas9 approach [37] to generate NF54/AP2-G-mScarlet lines expressing C-terminally tagged PfCK2α-GFP or PfCK2α-GFPDD. Successful editing of the *pfck2α* gene and absence of the WT locus was confirmed in both lines by PCR on genomic DNA (gDNA) (Supplementary Figs. 1 and 2). We also detected integration of donor plasmid concatamers downstream of the *pfck2α* locus in at least a subset of parasites in both populations (Supplementary Figs. 1 and 2). Such undesired recombination events have previously been reported in other studies as well [38,39]. However, since the 829 bp 3' homology region (HR) used for homology-directed repair seems to include the native terminator based on published RNA-seq data [40], expression of the modified *pfck2α* genes is likely not compromised by donor plasmid integration (Figs. 1 and 2 and Supplementary Figs. 1-3).

Conditional knockdown of PfCK2α-GFPDD expression has no effect on asexual growth but causes a defect late in gametocytogenesis

In the NF54/AP2-G-mScarlet/CK2α-GFP transgenic line, we investigated the expression and localisation of PfCK2α in asexual blood stage parasites by Western blot and live cell fluorescence imaging. Consistent with previous findings [10,27-29], we show that PfCK2α is expressed throughout the IDC with increased expression in trophozoites and schizonts and localises to both the nucleus and parasite cytoplasm (Fig. 1 and Supplementary Fig. 3). In the NF54/AP2-G-mScarlet/CK2α-GFPDD conditional knockdown (cKD) line, the functionality of the cKD system to regulate PfCK2α expression was confirmed by Western blot and live cell fluorescence imaging, showing a substantial reduction of PfCK2α protein levels upon removal of Shield-1 (-Shield-1) (Fig. 2a and Supplementary Fig. 2).

To identify a potential effect of the depletion of PfCK2α on asexual parasite growth, we performed multiplication assays comparing parasites cultured in presence or absence of Shield-1 (±Shield-1) over two generations by measuring fluorescence intensity of SYBR Green-stained parasites using flow cytometry. We did not observe a significant difference in the multiplication rates of PfCK2α-GFPDD-depleted parasites (–Shield-1) in comparison to the isogenic control population (+Shield-1) (Fig. 2b and Supplementary Fig. 4). This finding is in contrast to those obtained by Tham and colleagues, who observed a dramatic multiplication defect upon conditional depletion of PfCK2α in parasites expressing PfCK2α C-terminally tagged with a triple hemagglutinin (HA) tag fused to DD [31].

We next investigated whether reduction of PfCK2α expression levels affects the ability of parasites to undergo sexual commitment and/or sexual development. To study the potential effect of PfCK2α depletion on sexual commitment, we split synchronous NF54/AP2-G-mScarlet/CK2α-GFPDD ring stage cultures at 0-6 hours post invasion (hpi) and Shield-1 was removed from one of the paired cultures. 18 hours later (18-24 hpi), we induced sexual commitment using serum-free medium (–SerM) [36]. Parasites cultured

on –SerM medium supplemented with 2 mM choline chloride (–SerM/CC), a metabolite known to repress sexual commitment [36], were used as control. Sexual commitment rates were determined in the ring stage progeny by quantifying the proportion of PfAP2-G-mScarlet-positive parasites among all infected RBCs (iRBCs) identified by Hoechst staining. When comparing parasites cultured in presence or absence of Shield-1, no significant difference in sexual commitment rates was observed in either of the two medium conditions (–SerM and –SerM/CC) (Supplementary Fig. S5). We next monitored gametocyte maturation of sexually committed ring stage parasites cultured in presence or absence of Shield-1 over 11 days by visual inspection of Giemsa-stained thin blood smears. To perform these experiments, sexual commitment was induced in parasites previously split (±Shield-1) using –SerM culture medium as described above. The asexual/sexual ring stage progeny was subsequently maintained in culture medium supplemented with serum (+SerM) containing 50 mM N-acetyl-D-glucosamine (GlcNAc) to eliminate asexual parasites and obtain pure gametocyte populations [41]. Whereas the morphology of stage I-IV gametocytes (day 2 to 9) was comparable between NF54/AP2-G-mScarlet/CK2α-GFPDD parasites cultured in presence or absence of Shield-1, most PfCK2α-GFPDD-depleted gametocytes failed to develop into mature stage V gametocytes (day 11), even after prolonged periods of observation (Figs. 3a and 3b). Closer assessment of gametocyte morphology based on three independent gametocyte maturation assays revealed that from day 8 onwards the morphology of PfCK2α-GFPDD-depleted gametocytes changed considerably, resulting in stage IV-type cells with elongated and pointy tips that did not progress further to adopt the typcial stage V morphology observed for +Shield-1 control gametocytes on day 11 (Fig. 3b). Western blot analysis confirmed the efficient depletion of PfCK2α in day 11 gametocytes cultured in absence of Shield-1 (Fig. 3c and Supplementary Fig. 5). To obtain further insight into the functionality and viability of PfCK2α knockdown gametocytes we performed microsphiltration experiments. Microsphiltration experiments allow comparing differences in cell rigidity based on cell retention rates in microsphere filters that

represent an artificial spleen system [42,43]. Previous research has shown that stage I-IV gametocytes are more rigid than mature gametocytes and sequester in tissues such as the bone marrow and spleen and are thus absent from the blood circulation [42,44-46]. In contrast, mature stage V gametocytes become highly deformable, which likely allows them to leave their site of sequestration and re-enter the bloodstream from where they can be taken up by a mosquito vector [42,44,45]. Here, we performed microsphiltration experiments on stage III (day 7) and stage V (day 11) gametocytes by microsphiltration [43]. Our data reveal that gametocytes with depleted PfCK2α expression (–Shield-1) do not undergo a deformability switch since gametocytes on day 11 of development were still retained on the microsphere columns like immature gametocyte stages (Fig. 3d). In contrast, in the matching control population (+Shield-1) only stage III gametocytes were retained on the columns whereas stage V passed through efficiently as expected (Fig. 3d).

Once taken up by an *Anopheles* mosquito, male and female gametocytes become activated by several changes in the environment and consequently develop into gametes. Activation of both male and female gametocytes can be triggered *in vitro* by a drop in temperature and addition of xanthurenic acid (XA) [47] to the culture medium. Gametocyte activation can be observed by a change in shape since gametocytes egress from the iRBC and become spherical in a process termed “rounding up” [48]. Activation of male gametocytes further entails three rapid rounds of genome replication and production of eight male microgametes that can fuse with a female macrogamete to generate a zygote. The egress of eight motile microgametes from the iRBC is termed exflagellation and can be observed and quantified by bright-field microscopy [49,50]. Successful exflagellation was proposed as a suitable proxy for the viability of mature male gametocytes [49]. We observed that the majority of PfCK2α-depleted (-Shield-1) day 11 gametocytes with aberrant morphology (elongated, pointy tips) were unable to round up upon XA-induced activation whereas gametocytes of the matching control (+Shield-1) rounded up as expected (Figs. 3e and 3f). Consistent with this finding, PfCK2α-

depleted day 11 gametocytes were also unable to exflagellate in contrast to the control population grown in presence of Shield-1 (Fig. 3g).

In conclusion, conditional depletion of PfCK2α in NF54/AP2-G-mScarlet/CK2α-GFPDD parasites has no apparent effect on parasite multiplication and on their capacity to undergo and regulate sexual commitment in response to environmental triggers. However, PfCK2α-depleted late stage gametocytes show abnormal morphology, fail to undergo the deformability switch, are severely impaired in the process of rounding up and are unable to exflagellate.

PfCK2α is essential for asexual development

It was previously reported that conditional depletion of PfCK2α leads to a severe multiplication defect, where PfCK2α-depleted parasites completed schizogony but failed to give rise to ring stage progeny likely due to defective merozoite invasion [31]. Unexpectedly, we did not observe this phenotype in our NF54/AP2-G-mScarlet/CK2α-GFPDD cKD line. To address this discrepancy, we generated a conditional knockout (cKO) parasite line based on the DiCre/loxP system [51-53]. We performed two consecutive CRISPR/Cas9-based gene editing steps in NF54::DiCre parasites [51] to insert a loxP-intron/loxPint element [52] into the 5' end and fuse a GFP coding sequence followed by a loxP element to the 3' end of the *pfck2α* gene (NF54::DiCre/CK2α-GFP cKO line) (Supplementary Fig. 6). Successful editing of the *pfck2α* locus and absence of the WT locus was confirmed by PCR on gDNA (Supplementary Fig. 6). We again also detected integration of donor plasmid concatamers downstream of the *pfck2α* locus in a subset of parasites (Supplementary Fig. 6). In this parasite line, the *pfck2α-gfp* coding region can be excised by addition of rapamycin (RAPA) to the culture medium, which activates the DiCre recombinase to recombine the two inserted loxP sites [51]. PCR on gDNA isolated from late schizonts 40 hours after treating ring stage parasites with RAPA revealed the highly efficient excision of the *pfck2α-gfp* gene (Supplementary Fig. 6) and successful depletion of PfCK2α-GFP expression was observed by Western blot analysis and live

cell fluorescence imaging when compared to DMSO-treated control parasites (Fig. 4a). To assess the phenotype of PfCK2α KO parasites, we analysed parasite multiplication by visual inspection of Giemsa-stained blood smears and flow cytometry-based analysis of SYBR green-stained iRBCs (Supplementary Fig. 4). After triggering excision of *pfck2α-gfp* (RAPA-treated) in young ring stages (0-8 hpi), parasites developed similarly compared to the matching control population until the end of schizogony (Fig. 4b) but upon schizont rupture PfCK2α KO merozoites seemed unable to invade RBCs, as suggested by Tham and colleagues after knocking down expression of PfCK2α-3xHADD in 3D7 parasites [31] (Fig. 4c and 4d). A small subset of merozoites was still able to invade new erythrocytes, which was evident by a minor increase in parasitaemia in generation 2 (Figs. 4b, 4c and 4d). Notably, however, these PfCK2α KO progeny parasites arrested at the trophozoite stage and failed to develop further (Fig. 4b and 4c).

To investigate the PfCK2α KO phenotype in more detail, we performed flow cytometry measurements of synchronised parasite cultures at multiple time points during the IDC. Upon excision of *pfck2α-gfp* in young ring stages (0-4 hpi), RAPA-treated and DMSO-treated control parasites simultaneously entered the first round of genome replication at the onset of schizogony (32-36 hpi). However, PfCK2α KO parasites progressed more slowly through schizogony compared to the control population, showing a delay of approximately four hours towards the end of the IDC (44-48 hpi) (Supplementary Figs. 7 and 8). After an additional 10 hours, schizonts had disappeared from both cultures but the ring stage progeny produced by PfCK2α KO parasites was approximately five-fold lower compared to the control population (Supplementary Fig. 7), consistent with the results presented above (Fig. 4c). To confirm that PfCK2α KO parasites are able to release merozoites, we treated late stage schizonts with the PfPKG kinase inhibitor compound 2 (C2), an experimental compound that reversibly arrests schizonts at the very end of the IDC just prior to merozoite egress [54]. After reversing the developmental arrest by washing away C2, merozoite egress was observed for both DMSO-treated

control and RAPA-treated PfCK2α KO schizonts as revealed by both flow cytmetry analysis and inspection of Giemsa-stained blood smears (Supplementary Fig. 7).

In summary, our PfCK2α cKO line confirms the previously suggested essential function of PfCK2α in merozoite invasion and hence proliferation of asexual blood stage parasites [31]. We show that after knocking out *pfck2α* in ring stages, parasites progressed through schizogony more slowly but still produced and released merozoites. While the vast majority of PfCK2α KO merozoites failed to invade RBCs, a small subset of merozoites was still able to invade but were unable to develop past the trophozoite stage. Hence, PfCK2α has essential functions during the IDC in addition to its crucial role for merozoite invasion.

PfCK2α is essential for sexual development

Proteomics as well as transcriptomics data suggest that PfCK2α is expressed throughout sexual development [55,56]. Using the NF54::DiCre/CK2α-GFP cKO parasite line, we investigated the expression and localisation of PfCK2α-GFP during gametocytogenesis on a single cell level by live cell fluorescence imaging. Indeed, we observed PfCK2α-GFP expression throughout gametocyte maturation in all five stages in both the nuclear and cytoplasmic compartments of the parasite (Fig. 5), which is in line with our observations during the IDC (Fig. 1a and Supplementary Fig. 3). Next, we asked if knocking out PfCK2α at the onset of gametocytogenesis has more dramatic consequences for gametocyte maturation compared to knocking down PfCK2α expression in the cKD line (see above). To this end, we induced sexual commitment using –SerM medium [36], excised the *pfck2α-gfp* gene in the subsequent ring stage progeny by treatment with RAPA as described above and allowed gametocyte maturation to proceed in +SerM culture medium supplemented with 50 mM GlcNAc during the first six days. Strikingly, RAPA-treated PfCK2α KO gametocytes showed abnormal morphology during most of gametocyte development when compared to the matching DMSO-treated control (Fig. 6a) and this phenotype was more pronounced

compared to the PfCK2α-GFPDD-depleted gametocytes described above (Fig. 3a). Additional investigation of this phenotype revealed a drastic defect in gametocytogenesis from stage II (day 4 to 5) onwards with most gametocytes failing to develop further (Figs. 6a and 6b). On day 11 of development most PfCK2α KO gametocytes were severely deformed, rounded up or pyknotic in appearance (Figs. 6a and 6b). Furthermore, the gametocytaemia in RAPA-treated populations decreased by 87% (86.4%±4.8) from day 4 to day 11, showing that a large proportion of PfCK2α KO gametocytes died during maturation. In contrast, the corresponding decrease in gametocytaemia in control DMSO-treated populations was only 44% (43.8%±1.3), which is in line with our observations from routine gametocyte cultures and can be explained by normal turnover, for instance due the lysis of iRBCs over time [49]. Microscopy of magnet-purified gametocytes on day 11 of development illustrates the drastic morphological changes and lack of PfCK2α-GFP expression in PfCK2α KO gametocytes when compared to the respective DMSO-treated control (Figs. 6c and 6d).

In contrast to our observations made with NF54/AP2-G-mScarlet/CK2α-GFPDD gametocytes, in which the conditional knockdown of PfCK2α-GFPDD expression does not result in major morphological changes up to day 8 (stage IV) of gametocytogenesis, knocking out the *pfck2α* gene in sexual ring stages leads to dramatic morphological changes and defective cell differentiation already early during gametocytogenesis. In summary, these experiments demonstrate that PfCK2α is not only essential for asexual proliferation but also for sexual parasite development.

Activity of CK2 inhibitors in reducing asexual parasite multiplication

Whereas several studies proposed PfCK2α as an attractive drug target based on *in vitro* kinase inhibition assays using compounds targeting human CK2α [11-13], data on successful inhibition of parasite growth and multiplication by such compounds in cell-based assays is currently missing. To close this knowledge gap, we tested four commercially available cell-permeable and selective ATP-competitive inhibitors of

human CK2α (Quinalizarin, TTP 22, TBB and DMAT) for their ability to reduce or block parasite multiplication in a [^{3}H]-hypoxanthine incorporation assay [57]. Quinalizarin, described as one of the most potent human CK2α inhibitors, was previously reported to block the activity of recombinant PfCK2α *in vitro* with an IC_{50} of 2 µM [11,58]. We identified an IC_{50} of higher than 50 µM for Quinalizarin and at this concentration parasites still multiplied at a rate of about 65%, when compared to the drug-free control culture (Supplementary Fig. 9). Next, we tested TTP 22 that inhibits the human CK2α kinase *in vitro* with an IC_{50} value of 0.1 µM [59]. Like Quinalizarin, TTP 22 performed poorly (IC_{50} > 50 µM) in inhibiting *P. falciparum* parasite multiplication (Supplementary Fig. 9). Finally, we tested the polyhalogenated benzimidazole compound TBB that blocks recombinant human CK2α activity with an IC_{50} of 0.9 µM [60] and DMAT, a structural analog of TBB that shows improved activity and selectivity towards human CK2α [61] . TBB was previously tested on recombinant PfCK2α and shown to block kinase activity with an IC_{50} of 1.5 µM [12]. In our cell-based assay, TBB showed poor activity (IC_{50} > 50 µM) and for DMAT we determined an IC_{50} of 15.8 µM (17.3 µM; 14.4 µM) in inhibiting parasite proliferation (Supplementary Fig. 9).

In summary, we show that four selective inhibitors of human CK2α performed poorly in blocking parasite multiplication in a cell-based assay, despite two of them previously showed promising activity against recombinant PfCK2α in *in vitro* kinase assays.

Discussion

In model eukaryotes, the casein kinase CK2 has been implicated in the phosphorylation of a variety of substrates and executes essential cellular functions [17,22-24]. Similarly, in *P. falciparum* PfCK2 is suggested to phosphorylate a broad range of substrates [10,30,31] and both the regulatory and catalytic kinase subunits are essential for asexual parasite development [10,12,31]. In order to study the function of the catalytic subunit PfCK2α in asexual and sexual development, we generated several transgenic parasites lines using CRISPR/Cas9-based gene editing.

Flow cytometry assays performed using the NF54::DiCre/CK2α-GFP cKO line confirmed the essential role of PfCK2α in merozoite invasion into RBCs [31]. However, whereas the cKO parasite line indeed produced merozoites incapable of invading RBCs, our NF54/AP2-G-mScarlet/CK2α-GFPDD cKD parasite line showed no growth defect upon knocking down PfCK2α expression through Shield-1 removal. This is surprising since Tham and colleagues reported that a very similar cKD line produced in the 3D7 strain (a clonal line of the NF54 strain used in our study), in which the PfCK2α protein is expressed as a 3xHA-DD fusion (PfCK2α-HADD), showed a strong RBC invasion defect [31]. This discrepancy may be explained for instance by higher stability of the PfCK2α-GFPDD protein compared to the PfCK2α-HADD protein in absence of Shield-1, leading to less efficient PfCK2α degradation in our cKD line, or by a slightly higher PfCK2α expression threshold required for successful invasion of 3D7 merozoites. Previous studies have shown that PfCK2 is able to phosphorylate the cytoplasmic tails of both the Rh (Rh2b, Rh4) and EBA (EBA140, EBA175, EBA181) families of invasion ligands using *in vitro* kinase assays [30,31]. However, direct evidence of lack of phosphorylation of these adhesins in PfCK2-depleted parasites *in vivo*, for instance by phosphoproteomics studies, is still missing. Interestingly, however, mutational analyses of mapped CK2 phosphosites in the cytoplasmic tail of Rh4 highlighted their importance in the Rh4-dependent (sialic acid-independent) invasion pathway *in vivo* [31]. Since 3D7, a clone of the NF54 strain used here, relies on Rh4 for RBC invasion [62], it is likely that the invasion

defect in PfCK2α loss-of-function mutants in these strains is indeed due to the lack of PfCK2-dependent phosphorylation of Rh4 [62]. Whether PfCK2 is also required for invasion of parasites employing alternative sialic acid-dependent invasion pathways reliant on EBA family ligands is an interesting question to be addressed in the future, for instance by recapitulating PfCK2α loss-of-function mutants in such strains. In this context it is tempting to speculate that the small proportion of RAPA-treated PfCK2α cKO parasites that successfully invaded RBCs may have employed an Rh4-independent invasion pathway potentially dependent on invasion-ligand phosphorylation by another kinase [31]. Regardless of this hypothesis, the fact that these parasites failed to progress beyond the trophozoite stage suggests that PfCK2 exhibits essential functions during the IDC in addition to its role in merozoite invasion. This is in line with the proposed pleiotropic activity of CK2 and the variety of putative cellular functions identified for PfCK2 in *P. falciparum* [10]. Interestingly, Dastidar and colleagues revealed a potential function of PfCK2 in chromatin assembly and dynamics, DNA replication and mitosis and could show that PfCK2α is able to phosphorylate histones and nucleosome-assembly proteins *in vitro* [10]. Lack of post-translational modifications of important chromatin components and regulators such as histones could for instance lead to impaired DNA damage signaling and hence result in a DNA-damage induced cell cycle arrest [63]. Whether PfCK2 indeed phosphorylates histones and other chromatin components *in vivo* and whether lack of their phosphorylation is also involved in damage sensing and cell cycle arrest in *P. falciparum* has not yet been investigated [64].

We also studied the role of PfCK2α in gametocytes by analyzing both a conditional PfCK2α knockdown line (NF54/AP2-G-mScarlet/CK2α-GFPDD) and a DiCre-inducible PfCK2α knockout line (NF54::DiCre/CK2α-GFP) and demonstrate that PfCK2α is indispensable for gametocytogenesis. To our knowledge, this is the first example of a parasite kinase shown to be essential for sexual development of malaria parasites. The cKD of PfCK2α expression resulted in gametocytes with seemingly normal morphology up to stage IV, but mature crescent-shaped stage V gametocytes with rounded ends,

increased cellular deformability and ability to undergo gamete activation and exflagellation were not formed. In comparison to the PfCK2α cKD line, RAPA-induced *pfck2*α knockout gametocytes showed a more severe phenotype. These gametocytes did not progress past stage II/III of maturation, showed drastic morphological aberrations including lack of elongation and displayed a marked decrease in viability when compared to the DMSO-treated control. Previous research has shown that formation of the inner membrane complex (IMC) and the tightly associated underlying microtubule and F-actin cytoskeletal networks are main drivers of gametocyte shape and elongation during gametocyte maturation [45,65-68]. The nascent IMC and cytoskeletal structures already appear in stage I/II gametocytes and expand over the whole cell body in stage III/IV gametocytes [45,65-68]. At the stage IV to V transition, the microtubule and actin networks are disassembled and this is linked to the rounding up of both ends of the gametocyte [45,65,66,68] and probably also to their capacity to undergo gamete activation and exflagellation. Interestingly, upon conditional knockdown of two different IMC components (PfPHIL1, PfPIP1) gametocytes failed to develop morphologically beyond stage III, displayed aberrant morphology and a lack of elongation and gametocyte viability decreased drastically over time [66]. Moreover, treatment of gametocytes with the microtubule-destabilising compound trifluralin affects gametocyte morphology [69] and exposure to the actin-stabilising agent jasplakinolide causes marked deformation of late stage gametocytes and a complete lack of stage V formation [65]. The morphologically similar developmental defects observed in our PfCK2α knockdown and knockout gametocytes are therefore indicative for a direct or indirect role of PfCK2 in IMC maturation and/or microtubule or actin cytoskeleton dynamics during gametocytogenesis. While experimental evidence for PfCK2-dependent phosphorylation of IMC components is currently lacking, CK2 has been shown to interact directly with tubulin and microtubules in human cells and several *Trypanosoma* species [70-73] and to phosphorylate microtubule-associated proteins [74]. In addition, human CK2 is directly involved in the regulation of microtubule assembly and stability [75] and inhibition of CK2

activity induces alterations to the cytoskeleton and shape of astrocytes and endothelial cells [76]. Moreover, in the apicomplexan parasite *Toxoplasma gondii* phosphorylation of the actin-binding protein toxofilin by a CK2-like activity was shown to be important for the actin-toxofilin interaction and consequently actin dynamics [77].

In contrast to day 11 control gametocytes, PfCK2α knockdown gametocytes retained a high level of cellular rigidity similar to immature stage III gametocytes. While the elaborate IMC and cytoskeletal network structures in the parasite may contribute to the increased rigidity of immature gametocytes, parasite-induced remodeling of the membrane and underlying spectrin and actin networks of the host RBC seems to play a more dominant role in gametocyte rigidification [42,69,78-81]. The deformability switch occurring at the stage IV to V transition is linked to the dephosphorylation and dissociation of the parasite-encoded STEVOR protein from the iRBC membrane [42,79,81] and to the reversal of previously established cytoskeletal rearrangements underneath [69]. Our findings therefore indicate that PfCK2α-depleted stage IV gametocytes are either arrested in development prior to the initiation of the deformability switch or that PfCK2-dependent signaling is required to regulate this process. Given that PfCK2 is not known to be exported into the RBC cytosol, however, the direct phosphorylation of proteins in the iRBC by PfCK2 seems rather unlikely. In summary, our results show that PfCK2 is essential for the morphological and functional maturation of gametocytes and provide circumstantial evidence that PfCK2 may be required for the regulation of IMC biogenesis and cytoskeleton dynamics in the parasite and/or host RBC. Alternatively, it is also conceivable that PfCK2 may be important for the proper control of gene expression during gametocytogenesis. PfCK2 shows prominent nuclear localisation in gametocytes, interacts with chromatin components in asexual parasites [10] and CK2 is known to regulate the activity of transcriptional regulators in yeast [20,21]. Notwithstanding the above hypotheses, the findings and transgenic parasite lines generated in this study will allow for a detailed targeted analysis of PfCK2 function in gametocytes using complementary biochemical, cell biological and high throughput approaches.

The essential roles PfCK2α plays in asexual and sexual development of *P. falciparum* renders this kinase an even more attractive drug target than anticipated previously. A drug specifically targeting *P. falciparum* PfCK2α might therefore combine asexual parasite clearance and transmission-blocking properties. All CK2 kinase-specific motifs have been identified in PfCK2α protein and it shares 65% amino acid sequence identity with its human CK2α orthologue (HsCK2α) [12,25,26]. Despite the high similarity of PfCK2α and HsCK2α, Holland and colleagues (2009) showed by using the CK2 inhibitor Rottlerin that selective inhibition of PfCK2α is achievable [12]. In our study, we tested Quinalizarin. TTP 22, TBB and DMAT for their ability to inhibit parasite multiplication *in vivo*. The IC_{50} concentrations of DMAT and the other three CK2α inhibitors were found to be more than 1,000-fold higher (15.8µM; >50µM; >50µM; >50µM) when compared with the antimalarial control drugs Chloroquine and Artesunate (9.1 nM; 6.8 nM). Several previous studies have shown inhibition of recombinant or purified PfCK2α at low IC_{50} values [11-13]. Unfortunately, however, it becomes evident that these promising results from *in vitro* kinase assays do not translate into activity of the tested compounds against parasite growth and multiplication. Nevertheless, screening for *Plasmodium*-specific and membrane-permeable PfCK2α inhibitors and lead optimisation may still be worthwhile pursuing, given that PfCK2α is essential for both asexual proliferation and gametocytogenesis. Of note, several CK2 inhibitors have been produced or are under development for use in cancer treatment [82-84] and compounds stemming from these campaigns may be a promising starting point to discover compounds targeting PfCK2α *in vivo*.

Materials and Methods

Parasite culture

Culturing and sorbitol synchronization of *P. falciparum* NF54 parasites[85] were performed as described [86,87]. For routine parasite culture, parasites were propagated in AB+ or B+

human RBCs (Blood Donation Center, Zurich, Switzerland) at a hematocrit of 5% in complete parasite culture medium (PCM) consisting of 10.44 g/liter RPMI-1640, 25 mM HEPES, 100 µM hypoxanthine, 24 mM sodium bicarbonate and 0.5% AlbuMAX II (Gibco #11021-037). The medium was further complemented with 2 mM choline chloride (Sigma #C7527) to suppress sexual commitment [36], Parasite cultures were incubated at 37°C in air-tight containers filled with malaria gas (4% CO_2, 3% O_2, 93% N_2).

Cloning of transfection constructs

CRISPR/Cas9-based genome engineering of parasites was performed using a two-plasmid approach as previously described [37]. This system is based on co-transfection of a suicide and donor plasmid. The suicide plasmid contains expression cassettes for the Cas9 enzyme, the single guide RNA (sgRNA) and either the human dihydrofolate reductase (hDHFR) or blasticidin deaminase (BSD) resistance markers (pH-gC, pB-gC). In two additional suicide plasmids the resistance marker hDHFR or BSD is further fused to the negative selection marker yeast cytosine deaminase/uridyl phosphoribosyl transferase (yFCU) (pHF-gC or pBF-gC). A pD-derived donor plasmid is needed for homology-directed repair of the Cas9-induced DNA lesion [37]. For this study we generated an additional suicide plasmid, pY-gC, containing the yeast dihydroorotate dehydrogenase (yDHODH) resistance cassette conferring resistance to DSM1 [88] instead of the h*dhfr(-fcu)* or *bsd(-fcu)* cassettes. The y*dhodh* resistance cassette was amplified from the pUF1-Cas9 plasmid [89] by producing two overlapping PCR fragments (F1 and F2) in order to mutate the *BsaI* restriction enzyme recognition site present in the y*dhodh* coding sequence. To this end, we inserted a single point mutation in the complementary reverse and forward primers used to amplify the F1 and F2 fragments, respectively. F1 was amplified using primers Y_F and B_R and F2 using primers B_F and Y_R. The pY-gC plasmid was then generated in a three-fragment Gibson assembly joining the *BamHI* and *XhoI* fragment of the pBF-gC plasmid [37] and the two overlapping y*dhodh* fragments F1 and F2. The resulting pY-gC plasmid and the previously published suicide plasmids

pHF-gC and pBF-gC [37] were used for insertion of sgRNA-encoding sequences targeting the 3' end (sgt_*ck2a_1*) or 5' end (sgt_*ck2a_2*) of *pfckα*. For this purpose, complementary oligonucleotides were annealed and the resulting double-stranded fragments were ligated into the *BsaI* digested pY-gC, pBF-gC or pHF-gC plasmids using T4 DNA ligase generating the pY-gC_*ck2α_tag,* pBF-gC_*ck2α_tag*, and pHF-gC_*ck2α-cKO* plasmids.

Plasmids pBF-gC_*ck2a_tag* and pY-gC_*ck2a_tag,* both encoding the sgt_*ck2a_1* sgRNA, were used to generate parasites expressing PfCK2α-GFP and PfCK2α-GFPDD, respectively. The corresponding donor plasmids pD_*ck2α-gfp* and pD_*ck2α-gfpdd* were produced by assembling four PCR fragments in a Gibson reaction using (a) the plasmid backbone amplified from pUC19 using primers PCRA_F and PCRA_R [37], (b) the 5' homology region (HR) amplified from NF54 gDNA using primers H1_F and H1_R, (c) the *gfp* (primers G_F and G_R) or *gfpdd* (primers G_F and GD_R) sequence amplified from pHcamGDV1-GFP-DD [37], and (d) the 3' HR amplified from NF54 gDNA using primers H2_F and H2_R (pD_*ck2α-gfp*) or H2D_F and H2_R (pD_*ck2α-gfpdd*).

The NF54::DiCre/CK2α_cKO parasite line was generated in two consecutive transfection steps using the suicide plasmids pBF-gC_*ck2α_tag* (encoding the sgt_*ck2a_1* sgRNA) and pHF-gC_*ck2α-cKO* (encoding the sgt_*ck2a_2* sgRNA) and the corresponding donor plasmids pD_*ck2α-cKO1* and pD_*ck2α-cKO2*. The pD_*ck2α-cKO1* plasmid was generated in a three-fragment Gibson reaction joining (a) the plasmid backbone amplified from pUC19 using primers PCRA_F and PCRA_R as previously described [37], (b) the 5' HR followed by the in-frame *gfp* coding sequence amplified from pD_*ck2α-gfp* using primers H1_F and loxP1_R, and (c) the 3' HR amplified from pD_*ck2α-gfp* using primers loxP1_F and H2_R. The loxP sequence [53] downstream to the *gfp* coding sequence was introduced into the primers loxP1_F and loxP1_R used to amplify the corresponding PCR fragments. The second donor plasmid pD_*ck2α-cKO2* was generated by assembling four fragments in a Gibson reaction using (a) the plasmid backbone amplified from pUC19 using primers PCRA_F and PCRA_R [37], (b) the 5' HR

amplified from NF54 gDNA using primers H3_F and H3_R, (c) the *sera2* intron:loxP fragment (loxPint) [52] amplified from the pD_SIP2xGFP plasmid (I. Niederwieser, unpublished) using primers loxPINT_F and loxPINT_R, and (d) the 3' HR amplified from NF54 gDNA using primers H4_F and H4_R. All oligonucleotides used for the cloning of transfection constructs and annealing of sgRNA-encoding sequences are listed in Supplementary Table 1.

Transfection and transgenic cell lines

P. falciparum transfection using the CRISPR/Cas9 suicide and donor constructs was performed as explained previously [37]. All transgenic cell lines were generated by transfecting parasites with 50 µg each of the suicide plasmid and the respective donor plasmid. Depending on the suicide plasmid used (pBF-gC_*ck2α_tag*, pHF-gC_*ck2α-cKO*, pY-gC_*ck2α_tag*) the transfected populations were treated either with 2.5 µg/mL blasticidin-S-hydrochloride (for 10 subsequent days), 4 nM WR99210 (for six subsequent days) or 1.5 µM DSM1 (for 10 subsequent days). The plasmid combinations pBF-gC_*ck2_tag*/pD_*ck2α-gfp* and pY-gC_*ck2_tag*/pD_*ck2α-gfpdd* were transfected into the NF54/AP2-G-mScarlet line to generate the NF54/AP2-G-mScarlet/CK2α-GFP and NF54/AP2-G-mScarlet/CK2α-GFPDD lines, respectively. The NF54/AP2-G-mScarlet line has previously been engineered to express the PfAP2-G transcription factor as a C-terminal mScarlet fusion (Brancucci et al, manuscript in preparation). After transfection, NF54/AP2-G-mScarlet/CK2α-GFPDD parasites were constantly cultured on 625 nM Shield-1 to stabilize expressed PfCK2α-GFPDD proteins. The NF54::DiCre parasite line [51] (kind gift from Moritz Treeck) was transfected first with the pBF-gC_*ck2α_tag* suicide and pD_*ck2α-cKO1* donor plasmids. After successful selection of the transgenic line a second transfection step using the pHF-gC_*ck2α-cKO* suicide and pD_*ck2α-cKO2* donor plasmids was performed to obtain the NF54::DiCre/CK2α_cKO parasite line carrying loxP elements at the 5' and 3' end of the *pfck2α-gfp* gene. Transgenic populations were routinely obtained 2-3 weeks after transfection and correct editing of the engineered loci

was confirmed by PCR on gDNA. Because editing of the targeted locus was 100% efficient in all transgenic lines based on the diagnostic PCR results, the lines were not cloned out prior to further investigation. Schematic maps of the transfection plasmids, transgenic loci, PCR primer binding sites and results of the diagnostic PCRs can be found in Supplementary Figs. 1, 2 and 6. Sequences of all primers used for diagnostic PCR reactions are listed in Supplementary Table 2.

Fluorescence microscopy

For live cell fluorescence microscopy, parasite DNA was stained using 5 µg/ml Hoechst (Merck) and the microscopy slides were mounted using Vectashield (Vector Laboratories). Slides were viewed using the Leica DM5000 B fluorescence microscope (20x, 40x and 63x objectives and 10x or 16x microscope magnification) and images were acquired using the Leica DFC345 FX camera and the Leica application suite software (LAS 4.9.0). Images were processed using Adobe Photoshop CC 2018. In each experiment, identical settings were used for both image acquisition and processing.

Western blot analysis

Parasites were released from iRBCs using 0.15% saponin in PBS and incubation on ice for 10 min. Parasite pellets were washed in ice-cold PBS 2-3 times until the supernatant was clear. An Urea/SDS lysis buffer (8 M Urea, 5% SDS, 50 mM Bis-Tris, 2 mM EDTA, 25 mM HCl, pH 6.5) complemented with 1x protease inhibitor cocktail (Merck) and 1 mM DTT was used to obtain whole cell protein lysates. Nuclear and cytoplasmic lysates were obtained by first lysing parasite pellets in cytoplasmic lysis buffer (20 mM Hepes, 10 mM KCl, 1 mM EDTA, 0.65% Igepal) complemented with 1x protease inhibitor cocktail (Merck) and 1 mM DTT. The resulting supernatant containing the cytoplasmic protein fraction was collected. The nuclear pellet was washed in cytoplasmic lysis buffer until the supernatant was clear followed by lysis of the nuclei in Urea/SDS buffer. Protein lysates were separated either on NuPage 3-8% Tris-Acetate or 5-12% Bis-Tris gels

(Novex, Qiagen) using MES running buffer (Novex, Qiagen). Upon protein transfer, the nitrocellulose membrane was blocked in 5% milk in PBS/0.1% Tween (PBS-Tween) for 30 min. Protein detection was performed using mouse mAb α-GFP (1:1,000) (Roche Diagnostics #11814460001), mAb α-PfGAPDH (1:20,000) [90] and rabbit α-PfHP1 (1:5,000) [91] diluted in blocking buffer. Incubation with the first antibody was performed at 4°C over night. After 3-4 washing steps in PBS/Tween, the membrane was incubated for at least 1 hour using the secondary antibody goat α-mouse IgG (H&L)-HRP (1:10,000) (GE healthcare #NXA931) or donkey anti-rabbit IgG (H&L) HRP (1:5,000) (GE Healthcare #NA934) diluted in blocking buffer. Membranes were subsequently washed 3-4 times using PBS/Tween before signal detection. The α-GFP/α-GAPDH blot shown in Supplementary Fig. 3 was stripped in 2% SDS, 62.5 mM Tris-HCl (pH 6.8), 100mM β-mercaptoethanol for 30 min at 60°C and re-probed with rabbit α-PfHP1 antibodies [91].

Quantification of sexual commitment rates

NF54/AP2-G-mScarlet/CK2α-GFPDD parasites were synchronised to a 6-hour time window by two consecutive treatments with 5% sorbitol. In the following replication cycle, parasite cultures were exposed to ±Shield at 0-6 hpi and either –SerM (sexual commitment inducing) or –SerM/CC (sexual commitment inhibiting) conditions at 18-24 hpi (2% parasitaemia, 2.5% hematocrit) [36]. After a 48-hour incubation period, cultures were resuspended and 30 µL of this suspension was mixed with 50 µL PBS containing 8.1 µM DNA dye Hoechst 33342. Cells were incubated in a 96 well plate for 30 min, pelleted at 300 g for 5 min, washed twice using 200 µL PBS and resuspended in 180 µL PBS. 30 µL of this cell suspension were mixed with 150 µL PBS within wells of a clear-bottom 96 well plate (Greiner CELLCOAT microplate 655948, Poly-D-Lysine, flat µClear bottom) and cells were allowed to settle for 30 min prior to imaging. Images were acquired using an ImageXpress Micro widefield high content screening system (Molecular Devices) in combination with MetaXpress software (version 6.5.4.532, Molecular Devices) and a Sola SE solid state white light engine (Lumencor). Filtersets

for Hoechst (Ex: 377/50 nm, Em: 447/60 nm) and mScarlet (Ex: 543/22 nm, Em: 593/40 nm) were used with exposure times of 80 ms and 600 ms, respectively. 36 sites per well were imaged using a Plan-Apochromat 40x objective. Images were analysed using the MetaXpress software and Hoechst-positive as well as mScarlet-positive parasites were quantified allowing for the calculation of sexual commitment rates corresponding to the percentage of mScarlet-positive parasites amongst all parasites (Hoechst-positive).

Gametocyte cultures

Synchronous gametocyte populations were needed for morphological assessment, extraction of protein samples, microsphiltration experiments and exflagellation assays. For this purpose, sexual commitment was induced by culturing trophozoites in –SerM medium for 24 hours as described above [36]. After reinvasion (0-6 hpi) (asexual/sexual ring stages), parasites were cultured in PCM containing 10% human serum instead of 0.5% AlbuMAX II (+SerM). At 24-30 hpi (trophozoites and stage I gametocytes), 50 mM N-acetyl-D-glucosamine (Sigma) was added to the +SerM medium (+SerM/GlcNAc) for six consecutive days to eliminate asexual parasites [41]. From day seven onwards, gametocytes were cultured in +SerM and daily medium changes were performed on a 37°C heating plate.

Exflagellation assays

On day 14 of gametocyte maturation, stage V gametocytes were subjected to exflagellation assays [49]. In brief, gametocytes were activated using a temperature drop (from 37 °C to 22 °C/room temperature) and 100 µM xanthurenic acid (XA) for 15 min. Subsequently, the number of exflagellation centers and total RBCs per mL of culture were determined by bright-field microscopy using a Neubauer chamber. Gametocytaemia was determined by visual inspection of Giemsa-stained blood smears before exflagellation thus allowing to calculate exflagellation rates as the number of exflagellating parasites per total number of gametocytes.

Microsphiltration experiments

Synchronous NF54/AP2-G-mScarlet/CK2α-GFPDD parasites were split at 0-6 hpi and cultured either in presence of 0.675 µM Shield-1 (+Shield-1) or in absence of Shield-1 (-Shield-1). Induction of sexual commitment using –SerM medium and culturing of gametocytes using +SerM and +SerM/GlcNAc media was performed as described above. Microsphiltration experiments were conducted in two independent biological replicates as published previously [43] on day seven (stage III) and day 11 (stage V) of gametocyte development. In detail, aliquots of the cultures were transferred to 15 mL tubes and the hematocrit was lowered to 1.5% by addition of fresh PCM. Tubes were kept in a water bath at 37°C to inhibit rounding up and exflagellation of mature stage V gametocytes. For each condition (±Shield-1), six microsphiltration columns (technical replicates) were loaded. Per column, 600 µL of cell suspension was injected and washed through the column with 5 mL +SerM medium at 60 mL/h using a medical grade pump (Syramed µSP6000, Acromed AG, Switzerland). To determine gametocyte retention rates, Giemsa-stained thin smears were prepared before and after the samples were subjected to microsphiltration. The input gametocytaemia before passing the sample through the column ("UP" gametocytaemia) was determined as the average count from two Giemsa-stained blood smears. The gametocytaemia in the microsphiltration elution fractions ("DOWN" gametocytaemia) was determined from Giemsa-stained thin smears prepared from each individual elution tube. At least 1,000 total RBCs were counted per slide. Gametocyte retention rates were calculated as 1-("DOWN" gametocytaemia/ "UP" gametocytaemia). The blood smears prepared from the day 11 input samples additionally served as quality control to confirm that stage V gametocytes did not undergo rounding up and exflagellation.

Flow cytometry analysis

For parasite multiplication assays, synchronous NF54/AP2-G-mScarlet/CK2α-GFPDD parasites were split at 0-6 hpi (0.2 % parasitaemia) and cultured either in presence of

675 nM Shield-1 (+Shield-1) or in absence of Shield-1 (-Shield-1) during the whole duration of the assay. Synchronous NF54::DiCre/CK2α-GFP cKO parasites were split at 0-6 hpi (0.2% parasitaemia) and exposed for four hours to 100 nM RAPA to trigger excision of the *pfck2α-gfp* gene (DMSO was added to the control population instead of RAPA) [51,53]. Subsequently, the RBCs were washed once in PCM/2mM choline chloride and resuspended in this medium for onward *in vitro* culture. After 18 hours (18-24 hpi) parasite DNA was stained at 37°C for 30 min using SYBR Green DNA stain (1:10,000, Invitrogen) to determine the starting parasitaemia (day 1). Flow cytometry measurements were repeated on day 3 (generation 2) and day 5 (generation 3) for NF54/AP2-G-mScarlet/CK2α-GFPDD parasites (±Shield-1) and on day 3 (generation 2), day 5 (generation 3) and day 7 (generation 4) for NF54::DiCre/CK2α-GFP cKO parasites (RAPA/DMSO).

To analyse parasite progression through schizogony and merozoite egress, synchronized NF54::DiCre/CK2α-GFP cKO parasites (0-4 hpi) were treated with RAPA or DMSO as explained above. Samples were collected for DNA content analysis starting at 20-24 hpi up to 20-24 hpi in the following generation. For merozoite egress experiments, 1 µM compound 2 (C2) was added to the cultures from 36-40 hpi onwards to prevent schizont rupture [54]. At 50-54 hpi to 54-58 hpi, C2-arrested segmented schizont cultures were split and one half was directly inactivated by fixation in 4% formaldehyde/0.0075% glutaraldehyde (C2-arrested control). The other half of the sample was washed once in culture medium to remove C2, resuspended in culture medium and rotated at 37°C to allow merozoite egress and invasion for 45 min (replicate 1) and 45 min and 90 min (replicate 2) before samples were fixed in 4% formaldehyde/0.0075% glutaraldehyde. Fixed samples were washed twice in PBS and permeabilized for 15 min in PBS containing 0.1%Triton X-100 and 0.1 mg/ml RNase A. Fixed and permeabilized cells were washed twice in PBS and stained with SYBR Green DNA stain (1:5,000, Invitrogen) for 30 min.

Fluorescence intensities were measured using the MACS Quant Analyzer 10 (200,000

RBCs measured per sample). Data were analysed using the FlowJo_v10.6.1 software. Gating was performed to remove small debris (smaller than cell size), doublets (single measurement event consisting of two cells) and to separate uninfected from infected RBCs (using an uninfected RBC control sample) based on their SYBR green intensity (Supplementary Fig. 4). For the results presented in Supplementary Fig. 7b an additional gate was set to separate mature schizonts from remaining iRBCs based on SYBR green intensity (Supplementary Fig. 8).

Drug assays

Activity of CK2 kinase inhibitors on asexual NF54 parasite multiplication was determined using an [^{3}H] hypoxanthine incorporation assay [57]. The mean IC_{50} values were determined from two biological replicate assays. One of the biological replicates was performed in two technical replicates. Quinalizarin (CAS Number 81-61-8, Sigma #Q2763), TBB (CAS Number 17374-26-4, Selleckchem #S5265), DMAT (CAS Number 749234-11-5, Sigma #SML2044) and TTP 22 (CAS Number 329907-28-0, TOCRIS #4432), were resuspended in DMSO and used at a maximum starting concentration of 50 µM. In a six-step serial dilution, the compound concentration was diluted to half in each step to span a concentration range between 50 µM and 0.8 µM. Chloroquine (CAS Number 50-63-5, Sigma #C6628) and Artesunate (CAS Number 88495-63-0, Mepha #11665) served as control antimalarial compounds with a starting concentration of 193 nM and 26 nM, respectively. In a six-step serial dilution, the Chloroquine and Artesunate concentrations were diluted to half in each step to span a concentration range between 193 nM and 3 nM or between 26 nM and 0.4 nM, respectively.

Statistics and Reproducibility

All data from assays quantifying parasite multiplication, sexual commitment rates, morphological gametocyte staging, gametocyte deformability or exflagellation rates are represented as means with error bars defining the standard deviation. All data were derived from at least three biological replicate experiments. Statistical significance was

determined using paired or unpaired Student's *t* test as indicated in the figure legends. The exact number of biological replicates performed per experiment and the number of cells analysed per sample are indicated in the figure legends and in Supplementary Dataset 1. Data were analysed and plotted using RStudio Version 1.1.456 and package ggplot2.

Data availability

The source data for all the graphs and charts in the main figures are present in Supplementary Data 1 and any other remaining information can be available from the corresponding author upon reasonable request.

References

1 World Health Organisation. *World Malaria Report 2019*. 1-185 (WHO Press, 2019).

2 Talman, A. M., Clain, J., Duval, R., Ménard, R. & Ariey, F. Artemisinin Bioactivity and Resistance in Malaria Parasites. *Trends in Parasitology* **35**, 953-963, doi:https://doi.org/10.1016/j.pt.2019.09.005 (2019).

3 Sokhna, C., Ndiath, M. O. & Rogier, C. The changes in mosquito vector behaviour and the emerging resistance to insecticides will challenge the decline of malaria. *Clinical Microbiology and Infection* **19**, 902-907, doi:https://doi.org/10.1111/1469-0691.12314 (2013).

4 Ferguson, F. M. & Gray, N. S. Kinase inhibitors: the road ahead. *Nature reviews. Drug discovery* **17**, 353-377, doi:10.1038/nrd.2018.21 (2018).

5 Paquet, T. *et al.* Antimalarial efficacy of MMV390048, an inhibitor of Plasmodium phosphatidylinositol 4-kinase. *Sci Transl Med* **9**, doi:10.1126/scitranslmed.aad9735 (2017).

6 Alam, M. M. *et al.* Validation of the protein kinase Pfm>CLK3 as a multistage cross-species malarial drug target. *Science* **365**, eaau1682, doi:10.1126/science.aau1682 (2019).

7 Lucet, I. S., Tobin, A., Drewry, D., Wilks, A. F. & Doerig, C. Plasmodium kinases as targets for new-generation antimalarials. *Future medicinal chemistry* **4**, 2295-2310, doi:10.4155/fmc.12.183 (2012).

8 McNamara, C. W. *et al.* Targeting Plasmodium PI(4)K to eliminate malaria. *Nature* **504**, 248-253, doi:10.1038/nature12782 (2013).

9 Sinxadi, P. *et al.* Safety, tolerability, pharmacokinetics and antimalarial activity of the novel Plasmodium phosphatidylinositol 4-kinase inhibitor MMV390048 in healthy volunteers. *Antimicrobial Agents and Chemotherapy* **64**, AAC.01896-01819, doi:10.1128/AAC.01896-19 (2020).

10 Dastidar, E. G. *et al.* Involvement of Plasmodium falciparum protein kinase CK2 in the chromatin assembly pathway. *BMC Biol* **10**, 5, doi:10.1186/1741-7007-10-5 (2012).

11 Graciotti, M. *et al.* Malaria protein kinase CK2 (PfCK2) shows novel mechanisms of regulation. *PLoS One* **9**, e85391, doi:10.1371/journal.pone.0085391 (2014).
12 Holland, Z., Prudent, R., Reiser, J. B., Cochet, C. & Doerig, C. Functional analysis of protein kinase CK2 of the human malaria parasite Plasmodium falciparum. *Eukaryot. Cell* **8**, 388-397 (2009).
13 Ruiz-Carrillo, D. *et al.* The protein kinase CK2 catalytic domain from Plasmodium falciparum: crystal structure, tyrosine kinase activity and inhibition. *Scientific reports* **8**, 7365, doi:10.1038/s41598-018-25738-5 (2018).
14 Litchfield, D. W. Protein kinase CK2: structure, regulation and role in cellular decisions of life and death. *Biochem J* **369**, 1-15, doi:10.1042/BJ20021469 (2003).
15 Bian, Y. *et al.* Global screening of CK2 kinase substrates by an integrated phosphoproteomics workflow. *Scientific reports* **3**, 3460, doi:10.1038/srep03460 (2013).
16 Franchin, C. *et al.* Re-evaluation of protein kinase CK2 pleiotropy: new insights provided by a phosphoproteomics analysis of CK2 knockout cells. *Cellular and Molecular Life Sciences* **75**, 2011-2026, doi:10.1007/s00018-017-2705-8 (2018).
17 Meggio, F. & Pinna, L. A. One-thousand-and-one substrates of protein kinase CK2? *Faseb j* **17**, 349-368, doi:10.1096/fj.02-0473rev (2003).
18 Jung, S.-I. *et al.* Yeast casein kinase 2 governs morphology, biofilm formation, cell wall integrity, and host cell damage of Candida albicans. *PLOS ONE* **12**, e0187721, doi:10.1371/journal.pone.0187721 (2017).
19 Filhol, O. & Cochet, C. Protein Kinase CK2 in Health and Disease. *Cellular and Molecular Life Sciences* **66**, 1830-1839, doi:10.1007/s00018-009-9151-1 (2009).
20 Bhat, W., Boutin, G., Rufiange, A. & Nourani, A. Casein kinase 2 associates with the yeast chromatin reassembly factor Spt2/Sin1 to regulate its function in the repression of spurious transcription. *Mol Cell Biol* **33**, 4198-4211, doi:10.1128/mcb.00525-13 (2013).
21 Burns, L. T. & Wente, S. R. Casein kinase II regulation of the Hot1 transcription factor promotes stochastic gene expression. *The Journal of biological chemistry* **289**, 17668-17679, doi:10.1074/jbc.M114.561217 (2014).
22 Lou, D. Y. *et al.* The Alpha Catalytic Subunit of Protein Kinase CK2 Is Required for Mouse Embryonic Development. *Molecular and Cellular Biology* **28**, 131-139, doi:10.1128/MCB.01119-07 (2008).
23 Hermosilla, G. H., Tapia, J. C. & Allende, J. E. Minimal CK2 activity required for yeast growth. *Mol Cell Biochem* **274**, 39-46, doi:10.1007/s11010-005-3112-2 (2005).
24 Padmanabha, R., Chen-Wu, J. L., Hanna, D. E. & Glover, C. V. Isolation, sequencing, and disruption of the yeast CKA2 gene: casein kinase II is essential for viability in Saccharomyces cerevisiae. *Mol Cell Biol* **10**, 4089-4099, doi:10.1128/mcb.10.8.4089 (1990).
25 Ward, P., Equinet, L., Packer, J. & Doerig, C. Protein kinases of the human malaria parasite Plasmodium falciparum: the kinome of a divergent eukaryote. *BMC Genomics* **5**, 79 (2004).
26 Anamika, Srinivasan, N. & Krupa, A. A genomic perspective of protein kinases in Plasmodium falciparum. *Proteins* **58**, 180-189, doi:10.1002/prot.20278 (2005).
27 Pease, B. N. *et al.* Global analysis of protein expression and phosphorylation of three stages of Plasmodium falciparum intraerythrocytic development. *J Proteome Res* **12**, 4028-4045, doi:10.1021/pr400394g (2013).
28 Florens, L. *et al.* A proteomic view of the Plasmodium falciparum life cycle. *Nature* **419**, 520-526 (2002).
29 Le Roch, K. G. *et al.* Discovery of gene function by expression profiling of the malaria parasite life cycle. *Science* **301**, 1503-1508, doi:10.1126/science.1087025 (2003).

30 Engelberg, K. *et al.* Specific phosphorylation of the PfRh2b invasion ligand of Plasmodium falciparum. *Biochem. J* **452**, 457-466, doi:BJ20121694 [pii];10.1042/BJ20121694 [doi] (2013).
31 Tham, W. H. *et al.* Plasmodium falciparum Adhesins Play an Essential Role in Signalling and Activation of Invasion into Human Erythrocytes. *PLoS. Pathog* **11**, e1005343, doi:10.1371/journal.ppat.1005343 [doi];PPATHOGENS-D-14-02241 [pii] (2015).
32 Banaszynski, L. A., Chen, L. C., Maynard-Smith, L. A., Ooi, A. G. & Wandless, T. J. A rapid, reversible, and tunable method to regulate protein function in living cells using synthetic small molecules. *Cell* **126**, 995-1004 (2006).
33 Armstrong, C. M. & Goldberg, D. E. An FKBP destabilization domain modulates protein levels in Plasmodium falciparum. *Nat. Methods* **4**, 1007-1009 (2007).
34 Sinha, A. *et al.* A cascade of DNA-binding proteins for sexual commitment and development in Plasmodium. *Nature* **507**, 253-257, doi:10.1038/nature12970 (2014).
35 Kafsack, B. F. C. *et al.* A transcriptional switch underlies commitment to sexual development in malaria parasites. *Nature* **507**, 248-252, doi:10.1038/nature12920 (2014).
36 Brancucci, N. M. B. *et al.* Lysophosphatidylcholine Regulates Sexual Stage Differentiation in the Human Malaria Parasite Plasmodium falciparum. *Cell* **171**, 1532-1544 e1515, doi:10.1016/j.cell.2017.10.020 (2017).
37 Filarsky, M. *et al.* GDV1 induces sexual commitment of malaria parasites by antagonizing HP1-dependent gene silencing. *Science* **359**, 1259-1263, doi:359/6381/1259 [pii];10.1126/science.aan6042 [doi] (2018).
38 Walker, M. P. & Lindner, S. E. Ribozyme-mediated, multiplex CRISPR gene editing and CRISPR interference (CRISPRi) in rodent-infectious Plasmodium yoelii. **294**, 9555-9566, doi:10.1074/jbc.RA118.007121 (2019).
39 Mogollon, C. M. *et al.* Rapid Generation of Marker-Free P. falciparum Fluorescent Reporter Lines Using Modified CRISPR/Cas9 Constructs and Selection Protocol. *PLoS. ONE* **11**, e0168362, doi:10.1371/journal.pone.0168362 [doi];PONE-D-16-31427 [pii] (2016).
40 Toenhake, C. G. *et al.* Chromatin Accessibility-Based Characterization of the Gene Regulatory Network Underlying Plasmodium falciparum Blood-Stage Development. *Cell Host Microbe* **23**, 557-569 e559, doi:10.1016/j.chom.2018.03.007 (2018).
41 Fivelman, Q. L. *et al.* Improved synchronous production of Plasmodium falciparum gametocytes in vitro. *Mol. Biochem. Parasitol* **154**, 119-123 (2007).
42 Tiburcio, M. *et al.* A switch in infected erythrocyte deformability at the maturation and blood circulation of Plasmodium falciparum transmission stages. *Blood* **119**, e172-e180, doi:blood-2012-03-414557 [pii];10.1182/blood-2012-03-414557 [doi] (2012).
43 Lavazec, C. *et al.* Microsphiltration: a microsphere matrix to explore erythrocyte deformability. *Methods Mol Biol* **923**, 291-297, doi:10.1007/978-1-62703-026-7_20 (2013).
44 Aingaran, M. *et al.* Host cell deformability is linked to transmission in the human malaria parasite Plasmodium falciparum. *Cell Microbiol* **14**, 983-993, doi:10.1111/j.1462-5822.2012.01786.x [doi] (2012).
45 Dearnley, M. K. *et al.* Origin, composition, organization and function of the inner membrane complex of Plasmodium falciparum gametocytes. *J Cell Sci* **125**, 2053-2063, doi:10.1242/jcs.099002 (2012).
46 Joice, R. *et al.* Plasmodium falciparum transmission stages accumulate in the human bone marrow. *Sci. Transl. Med* **6**, 244re245, doi:6/244/244re5 [pii];10.1126/scitranslmed.3008882 [doi] (2014).
47 Billker, O., Shaw, M. K., Margos, G. & Sinden, R. E. The roles of temperature, pH and mosquito factors as triggers of male and female gametogenesis of Plasmodium berghei in vitro. *Parasitology* **115 (Pt 1)**, 1-7 (1997).

48 Sinden, R. E., Canning, E. U., Bray, R. S. & Smalley, M. E. Gametocyte and gamete development in Plasmodium falciparum. *Proc. R. Soc. Lond B Biol. Sci* **201**, 375-399 (1978).
49 Delves, M. J. *et al.* Routine in vitro culture of P. falciparum gametocytes to evaluate novel transmission-blocking interventions. *Nat. Protoc* **11**, 1668-1680, doi:nprot.2016.096 [pii];10.1038/nprot.2016.096 [doi] (2016).
50 Templeton, T. J., Keister, D. B., Muratova, O., Procter, J. L. & Kaslow, D. C. Adherence of erythrocytes during exflagellation of Plasmodium falciparum microgametes is dependent on erythrocyte surface sialic acid and glycophorins. *J. Exp. Med* **187**, 1599-1609 (1998).
51 Tiburcio, M. *et al.* A Novel Tool for the Generation of Conditional Knockouts To Study Gene Function across the Plasmodium falciparum Life Cycle. *MBio* **10**, doi:10.1128/mBio.01170-19 (2019).
52 Jones, M. L. *et al.* A versatile strategy for rapid conditional genome engineering using loxP sites in a small synthetic intron in Plasmodium falciparum. *Sci. Rep* **6**, 21800, doi:srep21800 [pii];10.1038/srep21800 [doi] (2016).
53 Collins, C. R. *et al.* Robust inducible Cre recombinase activity in the human malaria parasite Plasmodium falciparum enables efficient gene deletion within a single asexual erythrocytic growth cycle. *Mol. Microbiol* **88**, 687-701, doi:10.1111/mmi.12206 [doi] (2013).
54 Taylor, H. M. *et al.* The malaria parasite cyclic GMP-dependent protein kinase plays a central role in blood-stage schizogony. *Eukaryot. Cell* **9**, 37-45, doi:EC.00186-09 [pii];10.1128/EC.00186-09 [doi] (2010).
55 Young, J. A. *et al.* The Plasmodium falciparum sexual development transcriptome: a microarray analysis using ontology-based pattern identification. *Mol. Biochem. Parasitol* **143**, 67-79 (2005).
56 Lasonder, E. *et al.* Integrated transcriptomic and proteomic analyses of P. falciparum gametocytes: molecular insight into sex-specific processes and translational repression. *Nucleic Acids Res* **44**, 6087-6101, doi:gkw536 [pii];10.1093/nar/gkw536 [doi] (2016).
57 Snyder, C., Chollet, J., Santo-Tomas, J., Scheurer, C. & Wittlin, S. In vitro and in vivo interaction of synthetic peroxide RBx11160 (OZ277) with piperaquine in Plasmodium models. *Exp. Parasitol* **115**, 296-300 (2007).
58 Cozza, G. *et al.* Quinalizarin as a potent, selective and cell-permeable inhibitor of protein kinase CK2. *Biochemical Journal* **421**, 387-395, doi:10.1042/BJ20090069 (2009).
59 Golub, A. G. *et al.* Synthesis and biological evaluation of substituted (thieno[2,3-d]pyrimidin-4-ylthio)carboxylic acids as inhibitors of human protein kinase CK2. *European journal of medicinal chemistry* **46**, 870-876, doi:10.1016/j.ejmech.2010.12.025 (2011).
60 Sarno, S. *et al.* Selectivity of 4,5,6,7-tetrabromobenzotriazole, an ATP site-directed inhibitor of protein kinase CK2 ('casein kinase-2'). *FEBS Lett* **496**, 44-48, doi:10.1016/s0014-5793(01)02404-8 (2001).
61 Pagano, M. A. *et al.* 2-Dimethylamino-4,5,6,7-tetrabromo-1H-benzimidazole: a novel powerful and selective inhibitor of protein kinase CK2. *Biochemical and biophysical research communications* **321**, 1040-1044, doi:10.1016/j.bbrc.2004.07.067 (2004).
62 Stubbs, J. *et al.* Molecular Mechanism for Switching of P. falciparum Invasion Pathways into Human Erythrocytes. *Science* **309**, 1384-1387, doi:10.1126/science.1115257 (2005).
63 Rossetto, D., Avvakumov, N. & Côté, J. Histone phosphorylation: a chromatin modification involved in diverse nuclear events. *Epigenetics* **7**, 1098-1108, doi:10.4161/epi.21975 (2012).
64 Lee, A. H., Symington, L. S. & Fidock, D. A. DNA repair mechanisms and their biological roles in the malaria parasite Plasmodium falciparum. *Microbiol. Mol. Biol. Rev* **78**, 469-486, doi:78/3/469 [pii];10.1128/MMBR.00059-13 [doi] (2014).

65 Hliscs, M. *et al.* Organization and function of an actin cytoskeleton in Plasmodium falciparum gametocytes. *Cell Microbiol* **17**, 207-225, doi:10.1111/cmi.12359 (2015).
66 Parkyn Schneider, M. *et al.* Disrupting assembly of the inner membrane complex blocks Plasmodium falciparum sexual stage development. *PLoS Pathog* **13**, e1006659, doi:10.1371/journal.ppat.1006659 (2017).
67 Kono, M. *et al.* Evolution and architecture of the inner membrane complex in asexual and sexual stages of the malaria parasite. *Mol. Biol. Evol* **29**, 2113-2132, doi:mss081 [pii];10.1093/molbev/mss081 [doi] (2012).
68 Sinden, R. E. Gametocytogenesis of Plasmodium falciparum in vitro: an electron microscopic study. *Parasitology* **84**, 1-11 (1982).
69 Dearnley, M. *et al.* Reversible host cell remodeling underpins deformability changes in malaria parasite sexual blood stages. *Proc Natl Acad Sci U S A* **113**, 4800-4805, doi:10.1073/pnas.1520194113 (2016).
70 Faust, M., Schuster, N. & Montenarh, M. Specific binding of protein kinase CK2 catalytic subunits to tubulin. *FEBS Letters* **462**, 51-56, doi:https://doi.org/10.1016/S0014-5793(99)01492-1 (1999).
71 Serrano, L., Hernández, M. A., Díaz-Nido, J. & Avila, J. Association of casein kinase II with microtubules. *Experimental Cell Research* **181**, 263-272, doi:https://doi.org/10.1016/0014-4827(89)90200-0 (1989).
72 Boscan, B. E. *et al.* Interaction of tubulin and protein kinase CK2 in Trypanosoma equiperdum. *Zeitschrift fur Naturforschung. C, Journal of biosciences* **72**, 459-465, doi:10.1515/znc-2017-0019 (2017).
73 De Lima, A. R. *et al.* Tight binding between a pool of the heterodimeric alpha/beta tubulin and a protein kinase CK2 in Trypanosoma cruzi epimastigotes. *Parasitology* **132**, 511-523, doi:10.1017/s0031182005009352 (2006).
74 Avila, J., Ulloa, L., Gonzalez, J., Moreno, F. & Diaz-Nido, J. Phosphorylation of microtubule-associated proteins by protein kinase CK2 in neuritogenesis. *Cell Mol Biol Res* **40**, 573-579 (1994).
75 Lim, A. C., Tiu, S. Y., Li, Q. & Qi, R. Z. Direct regulation of microtubule dynamics by protein kinase CK2. *J Biol Chem* **279**, 4433-4439, doi:10.1074/jbc.M310563200 (2004).
76 Kramerov, A. A. *et al.* Treatment of cultured human astrocytes and vascular endothelial cells with protein kinase CK2 inhibitors induces early changes in cell shape and cytoskeleton. *Mol Cell Biochem* **349**, 125-137, doi:10.1007/s11010-010-0667-3 (2011).
77 Delorme, V., Cayla, X., Faure, G., Garcia, A. & Tardieux, I. Actin dynamics is controlled by a casein kinase II and phosphatase 2C interplay on Toxoplasma gondii Toxofilin. *Mol. Biol. Cell* **14**, 1900-1912 (2003).
78 Neveu, G. & Lavazec, C. Erythrocyte Membrane Makeover by Plasmodium falciparum Gametocytes. *Front Microbiol* **10**, 2652, doi:10.3389/fmicb.2019.02652 (2019).
79 Naissant, B. *et al.* Plasmodium falciparum STEVOR phosphorylation regulates host erythrocyte deformability enabling malaria parasite transmission. *Blood* **127**, e42-53, doi:10.1182/blood-2016-01-690776 (2016).
80 Tiburcio, M., Sauerwein, R., Lavazec, C. & Alano, P. Erythrocyte remodeling by Plasmodium falciparum gametocytes in the human host interplay. *Trends Parasitol* **31**, 270-278, doi:S1471-4922(15)00041-0 [pii];10.1016/j.pt.2015.02.006 [doi] (2015).
81 Ramdani, G. *et al.* cAMP-Signalling Regulates Gametocyte-Infected Erythrocyte Deformability Required for Malaria Parasite Transmission. *PLoS. Pathog* **11**, e1004815, doi:10.1371/journal.ppat.1004815 [doi];PPATHOGENS-D-14-02393 [pii] (2015).
82 Hanif, I. M., Hanif, I. M., Shazib, M. A., Ahmad, K. A. & Pervaiz, S. Casein Kinase II: An attractive target for anti-cancer drug design. *The International Journal of*

Biochemistry & Cell Biology **42**, 1602-1605, doi:https://doi.org/10.1016/j.biocel.2010.06.010 (2010).
83 Lian, H. *et al.* Protein Kinase CK2, a Potential Therapeutic Target in Carcinoma Management. *Asian Pacific journal of cancer prevention : APJCP* **20**, 23-32, doi:10.31557/apjcp.2019.20.1.23 (2019).
84 Siddiqui-Jain, A. *et al.* CX-4945, an orally bioavailable selective inhibitor of protein kinase CK2, inhibits prosurvival and angiogenic signaling and exhibits antitumor efficacy. *Cancer Res* **70**, 10288-10298, doi:10.1158/0008-5472.Can-10-1893 (2010).
85 Delemarre, B. J. & van der Kaay, H. J. [Tropical malaria contracted the natural way in the Netherlands]. *Ned. Tijdschr. Geneeskd* **123**, 1981-1982 (1979).
86 Lambros, C. & Vanderberg, J. P. Synchronization of Plasmodium falciparum erythrocytic stages in culture. *J. Parasitol* **65**, 418-420 (1979).
87 Jensen, J. B. & Trager, W. Plasmodium falciparum in culture: establishment of additional strains. *Am J Trop Med Hyg* **27**, 743-746, doi:10.4269/ajtmh.1978.27.743 (1978).
88 Ganesan, S. M. *et al.* Yeast dihydroorotate dehydrogenase as a new selectable marker for Plasmodium falciparum transfection. *Molecular and biochemical parasitology* **177**, 29-34, doi:10.1016/j.molbiopara.2011.01.004 (2011).
89 Ghorbal, M. *et al.* Genome editing in the human malaria parasite Plasmodium falciparum using the CRISPR-Cas9 system. *Nat. Biotechnol* **32**, 819-821, doi:nbt.2925 [pii];10.1038/nbt.2925 [doi] (2014).
90 Daubenberger, C. A. *et al.* The N'-terminal domain of glyceraldehyde-3-phosphate dehydrogenase of the apicomplexan Plasmodium falciparum mediates GTPase Rab2-dependent recruitment to membranes. *Biol Chem* **384**, 1227-1237, doi:10.1515/bc.2003.135 (2003).
91 Brancucci, N. M. B. *et al.* Heterochromatin protein 1 secures survival and transmission of malaria parasites. *Cell Host. Microbe* **16**, 165-176, doi:S1931-3128(14)00258-3 [pii];10.1016/j.chom.2014.07.004 [doi] (2014).

Acknowledgements

We thank M. Treeck for providing the NF54::DiCre line. This work was supported by funding from the Swiss National Science Foundation (BSCGI0_157729, 31003A_169347, 310030_184785) and the Rudolf Geigy Foundation.

Author Contributions

E.H. and O.G. generated all transgenic parasite lines, designed and performed experiments, analysed and interpreted data. E.H. prepared illustrations and wrote the manuscript. A.P. designed, performed and analysed microsphiltration experiments and NF54/AP2-G-mScarlet/CK2α-GFPDD gametocyte maturation assays. M. W. performed and analysed NF54::DiCre/CK2α-GFP cKO flow cytometry experiments. N.M.B.B and H.P.B helped designing and supervised experiments and provided resources. C.S. helped designing, performing and analysing drug assays and S.W. supervised these experiments and provided resources. T.S.V. conceived of the study, designed and supervised experiments, provided resources and wrote the manuscript. All authors contributed to editing of the manuscript.

Competing Interests

The authors declare no competing interests.

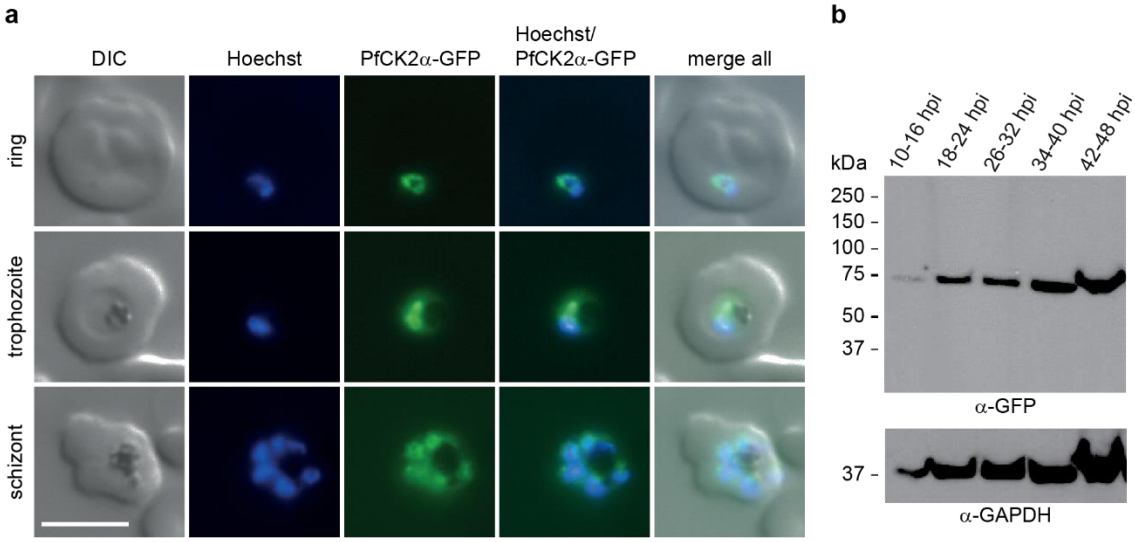

Fig 1 Expression and localisation of PfCK2α in NF54/AP2-G-mScarlet/CK2α-GFP parasites. a Expression and localisation of PfCK2α-GFP in ring, trophozoite and schizont stage parasites by live cell fluorescence imaging. Representative images are shown. Nuclei were stained with Hoechst. DIC, differential interference contrast. Scale bar = 5 µm. **b** Western blot analysis showing expression of PfCK2α-GFP at several time points during the IDC. Protein lysates derived from an equal number of parasites were loaded per lane. MW PfCK2α-GFP = 66.8 kDa, MW loading control PfGAPDH = 36.6 kDa.

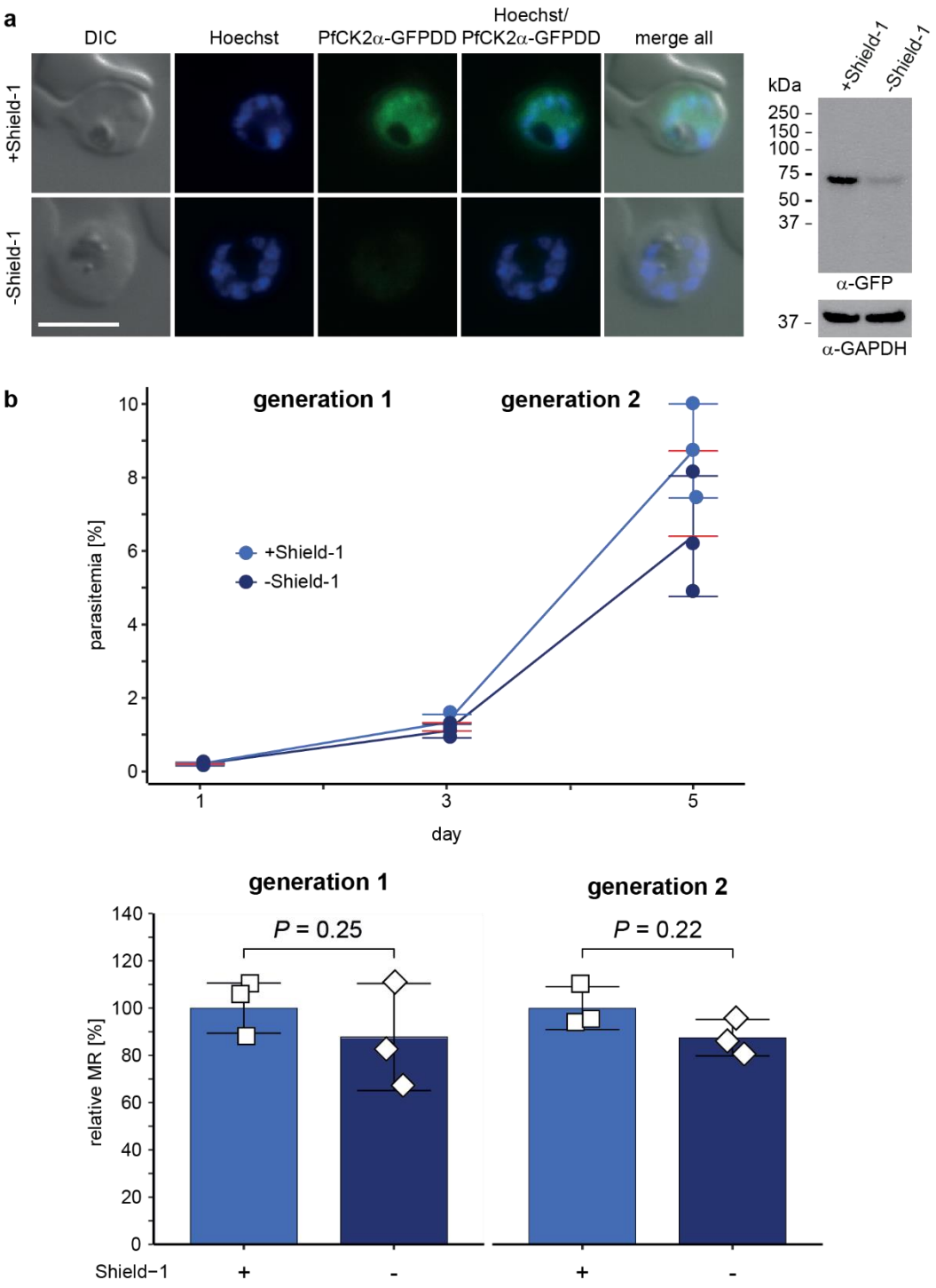

Fig 2 PfCK2α depletion in NF54/AP2-G-mScarlet/CK2α-GFPDD parasites has no effect on asexual parasite multiplication. a Expression of PfCK2α-GFPDD in schizonts cultured in presence (+Shield-1) and absence (-Shield-1) of Shield-1 by live cell fluorescence imaging and Western blot analysis. Parasites were split (±Shield-1) 40 hours before sample collection. Representative images are shown. Nuclei were stained with Hoechst. DIC, differential interference contrast. Scale bar = 5 µm. For Western blot

analysis, protein lysates derived from an equal number of parasites were loaded per lane. MW PfCK2α-GFPDD = 78.7 kDa, MW loading control PfGAPDH = 36.6 kDa. **b** Flow cytometry data showing the increase in parasitaemia (top) and parasite multiplication rates (bottom) in two subsequent generations of NF54/AP2-G-mScarlet/CK2α-GFPDD parasites cultured under protein-degrading (-Shield-1; dark blue) and protein-stabilizing (+Shield-1; light blue) conditions. Parasites were split (±Shield-1) at 0-6 hpi, 18 hours before the first measurement (day 1). The means ±s.d. (error bars) of three biological replicates are shown. Data points for individual replicates are represented by colored circles (top) or open squares (bottom). Differences in parasite multiplication rates were compared using a paired two-tailed Student's t test (*P* values are indicated above the graphs). MR, multiplication rate.

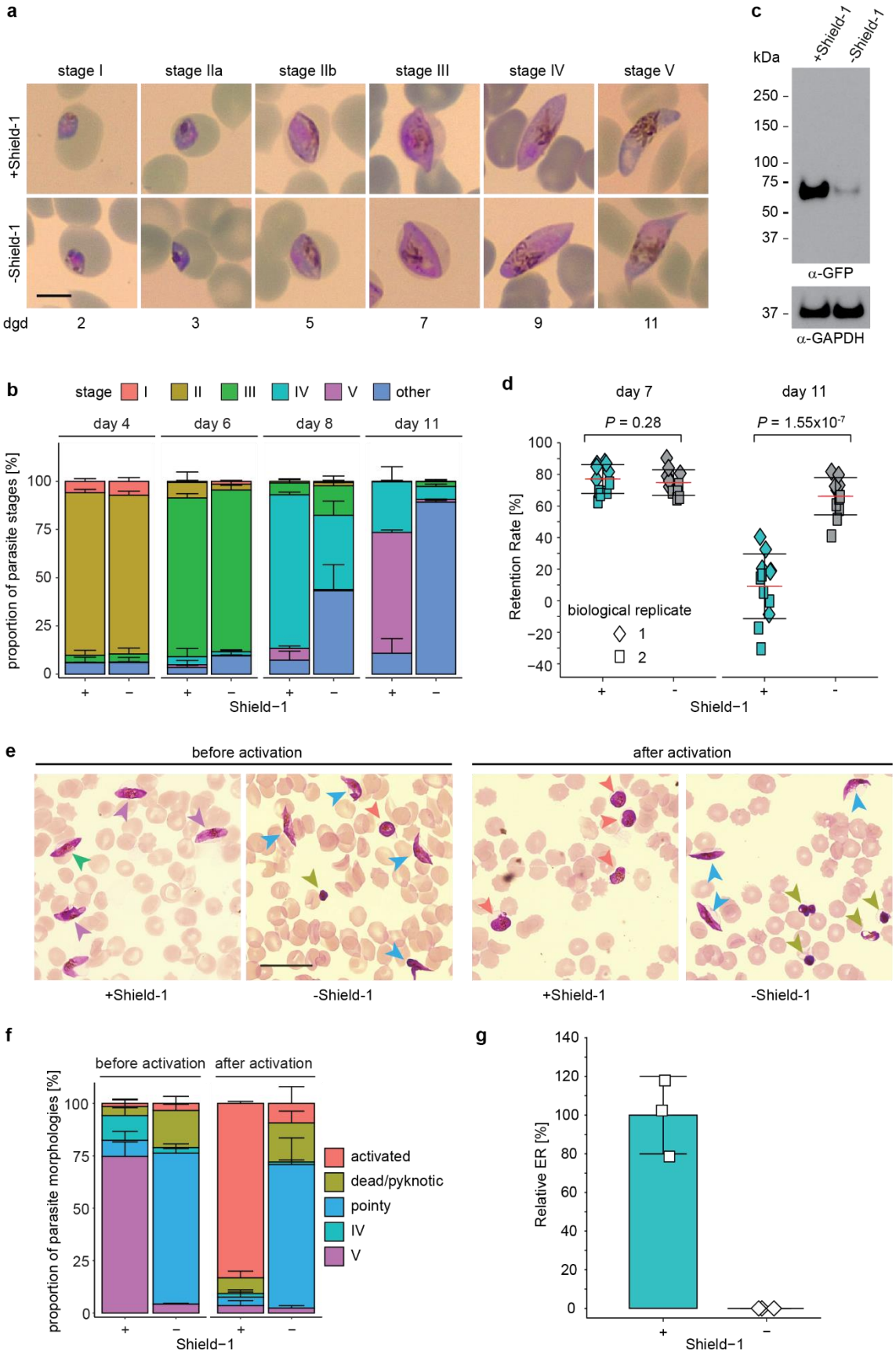

Fig 3 PfCK2α depletion in NF54/AP2-G-mScarlet/CK2α-GFPDD parasites prevents formation of mature stage V gametocytes. a Representative images of

morphologically distinct sexual stages (stage I-V) cultured in presence (+Shield-1) and absence (-Shield-1) of Shield-1 over 11 days of gametocyte development. Parasites were split (±Shield-1) at 0-6 hpi and transferred to –SerM at 18-24 hpi to induce sexual commitment [36] and subsequently cultured in presence or absence of Shield-1 until stage V gametocytes were obtained. From the ring stage progeny (asexual/sexual ring stages) until day six of gametocytogenesis, parasites were cultured in presence of 50 mM GlcNAc to eliminate asexual parasites [41]. Images were taken from Giemsa-stained thin blood smears. Scale bar = 5 µm. dgd, day of gametocyte development. **b** Proportion of gametocyte stages on day four, six, eight and eleven of gametocytogenesis in populations cultured in presence (+) and absence (–) of Shield-1, as assessed by morphological classification and counting from Giemsa-stained thin blood smears. Deformed gametocytes that could not be classified as one of the five distinct morphological stages I-V were classified as "other" (see colour code above the graph). Gametocytes were cultured as described above in panel a. The means ±s.d. (error bars) of three biological replicates are shown. At least 100 gametocytes were classified per sample (see Supplementary Dataset 1 for exact numbers). **c** Expression of PfCK2α-GFPDD in stage V gametocytes cultured in presence presence (+Shield-1) and absence (-Shield-1) of Shield-1 by Western blot analysis. Gametocytes were cultured as described above in panel a. Protein lysates derived from an equal number of parasites were loaded per lane. MW PfCK2α-GFPDD = 78.7 kDa, MW loading control PfGAPDH = 36.6 kDa. **d** Retention rates of gametocytes cultured in presence (+Shield-1; turqoise) or absence (-Shield-1; grey) of Shield-1 on day seven (stage III) and day 11 (stage V) of development as determined from microsphiltration experiments [43]. Gametocytes were cultured as described above in panel a. The means ±s.d. (error bars) of two biological replicates performed in five to six technical replicates each are shown. Individual data points of the technical replicates from the first and second biological replicate experiments are represented by coloured diamonds and squares, respectively. Differences in gametocyte retention rates were compared using the unpaired two-tailed

Student's t test (*P* values are indicated above the graphs). **e** Representative overview images showing gametocytes on day 14 of development before and after (10 min) the activation of gametogenesis (XA and drop in temperature) and cultured in presence (+Shield-1) or absence (-Shield-1) of Shield-1. Gametocytes were cultured as described above in panel a. Images were taken from Giemsa-stained thin blood smears. Coloured arrowheads mark the different morphological types observed according to the key provided in panel f below. Scale bar = 20 μm. **f** Proportion of gametocytes with stage IV (turquoise), stage V (purple), "pointy" (blue), activated (salmon) or dead/pyknotic (green) morphology on day 11 of gametocytogenesis in parasites cultured in presence presence (+) and absence (–) of Shield-1 before and 10 min after activation of gametogenesis by XA. Gametocytes were allocated to one of the five different classes of morphology based on visual inspection of Giemsa-stained thin blood smears. Gametocytes were cultured as described above in panel a. The means ±s.d. (error bars) of four biological replicates are shown. At least 100 gametocytes were classified per sample (see Supplementary Dataset 1 for exact numbers). **g** Relative exflagellation rates of gametocytes cultured in presence presence (+) and absence (–) of Shield-1. Gametocytes were cultured as described above in panel a. The means ±s.d. (error bars) of three biological replicates are shown and individual data points are represented by open squares. ER, exflagellation rate.

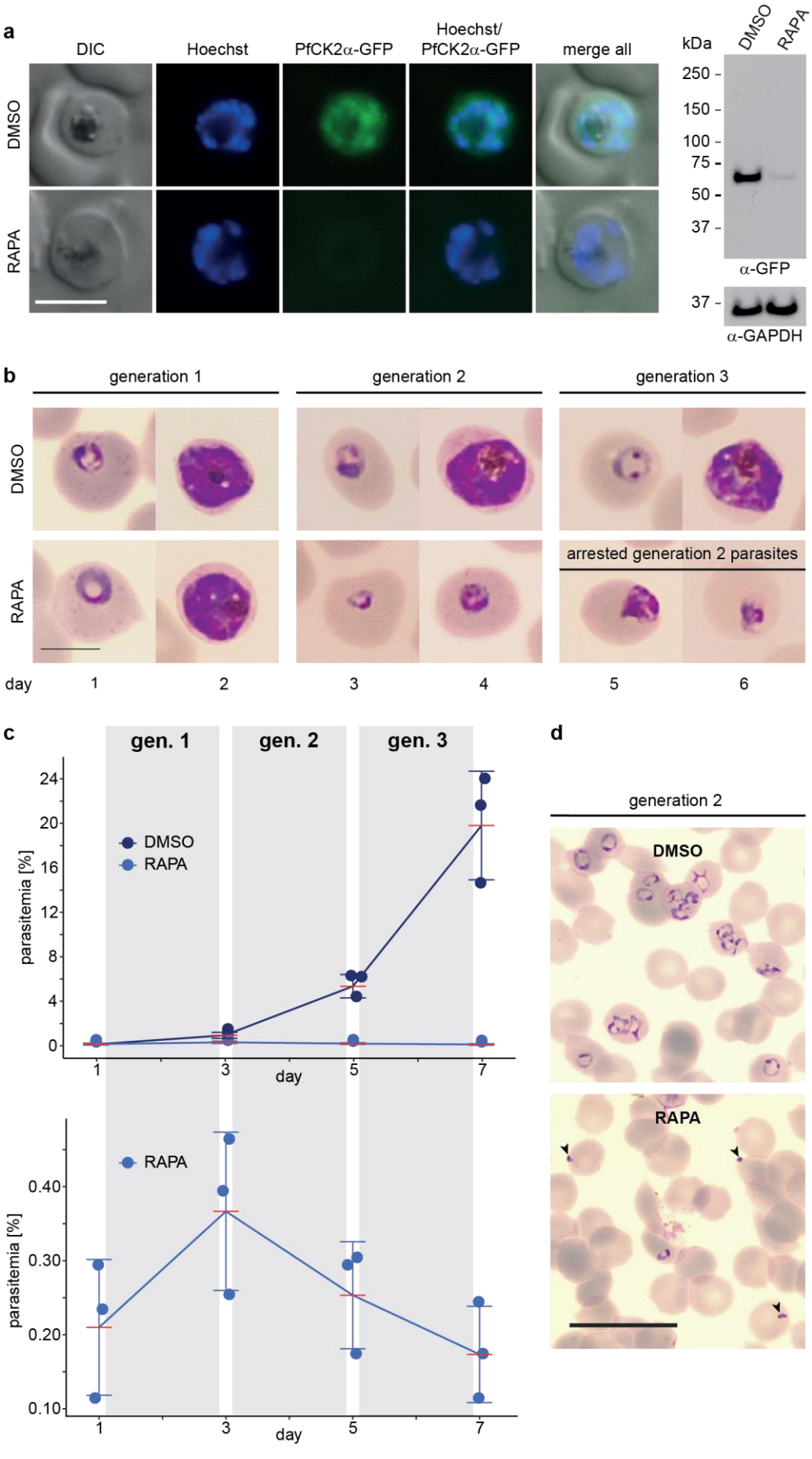
a
DIC
Hoechst
PfCK2α-GFP
Hoechst/
PfCK2α-GFP
merge all
DMSO
RAPA
kDa
DMSO
RAPA
250
150
100
75
50
37
α-GFP
37
α-GAPDH
b
generation 1
generation 2
generation 3
DMSO
RAPA
arrested generation 2 parasites
day
1
2
3
4
5
6
c
gen. 1
gen. 2
gen. 3
DMSO
RAPA
parasitemia [%]
day
RAPA
parasitemia [%]
day
d
generation 2
DMSO
RAPA

Fig 4 Deletion of *pfck2α* in NF54::DiCre/CK2α-GFP cKO parasites leads to a dramatic defect in asexual parasite multiplication. a Expression of PfCK2α-GFP in NF54::DiCre/CK2α-GFP KO (RAPA) and control (DMSO) schizonts by live cell fluorescence imaging and Western blot analysis. Parasites were split and exposed for four hours to either RAPA or DMSO 40 hours before sample collection. Representative images are shown. Nuclei were stained with Hoechst. DIC, differential interference contrast. Scale bar = 5 µm. For Western blot analysis, protein lysates derived from an equal number of parasites were loaded per lane. MW PfCK2α-GFP = 66.8 kDa, MW loading control PfGAPDH = 36.6 kDa. RAPA, rapamycin. **b** Representative images of NF54::DiCre/CK2α-GFP KO (RAPA) and control (DMSO) parasites taken from Giemsa-stained thin blood smears prepared daily for six consecutive days. Scale bar = 5 µm. RAPA, rapamycin. **c** Top: Flow cytometry data showing the increase in parasitaemia over three subsequent generations in NF54::DiCre/CK2α-GFP KO (RAPA; light blue) and control (DMSO; dark blue) parasites. Bottom: Zoom-in on the marginal increase in parasitaemia observed for the RAPA-treated population. Parasites were split at 0-6 hpi and treated for four hours with either RAPA or DMSO 18 hours before the first measurement (day 1). The means ±s.d. (error bars) of three biological replicates are shown. Data points for individual replicates are represented by closed circles. RAPA, rapamycin. gen., generation. **d** Representative overview images showing parasites in the progeny of RAPA- and DMSO-treated NF54::DiCre/CK2α-GFP parasites (0-8 hpi; generation 2) taken from Giemsa-stained thin blood smears. Black arrowheads indicate merozoites unable to invade new RBCs. Scale bar = 20 µm.

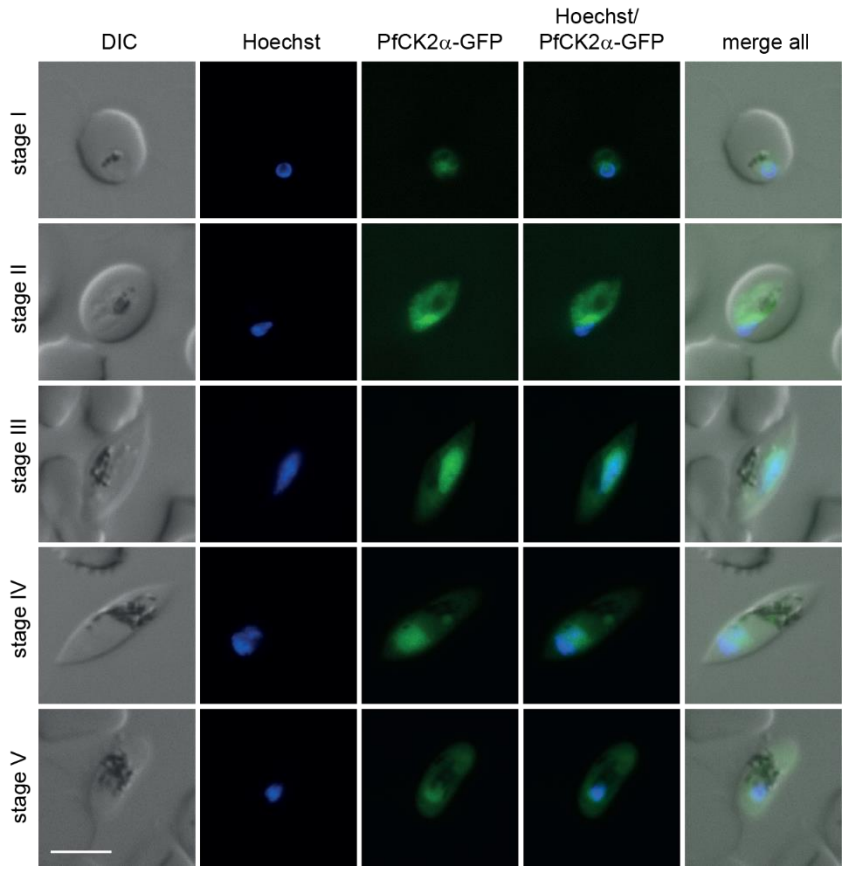

Fig 5 Expression and localisation of PfCK2α-GFP during gametocytogenesis (stage I-V) by live cell fluorescence imaging. Representative images are shown. Nuclei were stained with Hoechst. DIC, differential interference contrast. Scale bar = 5 µm.

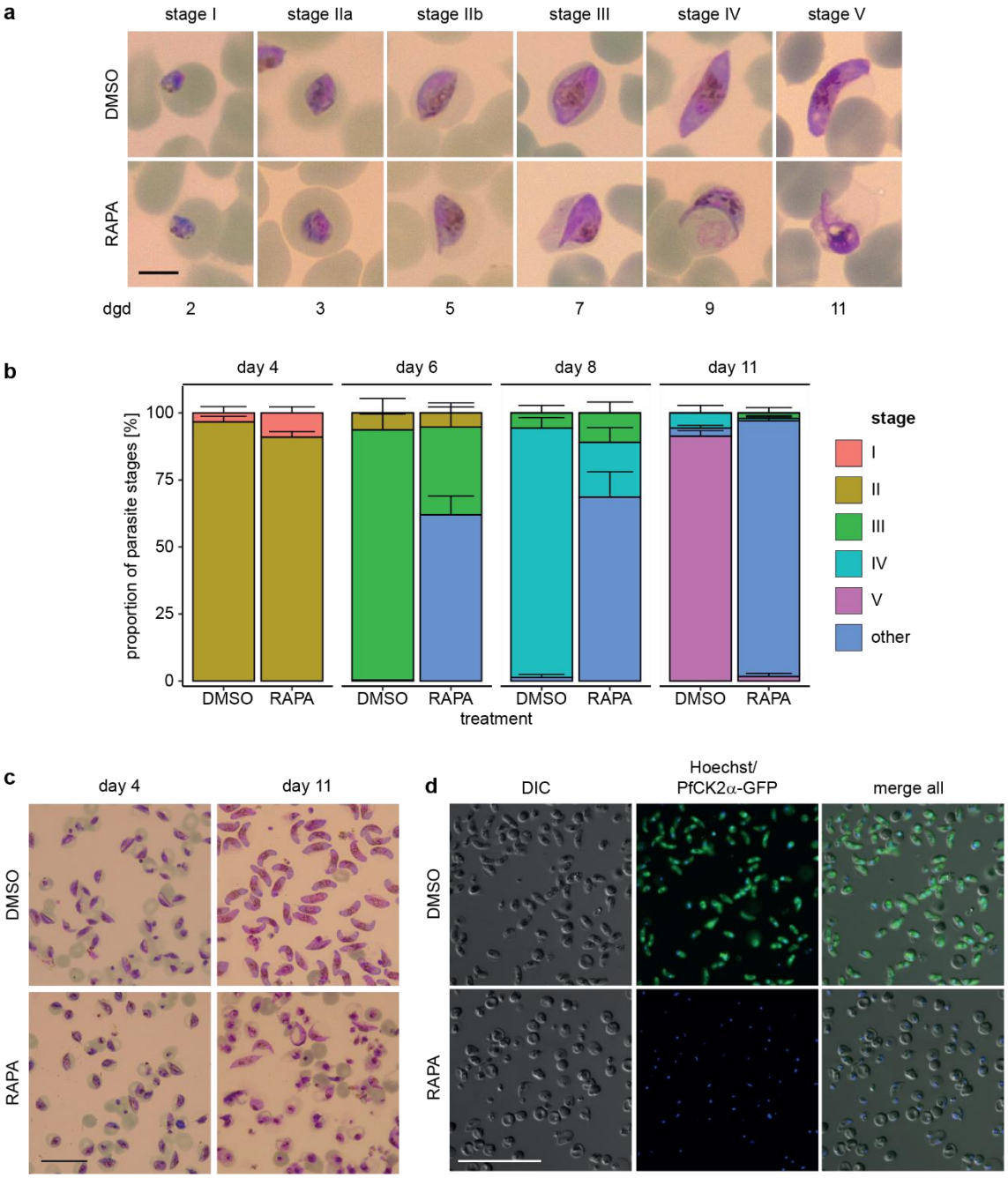

Fig 6 Deletion of *pfck2α* in NF54::DiCre/CK2α-GFP cKO parasites leads to defective gametocytogenesis. a Representative images of NF54::DiCre/CK2α-GFP KO (RAPA) and control (DMSO) gametocytes over 11 days of development taken from Giemsa-stained thin blood smears. Parasites were induced for sexual commitment using –SerM medium [36] and the ring stage progeny was split at 0-6 hpi, treated for four hours with either DMSO or RAPA and then cultured in presence of 50 mM GlcNAc for six consecutive days to eliminate asexual parasites [41]. Subsequently, gametocytes were cultured in +SerM medium until stage V gametocytes were observed in the DMSO-

treated control population. Scale bar = 5 µm. RAPA, rapamycin. dgd, day of gametocyte development. **b** Proportion of gametocyte stages on day four, six, eight and eleven of gametocytogenesis in PfCK2α-GFP KO (RAPA) and control (DMSO) populations as assessed by morphological classification and counting from Giemsa-stained thin blood smears. Deformed gametocytes that could not be classified as one of the five distinct morphological stages I-V were classified as “other” (see colour code above the graph). Gametocytes were cultured as described above in panel a. The means ±s.d. (error bars) of three biological replicates are shown. 100 gametocytes were classified per sample. **c** Representative overview images showing magnet-purified gametocytes on day 4 and day 11 of development in PfCK2α-GFP KO (RAPA) and control (DMSO) gametocytes. Images were taken from Giemsa-stained thin blood smears. Gametocytes were cultured as described above in panel a. Scale bar = 20 µm. RAPA, rapamycin. **d** Representative live cell fluorescence images showing an overview of magnet-purified NF54::DiCre/CK2α-GFP KO (RAPA) and control (DMSO) gametocytes on day 11 of development. Gametocytes were cultured as described above in panel a. Scale bar = 50 µm. RAPA, rapamycin.

Supplementary Information

The catalytic subunit of *Plasmodium falciparum* casein kinase 2 is essential for gametocytogenesis

Eva Hitz[1,2], Olivia Grüninger[1,2], Armin Passecker[1,2], Matthias Wyss[1,2], Christian Scheurer[1,2], Sergio Wittlin[1,2], Hans-Peter Beck[1,2], Nicolas M. B. Brancucci[1,2], Till S. Voss[1,2,*]

[1]Department of Medical Parasitology and Infection Biology, Swiss Tropical and Public Health Institute, 4051 Basel, Switzerland.

[2]University of Basel, 4001 Basel, Switzerland.

[*]Corresponding author: till.voss@swisstph.ch.

This Supplementary Information file includes:

- Supplementary Figures 1-9
- Supplementary Tables 1 and 2

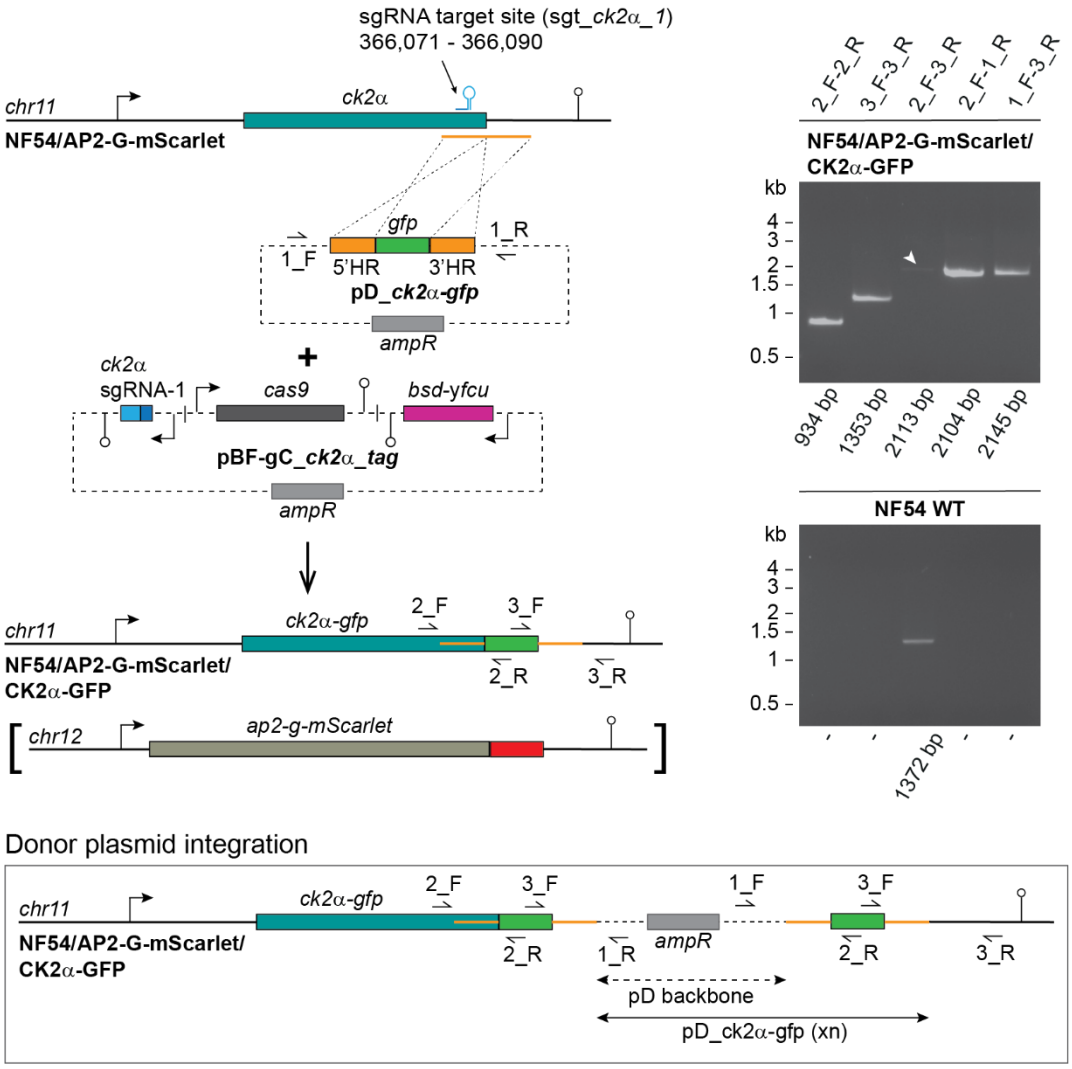

Donor plasmid integration

Supplementary Fig 1 CRISPR/Cas9-based engineering of the NF54/AP2-G-mScarlet/CK2α-GFP parasite line. Left: Schematic maps of the WT *pfck2α* locus, the CRISPR/Cas9 suicide and donor plasmids (pBF-gC_*ck2α_tag* and pD_*ck2α-gfp*) used to generate the NF54/AP2-G-mScarlet/CK2α-GFP parasite line and the modified *pfck2α* locus after editing (the modified *pfap2-g-mScarlet* locus in NF54/AP2-G-mScarlet parasites (Brancucci et al., manuscript in preparation) is schematically depicted in brackets) (bottom). A schematic illustrating a donor plasmid concatamer integration event by double-crossover recombination is shown in the box below (for simplicity integration of a tandem assembly is shown). Names and relative binding sites of the primers used for diagnostic PCRs are indicated. Right: PCRs performed on gDNA of NF54/AP2-G-mScarlet/CK2α-GFP parasites confirm correct tagging of the *pfck2α* gene (PCR reactions: 2_F-2_R, 3_F-3_R, 2_F-3_R) and donor plasmid concatamer

integration in a subset of parasites in the population (PCR reactions: 3_F-1_R and 1_F-4_R). PCRs performed on gDNA of NF54 WT parasites serve as control.

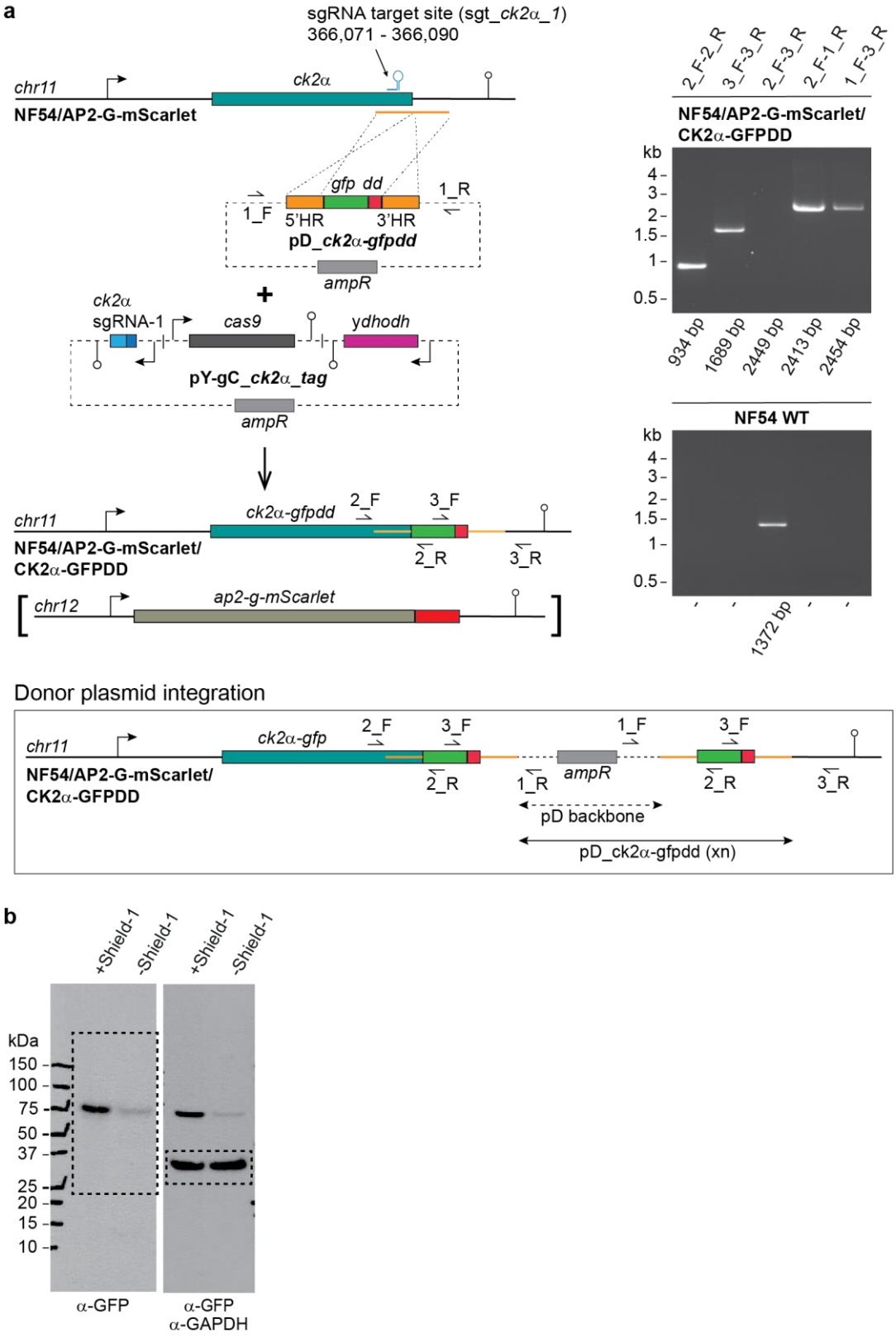

Supplementary Fig 2 CRISPR/Cas9-based engineering of the NF54/AP2-G-mScarlet/CK2α-GFPDD parasite line and full-size Western blot of the blot section shown in Fig. 2. a Left: Schematic maps of the WT *pfck2α* locus, the CRISPR/Cas9 suicide and donor plasmids (pY-gC_*ck2α_tag* and pD_*ck2α-gfpdd*) used to generate the

NF54/AP2-G-mScarlet/CK2α-GFPDD parasite line and the modified *pfck2α* locus after editing (the modified *pfap2-g-mScarlet* locus in NF54/AP2-G-mScarlet parasites (Brancucci et al., manuscript in preparation) is schematically depicted in brackets) (bottom). A schematic illustrating a donor plasmid concatamer integration event by double-crossover recombination is shown in the box below (for simplicity integration of a tandem assembly is shown). Names and relative binding sites of the primers used for diagnostic PCRs are indicated. Right: PCRs performed on gDNA of NF54/AP2-G-mScarlet/CK2α-GFPDD parasites confirm correct tagging of the *pfck2α* gene (PCR reactions: 2_F-2_R, 3_F-3_R). The PCRs also detected donor plasmid concatamer integration in all parasites in the population (PCR reactions: 2_F-1_R and 1_F-3_R), explained by the lack of a PCR product spanning the full modified locus (PCR reaction: 2_F-3_R). PCRs performed on gDNA of NF54 WT parasites serve as control. **b** Full-size Western blot showing expression of PfCK2α-GFPDD in NF54/AP2-G-mScarlet/CK2α-GFPDD schizonts cultured in presence (+Shield-1) and absence (-Shield-1) of Shield-1. Parasites were split (±Shield-1) 40 hours before sample collection. Protein lysates derived from an equal number of parasites were loaded per lane. The membrane was first probed with α-GFP antibodies (left) and subsequently with α-GAPDH control antibodies (right). MW PfCK2α-GFPDD = 78.7 kDa, MW loading control PfGAPDH = 36.6 kDa.

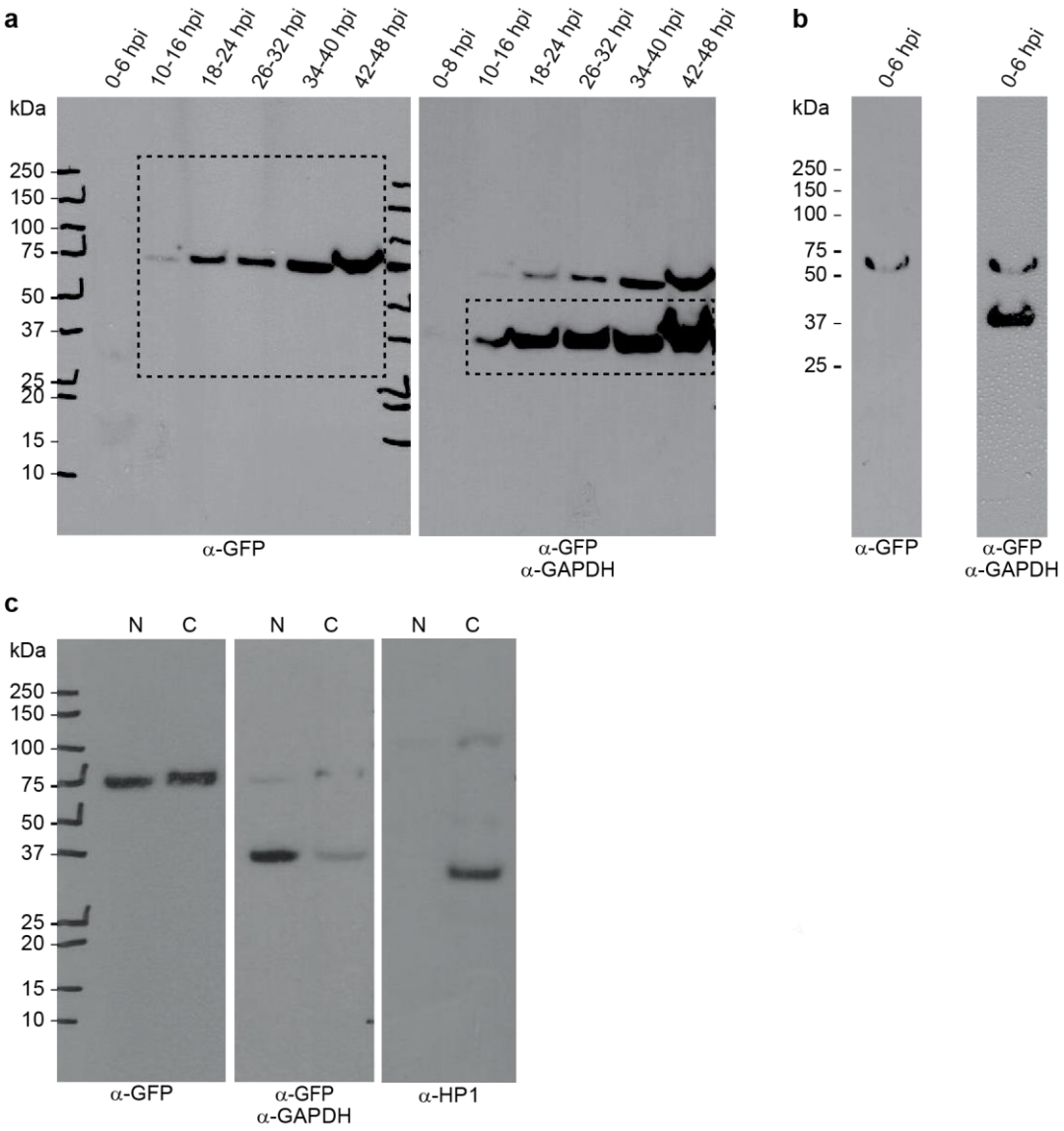

Supplementary Fig 3 Full-size Western blots of the blot sections shown in Fig. 1 and of cytoplasmic and nuclear protein fractions. a Full-size Western blot showing expression of PfCK2α-GFP in NF54/AP2-G-mScarlet/CK2α-GFP parasites at several time points during the IDC. Protein lysates derived from an equal number of parasites were loaded per lane. The membrane was first probed with α-GFP antibodies (left) and subsequently with α-GAPDH control antibodies (right). **b** Full-size Western blot showing expression of PfCK2α-GFP in early ring stage parasites (0-6 hpi) (three-fold higher amount of lysate loaded compared to panel a). The membrane was first probed with α-GFP antibodies (left) and subsequently with α-GAPDH control antibodies (right). **c** Full-size Western blot showing PfCK2α-GFP expression in nuclear and cytoplasmic extracts of NF54/AP2-G-mScarlet/CK2α-GFP parasites. The membrane was first probed with α-

GFP antibodies (left) and subsequently with α-GAPDH control antibodies (center). After stripping off the α-GFP/α-GAPDH and secondary antibodies, the membrane was re-probed using α-HP1 control antibodies. Nuclear and cytoplasmic protein extracts derived from the same parasite sample and equal proportions of both extracts were loaded. C, cytoplasmic extract; N, nuclear extract. MW PfCK2α-GFP = 66.8 kDa, MW loading control PfGAPDH = 36.6 kDa, MW PfHP1 = 31 kDa.

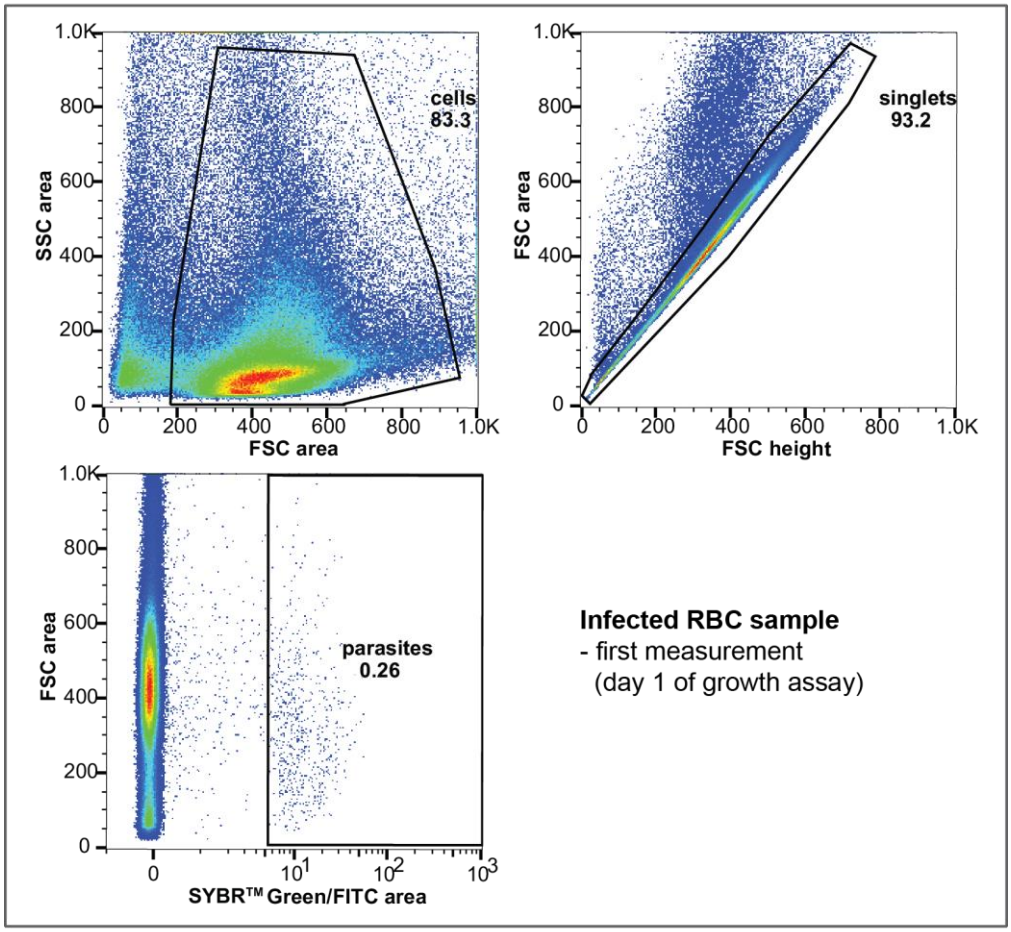

Infected RBC sample
- first measurement
  (day 1 of growth assay)

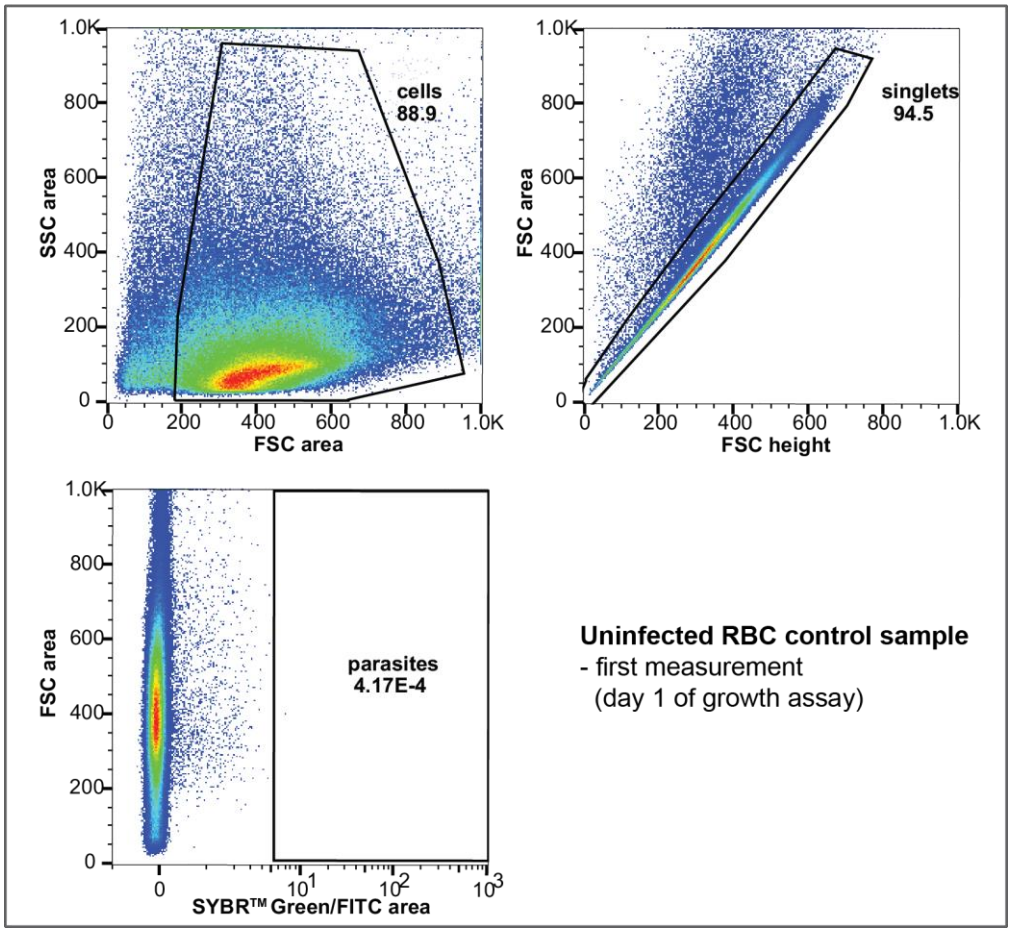

Uninfected RBC control sample
- first measurement
  (day 1 of growth assay)

Supplementary Fig 4 Gating strategy of flow cytometry data obtained from parasite multiplication assays. Representative flow cytometry plots of an infected (top frame; NF54/AP2-G-mScarlet/CK2α-GFPDD +Shield-1) and an uninfected RBC control sample (bottom frame) on the first day of the multiplication assay are shown. The first plot (top left) for both samples shows the gate set to remove small debris (smaller than cell size), keeping the “cells” used for further gating. The “cells” population was gated to remove doublets (single measurement events consisting of two cells), keeping “singlets” used for further gating (top right). Finally, SYBR green fluorescence intensity was used to separate uninfected from infected RBCs (bottom left). The numbers indicate the percentage of cells included in the infected RBC or “parasites” gate, directly reflecting the parasitaemia of the sample. This gating strategy was applied to the flow cytometry data shown in Figs. 2b and 4c.

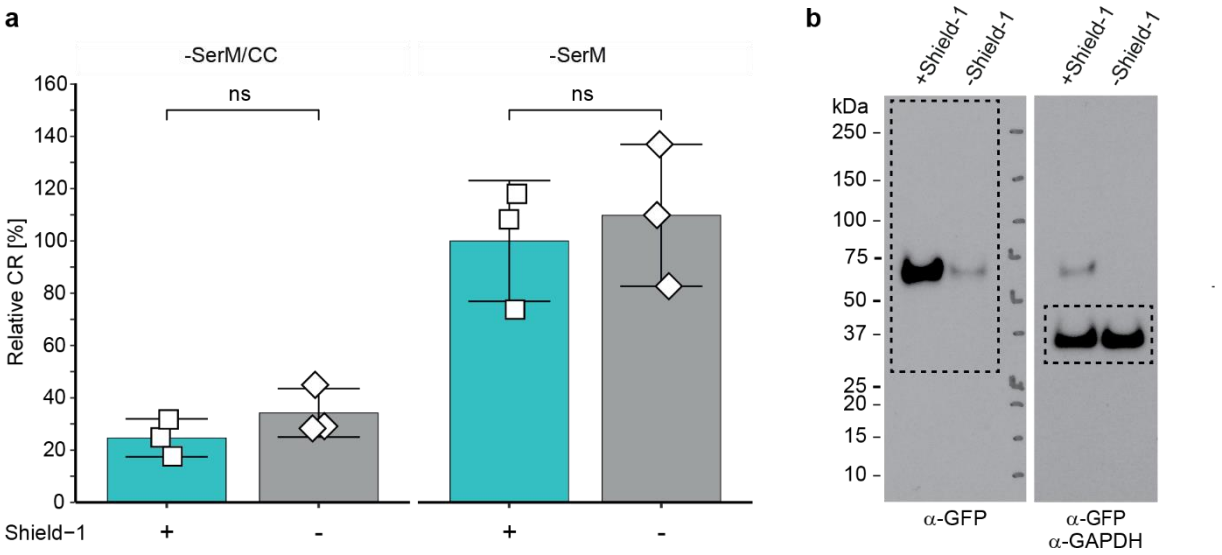

Supplementary Fig 5 Sexual commitment rates of NF54/AP2-G-mScarlet/CK2α-GFPDD parasites and full-size Western blot of the blot section shown in Fig. 3b. a Relative sexual commitment rates of parasites cultured in serum-free medium either in presence (–SerM/CC) or absence (–SerM) of 2 mM choline chloride [1]. Parasites cultured in presence (+Shield-1; turquoise) or absence (-Shield-1; grey) of Shield-1 are compared. Parasites were split (±Shield-1) at 0-6 hpi, transferred to –SerM or –SerM/CC medium conditions at 18-24 hpi and sexual commitment rates were assessed in the progeny at 18-24 hpi by quantifying AP2-G-mScarlet-positivity among all iRBCs (Hoechst-positive cells) by high content imaging (>3,000 iRBCs counted per experiment). The mean ±SD of three biological replicates is shown. Data points for individual replicates are represented by open squares. ns, not significant (paired two-tailed Student's t test). CR, commitment rate. **b** Full-size Western blot showing expression of PfCK2α-GFPDD in NF54/AP2-G-mScarlet/CK2α-GFPDD stage V gametocytes cultured in presence (+Shield-1) and absence (-Shield-1) of Shield-1. Parasites were split (±Shield-1) at 0-6 hpi, transferred to –SerM at 18-24 hpi to induce sexual commitment and subsequently cultured in presence or absence of Shield-1 until stage V gametocytes were obtained. From the ring stage progeny (asexual/sexual ring stages) until day six of gametocytogenesis, parasites were cultured in presence of 50 mM GlcNAc to eliminate asexual parasites. Protein lysates derived from an equal

number of parasites were loaded per lane. The membrane was first probed with α-GFP antibodies (left) and subsequently with α-GAPDH control antibodies (right). MW PfCK2α-GFPDD = 78.7 kDa, MW loading control PfGAPDH = 36.6 kDa.

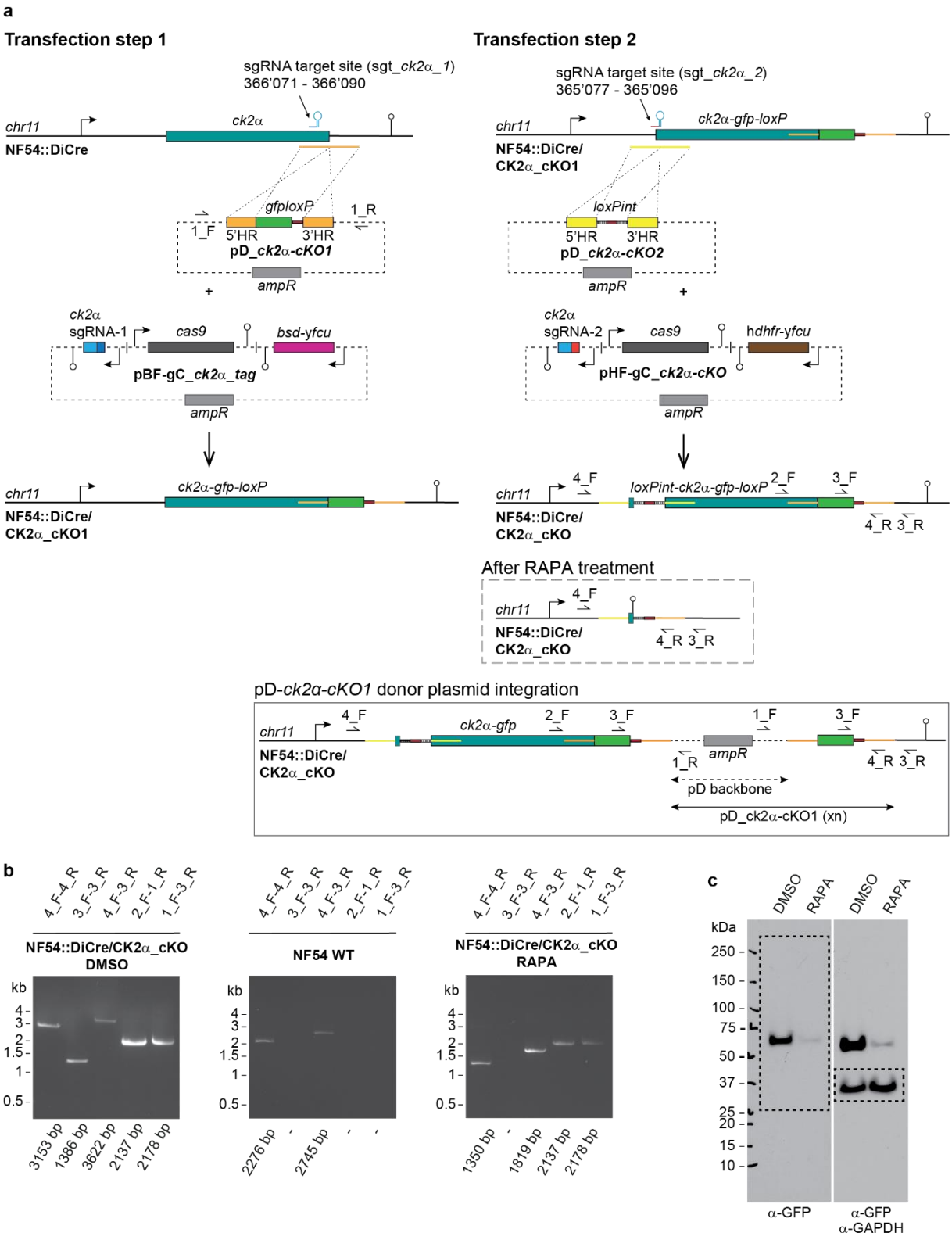

Supplementary Fig 6 CRISPR/Cas9-based engineering of the NF54::DiCre/CK2α_cKO parasite line. a Left: Schematic maps of the WT *pfck2α* locus, the CRISPR/Cas9 suicide and donor plasmids (pBF-gC_*ck2α_tag* and pD_*ck2α-cKO1*) used for the transfection of NF54::DiCre parasites[2] and the modified *pfck2α* locus after

editing. Right: Schematic maps the *pfck2α-gfp-loxP* locus, the CRISPR/Cas9 suicide and donor plasmids (pHF-gC_*ck2α-cKO* and pD_*ck2α-cKO2*) used for the transfection of NF54::DiCre/CK2α_cKO1 parasites and the modified *pfck2α* locus after editing, resulting in the generation of the NF54::DiCre/CK2α_cKO parasite line. The schematic map in the dashed box below shows the *pfck2α* locus after DiCre-mediated excision of the *pfck2α-gfp* gene. The schematic map in the box at the bottom illustrates a pD_*ck2α-cKO1* donor plasmid concatamer integration event by double-crossover recombination (for simplicity integration of a tandem assembly is shown). Names and relative binding sites of the primers used for diagnostic PCRs are indicated. **b** Left: PCRs performed on gDNA of NF54::DiCre/CK2α_cKO parasites treated with DMSO confirm correct editing of the locus (PCR reactions: 4_F-4_R, 3_F-3_R, 4_F-3_R) and reveal integration of pD_*ck2α-cKO1* donor plasmid concatamers in a subset of parasites in the population (PCR reactions: 2_F-1_R and 1_F-3_R). Center: Control PCRs performed on gDNA of NF54 WT parasites. Right: PCRs performed on gDNA of NF54::DiCre/CK2α_cKO parasites treated with RAPA at 0-6 hpi for four hours and harvested 40 hours later (40-46 hpi) confirm successful excision of the *pfck2α-gfp* gene upon action of the DiCre recombinase (PCR reactions: 4_F-4_R, 3_F-3_R, 4_F-3_R). Donor plasmid concatamer integration events were still detectable suggesting that DiCre-mediated excision was not 100% efficient (PCR reactions: 2_F-1_R and 1_F-3_R). However, these parasites were of very low abundance since even seven days after RAPA treatment no viable parasites were observed (Fig. 4). RAPA, rapamycin. **c** Full-size Western blot of the blot sections shown in Fig. 4. Full-size Western blot showing expression of PfCK2α-GFP in PfCK2α-GFP KO (RAPA) and control (DMSO) schizonts. Parasites were split and exposed for four hours to either RAPA or DMSO 40 hours before sample collection. Protein lysates derived from an equal number of parasites were loaded per lane. The membrane was first probed with α-GFP antibodies (left) and subsequently with α-GAPDH control antibodies (right). MW PfCK2α-GFP = 66.8 kDa, MW loading control PfGAPDH = 36.6 kDa. RAPA, rapamycin.

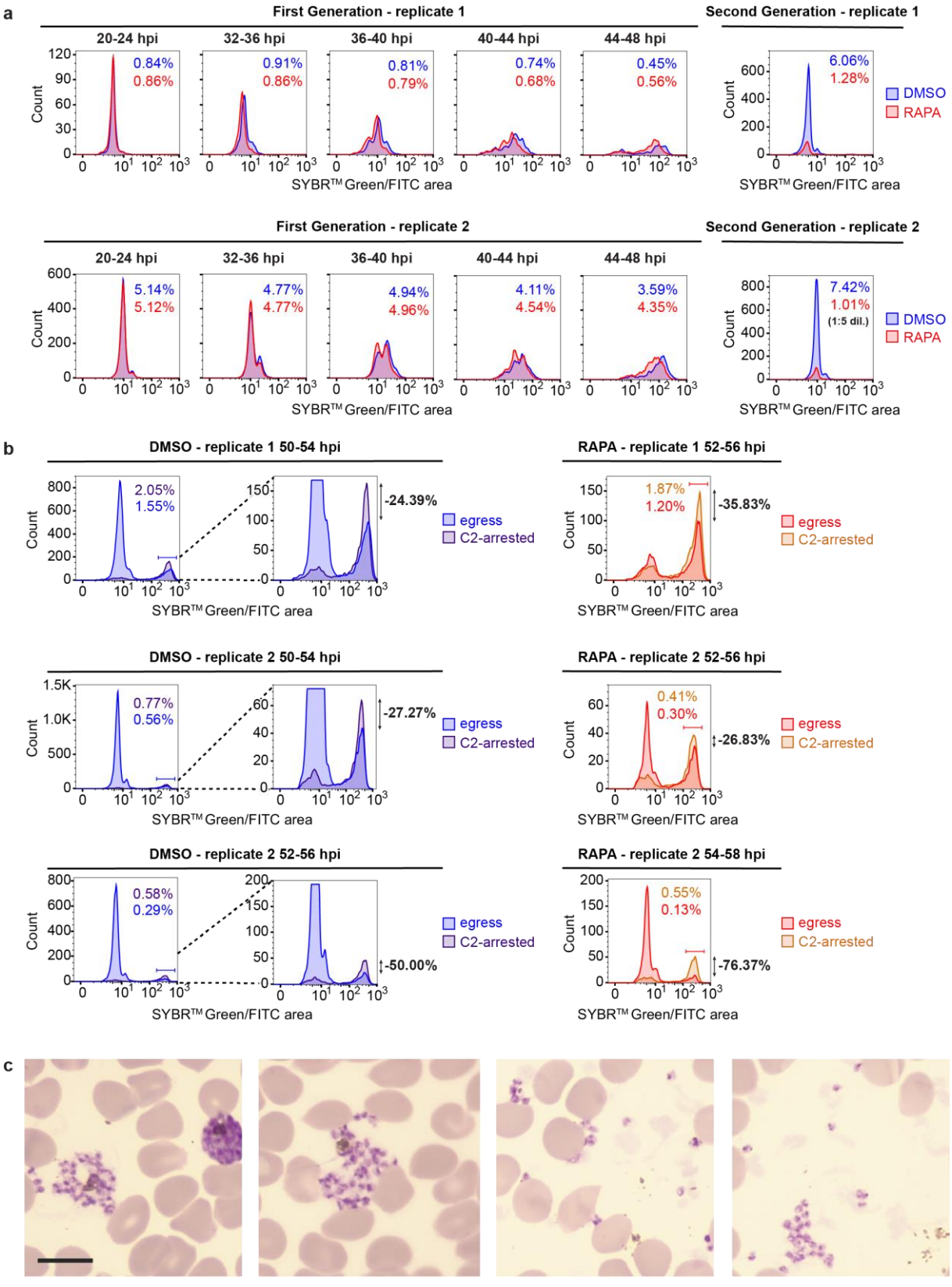

Supplementary Fig 7 Parasite progression through schizogony and merozoite egress and invasion in NF54::DiCre/CK2α-GFP KO (RAPA) and control (DMSO) parasites. a Flow cytometry time course experiment showing parasite progression

through schizogony as determined by quantifying the increase in genome content based on SYBR Green intensity (x-axis). Parasites were split at 0-4 hpi and treated for four hours with either RAPA (red) or DMSO (blue) before sampling five consecutive time points from 20-24 hpi (late ring stages) to 44-48 hpi (mature schizonts) in generation 1 and one ring stage time point in the subsequent progeny (generation 2). Numbers indicate total parasitaemia. Two independent time course experiments are shown. Note that for replicate 2 the parasitaemia has been diluted 1:5 prior to schizont rupture (1:5 dil.). hpi, hours post-invasion. **b** Flow cytometry experiment showing merozoite egress as determined by quantifying the percentage of schizont-infected RBCs based on SYBR reen intensity. Parasites were split at 0-4 hpi, treated for four hours with either RAPA or DMSO and exposed to C2 from 36-40 hpi onwards. Sampling was performed at 50-54 to 54-58 hpi from C2-arrested populations (RAPA, orange; DMSO, purple) and 45-90 min after release from C2-mediated developmental arrest (RAPA, red; DMSO, blue). Numbers indicate total schizontaemia. The relative reduction in schizontaemia after release from C2-mediated arrest compared to the C2-arrested control is shown to the right of the graphs. Two independent experiments are shown. hpi, hours post-invasion. **c** Representative images from Giemsa-stained thin blood smears prepared from RAPA-treated mature NF54::DiCre/CK2α-GFP KO schizonts 20 min after reversal of C2-mediated developmental arrest, showing ruptured schizonts and released merozoites. Scale bar = 10 µm.

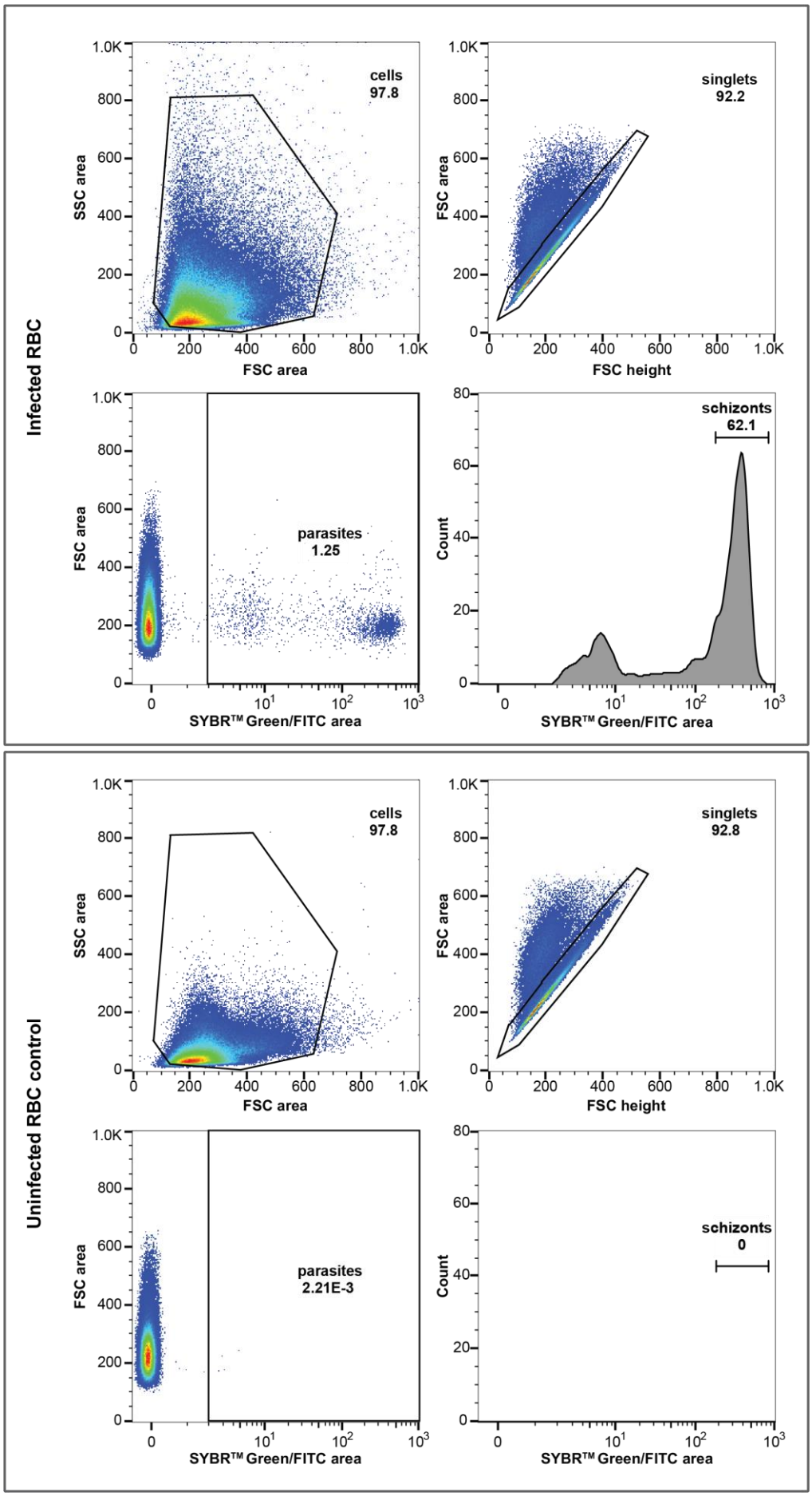
Infected RBC
cells
97.8
SSC area
FSC area
singlets
92.2
FSC area
FSC height
parasites
1.25
FSC area
SYBR™ Green/FITC area
schizonts
62.1
Count
SYBR™ Green/FITC area
Uninfected RBC control
cells
97.8
SSC area
FSC area
singlets
92.8
FSC area
FSC height
parasites
2.21E-3
FSC area
SYBR™ Green/FITC area
schizonts
0
Count
SYBR™ Green/FITC area

Supplementary Fig 8 Gating strategy of flow cytometry data obtained from parasite schizogony and merozoite egress assays. Representative flow cytometry plots of an infected (top frame; NF54::DiCre/CK2α_cKO, DMSO-treated control) and an uninfected RBC control sample (bottom frame). The first plot (top left) for both samples shows the gate set to remove small debris (smaller than cell size), keeping the “cells” used for further gating. The “cells” population was gated to remove doublets (single measurement events consisting of two cells), keeping “singlets” used for further gating (top right). SYBR green fluorescence intensity was used to separate uninfected from infected RBCs ("parasites"; bottom left) or mature schizonts from other iRBCs ("schizonts"; botttom right). The numbers indicate the percentage of cells included in the “parasites” or "schizonts" gates, directly reflecting the parasitaemia or schizontaemia of the sample, respectively. This gating strategy was applied to the flow cytometry data shown in Supplementary Fig. 7.

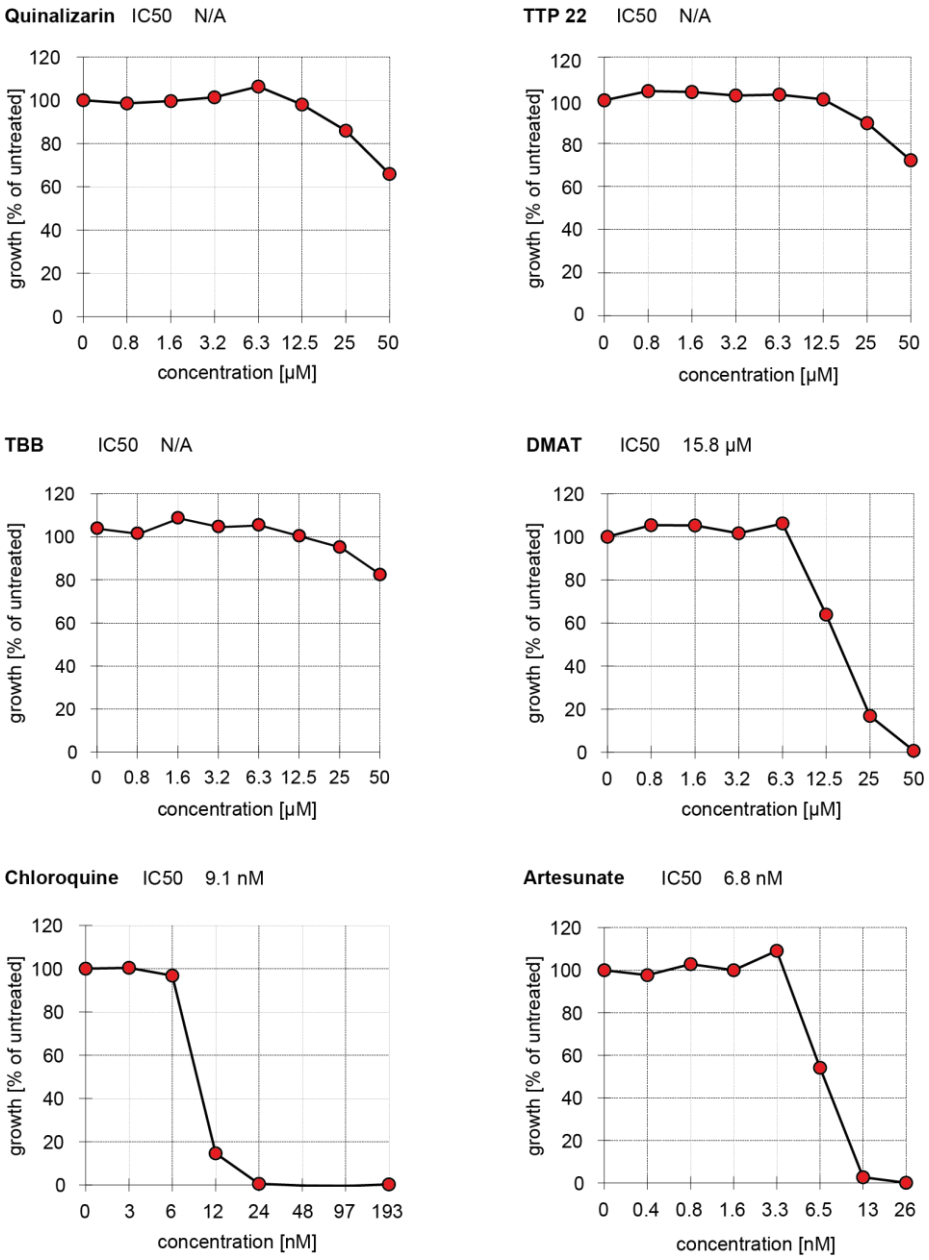

Supplementary Fig 9 Growth inhibition curves of compounds tested on NF54 asexual parasites in a [^{3}H] hypoxanthine incorporation assay. Growth inhibition curves of the four human CK2α inhibitors Quinalizarin, TTP 22, TBB and DMAT. Maximal concentration of compounds tested: 50 µM. Growth inhibition curves of the two antimalarial control compounds Chloroquine and Artesunate are shown at the bottom. Maximal concentrations for Chloroquine and Artesunate were 193 nM and 26 nM, respectively. The means of two biological replicates are shown. One of the biological replicate experiments was performed in two technical replicates. The fifty percent inhibitory concentration (IC_{50}) is indicated above each graph. N/A, not applicable.

Supplementary Table 1 Oligonucleotides used for cloning of CRISPR/Cas9 transfection constructs. Names of oligonucleotides, plasmids and cell lines as well as oligonucleotide sequences are shown. Sequences essential for Gibson assembly reactions (Gibson overhangs) or for T4 DNA ligase-dependent cloning of double-stranded sgRNA-encoding fragments (5' and 3' overhangs) are highlighted with capital or italicized capital letters, respectively.

Oligo-nucleotide	Sequence 5' → 3'	Plasmids	Cell line
Y_F	GACGGAGCTCGAATTCGcgaagatctgtcttaagcatttg	pY-gC mother plasmid	-
Y_R	CTTTTCTTCTTCAGGGTAGCccatggagttatcgatatgaattc	pY-gC mother plasmid	-
B_F	CTCGTTTAAGACCTGAAATCaaagttatcg	pY-gC mother plasmid	-
B_R	GATTTCAGGTCTTAAACGAGtgtaaaatgcacg	pY-gC mother plasmid	-
sgt_ck2a_1_F	*TATT*tcacggacttctctaaagta	pBF-gC_ck2α_tag; pY-gC_ck2α_tag	NF54/AP2-G-mScarlet/CK2α-GFP; NF54/AP2-G-mScarlet/CK2α-GFPDD; NF54::DiCre/CK2α_cKO
sgt_ck2a_1_R	*AAAC*tactttagagaagtccgtga	pBF-gC_ck2α_tag; pY-gC_ck2α_tag	NF54/AP2-G-mScarlet/CK2α-GFP; NF54/AP2-G-mScarlet/CK2α-GFPDD; NF54::DiCre/CK2α_cKO
sgt_ck2a_2_F	*TATT*aaaagagacaggaataatgt	pHF-gC_ck2α-cKO	NF54::DiCre/CK2α_cKO
sgt_ck2a_2_R	*AAAC*acattattcctgtctctttt	pHF-gC_ck2α-cKO	NF54::DiCre/CK2α_cKO
PCRA_F	CTGGCGTAATAGCGAAGAGG	pD_ck2α-gfp; pD_ck2α-gfpdd; pD_ck2α-cKO1; pD_ck2α-cKO2	NF54/AP2-G-mScarlet/CK2α-GFP; NF54/AP2-G-mScarlet/CK2α-GFPDD; NF54::DiCre/CK2α_cKO
PCRA_R	CATTAATGAATCGGCCAACG	pD_ck2α-gfp; pD_ck2α-gfpdd; pD_ck2α-cKO1; pD_ck2α-cKO2	NF54/AP2-G-mScarlet/CK2α-GFP; NF54/AP2-G-mScarlet/CK2α-GFPDD; NF54::DiCre/CK2α_cKO
H1_F	CGTTGGCCGATTCATTAATGctggtcaagaatataatgttcgtg	pD_ck2α-gfp; pD_ck2α-gfpdd; pD_ck2α-cKO1	NF54/AP2-G-mScarlet/CK2α-GFP; NF54/AP2-G-mScarlet/CK2α-GFPDD; NF54::DiCre/CK2α_cKO
H1_R	CTCTCTTCTCTAACCTCGCGgaaatagggatgctccatggcttcc	pD_ck2α-gfp; pD_ck2α-gfpdd	NF54/AP2-G-mScarlet/CK2α-GFP NF54/AP2-G-mScarlet/CK2α-GFPDD
G_F	CGCGAGGTTAGAGAAGAGAGtggatccagtggaatgagtaaag	pD_ck2α-gfp; pD_ck2α-gfpdd	NF54/AP2-G-mScarlet/CK2α-GFP NF54/AP2-G-mScarlet/CK2α-GFPDD

G_R	GATTCCTCACGTTATTTGTATAGttcatccatgccatg	pD_ck2α-gfp	NF54/AP2-G-mScarlet/CK2α-GFP
GD_R	GATTCCTCACGTCATTCTAAttttagaagctccacacgg	pD_ck2α-gfpdd	NF54/AP2-G-mScarlet/CK2α-GFPDD
H2_F	CTATACAAATAACGTGAGGAATCataataataataaaaaaaaatg	pD_ck2α-gfp	NF54/AP2-G-mScarlet/CK2α-GFP
H2D_F	TTAGAATGACGTGAGGAATCataataataataaaaaaaaatg	pD_ck2α-gfpdd	NF54/AP2-G-mScarlet/CK2α-GFPDD
H2_R	CCTCTTCGCTATTACGCCAGttgagcacatttttctctataagg	pD_ck2α-gfp; pD_ck2α-gfpdd; pD_ck2α-cKO1	NF54/AP2-G-mScarlet/CK2α-GFP; NF54/AP2-G-mScarlet/CK2α-GFPDD; NF54::DiCre/CK2α_cKO
loxP1_R	CGTATAATGTATGCTATACGaagttatttatttgtatagttcatccatgcc	pD_ck2α-cKO1	NF54::DiCre/CK2α_cKO
loxP1_F	CGTATAGCATACATTATACGaagttatgtgaggaatcataataataataaaaaaaaatg	pD_ck2α-cKO1	NF54::DiCre/CK2α_cKO
H3_F	CGTTGGCCGATTCATTAATGgataacaaaaatataaatcaagatcgt	pD_ck2α-cKO2	NF54::DiCre/CK2α_cKO
H3_R	TTTTTTATTTACCTAACAGACATTATTcctgtctcttttaaaaacg	pD_ck2α-cKO2	NF54::DiCre/CK2α_cKO
loxPINT_F	AATAATGTCTGTTAGGTAAATAAAAAAaataatatacaataacttcgtatag	pD_ck2α-cKO2	NF54::DiCre/CK2α_cKO
loxPINT_R	GGTATATAAATTTTTTTATTAATTGAGCTAAAAGAATATAAAATATATAAATATatatatatatac	pD_ck2α-cKO2	NF54::DiCre/CK2α_cKO
H4_F	ATATTTATATATTTTATATTCTTTTAGCTCAATTAATAAAAAAATTTATATACCaaaattttatg	pD_ck2α-cKO2	NF54::DiCre/CK2α_cKO
H4_R	CTTCGCTATTACGCCAGcagctagaccccaatcaa	pD_ck2α-cKO2	NF54::DiCre/CK2α_cKO

Supplementary Table 2 Primers used for PCRs on gDNA of transgenic parasite lines.

Primer names, sequences and names of the transgenic cell lines are shown.

Primer	**Sequence 5' → 3'**	**Cell line**
1_F	gcgaggaagcggaagagc	NF54/AP2-G-mScarlet/CK2α-GFP; NF54/AP2-G-mScarlet/CK2α-GFPDD; NF54::DiCre/CK2α_cKO
1_R	attcgccattcaggctgc	NF54/AP2-G-mScarlet/CK2α-GFP; NF54/AP2-G-mScarlet/CK2α-GFPDD; NF54::DiCre/CK2α_cKO
2_F	attaattgattggggtctagc	NF54/AP2-G-mScarlet/CK2α-GFP; NF54/AP2-G-mScarlet/CK2α-GFPDD; NF54::DiCre/CK2α_cKO
2_R	gtgtgagttatagttgtattcc	NF54/AP2-G-mScarlet/CK2α-GFP; NF54/AP2-G-mScarlet/CK2α-GFPDD
3_F	ggttatgtacaggaaagaac	NF54/AP2-G-mScarlet/CK2α-GFP; NF54/AP2-G-mScarlet/CK2α-GFPDD; NF54::DiCre/CK2α_cKO
3_R	gaaataagaaataaaaaataagaaataagaaaac	NF54/AP2-G-mScarlet/CK2α-GFP; NF54/AP2-G-mScarlet/CK2α-GFPDD; NF54::DiCre/CK2α_cKO

4_F	gtcataccacatttccaatc	NF54::DiCre/CK2α_cKO
4_R	cgtgcataaatcatacacac	NF54::DiCre/CK2α_cKO

Supplementary References

1 Brancucci, N. M. B. *et al.* Lysophosphatidylcholine Regulates Sexual Stage Differentiation in the Human Malaria Parasite Plasmodium falciparum. *Cell* **171**, 1532-1544 (2017).

2 Tiburcio, M. *et al.* A Novel Tool for the Generation of Conditional Knockouts To Study Gene Function across the Plasmodium falciparum Life Cycle. *MBio* **10**, e01170-19 (2019).

Chapter 5

cAMP-dependent protein kinase A (PKA)

This chapter contains the manuscript “A 3-phosphoinositide-dependent protein kinase-1 homologue is essential for activation of protein kinase A in malaria parasites” currently in preparation for submission to *Nature Microbiology* or *Nature Communications* (status April 2021). The Supplementary Dataset 1 is not included in this version, but is available upon request and will be included in the final manuscript version. I am first author of this manuscript and detailed information on the author contribution is given in the according manuscript section.

Chapter 5

A 3-phosphoinositide-dependent protein kinase-1 homologue is essential for activation of protein kinase A in malaria parasites

Eva Hitz[1,2], Natalie Wiedemar[1,2], Nicolas M. B. Brancucci[1,2], Armin Passecker[1,2], Ioannis Vakonakis[3], Pascal Mäser[1,2], Till S. Voss[1,2,*]

[1]Department of Medical Parasitology and Infection Biology, Swiss Tropical and Public Health Institute, 4051 Basel, Switzerland.

[2]University of Basel, 4001 Basel, Switzerland.

[3]Department of Biochemistry, University of Oxford, Oxford OX1 3QU, United Kingdom

[*]Corresponding author: till.voss@swisstph.ch.

Summary

In eukaryotic model organisms, the cAMP-dependent protein kinase PKA is a tetrameric holoenzyme in its inactive state. Upon binding of cAMP to the regulatory subunits (PKAr), the catalytic subunits (PKAc) are released. Subsequent activation of PKAc likely happens through phosphorylation by the 3-phosphoinositide-dependent protein kinase-1 (PDK1). In the human malaria parasite *Plasmodium falciparum*, PfPKA-dependent phosphorylation of the invasion factor AMA-1 is essential for merozoite invasion into erythrocytes. Following the release from PfPKAr, PfPKAc is phosphorylated in its activation segment, which is likely crucial for kinase activity. Here, we investigated the function of the catalytic kinase subunit PfPKAc in asexual and sexual parasite development by reverse genetics. Using a conditional PfPKAc knockdown line, we confirmed the essentiality of PfPKAc for erythrocyte invasion and its involvement in gametocyte-infected erythrocyte deformability. Furthermore, we demonstrate the lethality of PfPKAc overexpression and report the selection of overexpression-resistant

parasite survivors. Whole genome sequencing of PfPKAc overexpression-sensitive mother clones and -resistant survivors revealed that mutations in Pf3D7_1121900 are responsible for the tolerance of elevated PfPKAc levels, which suggests that Pf3D7_1121900 is the *P. falciparum* orthologue of PDK1. Our results demonstrate the importance of regulating PfPKAc expression and activity in asexual and sexual development and we report the identification of PfPDK1, an upstream regulator of PfPKA.

Introduction

Malaria is caused by protozoan parasites of the genus *Plasmodium*. Infections with *P. falciparum* are responsible for the vast majority of severe and fatal malaria cases. People get infected by female *Anopheles* mosquitoes that transmit sporozoites into the skin tissue during their blood meal. Having reached the liver, sporozoites infect and multiply inside hepatocytes, generating thousands of merozoites that are eventually released into the blood stream. Here, merozoites invade red blood cells (RBCs) and develop intracellularly through the ring stage into a trophozoite and finally a schizont stage parasite, which undergoes four to five rounds of nuclear division followed by cytokinesis to produce up to 32 new merozoites. Upon schizont rupture, these merozoites infect new erythrocytes to initiate another intra-erythrocytic developmental cycle (IDC). However, during each round of replication, a small subset of trophozoites commits to sexual development and their ring stage progeny differentiates over the course of 10-12 days and five distinct morphological stages (stage I-V) into mature male or female gametocytes. Sexual commitment occurs in response to environmental triggers that activate expression of the transcription factor PfAP2-G, the master regulator of sexual conversion [1-3]. When taken up by an *Anopheles* mosquito, mature stage V gametocytes develop into gametes that undergo fertilization. The resulting zygote develops into an ookinete that migrates through the midgut wall and transforms into an oocyst, which

generates thousands of infectious sporozoites ready to be injected into another human host.

The consecutive rounds of RBC invasion and intraerythrocytic parasite proliferation are responsible for all malaria-related pathology and deaths. Erythrocyte invasion by merozoites is a highly regulated multi-step process starting with the initial attachment of the merozoite to the RBC surface, followed by parasite reorientation and formation of a so-called tight junction [4]. The tight junction is the intimate contact area between the merozoite and RBC membranes that moves along the merozoite surface during the actin-myosin motor-driven invasion process [4]. Alongside the secreted rhoptry neck proteins, the micronemal transmembrane protein apical membrane antigen 1 (AMA1) is an integral component of the tight junction [4]. The cytoplasmic domain of AMA1 bears an essential role during merozoite invasion [5-7]. In particular, the phosphorylation of residues in the AMA1 cytoplasmic tail (S610 and T613) is essential for AMA1 function in RBC invasion [5-7]. Recent research has shown that the *P. falciparum* cyclic adenosine monophosphate (cAMP)-dependent protein kinase A (PfPKA) is responsible for AMA1 phosphorylation at S610 and hence essential for successful erythrocyte invasion [5,6,8,9].

PKA was discovered in the 1970s and is one of the most studied and best characterized eukaryotic protein kinases [10]. In its inactive state, the PKA holoenzyme is a tetramer consisting of two regulatory subunits (PKAr) and two catalytic subunits (PKAc) [11,12]. Upon binding of cAMP to PKAr, the catalytic PKAc subunits are released. PKAc release thus depends on cAMP levels, which are regulated by adenylate cyclases (ACs) or phosphodiesterases (PDEs) that synthesise or hydrolyse cAMP, respectively [11,12]. Furthermore, phosphorylation of PKAc is essential for its activity. *In vitro*, PKAc itself was shown to be active upon release from PKAr due to *cis*-auto-phosphorylation [13,14]. However, research in budding yeast and human cells has shown that the 3-phosphoinositide-dependent protein kinase-1 (PDK1) is important for the phosphorylation and thus activation of PKAc *in vivo* [15-20]. PDK1 is an essential activator of a variety of AGC family kinases including PKA, PKG and PKC in human cells [15,21-23].

Several PDK1-interacting AGC kinases including PKA contain a so-called PDK1-interacting fragment (PIF) [17,24,25]. This hydrophobic sequence binds to the PIF-binding pocket of PDK1 and this interaction is important for PDK1-dependent substrate phosphorylation [17,24,25]. In addition, PDK1-dependent phosphorylation of a specific activation loop site in PKAc (T197 in mammals) has been shown to play a crucial role for PKAc structure, activity and function [15,18,26-29].

In contrast to the tetrameric structure of PKA in model eukaryotes, the *P. falciparum* PfPKA kinase consists of only one catalytic (PfPKAc) and one regulatory (PfPKAr) subunit each [30,31]. Recent studies have also shown that cAMP levels in asexual parasites are regulated by the actions of *P. falciparum* PfPDEβ [32], which hydrolyses both cAMP and cGMP, and PfACβ that synthesises cAMP [8]. Analysis of conditional loss-of-function mutants identified PfPKAc as an essential kinase for the process of merozoite invasion into RBCs due to its crucial role in phosphorylation and subsequent shedding of the invasion ligand AMA-1 from the merozoite surface [5,6,8,9]. Likewise, depletion of cAMP levels through conditional disruption of the *pfacβ* gene phenocopied the invasion defect observed for the *pfpka*c mutant [8]. Interestingly, a conditional *pfpdeβ* mutant, which displays increased cAMP levels and PfPKAc hyperactivation, also showed severely reduced merozoite invasion that was linked to elevated phosphorylation and premature shedding of AMA1 [32]. Hence, tight regulation of PfPKAc activity is absolutely crucial for merozoite invasion and parasite proliferation. However, PfPKA seems to have additional functions in blood stage parasites. Phosphoproteomics studies of *pfpdeβ*, *pfacβ* as well as *pfpkac* conditional knockout cell lines revealed 39 proteins as high confidence targets of cAMP/PfPKA-dependent phosphorylation [8,32]. These proteins include not only invasion factors (e.g. AMA-1 and coronin), but also several unrelated proteins with predicted (e.g. chromatin organization and protein transport) or unknown functions [8,32]. In addition, cAMP/PfPKA-dependent signalling has been implicated in the regulation of ion channel conductance and establishment as well as dynamics of new permeability pathways (NPP) in asexual blood stage parasites and gametocytes as shown through the use of

pharmacological approaches (PKA/PDE inhibitors and increasing cAMP levels) and transgenic cell lines (deletion of PfPDEδ and overexpression of PfPKAr) [33,34]. Finally, another study identified a putative role for cAMP/PfPKA-dependent signalling in regulating gametocyte-infected erythrocyte deformability [35].

While several studies clearly demonstrated the importance of cAMP in activating PfPKAc, the role of PfPKAc phosphorylation in regulating its activity remains elusive. High throughput phosphoproteomics approaches identified several phosphorylated residues in PfPKAc, including T189 that corresponds to T197 in the activation segment of mammalian PKAc [36-39]. However, if and to what extent phosphorylation of T189 (and other residues) is important for PfPKAc activation in *P. falciparum* and if the phosphates are deposited via *cis*-auto-phosphorylation or by other kinases is unknown. Furthermore, although the essential function of PfPKAc in parasite invasion has been well described, other functions of PfPKA in asexual and sexual development are only poorly understood. Here, we used complementary CRISPR/Cas9-based reverse genetics approaches to study the function of PfPKAc in asexual blood stage parasites, sexual commitment and gametocytogenesis. Our results confirm the essential role of PfPKAc in merozoite invasion. We furthermore show that PfPKAc plays no obvious role in the control of sexual commitment or gametocyte maturation, but is involved in regulating gametocyte-infected erythrocyte deformability. In addition, we discovered that the conditional overexpression of PfPKAc is lethal in asexual blood stage parasites. Intriguingly, selection of survivor populations tolerant to PfPKAc overexpression followed by Illumina whole genome sequencing (WGS) revealed mutations exclusively in a gene encoding a putative serine/threonine kinase (Pf3D7_1121900), which we identified as the *P. falciparum* orthologue of phosphoinositide-dependent protein kinase-1 (PfPDK1). Targeted mutagenesis experiments confirmed that PfPKAc activity is strictly dependent on PfPDK1-mediated phosphorylation.

Results

Generation of a conditional PfPKAc loss-of-function mutant

We first aimed at studying the function of the catalytic kinase subunit PfPKAc in *P. falciparum* sexual commitment and development. We therefore generated a conditional kinase knockdown (cKD) parasite line using a selection-linked integration (SLI)-based [40] gene editing approach. The successful engineering of this PfPKAc cKD parasite line tags the *pfpkac* gene with the fluorescent marker *gfp* fused to the *fkbp* destabilization domain (*dd*) sequence [41,42], followed by a sequence encoding the 2A skip peptide [43,44], the blasticidin S deaminase coding sequence conferring drug resistance and finally the *glmS* ribozyme element [45] (Supplementary Fig. 1). The FKBP/DD system allows for protein stabilization using the small ligand molecule Shield-1 [41,42] whereas the *glmS* ribozyme causes degradation of the mRNA it is fused to in presence of glucosamine (GlcN) [45]. To be able to quantify parasite sexual commitment rates by live fluorescence imaging, we modified *pfpkac* in the previously generated reporter cell line NF54/AP2-G-mScarlet (Brancucci et al., manuscript in preparation). This line allows visualizing sexually committed cells by means of detecting expression of fluorophore-tagged PfAP2-G [3,46]. After transfection, we could confirm correct editing of the *pfpkac* locus by PCR on gDNA (Supplementary Fig. 1). This NF54/AP2-G-mScarlet/PKAc cKD parasite line allows for visualization of PfPKAc-GFPDD under protein and RNA stabilizing conditions (+Shield-1/–GlcN) and studying the effect of PfPKAc depletion upon protein and RNA degradation (–Shield-1/+GlcN). Using Western Blot analysis and live cell fluorescence imaging, we first confirmed efficient regulation of PfPKAc expression levels by comparing PfPKAc-depleted (–Shield-1/+GlcN) parasites with the matching control (+Shield-1/–GlcN) (Fig. 1a and Supplementary Fig. 1). With regard to subcellular localization, we observed PfPKAc in cytosolic and nuclear compartments in early schizonts before it localizes to the periphery of developing merozoites in late schizonts as described [8,9] (Fig. 1a and Supplementary Fig. 1). Previous research has shown that depletion of PfPKAc prevents merozoites from invading RBCs [8,9]. Hence, to further confirm the functionality and

effectiveness of the cKD system, we performed parasite multiplication assays. We split synchronous young ring stage parasites (0-6 hours post invasion, hpi) and cultured them separately under PfPKAc-depleting (–Shield-1/+GlcN) and -stabilizing (+Shield-1/–GlcN) conditions over three generations. The parasitaemia was determined by measuring SYBR Green-stained parasites using flow cytometry (Fig. 1b and Supplementary Fig. 2). As previously reported, depletion of PfPKAc produces merozoites unable to invade RBCs (Fig. 1b and 1c) [8,9]. In conclusion, we combined two inducible expression systems to engineer a conditional PfPKAc knockdown mutant that allows efficient depletion of PfPKAc expression and confirmed the essential role of this kinase in merozoite invasion.

PfPKAc is not essential for sexual commitment and development

We next investigated whether PfPKA activity is important for the ability of the parasite to undergo sexual commitment. We therefore split young ring stage parasites (0-6 hpi) and induced PfPKAc depletion in one of the cultures (–Shield-1/+GlcN), whereas the other culture was maintained under PfPKAc-expressing conditions (+Shield-1/–GlcN). Sexual commitment was induced 18 hours later in old ring stage parasites (18-24 hpi) in both populations using serum-free (–SerM) medium as described [3]. As control, both populations were also cultured on –SerM medium supplemented with choline chloride (–SerM/CC), which was previously shown to block sexual commitment [3]. In the late schizont stage (40-46 hpi), sexually committed parasites were visualized based on PfAP2-G-mScarlet positivity and quantified using high content imaging. We observed a slight difference in sexual commitment rates under both media conditions (–SerM and –SerM/CC) when comparing PfPKAc-depleted and control parasites (Supplementary Fig. 3). However, due to previous observations in transgenic lines cultured in presence and absence of GlcN, we suspected that GlcN itself might have an effect on sexual commitment. We therefore cultured NF54/AP2-G-mScarlet parasites carrying a wild type (WT) *pfpkac* locus either in presence or absence of GlcN (±GlcN). Indeed, GlcN itself altered the sexual commitment rate especially under –SerM/CC medium conditions

(Supplementary Fig. 3). As both the NF54/AP2-G-mScarlet/PKAc cKD and the NF54/AP2-G-mScarlet parasite lines showed a similar fold change in sexual commitment when comparing + and –GlcN conditions, we conclude that PfPKAc does not play a major role in regulating sexual commitment (Supplementary Fig. 3).

Next, we investigated gametocyte morphology during gametocytogenesis both under PfPKAc-depleting (–Shield-1/+GlcN) and -stabilizing (+Shield-1/–GlcN) conditions by visual inspection of Giemsa-stained thin blood smears (Fig. 2a). We could not detect morphological differences in any of the five gametocyte stages (I-V), although efficient depletion of PfPKAc in stage V gametocytes was confirmed by both Western blot analysis and live cell fluorescence imaging (Fig. 2a and Supplementary Fig. 3). We also tested whether depletion of PfPKAc affects male gametogenesis. To do so, we stimulated gametogenesis and exflagellation by exposing stage V gametocytes to a drop in temperature and the mosquito metabolite xanthurenic acid (XA) as previously described [47]. Exflagellation rates (ExR) were determined by quantifying the number of exflagellation centres formed by the egress of male gametes in relation to total gametocytaemia and RBC counts by microscopy as described [47]. We observed a significant decrease of the ExR in PfPKAc-depleted gametocytes (50%±24) when compared to the matching control (100%±28) ($p = 0.01$; paired two-tailed Student's t test) (Supplementary Fig. 4). Due to the demonstrated effect of GlcN on sexual commitment (Supplementary Fig. 3), we also quantified the ExR in parasites in which PfPKAc expression was depleted by removal of Shield-1 only (–Shield-1). Comparison to the control population (+Shield-1) did not reveal a significant defect in exflagellation, although we did observe efficient protein degradation of PfPKAc upon Shield-1 removal (–Shield-1) (Supplementary Fig. 4). In addition, GlcN itself had a profound negative effect on exflagellation of male NF54 WT gametocytes; the ExR of gametocytes cultured in presence of GlcN (+GlcN) was reduced to less than 50% (47%±12) compared to the control population (–GlcN) (100%±11) ($p = 0.04$; paired two-tailed Student's t test) (Supplementary Fig. 4).

Hence, we conclude that PfPKAc plays no major role in the regulation of sexual commitment, gametocytogenesis and male gametogenesis in *P. falciparum*. Furthermore, we show that GlcN substantially affects both sexual commitment and male gametogenesis, which needs to be taken into account when studying these processes in conditional mutants employing the *glmS* riboswitch system.

Depletion of PfPKAc increases gametocyte deformability

Immature gametocytes display high cellular rigidity and sequester in host tissues such as the bone marrow and spleen. In contrast, stage V gametocytes are more deformable, which allows them to leave their sites of sequestration and re-enter the bloodstream in order to be picked up by mosquitoes [48-50]. Interestingly, cAMP-dependent signalling is involved in regulating the rigidity of immature gametocyte-infected erythrocytes [35,48]. Using PKA and PDE inhibitors as well as a transgenic cell line overexpressing the regulatory subunit PfPKAr, Ramdani and colleagues showed that PfPKA likely plays a role in maintaining the rigidity of immature gametocyte-infected erythrocytes [35]. In addition, increased cAMP levels result in elevated stiffness of stage V gametocytes [35]. However, genetic evidence for a direct involvement of PfPKA activity in controlling gametocyte stiffness is missing so far. We therefore measured the deformability status of immature stage III and mature stage V gametocytes upon PfPKAc depletion in the NF54/AP2-G-mScarlet/PKAc cKD line using microsphiltration experiments [49]. Microsphiltration experiments exploit the fact that differences in cellular rigidity correlate with cell retention rates in a microsphere-based artificial spleen system [49,50]. Indeed, we observed a decrease in gametocyte retention rates and hence increased deformability upon depletion of PfPKAc (–Shield-1) compared to the matching control (+Shield-1) both on day six (stage III) and eleven (stage V) of gametocyte maturation (Fig. 2b). Whereas the difference in retention rates of stage III gametocytes cultured in presence or absence of Shield-1 was rather small (82%±6 vs. 76%±23, respectively), it became much more pronounced in stage V gametocytes (28%±15 vs. 14%±23, respectively) (Fig. 2b). To

exclude a potential effect of Shield-1 on the gametocyte-infected erythrocyte deformability, we performed a control experiment using NF54 WT gametocytes cultured in presence and absence of Shield-1 (±Shield-1) (Supplementary Fig. 4). As expected, no significant difference in the retention rates of NF54 WT stage III and stage V gametocytes were observed when comparing + and –Shield-1 culture conditions (Supplementary Fig. 4). Hence, PfPKAc activity contributes to the regulation of cellular rigidity in gametocytes.

PfPKAc overexpression is lethal

A previous study demonstrated that the severe merozoite invasion and post-invasion developmental defects observed for *pfpde* KO parasites was linked to increased cAMP levels and PfPKAc hyperactivity [32]. To get further insights into the function of PfPKAc in asexual blood stage parasites, we generated a PfPKAc conditional overexpression (cOE) line using a two-plasmid CRISPR/Cas9 gene editing approach [51]. To this end, we transfected NF54 WT parasites to insert an ectopic copy of the *pfpkac* gene fused to *gfp* and controlled by the *glmS* ribozyme into the non-essential *glp3* (*cg6,* Pf3D7_0709200) locus [52] (NF54/PKAc cOE) (Supplementary Fig. 5). Expression of PfPKAc-GFP in this line is driven by the constitutive *calmodulin* (PF3D7_1434200) promoter and cOE of PfPKAc-GFP can be triggered by removal of GlcN (–GlcN) from the culture medium. Since the transgenic NF54/PKAc cOE population was contaminated with WT parasites, the line was cloned out using limiting dilution cloning as previously described [53]. In two clones (NF54/PKAc cOE M1 and M2), correct integration of the PfPKAc-GFP expression cassette into the *glp3* locus and absence of WT parasites was confirmed by PCR (Supplementary Fig. 5). First, we confirmed the efficient induction of PfPKAc OE upon removal of GlcN (–GlcN) by live cell fluorescence imaging and Western blot analysis in clones M1 (Fig. 3a and Supplementary Fig. 6) and M2 (Supplementary Fig. 6). PfPKAc OE (–GlcN) resulted in a dramatic defect in intraerythrocytic development with parasites seemingly arresting development half way through the IDC (Supplementary Fig. 6). To

study this growth defect in more detail, we quantified the number of nuclei per parasite in Hoechst-stained late schizont stages (40-46 hpi), 40 hours after triggering PfPKAc-GFP OE (–GlcN) in young ring stages (0-6 hpi) of clone M1. This experiment revealed that PfPKAc OE parasites (–GlcN) did not develop beyond the late trophozoite/early schizont stage as most parasites contained only one or two nuclei as opposed to the control population (+GlcN) that progressed normally through several rounds of nuclear division during schizogony (Fig. 3b). To test whether these parasites are still able to proliferate, we performed multiplication assays using the NF54/PKAc cOE M1 line. Parasites were split (±GlcN) at 0-6 hpi and parasite multiplication was quantified over three generations by measuring SYBR Green-stained parasites by flow cytometry. PfPKAc OE (–GlcN) completely blocked parasite multiplication as no increase in parasitaemia was observed even after six days (Fig. 3c and Supplementary Fig. 6). Intriguingly, upon continuous maintenance of NF54/PKAc cOE M1 parasites in culture medium lacking GlcN, proliferating PfPKAc OE parasites re-appeared after approximately two weeks and we termed these parasites PfPKAc OE survivors (NF54/PKAc cOE S1). Importantly, the NF54/PKAc cOE S1 survivor population still overexpressed PfPKAc-GFP in absence of GlcN as shown by live cell fluorescence imaging and Western blot analysis (Fig. 3d and Supplementary Fig. 6). Furthermore, Sanger sequencing did not identify any mutations in both the endogenous and ectopic *pfpkac* genes. Quantification of the number of nuclei per parasite as well as parasite multiplication assays revealed that PfPKAc cOE S1 parasites were completely tolerant to PfPKAc OE and developed and multiplied identically in presence and absence of GlcN (Figs. 3e, 3f and Supplementary Fig. 6).

In conclusion, parasites overexpressing PfPKAc are unable to develop beyond the late trophozoite/early schizont stage of intraerythrocytic parasite development. However, selection of survivor parasites tolerating PfPKAc OE was possible and these parasites show no defect in intraerythrocytic development and multiplication.

Parasites tolerant to PfPKAc overexpression carry mutations in the *P. falciparum* phosphoinositide-dependent protein kinase-1 (PfPDK1)

The above findings suggested that a genomic mutation in the PfPKAc cOE survivor population might be responsible for their tolerance to elevated PfPKAc levels. To address this hypothesis, we performed WGS on gDNA of the two unselected PfPKAc cOE clones M1 and M2 and six independently grown PfPKAc cOE survivor populations (S1-S6), three each originating from the M1 and M2 clones, respectively. Intriguingly, we found that all six PfPKAc cOE survivors, but not the unselected M1 and M2 clones, carried mutations in the Pf3D7_1121900 gene encoding a putative serine/threonine protein kinase (www.plasmodb.org) (Fig. 4a). Importantly, all mutations identified are missense mutations causing amino acid changes in the protein sequence (Fig. 4a). Moreover, consistent with the Sanger sequencing data we identified no mutations in both the endogenous and ectopic *pfpkac* genes in any of the PfPKAc cOE survivors. Furthermore, the sequencing data revealed no other mutations consistently present in all six survivor populations and absent in the unselected clones M1 and M2. These findings provided compelling evidence that the missense mutations acquired by the Pf3D7_1121900 gene were the cause for PfPKAc OE tolerance. The orthologues of Pf3D7_1121900 in *P. vivax* (PVX_091715) and *P. cynomolgi* (PcyM_0925100) are annotated as putative 3-phosphoinositide dependent protein kinase-1 (PDK1) (www.plasmodb.org). A multiple sequence alignment supported that Pf3D7_1121900 is indeed an orthologue of well-characterized PDK1 variants from opisthokonts and plants (Supplementary Fig. 7). On this basis, we constructed a homology model of Pf3D7_1121900 based on the human PDK1 crystallographic structure, which allowed us to visualize the location of amino acids mutated in the six PfPKAc cOE survivors S1-S6 (Fig. 4b). None of these mutations altered the putative PIF-binding pocket; rather, all mutated amino acids locate at or in the periphery of the kinase ATP-binding cleft, although only one mutation (N45S) may directly influence ATP coordination (Fig. 4b and Supplementary Fig. 7). We hence surmise that the mutations identified in Pf3D7_1121900 may alter the catalytic activity

but not the protein interaction preferences of this putative kinase.

In conclusion, using whole genome Illumina sequencing, we identified missense mutations in the Pf3D7_1121900 gene in all six independently obtained PfPKAC cOE survivor populations, which likely confer tolerance to PfPKAc OE. Bioinformatic analysis indicates that this gene encodes the *P. falciparum* orthologue of PDK1 (PfPDK1). Modelling of the predicted PfPDK1 structure suggests that the acquired mutations affect the catalytic activity of PfPDK1.

Conditional depletion of PfPDK1 leads to no major difference in asexual parasite growth and does not affect sexual commitment and gametocytogenesis

To get further insight into the function of PfPDK1 in *P. falciparum*, we aimed at generating a *pfpdk1* knockout (KO) parasite line using a CRISPR/Cas9 single-plasmid approach [51]. Previous research has shown that this kinase is likely essential for the asexual IDC both in *P. falciparum* and *P. berghei* since attempts to disrupt the corresponding genes failed [36,54,55]. Consistent with these observations, we also failed to generate a *pfpdk1* KO parasite line. We therefore engineered a *pfpdk1* cKD parasite line by tagging the endogenous *pfpdk1* gene with g*fp* fused to the *dd* sequence (Supplementary Fig. 8). As confirmed by PCR on gDNA, generation of the NF54/PDK1 cKD line was successful but we detected integration of donor plasmid concatemers downstream of the *pfpdk1* locus in a subset of parasites (Supplementary Fig. 8). However, since the 551 bp 3' homology region (HR) used for homology-directed repair appears to include the native terminator [56], expression of *pfpdk1-gfpdd* gene is not compromised by donor plasmid integration (Fig. 5a and Supplementary Fig. 9). Using NF54/PDK1 cKD parasites cultured in presence of Shield-1, we show that PfPDK1 is expressed throughout the IDC as shown by Western blot analysis and live cell fluorescence imaging (Supplementary Fig. 9). These experiments also revealed peak expression in the schizont stage and PfPDK1 localization in the parasite cytosol and nucleus of all asexual stages (Supplementary Fig. 9). Furthermore, we confirmed the efficient depletion of PfPDK1-GFPDD upon removal

of Shield-1 (–Shield-1) when compared to the control (+Shield-1) (Fig. 5a and Supplementary Fig. 9). Next, we investigated the effect of PfPDK1 depletion on parasite multiplication. Surprisingly, we did not observe a growth defect upon PfPDK1 depletion; instead, we detected a small increase in the multiplication rate of PfPDK1-GFPDD-depleted parasites (–Shield-1) in comparison to the isogenic control population (+Shield-1) (Fig. 5b). This increased multiplication rate cannot be attributed to removal of Shield-1 itself, since NF54 WT parasites cultured in presence or absence of Shield-1 (±Shield-1) multiplied equally (Supplementary Fig. 9). We further asked whether depletion of PfPDK1 affects sexual commitment and development. For this purpose, synchronous NF54/PDK1 cKD ring stage parasites (0-6 hpi) were split and cultured either in presence (+Shield-1) or absence (–Shield-1) of Shield-1. Eighteen hours later (18-24 hpi) sexual commitment was induced using –SerM medium and parasites cultured on –SerM/CC served as a control [3]. Comparison of sexual commitment rates of parasites cultured in presence and absence of Shield-1 (±Shield-1) did not reveal any difference under both medium conditions (–SerM and –SerM/CC) (Supplementary Fig. 10). Similarly, we monitored gametocytogenesis over eleven days by visual inspection of Giemsa-stained blood smears and did not observe any morphological difference between PfPDK1-depleted (–Shield-1) gametocytes and the control population (+Shield-1) (Supplementary Fig. 10). Finally, we also assessed male gametogenesis using exflagellation assays. Again, we did not observe any difference in their ExR when comparing PfPDK1-depleted gametocytes with the matching control (Supplementary Fig. 10).

Taken together, these data suggest that PfPDK1 is essential in asexual blood stage parasites as previously reported, but they also show that residual PfPDK1 expression levels sustain parasite viability. Furthermore, PfPDK1 is expressed in both the parasite nucleus and cytosol throughout asexual development reaching its peak in the schizont stage. Lastly, our experiments revealed no major involvement of PfPDK1 in sexual

commitment, gametocytogenesis and male gametogenesis but it is again conceivable that residual PfPDK1 expression is sufficient for these processes.

Reversion of *pfpdk1* mutations restores PfPKAc overexpression sensitivity and targeted mutation of *pfpdk1* causes PfPKAc overexpression tolerance

To confirm the specific function of PfPDK1 in regulating PfPKAc activity, we intended to revert the PfPDK1 M51R mutation identified in PfPKAc OE S1 parasites to restore the WT PfPDK1 sequence (R51M) thus generating the NF54/PKAc cOE S1/PDK1_wt parasite line. Furthermore, we aimed at introducing the PfPDK1 M51R mutation found in the PfPKAc OE S1 survivor into the unselected clone M1 thereby generating the NF54/PKAc cOE M1/PDK1_mut parasite line. Using a two-plasmid CRISPR/Cas9 approach [51], we were able to generate both lines and correct *pfpdk1* mutagenesis was confirmed by Sanger sequencing (Supplementary Fig. 11). Noteworthy, however, two attempts to introduce the PfPDK1 M51R mutation into the NF54 WT genome failed, suggesting that functional PfPDK1 is strictly required for parasite viability under normal PfPKAc expression levels. First, we confirmed that efficient PfPKAc OE was still inducible upon GlcN removal (–GlcN) in the NF54/PKAc cOE S1/PDK1_wt parasite line by Western Blot analysis and live cell fluorescence imaging (Fig. 6a and Supplementary Fig. 11). Strikingly, reverting the *pfpdk1* mutation in the PfPKAc cOE S1 survivor (R51M) completely restored the PfPKAc OE-sensitive phenotype (Figs. 6a, 6b and Supplementary Fig. 11). Using multiplication assays and live cell fluorescence imaging, we showed that triggering PfPKAc OE (–GlcN) in the NF54/PKAc cOE S1/PDK1_wt cell line leads to a complete block in asexual development (Figs. 6a, 6b and Supplementary Fig. 11). Next, we also confirmed efficient OE of PfPKAc upon removal of GlcN (–GlcN) in the NF54/PKAc cOE M1/PDK1_mut line by both Western blot analysis and live cell fluorescence imaging (Fig.6c and Supplementary Fig. 11). Notably, mutating the *pfpdk1* gene in the unselected PfPKAc cOE M1 clone rendered these parasites tolerant to PfPKAc OE (–GlcN), although the multiplication rates reached only 60% to 80% of the

matching control (+GlcN) (Fig. 6d and Supplementary Fig. 11). The impaired multiplication observed upon triggering PfPKAc OE in this PfPKAc cOE M1 PfPDK1 mutant suggested that an additional selection step might have taken place in the PfPKAc cOE S1 population rendering them completely resistant to PfPKAc OE. Indeed, analysis of the Illumina sequencing data revealed that while the unselected PfPKAc cOE clone M1 carried seven PfPKAc cOE cassette copies inserted into the *glp3* locus, the PfPKAc cOE S1 survivor carried only two copies (Supplementary Fig. 12). We therefore believe that due to the negative impact of continuous PfPKAc OE on parasite viability, survivor parasites carrying fewer PfPKAc cOE cassettes and hence lower overall PfPKAc expression levels had a comparative advantage during the selection process for PfPKAc OE tolerance. Altogether, these data confirm the importance of *pfpdk1* mutations in providing resistance to PfPKAc OE, suggesting that PfPDK1 is the kinase that phosphorylates and activates PfPKAc.

Mutation of T189 in the activation loop renders PfPKAc resistant to PfPDK1-dependent activation

Previous research in different eukaryotes including humans and yeast identified a specific threonine residue in the activation loop of PKAc (T197 in mammals) as the target of PDK1-dependent phosphorylation, and phosphorylation of this residue is important for PKAc structure and activity [15,18,26-29]. In *P. falciparum*, phosphoproteomic analyses detected phosphorylated T189 of PfPKAc [36-39], which likely corresponds to the activation loop phosphorylation site identified in other PKA sequences (equivalent to T197 in mammalian PKAc). Hence, we tested whether T189 phosphorylation is indeed important for PfPKAc activity. We therefore generated a parasite line that conditionally overexpresses mutated PfPKAc carrying a T189V mutation that renders this residue inaccessible for phosphorylation (Supplementary Fig. 5) [57,58]. Correct insertion of the PfPKAcT189V cOE cassette into the *glp3* locus was verified by PCR on gDNA of NF54/PKAcT189V cOE parasites (Supplementary Fig. 13). PfPKAcT189V OE was

inducible by removal of GlcN (–GlcN) as confirmed by Western blot analysis and live cell fluorescence imaging (Supplementary Fig. 13). Strikingly, fluorescence microscopy and multiplication assays revealed that OE of the PfPKAcT189V mutant kinase (–GlcN) has no effect on parasite development, multiplication and survival when compared to the control population (+GlcN) (Supplementary Fig. 13).

In conclusion, and in stark contrast to OE of WT PfPKAc, OE of PfPKAcT189V does not affect asexual parasite development and proliferation, showing that PfPKAc activity is strictly dependent on the phosphorylation of T189 in the activation segment. In combination with the findings obtained through the mutational analysis of PfPDK1, these results demonstrate that PfPDK1 is directly or indirectly responsible for T189 phosphorylation and thus activation of PfPKAc.

Discussion

PfPKA was shown to be essential for the proliferation of asexual blood stage parasites due to its indispensable role in phosphorylating the invasion ligand AMA-1 [5,6,8,9]. In addition, recent research revealed the importance of the phosphodiesterase PfPDEβ and the adenylate cyclase PfACβ in regulating cAMP levels and hence PfPKA activity [8,32].

Here we aimed at studying the function and regulation of the catalytic PfPKA subunit PfPKAc with a focus on sexual commitment and development. For this purpose, we generated several transgenic cell lines based on CRISPR/Cas9 and SLI gene editing approaches. Using the NF54/AP2-G-mScarlet/PKAc cKD parasite line, we confirmed the essential role of PfPKAc in merozoite invasion. As previously described [8], we observed that PfPKAc-depleted merozoites attach to the erythrocyte surface but are unable to invade. Furthermore, we demonstrated that PfPKAc plays no major role in regulating sexual commitment. The dispensability of PfPKAc in sexual commitment seems rather surprising, since previous research claimed a potential involvement of cAMP-dependent signalling in sexual commitment [59,60]. However, these studies only indirectly suggested an involvement of cAMP/PfPKA-signalling in this process. For instance, Kaushal and

colleagues determined the effect of high cAMP concentrations (1 mM) on sexual commitment and reported that under static culture conditions (high parasitaemia without addition of uRBCs) nearly all parasites develop into gametocytes [59]. We hypothesize that this observation reflects the selective killing of asexual stages by high concentrations of cAMP (as reported in their study), rather than true induction of sexual commitment by cAMP-dependent signalling. In addition, the increase of sexual commitment rates at high parasitaemia observed by Kaushal et al. was likely stimulated by the depletion of LysoPC from the culture medium [3]. Our results further suggest that PfPKAc is not required for gametocytogenesis and male gametogenesis. However, since our cKD system efficiently, but not completely, abolishes PfPKAc protein expression, we cannot exclude the possibility that residual PfPKAc levels still support normal sexual development. The conditional PfPKAc KO lines generated in previous studies would provide excellent tools to test this hypothesis. At this point, we would also like to reiterate that our experiments conducted with the NF54/AP2-G-mScarlet/PKAc cKD line identified GlcN (2.5 mM) as a confounding factor when studying sexual commitment and male gametocyte exflagellation. We therefore advise to use the FKBP/DD-Shield-1 [41,42] or DiCre/rapamycin [61,62] conditional expression approaches when studying these processes in *P. falciparum*.

The stiffness of immature gametocytes is associated with the dynamic reorganization of the RBC spectrin and actin networks [48] as well as the presence of parasite-encoded STEVOR proteins in the iRBC membrane [63,64]. The increased cellular deformability gained by stage V gametocytes is linked to the reversal of these cytoskeletal rearrangements [48] and the dissociation of STEVOR from the iRBC membrane [63,64]. Interestingly, results obtained by treating gametocyte cultures with pharmacological agents to increase cellular cAMP levels or to inhibit PKA activity demonstrated that gametocyte rigidity is positively regulated by cAMP/PKA-dependent signalling [35,64]. While PKA substrates involved in this process are largely unknown, PKA-dependent phosphorylation of the cytoplasmic tail of STEVOR (S324) is important to maintain

cellular rigidity and dephosphorylation of this residue is linked to the increased deformability of stage V gametocytes [64]. However, given that PfPKA is not known to be exported into the iRBC cytosol, the PKA-dependent phosphorylation of STEVOR and possibly other components of RBC compartment are likely excerted by human PKA. Notably though, overexpression of the regulatory subunit PfPKAr, which is expected to lower PfPKAc activity, still causes increased gametocyte-infected erythrocyte deformability [35]. Consistent with these data, we demonstrated that PfPKAc depletion increases cellular deformability of both stage III and V gametocytes, providing direct evidence for a role of PfPKAc-dependent phosphorylation in regulating the biomechanical properties of gametocytes. We imagine that PfPKAc activity may regulate the expression, trafficking or function of parasite-encoded proteins destined for export into the iRBC or of proteins implicated in the formation of the extensive inner membrane complex and/or microtubular and actin networks underneath the parasite plasma membrane that play important roles in determining cellular shape during gametocytogenesis [65-67]. Comparative phosphoproteomic analyses of the conditional PfPKAc mutants generated here and elsewhere [8,9] may be a promising approach to test this hypothesis and identify the actual substrates involved.

Three recent studies employing DiCre-inducible KO parasites for PfPKAc [8,9], the phosphodiesterase PfPDEβ [32] and the adenylate cyclase PfACβ [8] highlighted the importance for tight regulation of PfPKA activity in asexual blood stage parasites [8,9,32,33]. Both the prevention of PfPKA activity (PfPKAc and PfACβ KOs [8]) and the hyper-activation of PfPKA through elevated cAMP levels (PfPDEβ KO [32]) caused no immediate phenotype in intra-erythrocytic development but resulted in a complete or severe block of merozoite invasion, respectively. The few PfPDEβ KO merozoites that successfully invaded RBCs were unable to progress further through the IDC [32], providing circumstantial evidence for a detrimental effect of PfPKAc hyper-activity on the survival in intra-erythrocytic parasites. Here, we showed that this phenotype is much more pronounced upon direct overexpression of PfPKAc, which completely prevented parasite

progression through schizogony. While we did not engage in further explorations towards identifying the molecular mechanisms underlying the lethal consequences of PfPKAc overexpression, we discovered the upstream kinase that is required for PfPKAc activation. We identified this function by selecting parasites tolerant to PfPKAc OE. All six independently selected PfPKAc OE survivor populations carried mutations in a gene encoding the putative serine/threonine kinase Pf3D7_1121900. Bioinformatic analyses and structural modelling identified this kinase as the putative orthologue of eukaryotic phosphoinositide-dependent protein kinase 1 (PDK1), hence termed PfPDK1.

All PfPDK1 mutations identified in the various survivor populations are proximal to the ATP-binding cleft and do not coincide with the PIF-binding pocket. We therefore hypothesize that the identified mutations impair the catalytic efficiency of PfPDK1 rather than its capacity to interact with its substrates. It therefore seems that the only possibility for the parasite to overcome the lethal effect of PfPKAc OE was to acquire mutations reducing the activity of the PfPKAc-activating kinase PfPDK1. We confirmed this scenario by (1) restoring the PfPDK1 mutation in the PfPKAc OE S1 survivor back to the WT sequence, which rendered these parasites again sensitive to PfPKAc OE; and (2) by introducing the M51R mutation identified in the PfPKAc OE S1 survivor into the WT PfPDK1 kinase in the OE-sensitive clone M1, which rendered these parasites resistant to PfPKAc OE. Strikingly, we could also show that OE of mutant PfPKAc, which carries a non-phosphorylatable residue in place of the putative PfPDK1 target threonine in the activation loop (T189V), has no negative effect on intra-erythrocytic parasite development and multiplication. This striking result demonstrates that in addition to the cAMP-mediated release of PfPKAc from the regulatory subunit, the phosphorylation of T189 is essential for full activation of PfPKAc, and provides compelling evidence that PfPDK1 is the kinase that targets this residue. Our results also imply that unphosphorylated PfPKAc still exerts residual activity because the reduction or lack of PfPDK1-dependent PfPKAc activation in the PfPDK1 mutants could be compensated for by increased PfPKAc expression levels.

Conditional depletion of PfPDK1 did not result in any obvious multiplication or developmental defects in asexual and sexual blood stage parasites. This finding shows that largely diminished PfPDK1 protein levels are still sufficient to activate PfPKAc and sustain parasite proliferation. However, the failure to obtain PfPDK1 null mutants in this study and elsewhere [36,54] strongly argues for an essential role for the PfPDK1 kinase in asexual parasite survival. We have shown that one of these vital functions is to activate PfPKAc. Given that PDK1 is widely conserved in eukaryotes and required to activate a multitude of other AGC class kinases [68], we expect PfPDK1 may also have a role in activating PfPKG and PfPKB, the only other two known members of the AGC family in *P. falciparum* that are both essential in blood stage parasites [36,69]. Interestingly, none of the mutations identified in any of the PfPKAc OE survivors introduced a pre-mature stop codon into the *pfpdk1* open reading frame, suggesting that the mutant PfPDK1 enzyme still retains residual kinase activity and performs an essential function in PfPKAc OE parasites. Whether this essential function lies in securing baseline phosphorylation of PfPKG, PfPKB and/or other potential PfPDK1 substrates, or if some level of PfPKAc phosphorylation is still vital despite PfPKAc being overexpressed, remains to be determined in future studies. Importantly, however, our unsuccessful efforts to mutate PfPDK1 in WT parasites not only corroborates the essential role for PfPDK1 in activating PfPKAc but also indicates that the PfPDK1-dependent phosphorylation of other substrates is either not essential or can still be executed at a functionally relevant level by mutated PfPDK1.

In summary, we provide unprecedented functional insight into the cAMP/PfPKA signalling pathway in the malaria parasite *P. falciparum*. Our results complement earlier studies highlighting the importance of tight regulation of PfPKA activity for parasite survival, showing that diminished as well as augmented PfPKAc expression levels are lethal for asexual blood stage parasites. In addition to the well-established roles of the PfPKAr regulatory subunit, the adenylate cyclase PfACβ and the phosphodiesterase PfPDEβ in regulating PfPKAc activity, we identified PfPDK1 as the upstream kinase

activating PfPKAc through phosphorylation. In light of the essential role of PfPDK1 in this pathway, and possibly also in other parasite AGC kinase-dependent signalling processes, PfPDK1 represents a worthwhile candidate for further functional and structural studies and to be explored as a possible new antimalarial drug target.

Materials and Methods

Parasite culture

P. falciparum NF54 parasites were cultured and asexual growth was synchronized using 5% sorbitol as described previously [70,71]. Parasites were cultured in AB+ or B+ human RBCs (Blood Donation Center, Zurich, Switzerland) at a hematocrit of 5%. The standard parasite culture medium (PCM) contains 10.44 g/L RPMI-1640, 25 mM HEPES, 100 µM hypoxanthine and is complemented with 24 mM sodium bicarbonate and 0.5% AlbuMAX II (Gibco #11021-037). 2 mM choline chloride (CC) was routinely added to PCM to block induction of sexual commitment [3]. To induce sexual commitment, parasites were cultured in serum-free medium (–SerM) as described previously [3]. –SerM medium contains fatty acid-free BSA (0.39%, Sigma #A6003) instead of AlbuMAX II and 30 µM oleic and 30 µM palmitic acid (Sigma #O1008 and #P0500) [3]. Gametocytes were cultured in PCM complemented with 10% human serum (Blood Donation Center, Basel, Switzerland) instead of AlbuMAX II (+SerM). Parasite cultures were kept in gassed (4% CO_2, 3% O_2, 93% N_2) airtight containers at 37 °C.

Transfection constructs

Transgenic parasite lines were generated using the SLI- [40] and CRISPR/Cas9-based [51] genome editing systems. The NF54/AP2-G-mScarlet/PKAc cKD parasite line was generated using a SLI-based single-plasmid approach [40]. For this purpose, the SLI_PKAc_cKD transfection construct was generated in three successive cloning steps using Gibson assembly reactions. First, the SLI_cKD precursor plasmid was generated by joining four fragments in a Gibson assembly reaction: (1) the plasmid backbone amplified from pUC19 (primers PCRA_F and PCRA_R) as previously described [51]; (2)

the *SpeI/BamHI* cloning site followed by the *gfp-dd* sequence amplified from pD_cOE_DD_SpeI/BamHI (Hitz et al., unpublished) using primers gfp_F and dd_R; (3) the *2a-bsd* sequence amplified from pSLI-BSD [40] (primers 2A_F and bsd_R); and (4) the *glmS-hrp2* 3' sequence amplified from pD_cOE (described below) (primers glmS1_F and term_R). Second, a four-fragment Gibson assembly reaction was performed using (1) the *SalI*- and *EcoRI*-digested SLI_cKD precursor plasmid*;* (2) the *calmodulin* (PF3D7_1434200) promoter amplified from pHcamGFP-DD [51] (primers cam1_F and cam1_R); (3) the y*dhodh* resistance gene amplified from the pUF1-Cas9 plasmid [72] (primers ydhodh_F and ydhodh_R); and (4) the *pbdt 3'* terminator amplified from pUF1-Cas9 [72] (primers pbdt3_F and pbdt3_R). Third, this SLI_cKD_ydhodh precursor plasmid was digested using *SpeI* and *BamHI* and joined with the 3' HR of *pfpkac* amplified from NF54 gDNA (primers pka3'_F and pka3'_R) in a two-fragment Gibson assembly reaction resulting in the final SLI_PKAc_cKD transfection construct.

The CRISPR/Cas9 gene editing system employed here is based on co-transfection of a suicide and donor plasmid. The pBF-gC- or pHF-gC-derived suicide plasmids encode the Cas9 enzyme, the single guide RNA (sgRNA) cassette and either the blasticidin deaminase or the human dihydrofolate reductase (hDHFR) resistance markers fused to the negative selection marker yeast cytosine deaminase/uridyl phosphoribosyl transferase (BSD-yFCU or hDHFR-yFCU) [51]. The pD-derived donor plasmid [51] contains the sequence assembly essential for homology-directed repair of the DNA double-strand break induced by Cas9.

To obtain the NF54/PKAc cOE parasite line, the pD_pkac_cOE donor plasmid was generated in several cloning steps using Gibson assembly reactions. First, a pD_cOE_DD precursor plasmid was generated using a two-fragment Gibson assembly joining (1) the plasmid backbone including the *glp3*-specific 5' and 3' HRs amplified from pD_*cg6_cam-gdv1-gfp-glmS* (Boltryk et al., manuscript in preparation) (primers glp3_F and glp3_R) and (2) the *cam 5'-gfpdd-hrp2 3'* sequence amplified from pHcamGFP-DD [51] (primers cam_F and hrp2_R). Second, the subsequent precursor plasmid

pD_cOE_glmS was generated by performing a Gibson assembly using two fragments (1) the pD_cOE_DD precursor plasmid digested using *SalI* and *AgeI* and the (2) *glmS* sequence amplified from pD_*cg6_cam-gdv1-gfp-glmS* (Boltryk et al., manuscript in preparation) (primers glmS_F and glmS_R). To insert a new cloning site and generate the next precursor plasmid pD_cOE, another Gibson assembly reaction was performed joining (1) the pD_cOE_glmS plasmid digested using *BamHI* and *NotI* and (2) annealed complementary oligonucleotides clon_F and clon_R. The final pD_pkac_cOE plasmid was generated by assembling two Gibson fragments: (1) the *BamHI*- and *SpeI*-digested pD_cOE plasmid and (2) the *pfpkac* sequence amplified from NF54 gDNA using primers pka_F and pka_R. The pBF_gC-*cg6* suicide plasmid that was co-transfected with pD_pkac_cOE to generate this NF54/PKAc cOE parasite line encodes the sgRNA targeting the *glp3* locus (Boltryk et al., manuscript in preparation).

To obtain the NF54/PKAcT189V cOE parasite line, the pD_pkacT189V_cOE donor plasmid was generated in a Gibson assembly joining three fragments: (1) the *BamHI*- and *SpeI*-digested pD_cOE plasmid; (2) the 5' fragment of the *pfpkac* sequence containing the single point mutation resulting in the T189V amino acid change (primers pka_F and T189V_R); and (3) the 3'fragment of the *pfpkac* sequence overlapping with the 5' fragment and coding for the same amino acid change (primers T189V_F and pka_R). As described above, the *glp3*-specific suicide plasmid pBF_gC-*cg6* was used for co-transfection.

The NF54/PDK1 cKD parasite line was obtained by co-transfection of pHF_gC_pdk1-gfpdd (encoding sgRNA_pdk1) and pD_pdk1-gfpdd. The previously published suicide mother plasmid pHF-gC [51] was used to insert the sgRNA sequence targeting the 3' end of *pfpdk1* (sgt_pdk1). For this purpose, complementary oligonucleotides were annealed and the resulting double-stranded fragment was ligated into the *BsaI*-digested pHF-gC plasmid using T4 DNA ligase generating the pHF_gC_pdk1-gfpdd suicide plasmid. The pD_pdk1-gfpdd plasmid was generated by performing a four-fragment Gibson assembly joining (1) the plasmid backbone amplified from pUC19 (primers PCRA_F and PCRA_R)

as previously described [51]; (2) the 5' HR amplified from NF54 gDNA (primers hr1KD_F and hr1KD_R); (3) the *gfpdd* sequence (primers gfpdd_F and gfpdd_R) amplified from pHcamGDV1-GFP-DD [51]; and (4) the 3' HR amplified from NF54 gDNA (hr2KD_F and hr2KD_R).

The parasite lines NF54/PKAc cOE M1/PDK1_mut and NF54/PKAc cOE S1/PDK1_wt were generated as follows. Plasmids pHF_gC_S1rev and pHF_gC_M1mut were generated by inserting annealed complementary oligonucleotides encoding the respective sgRNAs (sgRNA_S1rev or sgRNA_M1mut) into the *BsaI*-digested pHF_gC suicide vector [51]. The donor plasmids pD_S1rev and pD_M1mut were generated in a three-fragment Gibson assembly joining (1) the plasmid backbone amplified from pUC19 (primers PCRA_F and PCRA_R) as previously described [51]; (2) the corresponding 5' HRs amplified from NF54 gDNA (primers hr1_F and either rev_R or mut_R); and (3) the respective 3' HRs amplified from NF54 gDNA (primers hr2_R and either rev_F or mut_F). The primers rev_F/rev_R or mut_F/mut_R encode the WT (M) or mutated (R) amino acid number 51 of PfPDK1, respectively.

All primers used for cloning of the described transfection constructs are listed in Supplementary Table 1.

Transfection and transgenic cell lines

P. falciparum ring stage parasite transfection was performed as described [51]. A total of 100 µg plasmid DNA was used to transfect NF54/AP2-G-mScarlet and NF54 WT parasites (100 µg of the SLI_PKAc_cKD plasmid; 50 µg each of all described CRISPR/Cas9 suicide and donor plasmids). 24 hours after transfection of the SLI_PKAc_cKD plasmid, parasites were cultured on 1.5 µM DSM1 until a stably growing parasite population was obtained. This culture was subsequently treated with 2.5 µg/mL blasticidin-S-hydrochloride to select for parasites in which the *pfpkac* gene was successfully tagged. Similarly, 24 hours after transfection of CRISPR/Cas9-based plasmids, the cultures were treated with 2.5 µg/mL blasticidin-S-hydrochloride (for ten

subsequent days) or 4 nM WR99210 (for six subsequent days) depending on the resistance cassette encoded by the suicide plasmid (BSD or hDHFR, respectively). NF54/AP2-G-mScarlet/PKAc cKD and NF54/PDK1 cKD parasites were constantly cultured on 675 nM Shield-1 (+Shield-1) to stabilize the PfPKAc-GFPDD or PfPDK1-GFPDD protein, respectively. NF54/PKAc cOE, NF54/PKAcT189V cOE as well as NF54/PKAc cOE M1/PDK1_mut and NF54/PKAc cOE S1/PDK1_wt parasites were constantly cultured on 2.5 mM GlcN to block PfPKAc or PfPKAcT189V OE. About two to three weeks after transfection, stably growing parasite cultures were obtained and diagnostic PCRs on gDNA were used to confirm correct genome editing. The results of these PCR reactions are displayed in Supplementary Figs. 1, 5, 8 and 13. Primers used to check for correct gene editing are listed in Supplementary Table 2. Correct editing of the *pfpdk1* sequence in NF54/PKAc cOE M1/PDK1_mut and NF54/PKAc cOE S1/PDK1_wt parasites was confirmed by Sanger sequencing as shown in Supplementary Fig. 11.

Limiting dilution cloning

Limiting dilution cloning was performed as previously described [53]. In brief, synchronous ring stage parasite cultures were diluted with fresh PCM and RBCs to a haematocrit of 0.75 % and a parasitaemia of 0.0006 % (=parasite cell suspension). Each well of a flat-bottom 96 well microplate (Costar #3596) was filled with 200 µL PCM/0.75% haematocrit (=RBC suspension). In each well of row A, 100 µL of the parasite cell suspension was mixed with the 200 µL RBC suspension (1/3 dilution) resulting in a parasitaemia of 0.0002% which equals approximately 30 parasites per well. Subsequently, 100 µL of the row A parasite cell suspensions were mixed with 200 µL RBC suspension in the wells of row B resulting again in a 1/3 dilution (approximately 10 parasites/well). This serial dilution was continued until the last row of the plate was reached. The 96-well microplate was kept in a gassed airtight container at 37 °C for 11-14 days without medium change. Subsequently, using the Perfection V750 Pro scanner (Epson), the 96-well microplate

was imaged to visualize plaques in the RBC layer. The content of wells containing a single plaque was then transferred individually into 5 mL cell culture plates and cultured using PCM until a stably growing parasite culture was obtained.

Flow cytometry growth assay

Quantification of parasite multiplication was performed using flow cytometry measurements of fluorescence intensity. For this purpose, synchronous NF54/AP2-G-mScarlet/PKAc cKD parasites (0.2 % parasitaemia) were split at 0-6 hpi and cultured either in presence of Shield-1 and absence of GlcN (+Shield-1/–GlcN) or in absence of Shield-1 and presence of GlcN (–Shield-1/+GlcN) during the entire duration of the multiplication assay. Synchronous NF54/PKAc cOE M1 and S1, NF54/PKAc cOE S1/PDK1_wt, NF54/PKAc cOE M1/PDK1_mut and NF54/PKAcT189V cOE parasites (0.2 % parasitaemia) were split at 0-6 hpi and cultured either in presence of absence of GlcN (±GlcN) for the entire duration of the multiplication assay. Similarly, synchronous NF54/PDK1 cKD parasites (0.2 % parasitaemia) were split at 0-6 hpi and cultured in presence or absence of Shield-1 (±Shield-1) during the entire duration of the multiplication assay. To determine the exact starting parasitaemia on day 1 of the assay, gDNA of synchronous ring stage parasites (18-24 hpi) was stained for 30 min using SYBR Green DNA stain (Invitrogen, 1:10,000) at 37 °C. Subsequently, parasites were washed twice in PBS and fluorescence intensity was measured using the MACS Quant Analyzer 10. 200,000 RBCs were measured per sample. The measurement was repeated in two (day 3 and 5) or three (day 3, 5 and 7) subsequent generations. The FlowJo_v10.6.1 software was used to analyse the flow cytometry data. The measurements were gated to remove small debris (< cell size) and doublets (two cells in a single measurement). Using an uninfected RBC (uRBC) control sample, uRBCs were separated from iRBCs based on their SYBR Green intensity. Representative plots showing the gating strategy used for all flow cytometry data are presented in Supplementary Fig. 2.

Fluorescence microscopy

Live cell fluorescence imaging was performed to visualize protein expression as described [73]. Parasite nuclei were stained using 5 µg/ml Hoechst (Merck) and Vectashield (Vector Laboratories) was used to mount the microscopy slides. Live cell fluorescence microscopy was performed using a Leica DM5000 B fluorescence microscope (20x, 40x and 63x objectives) and images were acquired using the Leica application suite (LAS) software Version 4.9.0 and the Leica DFC345 FX camera. Images were processed using Adobe Photoshop CC 2018 and for each experiment, identical settings for both image acquisition and processing were used for all samples analysed.

For the quantification of the number of nuclei per schizont, synchronous NF54/PfPKAc cOE M1 and S1 ring stage parasites (0-6 hpi) were split and cultured either in presence (+GlcN) or absence (–GlcN) of GlcN. 40 hours later (40-46 hpi), the schizonts were stained using 5 µg/ml Hoechst and Vectashield-mounted slides were visually screened using the Leica fluorescence microscope and the LAS software. Three biological replicate experiments were performed per condition and cell line and the number of nuclei of 100 parasites were quantified per replicate experiment.

Western blot analysis

A parasite pellet was obtained by lysis of the RBC membrane using 0.15% saponin in PBS (10 min on ice) followed by centrifugation and subsequently washed in ice-cold PBS until the supernatant was clear. Whole cell protein lysates were generated by lysing the parasite pellet in an UREA/SDS buffer (8 M Urea, 5% SDS, 50 mM Bis-Tris, 2 mM EDTA, 25 mM HCl, pH 6.5) complemented with 1x protease inhibitor cocktail (Merck) and 1 mM DTT. Protein lysates were separated on NuPage 5-12% Bis-Tris or 3-8% Tris-Acetate gels (Novex, Qiagen) using MES running buffer (Novex, Qiagen). Following protein transfer to a nitrocellulose membrane, the membrane was blocked for 30 min using 5% milk in PBS/0.1% Tween (PBS/Tween). Primary antibodies mouse mAb α-GFP (1:1,000)

(Roche Diagnostics #11814460001) and mAb α-PfGAPDH [74] (1:20,000) diluted in blocking buffer were used for protein detection. Primary antibody incubation was performed at 4 °C overnight in PBS/Tween and the membrane was subsequently washed three times. Incubation using the secondary antibody α-mouse IgG (H&L)-HRP (1:10,000) (GE healthcare #NXA931) diluted in blocking buffer was performed for two hours. The membrane was washed three times using PBS/Tween before chemiluminescent signal detection using KPL LumiGLO Chemiluminescent Substrate System (SeraCare).

Quantification of sexual commitment rates

High content imaging was performed to quantify sexual commitment rates of NF54/AP2-G-mScarlet/PKAc cKD and NF54/AP2-G-mScarlet parasites. For this purpose, synchronous (0-6 hpi) NF54/AP2-G-mScarlet/PKAc cKD and NF54/AP2-G-mScarlet parasites were split (±Shield-1/±GlcN and ±GlcN, respectively) and 18 hours later (18-24 hpi) parasites were exposed to either –SerM (sexual commitment-inducing) or –SerM/CC (sexual commitment-inhibiting) conditions (2% parasitaemia, 2.5% hematocrit). 22 (committed schizonts) or 48 (NF54/AP2-G-mScarlet) hours later, 30 µL of re-suspended parasites were mixed with 50 µL Hoechst/PBS solution (8.1 µM Hoechst) and incubated in a 96-well plate for 30 min. The parasites were then pelleted (300 g, 5 min) and washed twice using 200 µL PBS. Subsequently, the parasite pellet was resuspended using 180 µL PBS and 30 µL of this suspension was pipetted into the wells of a clear-bottom 96-well plate (Greiner CELLCOAT microplate 655948, Poly-D-Lysine, flat µClear bottom) containing 150 µL PBS per well. Prior to imaging, the cells were allowed to settle for 30 min at 37 °C. The MetaXpress software (version 6.5.4.532, Molecular Devices), the ImageXpress Micro widefield high content screening system using the Plan-Apochromat 40x objective (Molecular Devices) and the Sola SE solid state white light engine (Lumencor) were used for automated image acquisition. The Hoechst (Ex: 377/50 nm, Em: 447/60 nm, 80 ms exposure) and mScarlet (Ex: 543/22

nm, Em: 593/40 nm, 600 ms exposure) filter sets were used for imaging of all iRBCs and sexually committed parasites, respectively. Per well, 36 sites were imaged allowing to capture at least 3,000 iRBCs per sample. Image analysis was performed using the MetaXpress software (Brancucci et al., manuscript in preparation). Quantification of both Hoechst-positive and mScarlet-positive parasites allowed calculating sexual commitment rates (percentage of mScarlet-positive parasites amongst Hoechst-positive parasites).

To quantify the sexual commitment rate of NF54/PDK1 cKD parasites, N-acetyl-D-glucosamine (GlcNAc) assays were performed [75]. For this purpose, synchronous (0-6 hpi) NF54/PDK1 cKD parasites were split (±Shield-1) and 18 hours later (18-24 hpi) parasites were exposed to either –SerM (sexual commitment-inducing) or –SerM/CC (sexual commitment-inhibiting) conditions (2% parasitaemia, 5% haematocrit). Upon reinvasion, parasites were cultured in +SerM medium and the parasitaemia was quantified from Giemsa-stained blood smears prepared at 18-24 hpi. This parasitaemia corresponds to the cumulative counts of asexual and sexual (day one of gametocytogenesis) ring stage parasites. From 24-30 hpi onwards, parasites were cultured in +SerM medium supplemented with 50 mM GlcNAc (Sigma) to eliminate asexual parasites [75]. On day four of gametocytogenesis (stage II gametocytes), the parasitaemia was again quantified from Giemsa-stained blood smears. The sexual commitment rate was quantified as the proportion of the parasitaemia on day four (gametocytes only) of the total parasitaemia on day one (asexual and sexual ring stage parasites).

Gametocyte cultures

Synchronous gametocyte cultures were used to study gametocyte morphology, to extract protein samples and for microsphiltration and exflagellation assays. Sexual commitment was induced using –SerM medium (at 18-24 hpi) as described above. Upon reinvasion (0-6 hpi) (asexual and sexual ring stages, day one of gametocytogenesis),

parasites were cultured in +SerM medium. Another 24 hours later (24-30 hpi, trophozoites and stage I gametocytes, day two of gametocytogenesis), GlcNAc was added to the +SerM medium (+SerM/GlcNAc) to eliminate asexual parasites [75]. The +SerM/GlcNAc medium was changed daily for six consecutive days. Subsequently, from day seven onwards, gametocytes were cultured in +SerM medium only. The +SerM medium was changed daily on a 37 °C heating plate to prevent gametocyte activation and exflagellation.

Microsphiltration experiments

Synchronous NF54/AP2-G-mScarlet/PKAc cKD and NF54 WT parasites were split at 0-6 hpi and cultured either in presence or absence of Shield-1 (±Shield-1). Subsequently, at 18-24 hpi sexual commitment was induced using –SerM medium and upon reinvasion gametocytes were cultured using +SerM/GlcNAc and then +SerM medium as described above. On day seven (stage III) and eleven (mature stage V) of gametocytogenesis, microsphiltration experiments were conducted as described previously [49]. Per sample and condition, either one (NF54 WT) or two (NF54/AP2-G-mScarlet/PKAc cKD) independent biological replicate experiments with six technical replicates each were conducted. The experiment starts by transferring gametocyte culture aliquots into 15 mL tubes and lowering the haematocrit to 1.5% by addition of PCM. Six microsphere filters (technical replicates) were loaded per sample and condition (±Shield-1). After injection of 600 µL of cell suspension per filter, filters were washed with 5 mL +SerM medium at a speed of 60 mL per hour using a medical grade pump (Syramed µSP6000, Acromed AG, Switzerland). Gametocytaemia before (“UP”) and after (“DOWN”) the microsphiltration process were determined from Giemsa-stained blood smears by counting at least 1,000 RBCs. The “UP” or input gametocytaemia was determined as the average of the gametocytaemia calculated from two independent Giemsa-stained blood smears. The “DOWN” gametocytaemia was determined for each filter separately. The retention rate of the gametocytes was then calculated as 1-(“DOWN” gametocytaemia

divided by “UP” gametocytaemia). To ensure healthy gametocyte cultures and to prevent gametocyte activation samples were kept at 37 °C whenever possible. The Giemsa-stained smears of the gametocyte input/”UP” samples were further used to control for the quality and lack of activation (stage V) of gametocytes.

Exflagellation assays

On day 14 of gametocytogenesis (mature stage V), exflagellation assays were performed as described previously [47]. Briefly, in a Neubauer chamber gametocytes were activated using 100 µM xanthurenic acid (XA) and a drop in temperature (from 37 °C to 22 °C). After 15 min of activation, the total number of RBCs per mL of culture and the number of exflagellation centers formed by exflagellating male gametocytes were quantified by bright-field microscopy (40x objective). The gametocytaemia before activation was determined from Giemsa-stained thin blood smears. The exflagellation rate was calculated as the number of exflagellating male gametocytes per total gametocytes. Per experiment at least three biological replicates were performed.

Illumina whole genome sequencing

To perform WGS, gDNA of two PfPKAc cOE mother clones (NF54/PKAc cOE M1and M2) and six independently grown PfPKAc OE survivors (NF54/PKAc cOE S1-S6) was isolated using a phenol/chloroform-based extraction protocol as published previously [76]. To avoid an amplification bias due to the high AT-content of *P. falciparum* gDNA, DNA sequencing libraries were prepared with the PCR-free KAPA HyperPrep Kit. Libraries were sequenced on an Illumina NextSeq 500 and the quality of the raw sequencing reads was analyzed with fastqc [77]. The raw reads were mapped to the *P. falciparum* 3D7 reference genome (PlasmoDB version 39) complemented with the transfection plasmid sequences using the Burrows-Wheeler Aligner [78] with default parameters. The alignment files in SAM format were converted to binary BAM files with SAMtools [79] and the BAM files were coordinate-sorted, indexed and read-groups were added with Picard [80].

Sequence variants (SNP and Indels) were directly called with the Genome Analysis Toolkits' (GATK) HaplotypeCaller in the GVCF mode to allow multi-sample analysis [81]. The resulting g.vcf files of the different samples were combined into one file and genotyped using GATK [81]. To predict the consequences of the obtained variants, they were annotated with SnpEff [82] using the SnpEff database supplemented manually with the 3D7 genome annotation (PlasmoDB version 39). The detected variants were filtered for "HIGH" or "MODERATE" impact (according to SnpEff); absence in the "unselected clones/M1 and M2" control samples; and an allele frequency of the alternative allele of >40% in at least one of the survivor samples (S1-S6). The obtained list of 83 candidate variants was first screened manually (1) for variants present in all survivor samples; and (2) for genes mutated in all survivors, leaving the variants identified in Pf3D7_1121900 as only candidates. Additionally, all 83 original candidate variants were inspected visually with the Integrative Genomics Viewer [83]. Variants were excluded if they were suspected to be false-positives because they were (i) only supported by a very small number of reads, and (iia) also detected in reads of the mother clones and not called because of low allele frequencies or (iib) insertions and deletions after/before large homopolymers or repeats. This again left the variants in Pf3D7_1121900 as only candidates.

To analyse the PfPKAc OE cassette copy numbers, the sequencing coverage over the whole genome was determined in 50-nucleotide windows using the software igvtools [83]. The coverage of the endogenous and ectopic (plasmid-derived) *pfpkac* was summed up, as both sequences are identical and reads derived from ectopic *pfpkac* were mapped to both alleles. *pfpkac* coverage was normalized to the genome-wide coverage (assuming the copy number of the genome is 1) and to sequencing data of PfPKAc WT parasites . Finally, the endogenous *pfpkac* was subtracted (-1) to obtain the approximate copy number of ectopic PfPKAc OE cassettes.

Sequence alignments and modelling of protein structure

Alignment of the PfPDK1 (Pf3D7_1121900) amino acid sequence with PDK1 from *Arabidopsis thaliana* (UniProt ID Q9XF67), *Caenorhabditis elegans* (UniProt ID Q9Y1J3) and humans (UniProt ID O15530) was performed using Clustal Omega [84]. A homology model of PfPDK1 structure was built using SWISS-MODEL [85] based on the human PDK1 crystallographic structure (PDB ID 1UU9) [86]. The mean homology model quality (Global Model Quality Estimation, GMQE) was assessed as 0.49, suggesting a model of average quality (possible GMQE values are 0-1 on a linear scale, higher values indicate better quality). A large, predicted disordered loop (amino acids 180-310) present in PfPDK1 but not in its homologues was not built in the model. Amino acids of the ATP-binding cleft were defined as those within 4 Å of any ATP atom in the human PDK1 structure. The PIF-binding pocket was defined as suggested by Biondi and colleagues [17].

Acknowledgements

This work was supported by funding from the Swiss National Science Foundation (BSCGI0_157729) and the Rudolf Geigy Foundation. I.V. thanks the the Medical Research Council UK (MR/N009274/1) and the EPA Cephalosporin Fund (CF 329) for their support.

Author Contributions

E.H. produced transgenic parasite lines, designed and performed experiments, analysed and interpreted data, prepared illustrations and wrote the manuscript. N.W. analysed the WGS data and P.M. supervised these experiments and provided resources. N.M.B.B generated the PfPKAc cKD parasite line, performed the control sexual commitment experiment using high content microscopy (NF54/AP2-G-mScarlet line) and helped performing additional experiments, designed and supervised experiments and interpreted data. A.P. performed and analysed microsphiltration experiments. I.V. performed the bioinformatic analysis and structure modelling of PfPDK1/Pf3D7_1121900. T.S.V. conceived of the study, designed and supervised experiments, provided resources and wrote the manuscript. All authors contributed to editing of the manuscript.

Competing Interests

The authors declare no competing interests.

References

1 Sinha, A. *et al.* A cascade of DNA-binding proteins for sexual commitment and development in Plasmodium. *Nature* **507**, 253-257, doi:10.1038/nature12970 (2014).

2 Kafsack, B. F. *et al.* A transcriptional switch underlies commitment to sexual development in malaria parasites. *Nature* **507**, 248-252, doi:10.1038/nature12920 (2014).

3 Brancucci, N. M. B. *et al.* Lysophosphatidylcholine Regulates Sexual Stage Differentiation in the Human Malaria Parasite Plasmodium falciparum. *Cell* **171**, 1532-1544.e1515, doi:10.1016/j.cell.2017.10.020 (2017).

4 Cowman, A. F., Tonkin, C. J., Tham, W.-H. & Duraisingh, M. T. The Molecular Basis of Erythrocyte Invasion by Malaria Parasites. *Cell Host & Microbe* **22**, 232-245, doi:https://doi.org/10.1016/j.chom.2017.07.003 (2017).

5 Prinz, B. *et al.* Hierarchical phosphorylation of apical membrane antigen 1 is required for efficient red blood cell invasion by malaria parasites. *Sci Rep* **6**, 34479, doi:10.1038/srep34479 (2016).

6 Leykauf, K. *et al.* Protein kinase a dependent phosphorylation of apical membrane antigen 1 plays an important role in erythrocyte invasion by the malaria parasite. *PLoS Pathog* **6**, e1000941, doi:10.1371/journal.ppat.1000941 (2010).

7 Treeck, M. *et al.* Functional analysis of the leading malaria vaccine candidate AMA-1 reveals an essential role for the cytoplasmic domain in the invasion process. *PLoS Pathog* **5**, e1000322, doi:10.1371/journal.ppat.1000322 (2009).

8 Patel, A. *et al.* Cyclic AMP signalling controls key components of malaria parasite host cell invasion machinery. *PLOS Biology* **17**, e3000264, doi:10.1371/journal.pbio.3000264 (2019).

9 Wilde, M.-L. *et al.* Protein Kinase A Is Essential for Invasion of Plasmodium falciparum into Human Erythrocytes. **10**, e01972-01919, doi:10.1128/mBio.01972-19 %J mBio (2019).

10 Walsh, D. A., Perkins, J. P. & Krebs, E. G. An adenosine 3',5'-monophosphate-dependant protein kinase from rabbit skeletal muscle. *J Biol Chem* **243**, 3763-3765 (1968).

11 Taylor, S. S. & Radzio-Andzelm, E. in *Handbook of Cell Signaling (Second Edition)* (eds Ralph A. Bradshaw & Edward A. Dennis) 1461-1469 (Academic Press, 2010).

12 Taylor, S. S., Zhang, P., Steichen, J. M., Keshwani, M. M. & Kornev, A. P. PKA: lessons learned after twenty years. *Biochim Biophys Acta* **1834**, 1271-1278, doi:10.1016/j.bbapap.2013.03.007 (2013).

13 Moore, M. J., Kanter, J. R., Jones, K. C. & Taylor, S. S. Phosphorylation of the Catalytic Subunit of Protein Kinase A: AUTOPHOSPHORYLATION VERSUS PHOSPHORYLATION BY PHOSPHOINOSITIDE-DEPENDENT KINASE-1. **277**, 47878-47884, doi:10.1074/jbc.M204970200 (2002).

14 Yonemoto, W., McGlone, M. L., Grant, B. & Taylor, S. S. Autophosphorylation of the catalytic subunit of cAMP-dependent protein kinase in Escherichia coli. *Protein engineering* **10**, 915-925, doi:10.1093/protein/10.8.915 (1997).

15 Cheng, X., Ma, Y., Moore, M., Hemmings, B. A. & Taylor, S. S. Phosphorylation and activation of cAMP-dependent protein kinase by phosphoinositide-dependent protein kinase. **95**, 9849-9854, doi:10.1073/pnas.95.17.9849 %J Proceedings of the National Academy of Sciences (1998).

16 Voordeckers, K. *et al.* Yeast 3-phosphoinositide-dependent protein kinase-1 (PDK1) orthologs Pkh1-3 differentially regulate phosphorylation of protein kinase A (PKA) and the protein kinase B (PKB)/S6K ortholog Sch9. *The Journal of biological chemistry* **286**, 22017-22027, doi:10.1074/jbc.M110.200071 (2011).

17 Biondi, R. M. *et al.* Identification of a pocket in the PDK1 kinase domain that interacts with PIF and the C-terminal residues of PKA. *The EMBO journal* **19**, 979-988, doi:10.1093/emboj/19.5.979 (2000).
18 Cauthron, R. D., Carter, K. B., Liauw, S. & Steinberg, R. A. Physiological phosphorylation of protein kinase A at Thr-197 is by a protein kinase A kinase. *Molecular and cellular biology* **18**, 1416-1423, doi:10.1128/mcb.18.3.1416 (1998).
19 Frödin, M. *et al.* A phosphoserine/threonine-binding pocket in AGC kinases and PDK1 mediates activation by hydrophobic motif phosphorylation. *The EMBO journal* **21**, 5396-5407, doi:10.1093/emboj/cdf551 (2002).
20 Nirula, A., Ho, M., Phee, H., Roose, J. & Weiss, A. Phosphoinositide-dependent kinase 1 targets protein kinase A in a pathway that regulates interleukin 4. *The Journal of experimental medicine* **203**, 1733-1744, doi:10.1084/jem.20051715 (2006).
21 Alessi, D. R. *et al.* Characterization of a 3-phosphoinositide-dependent protein kinase which phosphorylates and activates protein kinase Balpha. *Current biology : CB* **7**, 261-269, doi:10.1016/s0960-9822(06)00122-9 (1997).
22 Chou, M. M. *et al.* Regulation of protein kinase C zeta by PI 3-kinase and PDK-1. *Current biology : CB* **8**, 1069-1077, doi:10.1016/s0960-9822(98)70444-0 (1998).
23 Dutil, E. M., Toker, A. & Newton, A. C. Regulation of conventional protein kinase C isozymes by phosphoinositide-dependent kinase 1 (PDK-1). *Current biology : CB* **8**, 1366-1375, doi:10.1016/s0960-9822(98)00017-7 (1998).
24 Balendran, A., Currie, R., Armstrong, C. G., Avruch, J. & Alessi, D. R. Evidence that 3-phosphoinositide-dependent protein kinase-1 mediates phosphorylation of p70 S6 kinase in vivo at Thr-412 as well as Thr-252. *J Biol Chem* **274**, 37400-37406, doi:10.1074/jbc.274.52.37400 (1999).
25 Balendran, A. *et al.* PDK1 acquires PDK2 activity in the presence of a synthetic peptide derived from the carboxyl terminus of PRK2. *Current biology : CB* **9**, 393-404, doi:10.1016/s0960-9822(99)80186-9 (1999).
26 Langer, T. *et al.* Folding and activity of cAMP-dependent protein kinase mutants. *FEBS Letters* **579**, 4049-4054, doi:https://doi.org/10.1016/j.febslet.2005.06.015 (2005).
27 Steichen, J. M. *et al.* Global consequences of activation loop phosphorylation on protein kinase A. *J Biol Chem* **285**, 3825-3832, doi:10.1074/jbc.M109.061820 (2010).
28 Tang, Y. & McLeod, M. In vivo activation of protein kinase A in Schizosaccharomyces pombe requires threonine phosphorylation at its activation loop and is dependent on PDK1. *Genetics* **168**, 1843-1853, doi:10.1534/genetics.104.032466 (2004).
29 Keshwani, M. M. *et al.* Cotranslational cis-phosphorylation of the COOH-terminal tail is a key priming step in the maturation of cAMP-dependent protein kinase. *Proc Natl Acad Sci U S A* **109**, E1221-1229, doi:10.1073/pnas.1202741109 (2012).
30 Li, J. & Cox, L. S. Isolation and characterisation of a cAMP-dependent protein kinase catalytic subunit gene from Plasmodium falciparum. *Mol Biochem Parasitol* **109**, 157-163, doi:10.1016/s0166-6851(00)00242-5 (2000).
31 Baker, D. A. *et al.* Cyclic nucleotide signalling in malaria parasites. *Open Biol* **7**, doi:10.1098/rsob.170213 (2017).
32 Flueck, C. *et al.* Phosphodiesterase beta is the master regulator of cAMP signalling during malaria parasite invasion. *PLOS Biology* **17**, e3000154, doi:10.1371/journal.pbio.3000154 (2019).
33 Merckx, A. *et al.* Plasmodium falciparum regulatory subunit of cAMP-dependent PKA and anion channel conductance. *PLoS Pathog* **4**, e19, doi:10.1371/journal.ppat.0040019 (2008).

34 Bouyer, G. *et al.* Plasmodium falciparum sexual parasites regulate infected erythrocyte permeability. *bioRxiv*, 2020.2005.2018.101576, doi:10.1101/2020.05.18.101576 (2020).
35 Ramdani, G. *et al.* cAMP-Signalling Regulates Gametocyte-Infected Erythrocyte Deformability Required for Malaria Parasite Transmission. *PLoS Pathog* **11**, e1004815, doi:10.1371/journal.ppat.1004815 (2015).
36 Solyakov, L. *et al.* Global kinomic and phospho-proteomic analyses of the human malaria parasite Plasmodium falciparum. *Nat Commun* **2**, 565, doi:10.1038/ncomms1558 (2011).
37 Lasonder, E., Green, J. L., Grainger, M., Langsley, G. & Holder, A. A. Extensive differential protein phosphorylation as intraerythrocytic Plasmodium falciparum schizonts develop into extracellular invasive merozoites. *Proteomics* **15**, 2716-2729, doi:10.1002/pmic.201400508 (2015).
38 Lasonder, E. *et al.* The Plasmodium falciparum schizont phosphoproteome reveals extensive phosphatidylinositol and cAMP-protein kinase A signaling. *J Proteome Res* **11**, 5323-5337, doi:10.1021/pr300557m (2012).
39 Treeck, M., Sanders, J. L., Elias, J. E. & Boothroyd, J. C. The phosphoproteomes of Plasmodium falciparum and Toxoplasma gondii reveal unusual adaptations within and beyond the parasites' boundaries. *Cell Host Microbe* **10**, 410-419, doi:10.1016/j.chom.2011.09.004 (2011).
40 Birnbaum, J. *et al.* A genetic system to study Plasmodium falciparum protein function. *Nat Methods* **14**, 450-456, doi:10.1038/nmeth.4223 (2017).
41 Armstrong, C. M. & Goldberg, D. E. An FKBP destabilization domain modulates protein levels in Plasmodium falciparum. *Nat Methods* **4**, 1007-1009, doi:10.1038/nmeth1132 (2007).
42 Banaszynski, L. A., Chen, L. C., Maynard-Smith, L. A., Ooi, A. G. & Wandless, T. J. A rapid, reversible, and tunable method to regulate protein function in living cells using synthetic small molecules. *Cell* **126**, 995-1004, doi:10.1016/j.cell.2006.07.025 (2006).
43 Straimer, J. *et al.* Site-specific genome editing in Plasmodium falciparum using engineered zinc-finger nucleases. *Nat Methods* **9**, 993-998, doi:10.1038/nmeth.2143 (2012).
44 Szymczak, A. L. *et al.* Correction of multi-gene deficiency in vivo using a single 'self-cleaving' 2A peptide-based retroviral vector. *Nature biotechnology* **22**, 589-594, doi:10.1038/nbt957 (2004).
45 Prommana, P. *et al.* Inducible Knockdown of Plasmodium Gene Expression Using the glmS Ribozyme. *PLOS ONE* **8**, e73783, doi:10.1371/journal.pone.0073783 (2013).
46 Brancucci, N. M. B. *et al.* Probing Plasmodium falciparum sexual commitment at the single-cell level. *Wellcome open research* **3**, 70, doi:10.12688/wellcomeopenres.14645.4 (2018).
47 Delves, M. J. *et al.* Routine in vitro culture of P. falciparum gametocytes to evaluate novel transmission-blocking interventions. *Nat Protoc* **11**, 1668-1680, doi:10.1038/nprot.2016.096 (2016).
48 Dearnley, M. *et al.* Reversible host cell remodeling underpins deformability changes in malaria parasite sexual blood stages. **113**, 4800-4805, doi:10.1073/pnas.1520194113 %J Proceedings of the National Academy of Sciences (2016).
49 Lavazec, C. *et al.* Microsphiltration: a microsphere matrix to explore erythrocyte deformability. *Methods in molecular biology (Clifton, N.J.)* **923**, 291-297, doi:10.1007/978-1-62703-026-7_20 (2013).
50 Tiburcio, M. *et al.* A switch in infected erythrocyte deformability at the maturation and blood circulation of Plasmodium falciparum transmission stages. *Blood* **119**, e172-e180, doi:blood-2012-03-414557 [pii];10.1182/blood-2012-03-414557 [doi] (2012).

51 Filarsky, M. *et al.* GDV1 induces sexual commitment of malaria parasites by antagonizing HP1-dependent gene silencing. *Science* **359**, 1259-1263, doi:359/6381/1259 [pii];10.1126/science.aan6042 [doi] (2018).
52 Nkrumah, L. J. *et al.* Efficient site-specific integration in Plasmodium falciparum chromosomes mediated by mycobacteriophage Bxb1 integrase. *Nat Methods* **3**, 615-621, doi:10.1038/nmeth904 (2006).
53 Thomas, J. A. *et al.* Development and Application of a Simple Plaque Assay for the Human Malaria Parasite Plasmodium falciparum. *PLoS One* **11**, e0157873, doi:10.1371/journal.pone.0157873 (2016).
54 Zhang, M. *et al.* Uncovering the essential genes of the human malaria parasite Plasmodium falciparum by saturation mutagenesis. **360**, eaap7847, doi:10.1126/science.aap7847 %J Science (2018).
55 Tewari, R. *et al.* The systematic functional analysis of Plasmodium protein kinases identifies essential regulators of mosquito transmission. *Cell Host Microbe* **8**, 377-387, doi:10.1016/j.chom.2010.09.006 (2010).
56 Toenhake, C. G. *et al.* Chromatin Accessibility-Based Characterization of the Gene Regulatory Network Underlying Plasmodium falciparum Blood-Stage Development. *Cell Host Microbe* **23**, 557-569 e559, doi:10.1016/j.chom.2018.03.007 (2018).
57 Dephoure, N., Gould, K. L., Gygi, S. P. & Kellogg, D. R. Mapping and analysis of phosphorylation sites: a quick guide for cell biologists. *Molecular biology of the cell* **24**, 535-542, doi:10.1091/mbc.E12-09-0677 (2013).
58 Orr, J. W. & Newton, A. C. Requirement for negative charge on "activation loop" of protein kinase C. *J Biol Chem* **269**, 27715-27718 (1994).
59 Kaushal, D. C., Carter, R., Miller, L. H. & Krishna, G. Gametocytogenesis by malaria parasites in continuous culture. *Nature* **286**, 490-492, doi:10.1038/286490a0 (1980).
60 Read, L. K. & Mikkelsen, R. B. Comparison of adenylate cyclase and cAMP-dependent protein kinase in gametocytogenic and nongametocytogenic clones of Plasmodium falciparum. *The Journal of parasitology* **77**, 346-352 (1991).
61 Jullien, N. *et al.* Conditional transgenesis using Dimerizable Cre (DiCre). *PLoS One* **2**, e1355, doi:10.1371/journal.pone.0001355 (2007).
62 Jullien, N., Sampieri, F., Enjalbert, A. & Herman, J. P. Regulation of Cre recombinase by ligand-induced complementation of inactive fragments. *Nucleic Acids Res* **31**, e131, doi:10.1093/nar/gng131 (2003).
63 Tiburcio, M. *et al.* A switch in infected erythrocyte deformability at the maturation and blood circulation of Plasmodium falciparum transmission stages. *Blood* **119**, e172-180, doi:10.1182/blood-2012-03-414557 (2012).
64 Naissant, B. *et al.* Plasmodium falciparum STEVOR phosphorylation regulates host erythrocyte deformability enabling malaria parasite transmission. *Blood* **127**, e42-53, doi:10.1182/blood-2016-01-690776 (2016).
65 Dearnley, M. K. *et al.* Origin, composition, organization and function of the inner membrane complex of Plasmodium falciparum gametocytes. *Journal of cell science* **125**, 2053-2063, doi:10.1242/jcs.099002 (2012).
66 Kono, M. *et al.* Evolution and architecture of the inner membrane complex in asexual and sexual stages of the malaria parasite. *Mol Biol Evol* **29**, 2113-2132, doi:10.1093/molbev/mss081 (2012).
67 Parkyn Schneider, M. *et al.* Disrupting assembly of the inner membrane complex blocks Plasmodium falciparum sexual stage development. *PLOS Pathogens* **13**, e1006659, doi:10.1371/journal.ppat.1006659 (2017).
68 Leroux, A. E., Schulze, J. O. & Biondi, R. M. AGC kinases, mechanisms of regulation and innovative drug development. *Seminars in Cancer Biology* **48**, 1-17, doi:https://doi.org/10.1016/j.semcancer.2017.05.011 (2018).
69 Taylor, H. M. *et al.* The malaria parasite cyclic GMP-dependent protein kinase plays a central role in blood-stage schizogony. *Eukaryot Cell* **9**, 37-45, doi:10.1128/ec.00186-09 (2010).

70 Lambros, C. & Vanderberg, J. P. Synchronization of Plasmodium falciparum erythrocytic stages in culture. *The Journal of parasitology* **65**, 418-420 (1979).
71 Jensen, J. B. & Trager, W. Plasmodium falciparum in culture: establishment of additional strains. *The American journal of tropical medicine and hygiene* **27**, 743-746, doi:10.4269/ajtmh.1978.27.743 (1978).
72 Ghorbal, M. *et al.* Genome editing in the human malaria parasite Plasmodium falciparum using the CRISPR-Cas9 system. *Nature biotechnology* **32**, 819-821, doi:10.1038/nbt.2925 (2014).
73 Witmer, K. *et al.* Analysis of subtelomeric virulence gene families in Plasmodium falciparum by comparative transcriptional profiling. *Mol. Microbiol* **84**, 243-259, doi:10.1111/j.1365-2958.2012.08019.x [doi] (2012).
74 Daubenberger, C. A. *et al.* The N'-terminal domain of glyceraldehyde-3-phosphate dehydrogenase of the apicomplexan Plasmodium falciparum mediates GTPase Rab2-dependent recruitment to membranes. *Biological chemistry* **384**, 1227-1237, doi:10.1515/bc.2003.135 (2003).
75 Fivelman, Q. L. *et al.* Improved synchronous production of Plasmodium falciparum gametocytes in vitro. *Mol. Biochem. Parasitol* **154**, 119-123 (2007).
76 Beck, H. P. Extraction and purification of Plasmodium parasite DNA. *Methods in molecular medicine* **72**, 159-163, doi:10.1385/1-59259-271-6:159 (2002).
77 Babraham-Bioinformatics. *FastQC A Quality Control tool for High Throughput Sequence Data* <http://www.bioinformatics.babraham.ac.uk/projects/fastqc/> (2017).
78 Li, H. & Durbin, R. Fast and accurate short read alignment with Burrows-Wheeler transform. *Bioinformatics (Oxford, England)* **25**, 1754-1760, doi:10.1093/bioinformatics/btp324 (2009).
79 Li, H. *et al.* The Sequence Alignment/Map format and SAMtools. *Bioinformatics (Oxford, England)* **25**, 2078-2079, doi:10.1093/bioinformatics/btp352 (2009).
80 Broad_Institute. *Picard Tools*, <http://broadinstitute.github.io/picard/> (2017).
81 McKenna, A. *et al.* The Genome Analysis Toolkit: a MapReduce framework for analyzing next-generation DNA sequencing data. *Genome Res* **20**, 1297-1303, doi:10.1101/gr.107524.110 (2010).
82 Cingolani, P. *et al.* A program for annotating and predicting the effects of single nucleotide polymorphisms, SnpEff: SNPs in the genome of Drosophila melanogaster strain w1118; iso-2; iso-3. *Fly* **6**, 80-92, doi:10.4161/fly.19695 (2012).
83 Thorvaldsdottir, H., Robinson, J. T. & Mesirov, J. P. Integrative Genomics Viewer (IGV): high-performance genomics data visualization and exploration. *Briefings in bioinformatics* **14**, 178-192, doi:10.1093/bib/bbs017 (2013).
84 Madeira, F. *et al.* The EMBL-EBI search and sequence analysis tools APIs in 2019. *Nucleic Acids Res* **47**, W636-w641, doi:10.1093/nar/gkz268 (2019).
85 Waterhouse, A. *et al.* SWISS-MODEL: homology modelling of protein structures and complexes. *Nucleic Acids Res* **46**, W296-w303, doi:10.1093/nar/gky427 (2018).
86 Komander, D. *et al.* Interactions of LY333531 and other bisindolyl maleimide inhibitors with PDK1. *Structure* **12**, 215-226, doi:10.1016/j.str.2004.01.005 (2004).

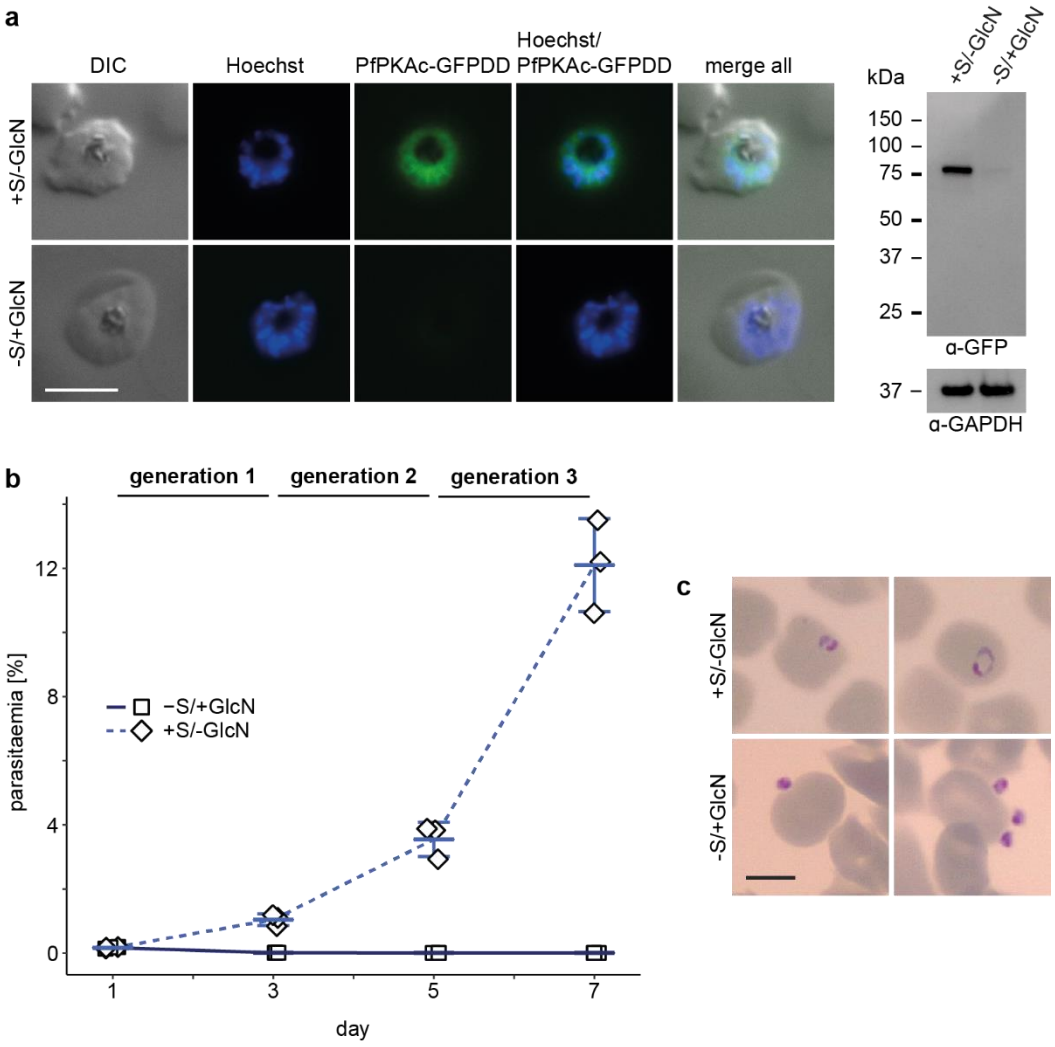

Figure 1. Depletion of PfPKAc in NF54/AP2-G-mScarlet/PKAc cKD parasites leads to a complete block in merozoite invasion. **(a)** Expression of PfPKAc-GFPDD under protein- and RNA-depleting (–Shield-1/+GlcN) and control (+Shield-1/–GlcN) conditions by Western blot analysis and live cell fluorescence imaging. Synchronous parasites (0-8 hpi) were split (±Shield-1/±GlcN) 40 hours before collection of the samples. Representative fluorescence images are shown. Parasite DNA was stained with Hoechst. S, Shield-1; DIC, differential interference contrast. Scale bar = 5 µm. For the Western blot analysis, parasite lysates derived from equal numbers of parasites were loaded per lane. The membrane was first probed with α-GFP followed by α-GAPDH control antibodies. MW PfPKAc-GFPDD = 79.8 kDa, MW PfGAPDH = 36.6 kDa. **(b)** Increase in parasitaemia over three generations under PfPKAc-GFPDD-depleting (–Shield-1/+GlcN) and control (+Shield-1/–GlcN) conditions. Synchronous parasites (0-6

hpi) were split (±Shield-1/±GlcN) 18 hours before the first measurement (day 1). Open squares represent data points for individual replicates and the means±SD of three biological replicates are shown. S, Shield-1. **(c)** Representative images showing the progeny of parasites (0-6 hpi, generation 2) cultured under PfPKAc-GFPDD-depleting (–Shield-1/+GlcN) or control (+Shield-1/–GlcN) conditions. Parasites were split (±Shield-1/±GlcN) 48 hours before the images were captured from Giemsa-stained blood smears. Merozoites under PfPKAc-GFPDD-depleting conditions are unable to invade new RBCs. Scale bar = 5 µm. S, Shield-1.

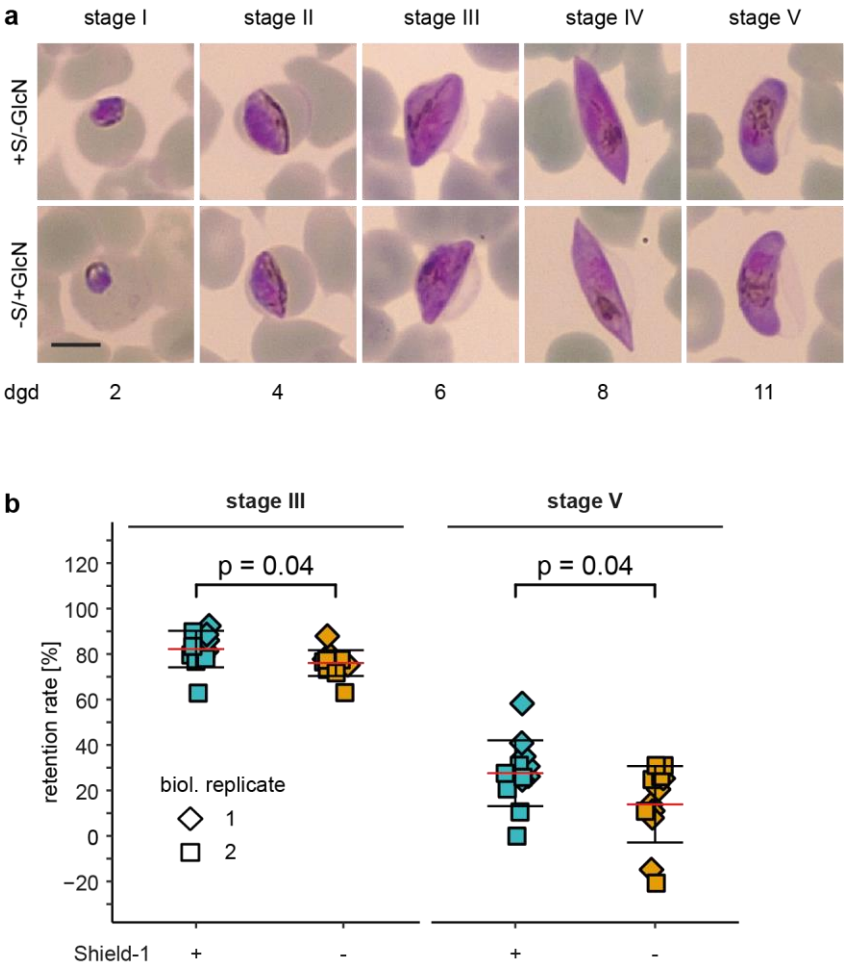

Figure 2. Depletion of PfPKAc in NF54/AP2-G-mScarlet/PKAc cKD parasites has no effect on gametocytogenesis and exflagellation but increases the deformability of stage III and stage V gametocytes. **(a)** Representative images of the distinct morphology of stage I-V gametocytes cultured under PfPKAc-GFPDD-depleting (–Shield-1/+GlcN) and control (+Shield-1/–GlcN) conditions over eleven days of maturation. Synchronous parasites were split (±Shield-1/±GlcN) as sexual/asexual ring stage parasites 24 hours after the induction of sexual commitment in the preceding IDC. To eliminate asexual parasites, gametocytes were cultured in +SerM supplemented with 50 mM GlcNAc from day one to six of gametocytogenesis. Images were captured from Giemsa-stained blood smears. Scale bar = 5 µm. dgd, day of gametocyte development; S, Shield-1. **(b)** Retention rates of stage III (day 6, left) and stage V (day 11, right) gametocytes cultured under PfPKAc-GFPDD protein-depleting (–Shield-1) and control conditions (+Shield-1) over 11 days of maturation. To eliminate asexual parasites, gametocytes were cultured

in +SerM supplemented with 50 mM GlcNAc from day one to six of gametocytogenesis. Coloured squares represent data points for individual replicates (technical and biological) and the means±SD of two biological replicate experiments with six technical replicates each are shown. Significant differences are indicated ($p = 0.04$; unpaired two-tailed Student's t test).

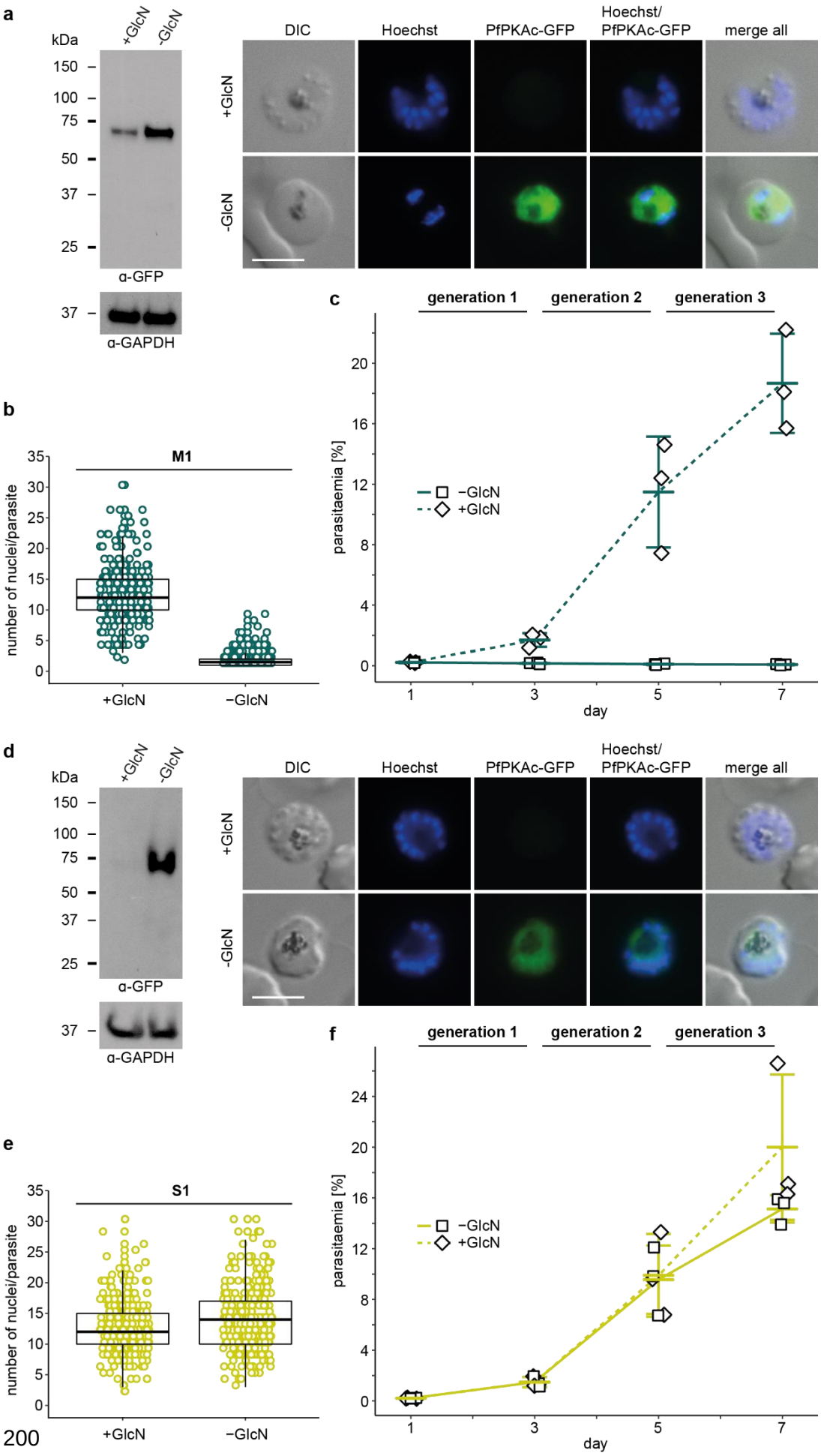
a
kDa
+GlcN
-GlcN
150
100
75
50
37
25
α-GFP
37
α-GAPDH
DIC
Hoechst
PfPKAc-GFP
Hoechst/
PfPKAc-GFP
merge all
+GlcN
-GlcN
b
M1
number of nuclei/parasite
+GlcN
−GlcN
c
generation 1
generation 2
generation 3
parasitaemia [%]
−GlcN
+GlcN
day
d
e
S1
f

Figure 3. Overexpression of PfPKAc in NF54/PKAc cOE M1 parasites is lethal but survivor populations tolerant to PfPKAc OE can be selected. **(a)** Expression of PfPKAc-GFP in NF54/PKAc cOE M1 parasites under overexpression-inducing (–GlcN) and control (+GlcN) conditions by Western blot analysis and live cell fluorescence imaging. Synchronous parasites (0-8 hpi) were split (±GlcN) 40 hours before collection of the samples. Representative fluorescence images are shown. Parasite DNA was stained with Hoechst. DIC, differential interference contrast. Scale bar = 5 µm. For the Western blot analysis, parasite lysates derived from equal numbers of parasites were loaded per lane. The membrane was first probed with α-GFP followed by α-GAPDH control antibodies. MW PfPKAc-GFP = 67.3 kDa, MW PfGAPDH = 36.6 kDa. **(b)** Number of nuclei per schizont in NF54/PKAc cOE M1 parasites under overexpression-inducing (–GlcN) and control (+GlcN) conditions. Synchronous parasites (0-6 hpi) were split (±GlcN) 40 hours before collection of the samples (40-46 hpi). Quantification of the number of nuclei per parasites was performed by live cell imaging of Hoechst-stained parasites. Each open circle represents one parasite. Data from three biological replicate experiments are shown and 100 parasites were counted in each experiment. The boxplots show data distribution (median, upper and lower quartile and whiskers). **(c)** Increase in parasitaemia in NF54/PKAc cOE M1 parasites over three generations under overexpression-inducing (–GlcN) and control (+GlcN) conditions. Synchronous parasites (0-6 hpi) were split (±GlcN) 18 hours before the first measurement (day 1). Open squares represent data points for individual replicates and the means±SD of three biological replicates are shown. **(d)** Expression of PfPKAc-GFP in NF54/PKAc cOE S1 survivor parasites under overexpression-inducing (–GlcN) and control (+GlcN) conditions by Western blot analysis and live cell fluorescence imaging. Parasites were cultured and samples prepared as described in panel a. DIC, differential interference contrast. Scale bar = 5 µm. MW PfPKAc-GFP = 67.3 kDa, MW PfGAPDH = 36.6 kDa. **(e)** Number of nuclei per schizont in NF54/PKAc cOE S1 survivor parasites under overexpression-inducing (–GlcN) and control (+GlcN) conditions. Parasites were cultured and samples

prepared as described in panel b. Each open circle represents one parasite. The boxplots show data distribution (median, upper and lower quartile and whiskers). **(f)** Increase in parasitaemia in NF54/PKAc cOE S1 survivor parasites over three generations under overexpression-inducing (–GlcN) and control (+GlcN) conditions. Synchronous parasites (0-6 hpi) were split (±GlcN) 18 hours before the first measurement (day 1). Open squares represent data points for individual replicates and the means±SD of three biological replicates are shown.

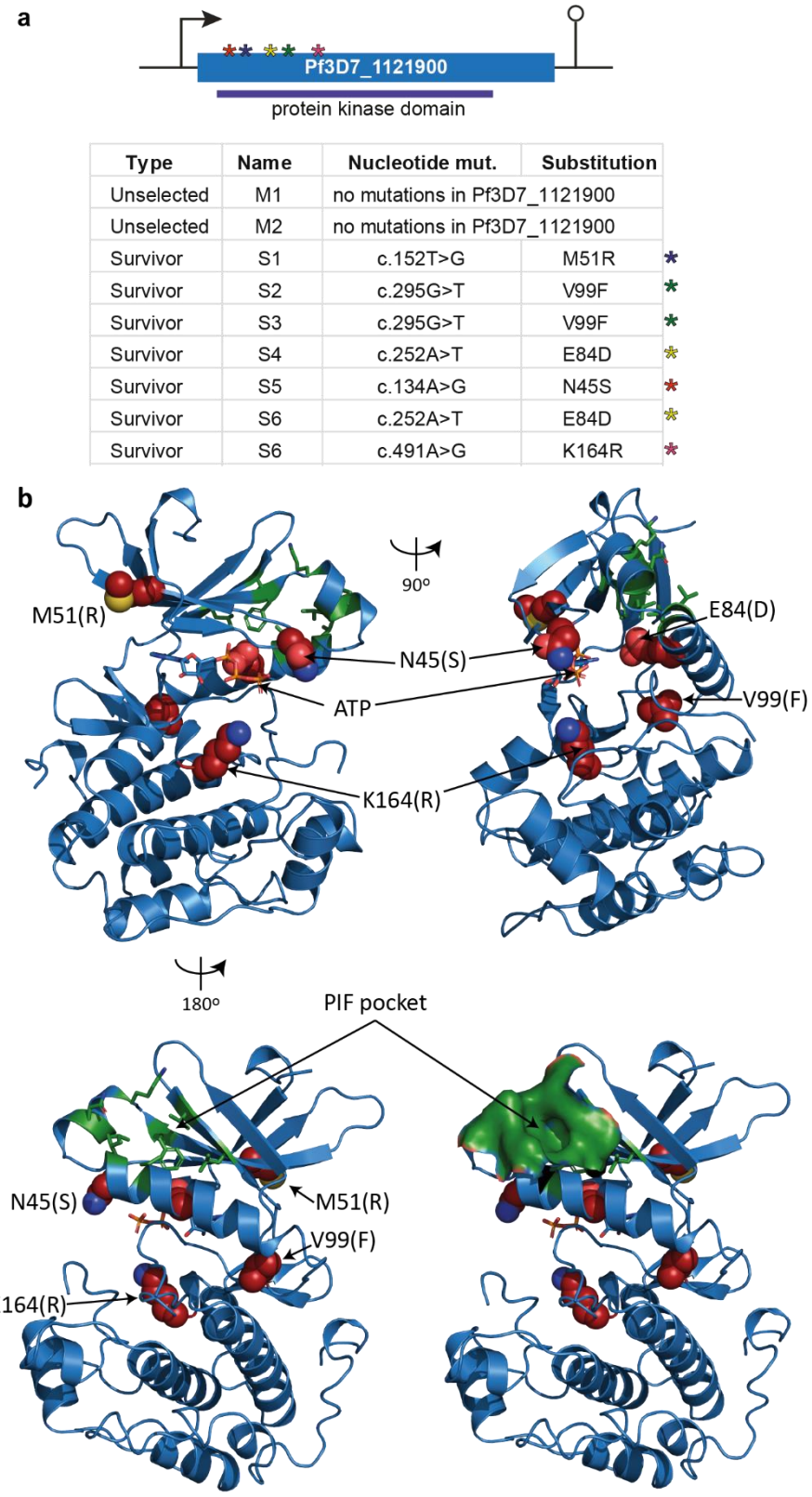

Type	Name	Nucleotide mut.	Substitution	
Unselected	M1	no mutations in Pf3D7_1121900		
Unselected	M2	no mutations in Pf3D7_1121900		
Survivor	S1	c.152T>G	M51R	*
Survivor	S2	c.295G>T	V99F	*
Survivor	S3	c.295G>T	V99F	*
Survivor	S4	c.252A>T	E84D	*
Survivor	S5	c.134A>G	N45S	*
Survivor	S6	c.252A>T	E84D	*
Survivor	S6	c.491A>G	K164R	*

Figure 4. Whole genome Illumina sequencing reveals mutations in the Pf3D7_1121900/*pfpdk1* gene in six independently grown NF54/PKAc cOE survivor

populations. **(a)** Top: Schematic of the Pf3D7_1121900/*pfpdk1* gene. Asterisks indicate the approximate localization of the five point mutations identified in the six (S1-S6) different survivor populations. Bottom: Summary of the information obtained from WGS performed on gDNA of two unselected NF54/PKAc cOE clones (M1, M2) and six independently grown survivors (S1-S6). Nucleotide mutations and their position on *pfpdk1* cDNA level as well as the corresponding amino acid substitutions in PfPDK1 are shown. mut., mutations; c., cDNA. **(b)** Predicted PfPDK1 structure shown in schematic representation, and orthogonal (top left vs top right) or opposing (top left vs lower left) views. PfPDK1 was modelled on the structure of human PDK1 [86]. PfPDK1 segments with no correspondence in human PDK1 (amino acids 1-27, 188-307 and 423-525) are not shown. The ATP substrate (sticks), mutated amino acids (substitution in parenthesis; red spheres) and residues forming the PIF-binding pocket [17] (green sticks) are indicated. The PIF-binding pocket is shown in surface representation in the lower right view.

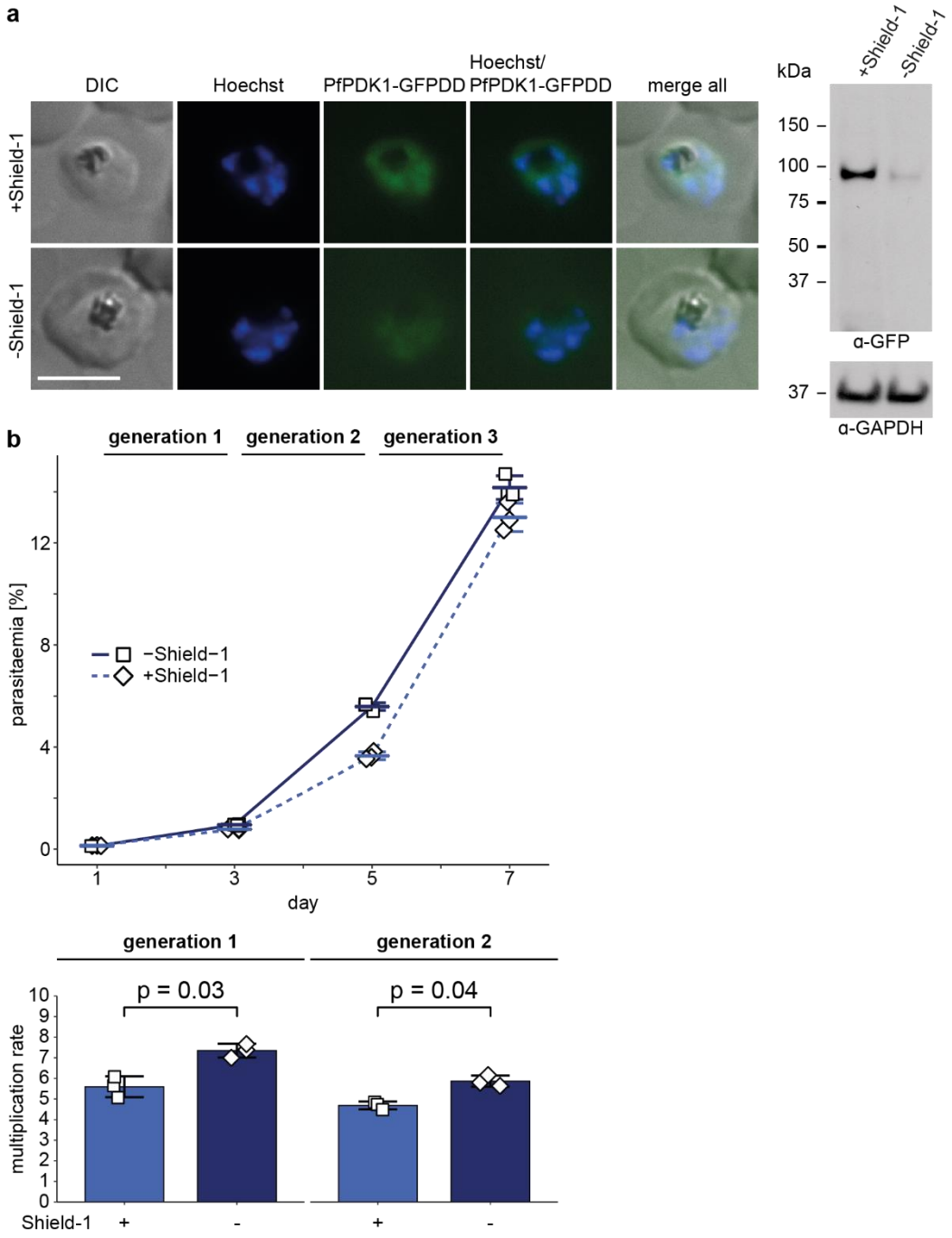

Figure 5. Knockdown of PfPDK1 expression in NF54/PDK1 cKD parasites has no major effect on asexual parasite growth. **(a)** Expression of PfPDK1-GFPDD under protein-depleting (–Shield-1) and control (+Shield-1) conditions by Western blot analysis and live cell fluorescence imaging. Synchronous parasites (0-8 hpi) were split (±Shield-1) 40 hours before collection of the samples. Representative fluorescence images are shown. Parasite DNA was stained with Hoechst. DIC, differential interference contrast. Scale bar = 5 µm. For the Western blot analysis, parasite lysates derived from equal numbers of

parasites were loaded per lane. The membrane was first probed with α-GFP followed by α-GAPDH control antibodies. MW PfPDK1-GFPDD = 101.1 kDa, MW PfGAPDH = 36.6 kDa. **(b)** Increase in parasitaemia (top) and parasite multiplication rates (bottom) under PfPDK1-GFPDD-depleting (–Shield-1) and control (+Shield-1) conditions. Synchronous parasites (0-6 hpi) were split (±Shield-1) 18 hours before the first measurement (day 1). Open squares represent data points for individual replicates and the means±SD of three biological replicates are shown. Significant differences in multiplication rates were determined using a paired two-tailed Student's t test.

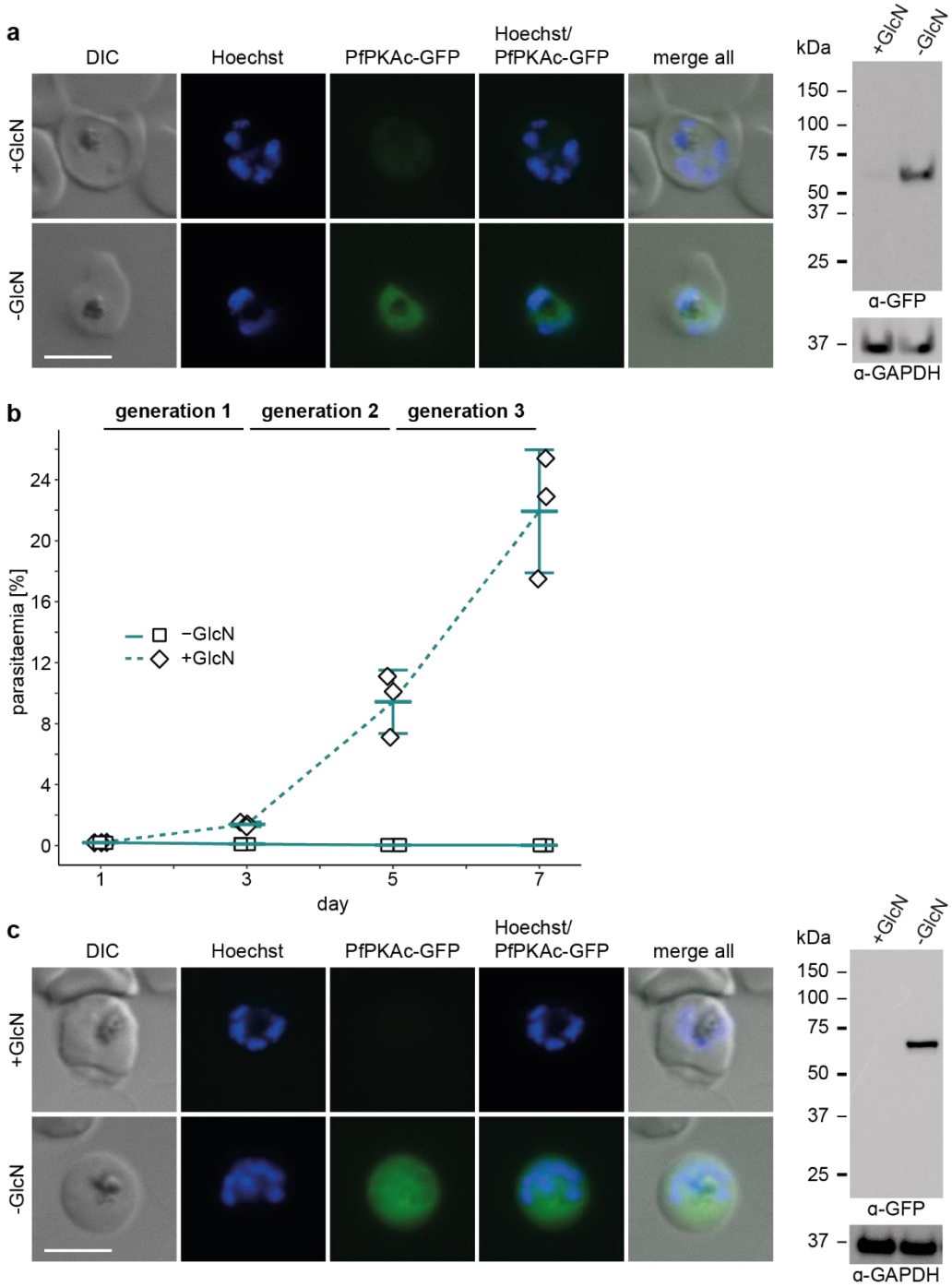
a
DIC
Hoechst
PfPKAc-GFP
Hoechst/
PfPKAc-GFP
merge all
+GlcN
-GlcN
kDa
+GlcN
-GlcN
150
100
75
50
37
25
α-GFP
37
α-GAPDH
b
generation 1
generation 2
generation 3
parasitaemia [%]
−GlcN
+GlcN
day
c
DIC
Hoechst
PfPKAc-GFP
Hoechst/
PfPKAc-GFP
merge all
+GlcN
-GlcN
kDa
+GlcN
-GlcN
150
100
75
50
37
25
α-GFP
37
α-GAPDH
d
generation 1
generation 2
generation 3
parasitaemia [%]
−GlcN
+GlcN
day

Figure 6. Targeted mutagenesis of PfPDK1 confirms its essential role in activating PfPKAc. **(a)** Expression of PfPKAc-GFP in NF54/PKAc cOE S1/PDK1_wt parasites under overexpression-inducing (–GlcN) and control (+GlcN) conditions by Western blot analysis and live cell fluorescence imaging. Synchronous parasites (0-8 hpi) were split (±GlcN) 40 hours before collection of the samples. Representative fluorescence images are shown. Parasite DNA was stained with Hoechst. DIC, differential interference contrast. Scale bar = 5 µm. For the Western blot analysis, parasite lysates derived from an equal number of parasites were loaded per lane. The membrane was first probed with α-GFP followed by α-GAPDH control antibodies. MW PfPKAc-GFP = 67.3 kDa, MW PfGAPDH = 36.6 kDa. **(b)** Increase in parasitaemia of NF54/PKAc cOE S1/PDK1_wt parasites over three generations under overexpression-inducing (–GlcN) and control (+GlcN) conditions. Synchronous parasites (0-6 hpi) were split (±GlcN) 18 hours before the first measurement (day 1). Open squares represent data points for individual replicates and the means±SD of three biological replicates are shown. **(c)** Expression of PfPKAc-GFP in NF54/PKAc cOE M1/PDK1_mut parasites under overexpression-inducing (–GlcN) and control (+GlcN) conditions by Western blot analysis and live cell fluorescence imaging. Parasites were cultured and samples prepared as described in panel a. DIC, differential interference contrast. Scale bar = 5 µm. MW PfPKAc-GFP = 67.3 kDa, MW PfGAPDH = 36.6 kDa. **(d)** Increase in parasitaemia of NF54/PKAc cOE M1/PDK1_mut parasites over three generations under overexpression-inducing (–GlcN) and control (+GlcN) conditions. Synchronous parasites (0-6 hpi) were split (±GlcN) 18 hours before the first measurement (day 1). Open squares represent data points for individual replicates and the means±SD of three biological replicates are shown.

Supplementary Information

A 3-phosphoinositide-dependent protein kinase-1 homologue is essential for activation of protein kinase A in malaria parasites

Eva Hitz[1,2], Natalie Wiedemar[1,2], Nicolas M. B. Brancucci[1,2], Armin Passecker[1,2], Ioannis Vakonakis[3], Pascal Mäser[1,2], Till S. Voss[1,2,*]

[1]Department of Medical Parasitology and Infection Biology, Swiss Tropical and Public Health Institute, 4051 Basel, Switzerland.

[2]University of Basel, 4001 Basel, Switzerland.

[3]Department of Biochemistry, University of Oxford, Oxford OX1 3QU, United Kingdom

[*]Corresponding author: till.voss@swisstph.ch.

The Supplementary Information file includes:

- Supplementary Figures 1-13
- Supplementary Tables 1 and 2
- Supplementary Dataset 1

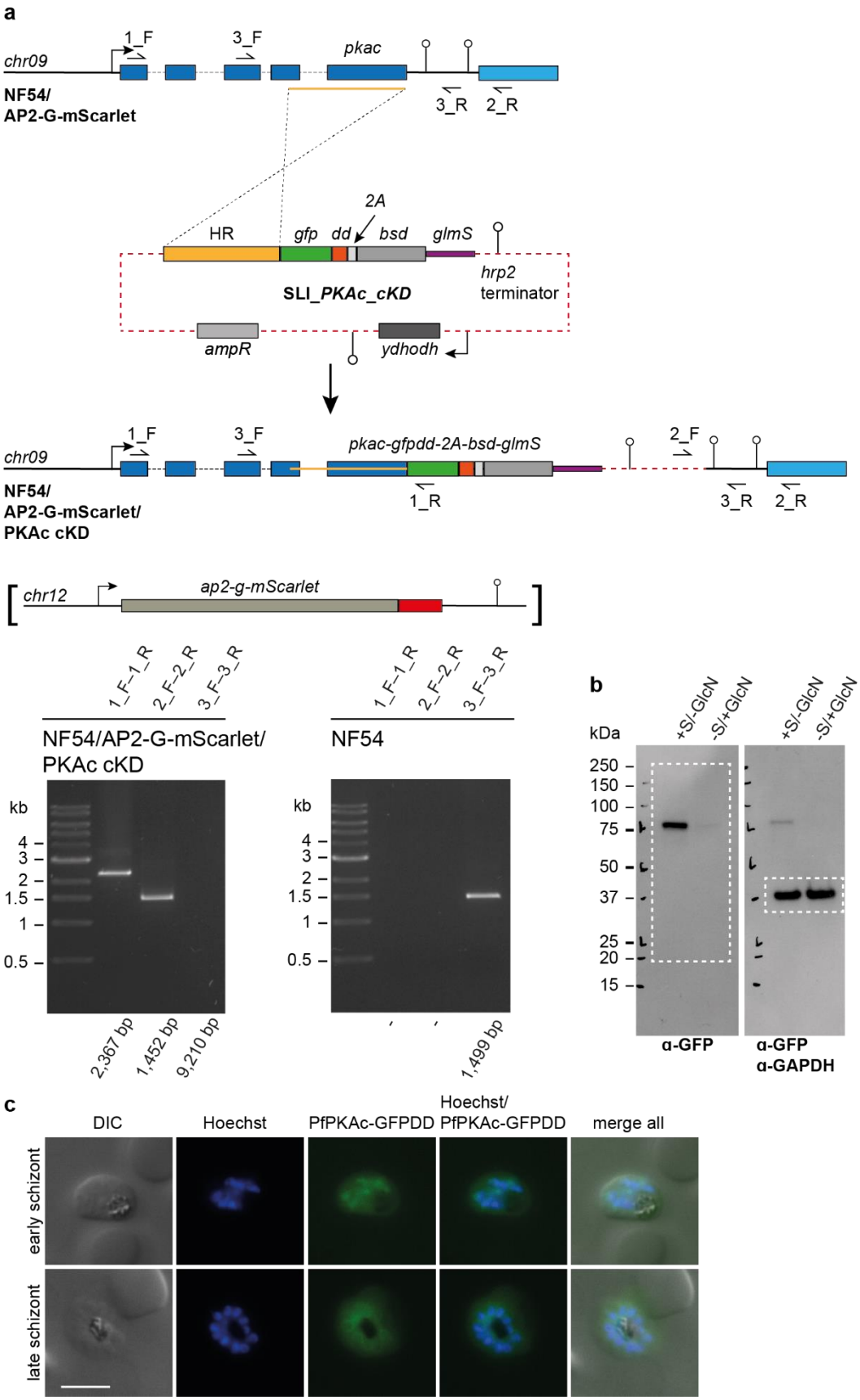

Supplementary Figure 1. SLI-based engineering of the NF54/AP2-G-mScarlet/PKAc cKD parasite line, full size Western blot of the section shown in Fig. 1a and PfPKAc

expression in schizonts. **(a)** Top: Scheme depicting the wild type *pfpkac* locus, the SLI_PKAc_cKD construct transfected into NF54/AP2-G-mScarlet parasites and the edited *pfpkac* locus in NF54/AP2-G-mScarlet/PKAc cKD parasites. Primers used for diagnostic PCRs are indicated. Middle: The schematic map of the edited *pfap2-g-mScarlet* locus in the NF54/AP2-G-mScarlet parasite line (Brancucci et al., manuscript in preparation) is shown in brackets. Bottom: Results of PCR reactions performed on gDNA of NF54/AP2-G-mScarlet/PKAc cKD and NF54 WT control parasites confirm correct gene editing. **(b)** Full size Western blot shows expression of PfPKAc-GFPDD under protein- and RNA-depleting (–Shield-1/+GlcN) and control (+Shield-1/–GlcN) conditions. Synchronous parasites (0-8 hpi) were split (±Shield-1/±GlcN) 40 hours before collection of the samples. Parasite lysates derived from an equal number of parasites were loaded per lane. The membrane was first probed with α-GFP followed by α-GAPDH control antibodies. Dashed lines mark the blot section shown in Fig.1a. MW PfPKAc-GFPDD = 79.8 kDa, MW PfGAPDH = 36.6 kDa. S, Shield-1. **(c)** Expression of PfPKAc-GFPDD in early and late schizonts under protein- and RNA-stabilizing (+Shield-1/–GlcN) conditions by live cell fluorescence imaging. Parasites were previously synchronized to an 8-hour window and imaged at 40-48 hpi. Representative fluorescence images are shown. Parasite DNA was stained with Hoechst. DIC, differential interference contrast. Scale bar = 5 µm.

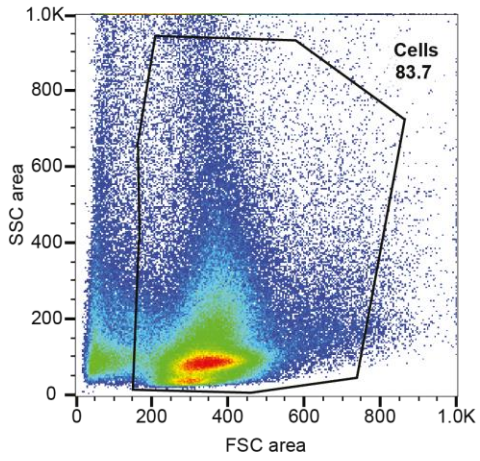

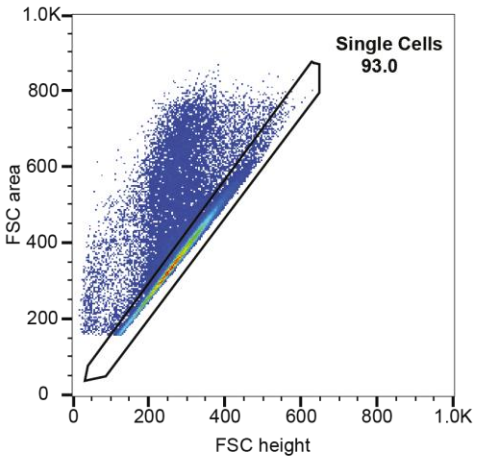

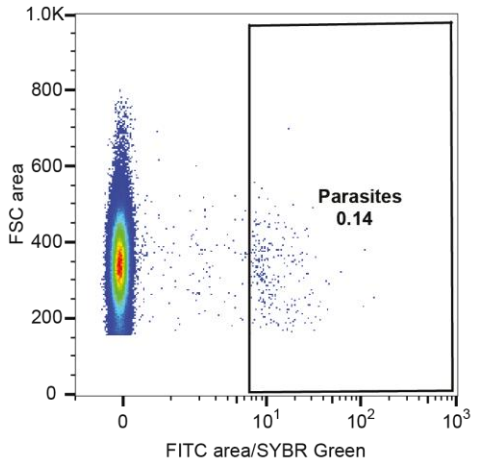

Infected RBC sample
- first measurement
  (day 1 of multiplication assay)

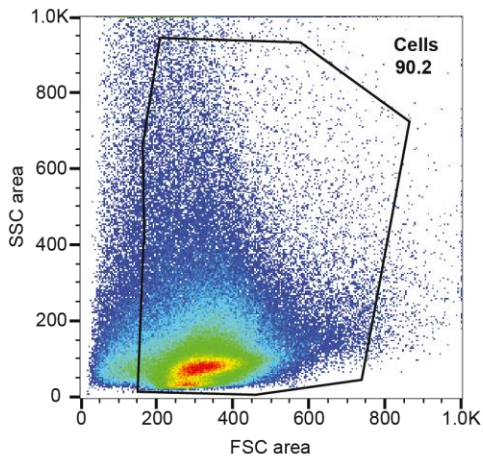

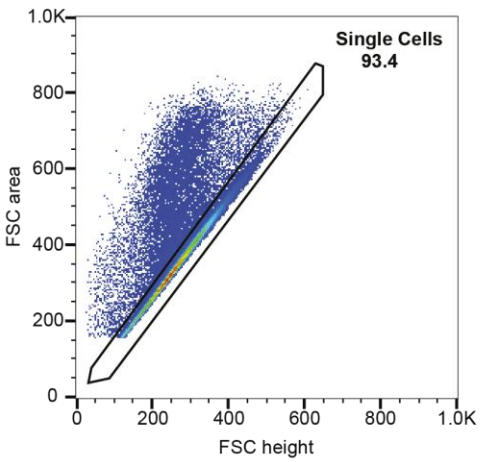

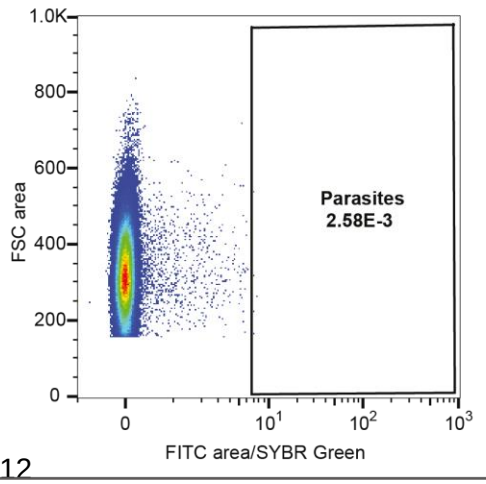

Uninfected RBC control sample
- first measurement
  (day 1 of multiplication assay)

Supplementary Figure 2. Gating strategy of flow cytometry data obtained from parasite multiplication assays. Representative flow cytometry plots of an infected (top frame; NF54/AP2-G-mScarlet/PKAc cKD +Shield-1/–GlcN) and an uninfected RBC control sample (bottom frame) on day one of the multiplication assay are shown. For both samples, the first plot (top left) shows the gating strategy used to remove small debris (smaller than cell size) and keep the “Cells” which are further gated. The next gating strategy of the “Cells” population was to remove doublets (single measurement events consisting of two cells) and keep the “Single Cells” (top right). In the last gating step, separation of uninfected from infected RBCs (bottom left) was based on SYBR Green fluorescence intensity. The percentage of cells included in the “Parasites” gate directly corresponds to the parasitaemia of the sample. All flow cytometry data was gated using this strategy and the resulting parasite multiplication plots are shown in Figs. 1, 3, 5 and 6 and in Supplementary Figs. 6, 9, 11 and 13.

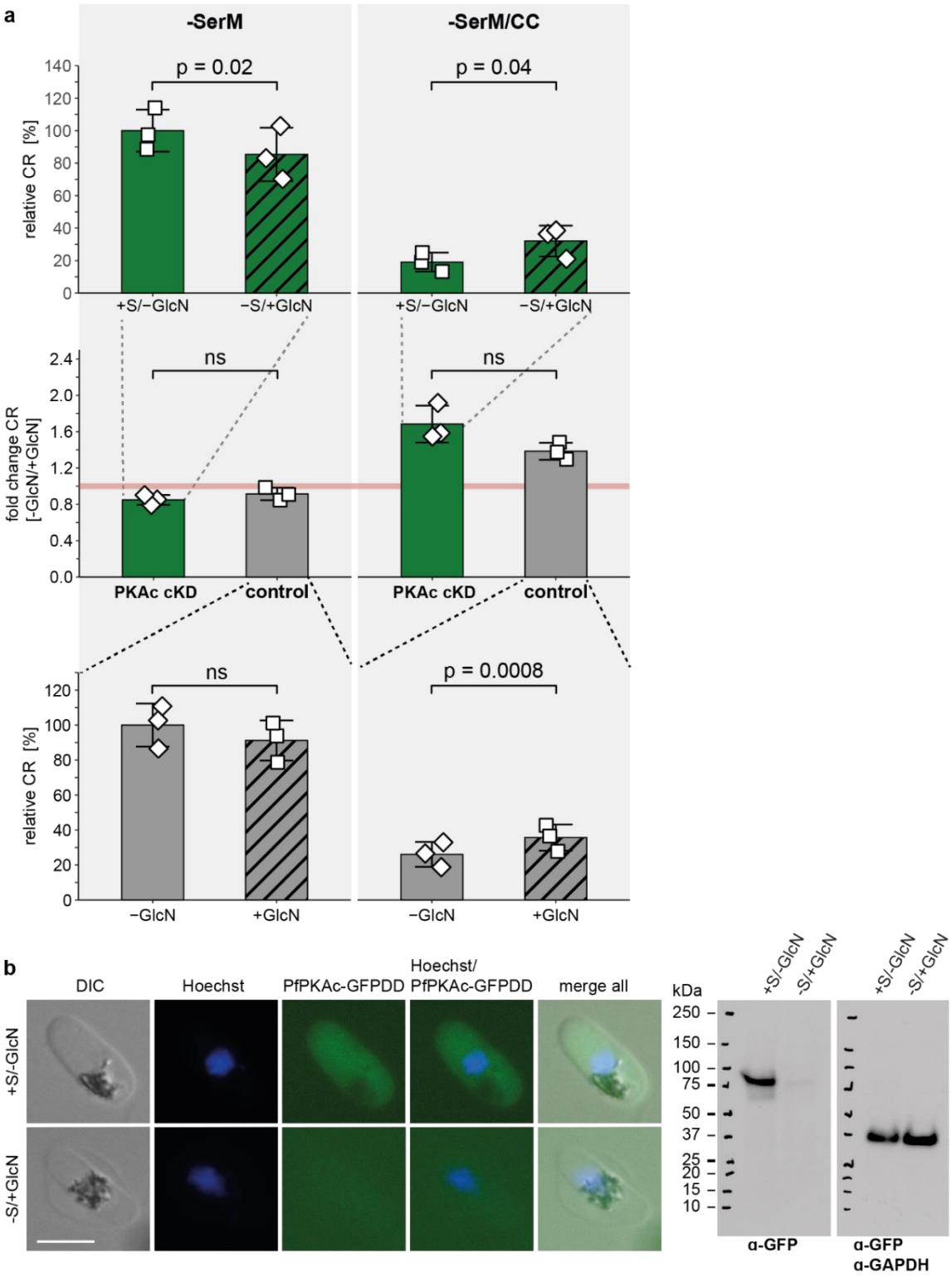

Supplementary Figure 3. Sexual commitment rates of NF54/AP2-G-mScarlet/PKAc cKD and NF54/AP2-G-mScarlet parasites and expression of PfPKAc-GFPDD in stage V gametocytes. **(a)** Top: Relative sexual commitment rates of NF54/AP2-G-mScarlet/PKAc cKD parasites cultured under protein- and RNA-depleting (–Shield-1/+GlcN) and control (+Shield-1/–GlcN) conditions and in serum-free medium in absence (–SerM,

commitment-inducing) or presence (–SerM/CC, commitment-inhibiting) of choline chloride [1]. Sexual commitment rates were determined by high content imaging and automated image analysis by assessing PfAP2-G-mScarlet positivity among the total number of iRBCs (Hoechst-stained parasite DNA). For each experiment, at least 3,000 Hoechst-positive cells were assessed for PfAP2-G-mScarlet expression. Open squares represent data points for individual replicates and the means±SD of three biological replicate experiments are shown. Middle: Fold change in sexual commitment rates between NF54/AP2-G-mScarlet/PKAc cKD parasite cultured under –Shield-1/+GlcN or +Shield-1/–GlcN conditions (green) and between NF54/AP2-G-mScarlet control parasites cultured under +GlcN or –GlcN conditions (grey). Bottom: Relative sexual commitment rates of NF54/AP2-G-mScarlet control parasites in presence (+GlcN) or absence (–GlcN) of GlcN cultured under commitment-inducing (–SerM) and –inhibiting (–SerM/CC) conditions [1]. Open squares represent data points for individual replicates and the means±SD of three biological replicate experiments are shown. Significant differences in sexual commitment rates were determined using a paired two-tailed Student's t test. ns, not significant; S, Shield-1; CR, commitment rate; –SerM, serum-free medium; CC, choline chloride; control, NF54/AP2-G-mScarlet. **(b)** Expression of PfPKAc-GFPDD under protein- and RNA-depleting (–Shield-1/+GlcN) and control (+Shield-1/–GlcN) conditions by live cell fluorescence imaging and Western blot analysis of mature stage V gametocytes (day 11). Synchronous parasites were split (±Shield-1/±GlcN) as sexual/asexual ring stages 24 hours after the induction of sexual commitment using –SerM medium [1]. To eliminate asexual parasites, gametocytes were cultured in +SerM supplemented with 50 mM GlcNAc from day one to six of gametocytogenesis [2]. Representative fluorescence images are shown. Parasite DNA was stained with Hoechst. DIC, differential interference contrast. Scale bar = 5 µm. For the Western blot analysis, parasite lysates derived from an equal number of parasites were loaded per lane. The membrane was first probed with α-GFP followed by α-GAPDH

control antibodies. MW PfPKAc-GFPDD = 79.8 kDa, MW PfGAPDH = 36.6 kDa. S, Shield-1.

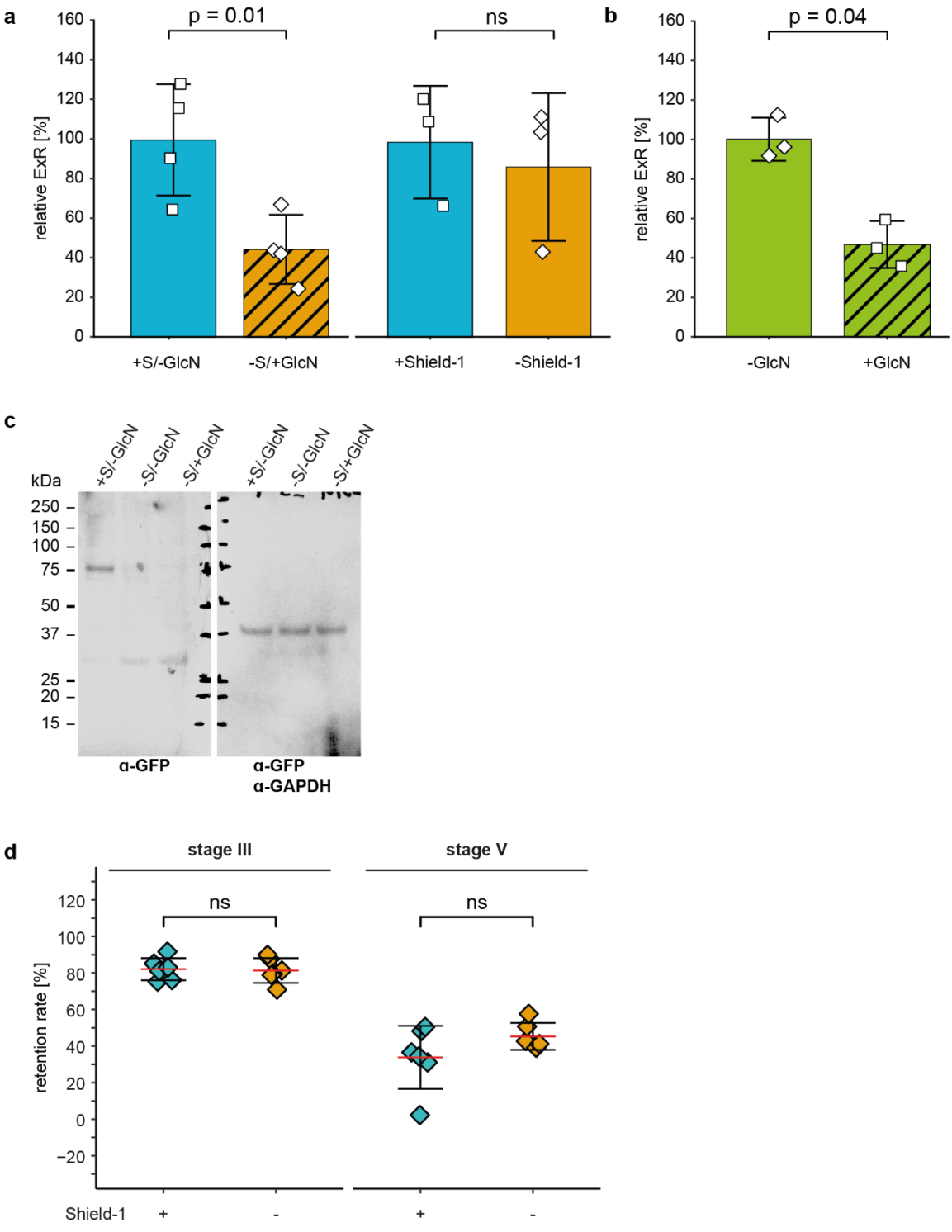

Supplementary Figure 4. Expression of PfPKAc in NF54/AP2-G-mScarlet/PKAc cKD gametocytes and exflagellation as well as retention rates of NF54 wild type gametocytes. **(a)** Relative exflagellation rates of mature stage V gametocytes (day 14) cultured under protein- and RNA-depleting (–Shield-1/+GlcN) and control (+Shield-1/–GlcN) conditions (left) or under protein-depleting conditions only (–Shield-1) and control (+Shield-1) conditions. Synchronous parasites were split (±Shield-1/±GlcN) as sexual/asexual ring

stages 24 hours after the induction of sexual commitment in the preceding IDC. To eliminate asexual parasites, gametocytes were cultured in +SerM supplemented with 50 mM GlcNAc from day one to six of gametocytogenesis [2]. Open squares represent data points for individual replicates and the means±SD of four (left) or three (right) biological replicate experiments are shown. Significant differences in exflagellation rates were determined using a paired two-tailed Student's t test. ns, not significant; ExR, exflagellation rate; S, Shield-1. **(b)** Relative exflagellation rates of mature NF54 WT stage V gametocytes (day 14) cultured in presence (+GlcN) and absence (–GlcN) of GlcN. Parasites were cultured as described in panel a. Open squares represent data points for individual replicates and the means±SD of three biological replicate experiments are shown. A significant difference in exflagellation rates was determined using a paired two-tailed Student's t test. ExR, exflagellation rate. **(c)** Full size Western blot shows expression of PfPKAc-GFPDD under protein- and RNA-depleting (–Shield-1/+GlcN), protein-depleting (–Shield-1/–GlcN) and control (+Shield-1/–GlcN) conditions in mature stage V gametocytes (day 11). Synchronous parasites were split (±Shield-1/±GlcN) as sexual/asexual ring stages upon reinvasion after the induction of sexual commitment during the preceding IDC. To eliminate asexual parasites, gametocytes were cultured in +SerM supplemented with 50 mM GlcNAc from day one to six of gametocytogenesis [2]. Parasite lysates derived from equal numbers of parasites were loaded per lane. The membrane was first probed with α-GFP followed by α-GAPDH control antibodies. MW PfPKAc-GFPDD = 79.8 kDa, MW PfGAPDH = 36.6 kDa. S, Shield-1. **(d)** Retention rates of NF54 WT stage III (day 6) and stage V (day 11) gametocytes cultured in presence (+Shield-1) and absence (–Shield-1) of Shield-1 over eleven days of maturation. To eliminate asexual parasites, gametocytes were cultured in +SerM medium supplemented with 50 mM GlcNAc from day one to six of gametocytogenesis [2]. Coloured squares represent data points for individual replicates and the means±SD of one biological replicate experiment with six technical replicates are shown. ns, not significant (unpaired two-tailed Student's t test).

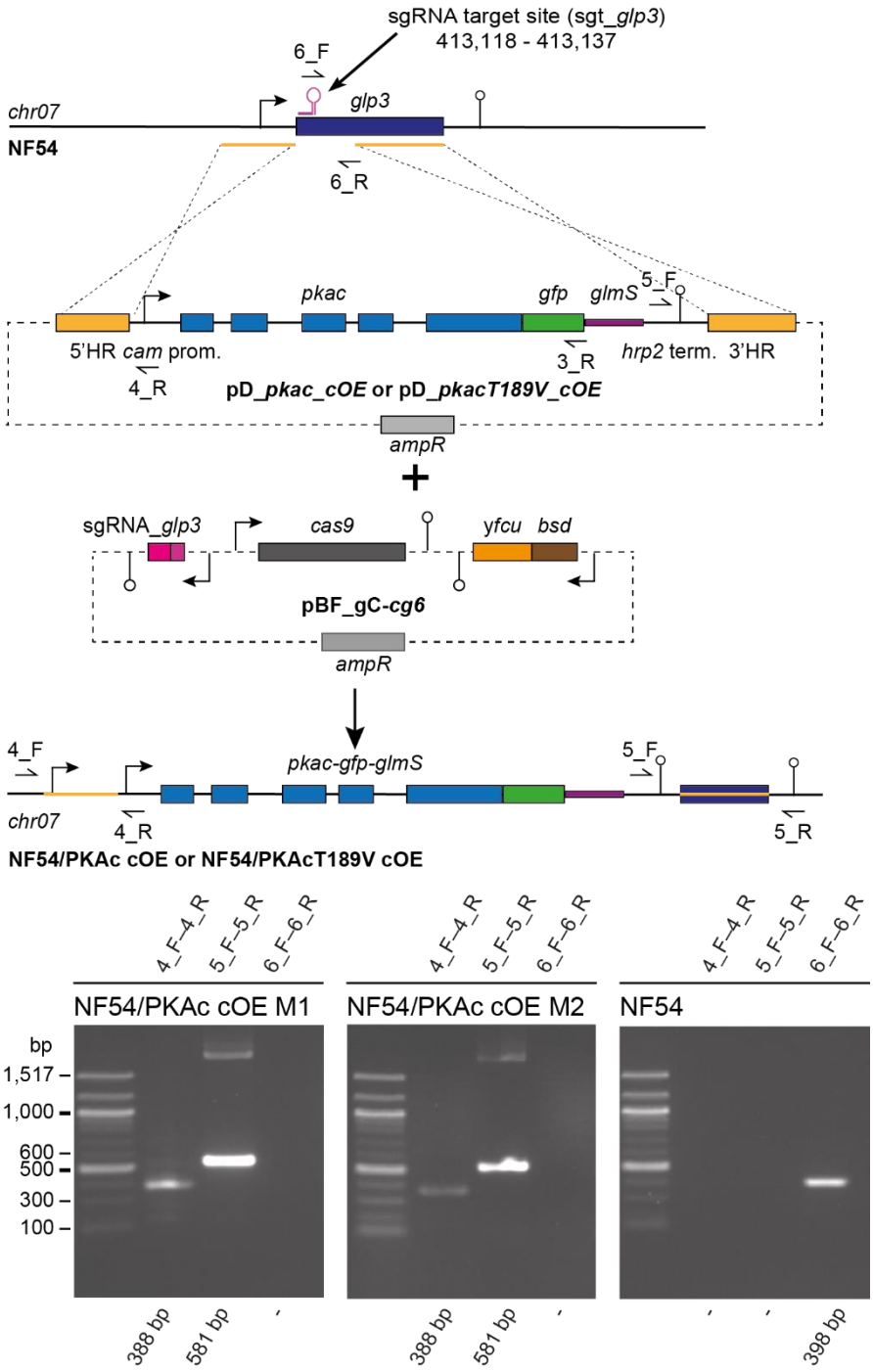

Supplementary Figure 5. CRISPR/Cas9-based engineering of the NF54/PKAc cOE and the NF54/PKAcT189V cOE parasite lines. Top: Scheme depicting the wild type *glp3* target locus, the donor (pD_pkac_cOE or pD_pkacT189V_cOE) and pBF_gC-cg6 suicide constructs transfected into NF54 WT parasites to generate the NF54/PKAc cOE and NF54/PKAcT189V cOE parasite lines and the edited *glp3* locus. Primers used for diagnostic PCRs are indicated. Middle: Results of PCR reactions performed on gDNA of

two clones (M1 and M2) of the NF54/PKAc cOE line. NF54 WT control parasites confirm successful insertion of the PfPKAc cOE cassettes into the *glp3* locus.

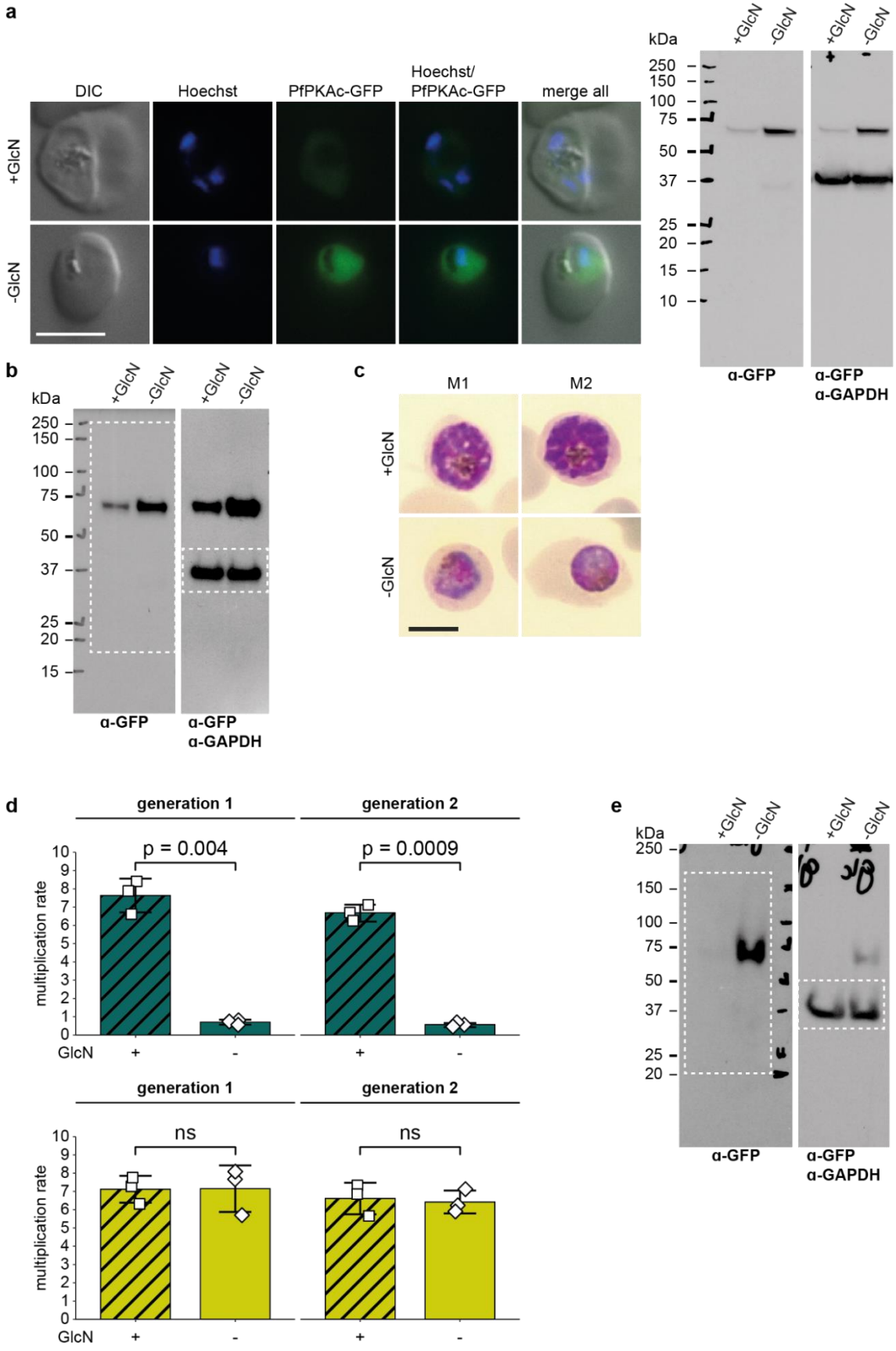

Supplementary Figure 6. Overexpression of PfPKAc in NF54/PKAc cOE M1 and M2 parasites leads to parasite death; full size Western blots of the sections shown in Fig. 3

and multiplication rates of NF54/PKAc cOE M1 and S1 parasites. **(a)** Expression of PfPKAc-GFP in NF54/PKAc cOE M2 parasites under overexpression-inducing (–GlcN) and control (+GlcN) conditions by Western blot analysis and live cell fluorescence imaging. Synchronous parasites (0-8 hpi) were split (±GlcN) 40 hours before collection of the samples. Representative fluorescent images are shown. Parasite DNA was stained with Hoechst. DIC, differential interference contrast. Scale bar = 5 µm. For the Western blot analysis, parasite lysates derived from equal numbers of parasites were loaded per lane. The membrane was first probed with α-GFP followed by α-GAPDH control antibodies. MW PfPKAc-GFP = 67.3 kDa, MW PfGAPDH = 36.6 kDa. **(b)** Full size Western blot shows expression of PfPKAc-GFP in NF54/PKAc cOE M1 parasites under overexpression-inducing (–GlcN) and control (+GlcN) conditions. Parasites were cultured and samples prepared as described in panel a. Dashed lines mark the blot sections shown in Fig. 3a. MW PfPKAc-GFP = 67.3 kDa, MW PfGAPDH = 36.6 kDa. **(c)** Representative images showing NF54/PKAc cOE M1 and M2 parasites under overexpression-inducing (–GlcN) and control (+GlcN) conditions. Synchronous parasites (0-8 hpi) were split (±GlcN) 40 hours before the images were captured from Giemsa-stained blood smears. Scale bar = 5 µm. **(d)** Parasite multiplication rates of NF54/PKAc cOE M1 (top) and S1 survivor (bottom) parasites under overexpression-inducing (–GlcN) and control (+GlcN) conditions over two generations. Synchronous parasites (0-6 hpi) were split (±GlcN) 18 hours before the first measurement (day 1). Open squares represent data points for individual replicates and the means±SD of three biological replicates are shown. Significant differences in parasite multiplication rates were determined using a paired two-tailed Student's t test. ns, not significant. Note that the same data is presented as an increase in parasitaemia over time in Figs. 3c and 3f. **(e)** Full size Western blot shows expression of PfPKAc-GFP in NF54/PKAc cOE S1 parasites under overexpression-inducing (–GlcN) and control (+GlcN) conditions. Parasites were cultured and samples prepared as described in panel a. Dashed lines

mark the blot sections shown in Fig. 3d. MW PfPKAc-GFP = 67.3 kDa, MW PfGAPDH = 36.6 kDa.

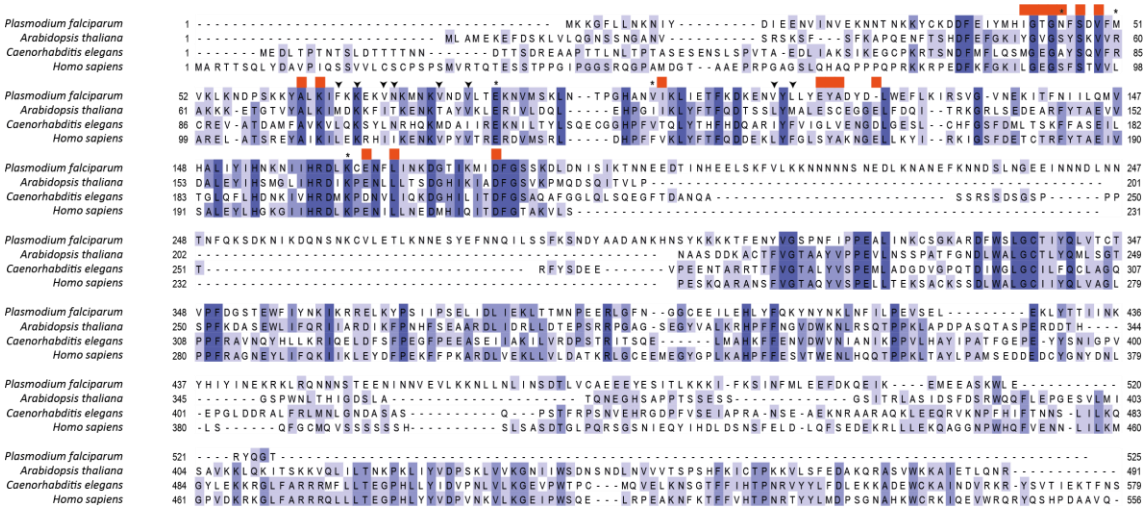

Supplementary Figure 7. Clustal Omega [4] multiple sequence alignment of PfPDK1 (Pf3D7_1121900) (shown as *P. falciparum*) with well-characterised PDK1 homologues from diverse species as indicated. Residues are highlighted in blue gradient depending on fractional conservation. Arrowheads denote residues forming the PIF-binding pocket [5], asterisks denote residues mutated in PfPKAc OE survivors identified in this study and red bars denote residues that form part of the ATP-binding cleft.

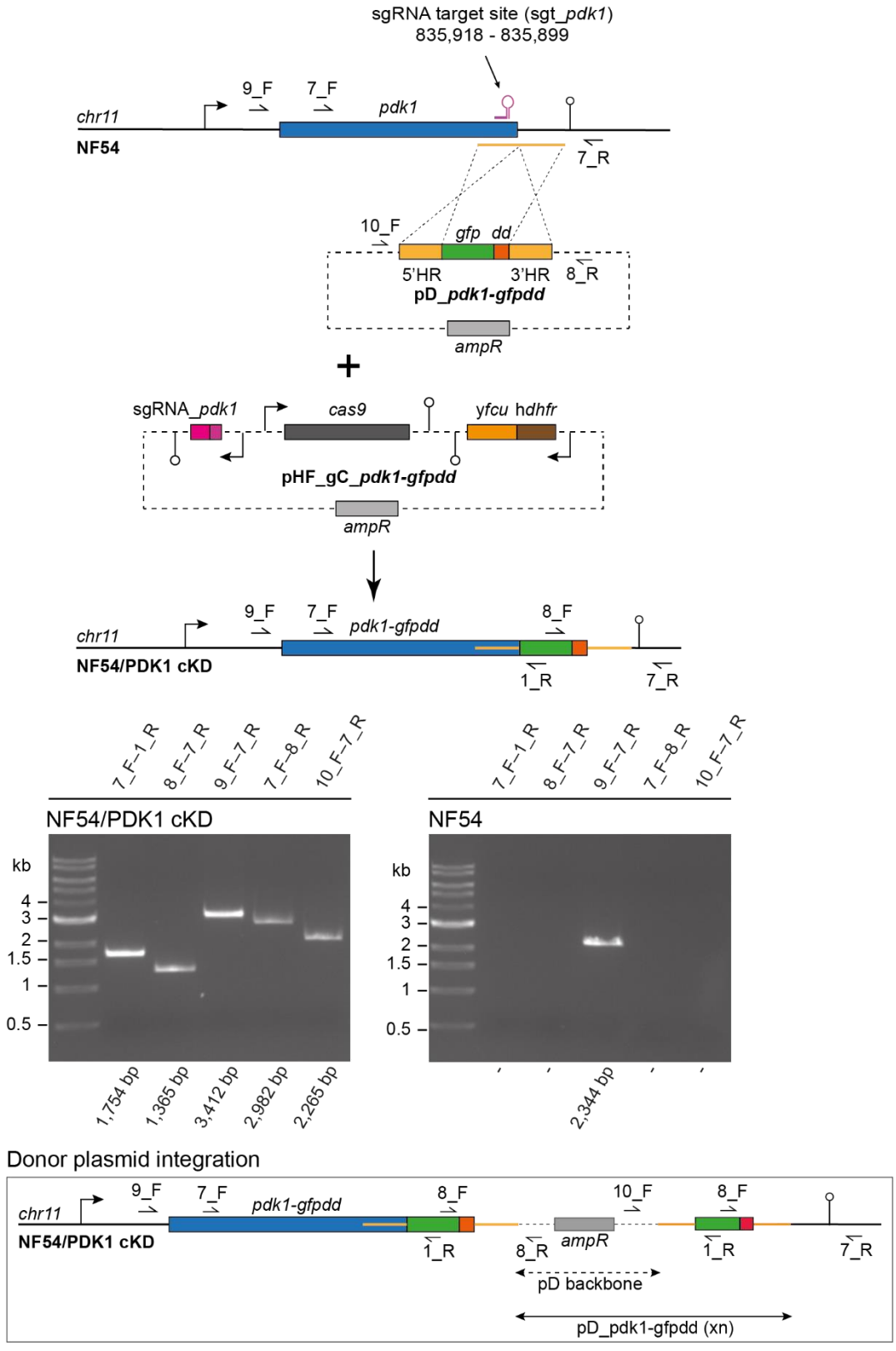

Supplementary Figure 8. CRISPR/Cas9-based engineering of the NF54/PDK1 cKD parasite line. Top: Scheme depicting the wild type *pfpdk1* locus, the donor (pD_pdk1-gfpdd) and the suicide (pHF_gC_pdk1-gfpdd) constructs transfected into NF54 WT parasites to generate the NF54/PDK1 cKD parasite line and the edited *pfpdk1* locus.

Primers used for diagnostic PCRs are indicated. Middle: Results of PCR reactions performed on gDNA of NF54/PDK1 cKD and NF54 WT control parasites confirm correct editing of the *pfpdk1* locus as well as plasmid concatemer integration. Bottom: Schematic map illustrating the integration of a donor plasmid concatemer based on double-crossover recombination of non-adjacent homology regions on the concatemer. To simplify the scheme, the integration of a tandem assembly only is shown.

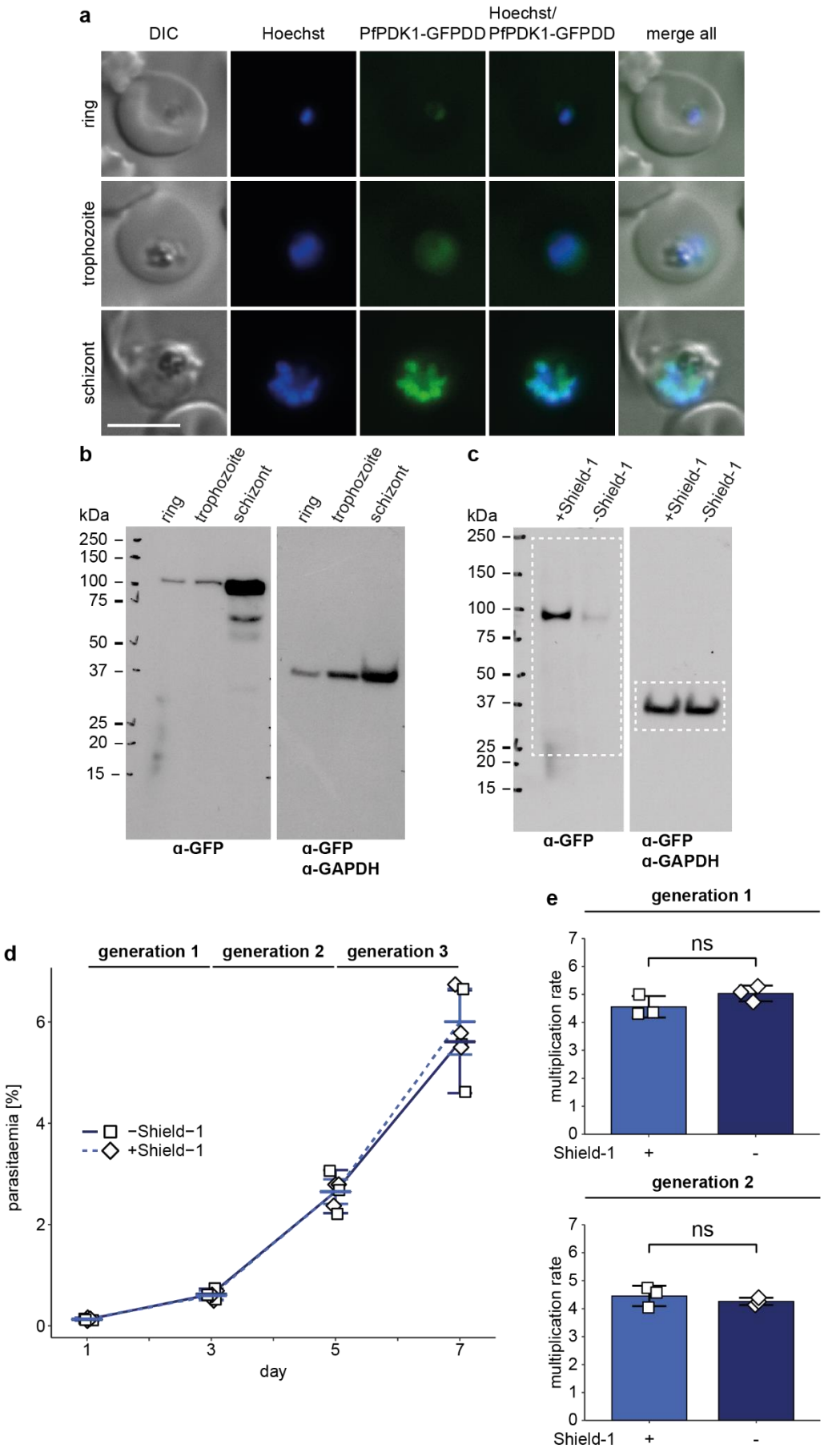

Supplementary Figure 9. Expression of PfPDK1 in NF54/PDK1 cKD parasites,

multiplication of NF54 wild type parasites in presence and absence of Shield-1 and full size Western blot of the sections shown in Fig. 5a. **(a)** Expression of PfPDK1-GFPDD in ring (18-24 hpi), trophozoite (24-30 hpi) and schizont (42-48 hpi) stages of NF54/PDK1 cKD parasites under protein-stabilizing (+Shield-1) conditions by live cell fluorescence imaging. Representative fluorescent images are shown. Parasite DNA was stained with Hoechst. DIC, differential interference contrast. Scale bar = 5 µm. **(b)** Expression of PfPDK1-GFPDD in ring (18-24 hpi), trophozoite (24-30 hpi) and schizont (42-48 hpi) stages of NF54/PDK1 cKD parasites under protein-stabilizing (+Shield-1) conditions by Western blot analysis. Parasite lysates derived from equal numbers of parasites were loaded per lane. The membrane was first probed with α-GFP followed by α-GAPDH control antibodies. MW PfPDK1-GFPDD = 101.1 kDa, MW PfGAPDH = 36.6 kDa. **(c)** Full size Western blot shows expression of PfPDK1-GFPDD in NF54/PDK1 cKD parasites under protein-depleting (–Shield-1) and control (+Shield-1) conditions. Synchronous parasites (0-8 hpi) were split (±Shield-1) 40 hours before collection of the samples. Parasite lysates derived from equal numbers of parasites were loaded per lane. The membrane was first probed with α-GFP followed by α-GAPDH control antibodies. Dashed lines mark the blot sections shown in Fig. 5a. MW PfPDK1-GFPDD = 101.1 kDa, MW PfGAPDH = 36.6 kDa. **(d)** Increase in parasitaemia of NF54 WT parasites in presence (+Shield-1) and absence (–Shield-1) of Shield-1 over three generations. Synchronous parasites (0-6 hpi) were split (±Shield-1) 18 hours before the first measurement (day 1). Open squares represent data points for individual replicates and the means±SD of three biological replicates are shown. **(e)** Parasite multiplication rates of NF54 WT parasites in presence (+Shield-1) and absence (–Shield-1) of Shield-1 over two generations (same data as shown in panel d). Open squares represent data points for individual replicates and the means±SD of three biological replicates are shown. ns, not significant (paired two-tailed Student’s t test).

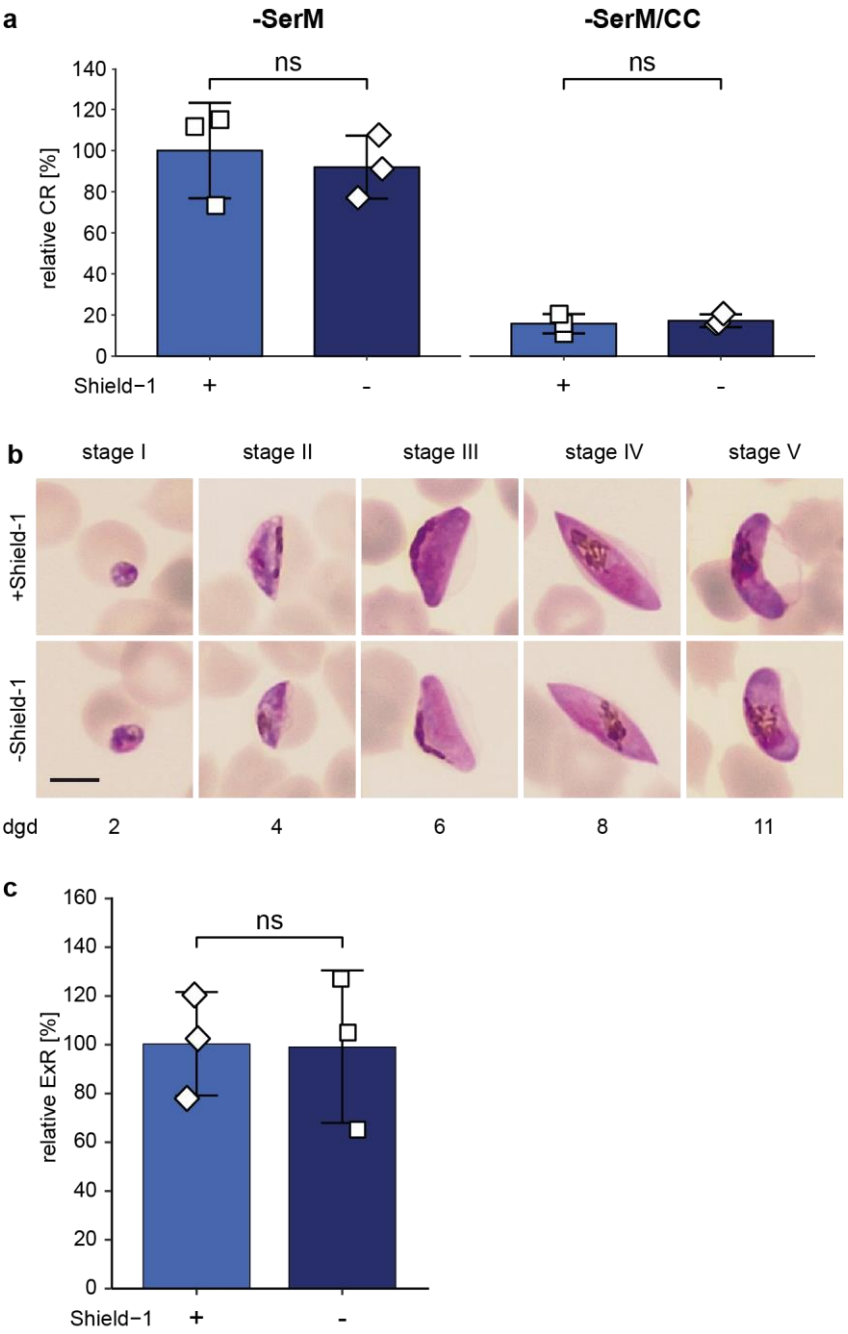

Supplementary Figure 10. Sexual commitment, gametocytogenesis and male gametogenesis of NF54/PDK1 cKD parasites. **(a)** Relative sexual commitment rates of NF54/PDK1 cKD parasites in presence (+Shield-1) or absence (–Shield-1) of Shield-1 cultured under commitment-inducing (–SerM) and -inhibiting (–SerM/CC) conditions [1]. Sexual commitment rates were determined using GlcNAc assays as described in the Methods section. Open squares represent data points for individual replicates and the means±SD of three biological replicate experiments are shown. ns, not significant (paired two-tailed Student's t test); CR, commitment rate; CC, choline chloride. **(b)**

Representative images of the distinct morphology of stage I-V gametocytes cultured under PfPDK1-GFPDD-depleting (–Shield-1) and control (+Shield-1) conditions over eleven days of maturation. Synchronous parasites (0-6 hpi) were split (±Shield-1) and 18 hours later sexual commitment was induced using –SerM medium [1]. To eliminate the asexual parasites, gametocytes were cultured in +SerM supplemented with 50 mM GlcNAc from day one to six of gametocytogenesis [2]. Images were captured from Giemsa-stained blood smears. Scale bar = 5 µm. dgd, day of gametocyte development. **(c)** Relative exflagellation rates of mature NF54/PDK1 cKD stage V gametocytes (day 14) cultured in presence (+Shield-1) and absence (–Shield-1) of Shield-1. Synchronous parasites were split (±Shield-1) and cultured as described in panel b. Open squares represent data points for individual replicates and the means±SD of three biological replicate experiments are shown. ns, not significant (paired two-tailed Student's t test); ExR, exflagellation rate.

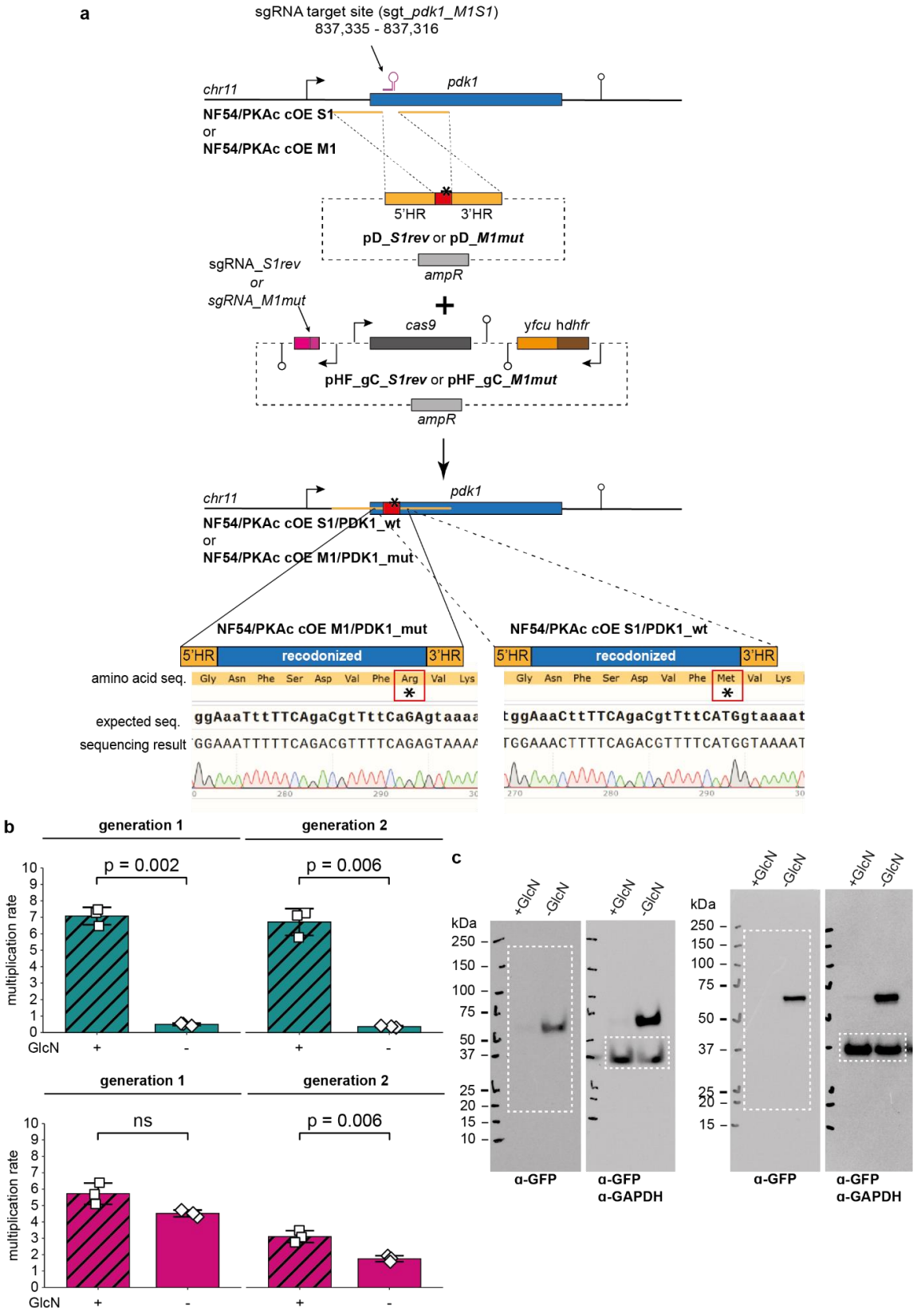

Supplementary Figure 11. CRISPR/Cas9-based engineering and multiplication rates of NF54/PKAc cOE M1/PDK1_mut and NF54/ PKAc cOE S1/PDK1_wt parasite lines and full size Western blots of the sections shown in Fig. 6. **(a)** Top: Scheme depicting

the *pfpdk1* locus of NF54/PKAc cOE S1 or M1 parasites, the donor (pD_S1rev or pD_M1mut) and the suicide (pHF_gC_S1rev or pHF_gC_M1mut) constructs transfected into either NF54/PKAc cOE S1 or NF54/PKAc cOE M1 parasites to generate the NF54/PKAc cOE S1/PDK1_wt and NF54/PKAc cOE M1/PDK1_mut parasite line, respectively, and the edited *pfpdk1* locus. Bottom: Sanger sequencing results of modified *pfpdk1* genes after targeted mutagenesis in NF54/PKAc cOE S1/PDK1_wt and NF54/PKAc cOE M1/PDK1_mut parasites confirms correct editing. The expected sequences after successful editing, the corresponding amino acid sequences and sequencing chromatograms are indicated (data analysis and visualisation was performed using SnapGene software 4.1.6 (Insightful Science; www.snapgene.com)). The asterisk (*) marks the mutated residues (M51 or R51). Capital letters highlight the nucleotide changes introduced by CRISPR/Cas9 editing to recodonize the sgRNA target site and to introduce the aspired amino acid changes (M51 or R51). **(b)** Parasite multiplication rates of NF54/PKAc cOE S1/PDK1_wt (top) and NF54/PKAc cOE M1/PDK1_mut (bottom) parasites under overexpression-inducing (–GlcN) and control (+GlcN) conditions over two generations. Synchronous parasites (0-6 hpi) were split (±GlcN) 18 hours before the first measurement (day 1). Open squares represent data points for individual replicates and the means±SD of three biological replicates are shown. Significant differences in parasite multiplication rates were determined using a paired two-tailed Student's t test. ns, not significant. Note that the same data is presented as an increase in parasitaemia over time in Figs. 6b and 6d. **(c)** Full size Western blots show expression of PfPKAc-GFP in NF54/PKAc cOE S1/PDK1_wt (left) and NF54/PKAc cOE M1/PDK1_mut (right) parasites under overexpression-inducing (–GlcN) and control (+GlcN) conditions. Synchronous parasites (0-8 hpi) were split (±GlcN) 40 hours before collection of the samples. Parasite lysates derived from equal numbers of parasites were loaded per lane. The membranes were first probed with α-GFP followed by α-GAPDH control antibodies. Dashed lines mark the blot sections shown in Figs. 6a and 6c. MW PfPKAc-GFP = 67.3 kDa, MW PfGAPDH = 36.6 kDa.

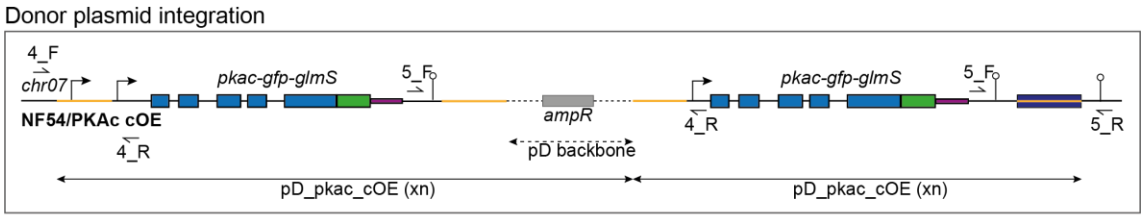

Type	Name	Copy number pD_pkac_cOE
Unselected	M1	7.8
Unselected	M2	7.2
Survivor	S1	2
Survivor	S2	6.3
Survivor	S3	2.6
Survivor	S4	6.1
Survivor	S5	1
Survivor	S6	5.9

Supplementary Figure 12. Scheme of the integration of pD_pkac_cOE donor plasmid concatemers upon CRISPR/Cas9 editing and estimated plasmid copy numbers present in the *glp3* locus of NF54/PKAc cOE M1, M2 and S1-S6 parasites. Top: Schematic map illustrating the integration of a pD_pkac_cOE donor plasmid concatemer into the parasite genome based on double-crossover recombination of non-adjacent homology regions on the concatemer. To simplify the scheme, only the integration of a tandem assembly is shown. Primers and annotations correspond to the scheme depicted in Supplementary Fig. 5. Bottom: Estimated pD_pkac_cOE copy numbers present in the *glp3* locus of the two unselected NF54/PKAc cOE clones (M1, M2) and six independently grown survivors (S1-S6). WGS data was used to determine the plasmid copy numbers and the analysis steps are described in the Methods section.

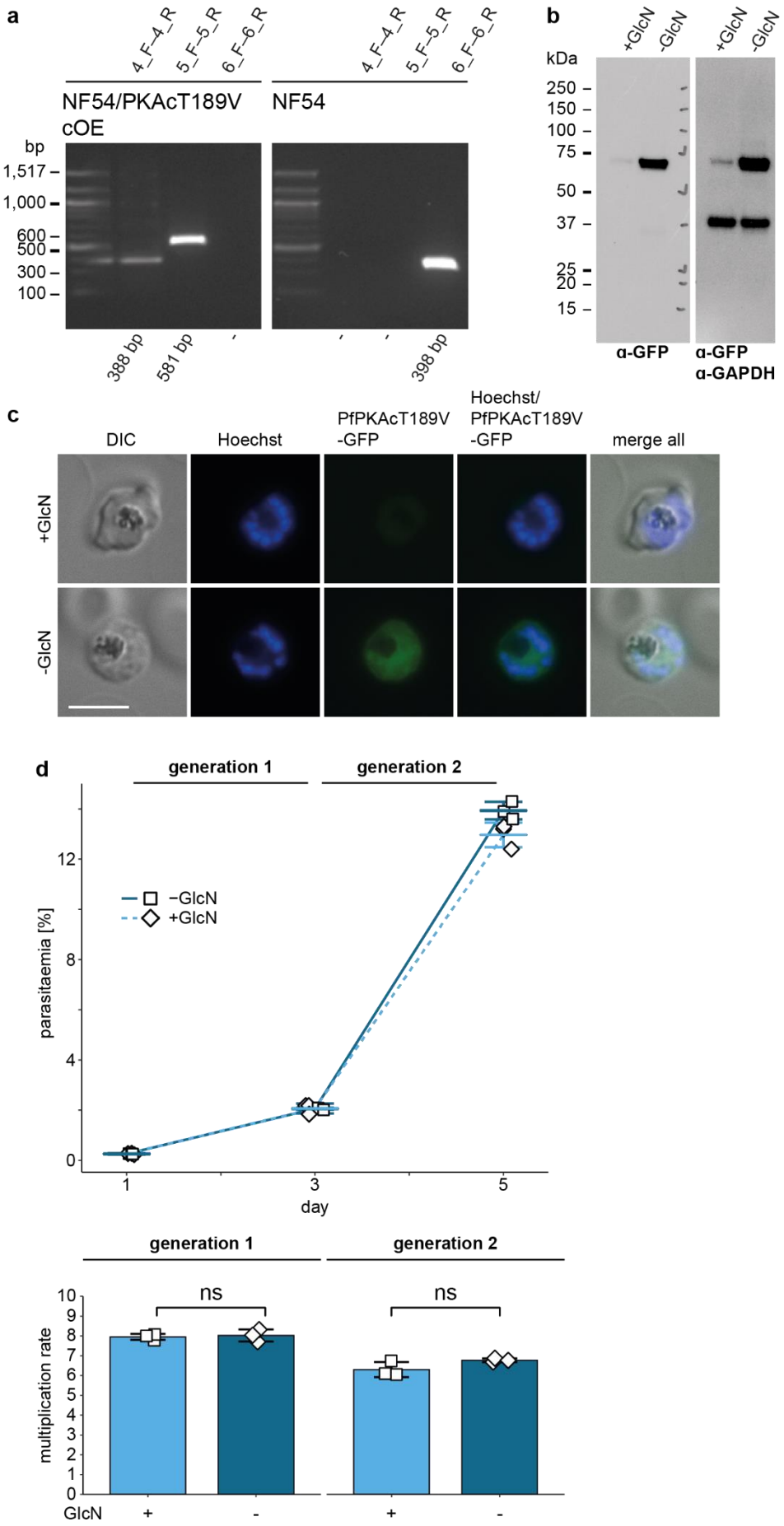
a
4_F–4_R
5_F–5_R
6_F–6_R
NF54/PKAcT189V cOE
NF54
bp
1,517
1,000
600
500
300
100
388 bp
581 bp
398 bp
b
+GlcN
-GlcN
kDa
250
150
100
75
50
37
25
20
15
α-GFP
α-GFP
α-GAPDH
c
DIC
Hoechst
PfPKAcT189V -GFP
Hoechst/ PfPKAcT189V -GFP
merge all
+GlcN
-GlcN
d
generation 1
generation 2
parasitaemia [%]
−GlcN
+GlcN
day
multiplication rate
ns
GlcN

Supplementary Figure 13. Diagnostic PCRs, over-expression of PfPKAcT189V and multiplication of NF54/PKAcT189V cOE parasites. **(a)** Results of diagnostic PCRs performed on gDNA of NF54/PKAcT189V cOE and NF54 WT control parasites confirm successful insertion of the PfPKAcT189V cOE cassette into the *glp3* locus. The schematic maps depicting the CRISPR/Cas9 approach used to generate the NF54/PKAcT189V cOE parasite line are shown in Supplementary Fig. 5. **(b)** Full size Western blot shows expression of PfPKAcT189V-GFP in NF54/PKAcT189V cOE parasites under overexpression-inducing (–GlcN) and control (+GlcN) conditions. Synchronous parasites (0-8 hpi) were split (±GlcN) 40 hours before collection of the samples. Parasite lysates derived from equal numbers of parasites were loaded per lane. The membrane was first probed with α-GFP followed by α-GAPDH control antibodies. MW PfPKAcT189V-GFP = 67.3 kDa, MW PfGAPDH = 36.6 kDa. **(c)** Expression of PfPKAcT189V-GFP in NF54/PKAcT189V cOE parasites under overexpression-inducing (–GlcN) and control (+GlcN) conditions by live cell fluorescence imaging. Synchronous parasites (0-8 hpi) were split (±GlcN) 40 hours before collection of the samples. Representative fluorescent images are shown. Parasite DNA was stained with Hoechst. DIC, differential interference contrast. Scale bar = 5 µm. **(d)** Increase in parasitaemia (top) and parasite multiplication rates (bottom) of NF54/PKAcT189V cOE parasites over two generations under overexpression-inducing (–GlcN) and control (+GlcN) conditions. Synchronous parasites (0-6 hpi) were split (±GlcN) 18 hours before the first measurement (day 1). Open squares represent data points for individual replicates and the means±SD of three biological replicates are shown. ns, not significant (paired two-tailed Student's t test).

Supplementary Table 1. Oligonucleotides used for cloning of transfection constructs. Names and sequences of oligonucleotides, plasmids and cell lines are indicated. Sequences essential for Gibson assembly reactions (Gibson overhangs) or for T4 DNA ligase-dependent cloning of double-stranded sgRNA-encoding fragments (5' and 3' overhangs) are highlighted with capital letters. Italicized letters highlight the annealed sequences (sgRNAs) and colour-highlighted letters represent introduced sequence mutations.

Oligo-nucleotide name	**Oligonucleotide sequence 5' → 3'**	**Plasmids**	**Cell lines**
PCRA_F	CTGGCGTAATAGCGAAGAGG	SLI_PKAc_cKD; pD_S1rev; pD_M1mut	NF54/AP2-G-mScarlet/PKAc cKD; NF54/ PKAc cOE S1/PDK1_wt; NF54/PKAc cOE M1/PDK1_mut
PCRA_R	CATTAATGAATCGGCCAACG	SLI_PKAc_cKD; pD_S1rev; pD_M1mut	NF54/AP2-G-mScarlet/PKAc cKD; NF54/ PKAc cOE S1/PDK1_wt; NF54/PKAc cOE M1/PDK1_mut
gfp_F	CGTTGGCCGATTCATTAATGactagtagcataggatccagtggaatgagt	SLI_PKAc_cKD	NF54/AP2-G-mScarlet/PKAc cKD
dd_R	CGCTACCACTTTCCAGTTTTAGAagctcc	SLI_PKAc_cKD	NF54/AP2-G-mScarlet/PKAc cKD
2A_F	TCTAAAACTGGAAAGTGGTAGCGgagaaggaaga	SLI_PKAc_cKD	NF54/AP2-G-mScarlet/PKAc cKD
bsd_R	GAACAAGATTACTCGAGTTAGCCCtcc	SLI_PKAc_cKD	NF54/AP2-G-mScarlet/PKAc cKD
glmS1_F	GGGCTAACTCGAGTAATCTTGTTCttattttctcaatagg	SLI_PKAc_cKD	NF54/AP2-G-mScarlet/PKAc cKD
term_R	CCTCTTCGCTATTACGCCAGgtcgacgaattctagatttaataaatatgttctt	SLI_PKAc_cKD	NF54/AP2-G-mScarlet/PKAc cKD
ydhodh_F	AGAAATATATCATGACAGCCAGtttaactaccaagt	SLI_PKAc_cKD	NF54/AP2-G-mScarlet/PKAc cKD
ydhodh_R	ATATCCTTAATTAATTAAATGCTGTTCaacttcccacg	SLI_PKAc_cKD	NF54/AP2-G-mScarlet/PKAc cKD
pbdt3_F	GAACAGCATTTAATTAATTAAGGATATggcagcttaatgttc	SLI_PKAc_cKD	NF54/AP2-G-mScarlet/PKAc cKD
pbdt3_R	TCGCTATTACGCCAGgtcgacctaccctgaagaagaaaagtcc	SLI_PKAc_cKD	NF54/AP2-G-mScarlet/PKAc cKD
cam1_F	ATTTCTCATTATATATAAGAACATATTTATTAAATgctatccgatcttataaggaaattcc	SLI_PKAc_cKD	NF54/AP2-G-mScarlet/PKAc cKD
cam1_R	CTGGCTGTCATGATATATTTCTattaggtatttattattataaaatataaatcttg	SLI_PKAc_cKD	NF54/AP2-G-mScarlet/PKAc cKD
pka3'_F	CGTTGGCCGATTCATTAATGagctaaaatagtcgagacgagaac	SLI_PKAc_cKD	NF54/AP2-G-mScarlet/PKAc cKD
pka3'_R	TTCTCCTTTACTCATTCCACTGgatccccaatcataaaatggatcattttcatttg	SLI_PKAc_cKD	NF54/AP2-G-mScarlet/PKAc cKD
glp3_F	CTTCTTCAGGGTAGCATGaac	pD_pkac_cOE;	NF54/PKAc cOE
glp3_R	GGATAGCTACATGTTCATAtttatatttatttattc	pD_pkac_cOE;	NF54/PKAc cOE
cam_F	TATGAACATGTAGCTATCCgatcttataaggaaattccc	pD_pkac_cOE;	NF54/PKAc cOE
hrp2_R	CATGCTACCCTGAAGAAGgaattctagatttaataaatatgttc	pD_pkac_cOE;	NF54/PKAc cOE

glmS_F	GCATGGATGAACTATACAAAtaatcttgttcttatttt ctcaatag	pD_pkac_cOE;	NF54/PKAc cOE
glmS_R	CTCATATACTTCCCTAGATGAGatttttcttcctcct aagattg	pD_pkac_cOE;	NF54/PKAc cOE
clon_F	TAATAAATACCTAATAGAAATATATC*actagta gtggatccagtgga*	pD_pkac_cOE;	NF54/PKAc cOE
clon_R	GAAAAGTTCTTCTCCTTTACTCAT*tccactggat ccactactagt*	pD_pkac_cOE;	NF54/PKAc cOE
pka_F	TACCTAATAGAAATATATCACTAGTatgcagttt attaaaaatttgc	pD_pkac_cOE; pD_pkacT189V_c OE	NF54/PKAc cOE
pka_R	CTCCTTTACTCATTCCACTGgatccccaatcataa aatggatcat	pD_pkac_cOE; pD_pkacT189V_c OE	NF54/PKAc cOE
T189V_F	ATGTTTTATGTGGAACTCCAgaatatatc	pD_pkacT189V_c OE	NF54/PKAcT189V cOE
T189V_R	TGGAGTTCCACATAAAACATaagttctcgtctcga c	pD_pkacT189V_c OE	NF54/PKAcT189V cOE
hr1_F	CGTTGGCCGATTCATTAATGgtgtaaaagttaaa aaaacatgc	pD_S1rev; pD_M1mut	NF54/PDK1_S1rev; NF54/PKAc cOE M1/PDK1_mut
rev_F	CTTTTCAGACGTTTTCATGGtaaaattaaaaaatg atccttcaaaaaaatatg	pD_S1rev	NF54/PKAc cOE S1/PDK1_wt
rev_R	CCATGAAAACGTCTGAAAAGtttccagttcctatgt gcatatatatttc	pD_S1rev	NF54/PKAc cOE S1/PDK1_wt
mut_F	TTTTTCAGACGTTTTCAGAGtaaaattaaaaaatg atccttcaaaaaaatatg	pD_M1mut	NF54/PKAc cOE M1/PDK1_mut
mut_R	CTCTGAAAACGTCTGAAAAAtttccagttcctatgtg catatatatttc	pD_M1mut	NF54/PKAc cOE M1/PDK1_mut
hr2_R	CCTCTTCGCTATTACGCCAGagctattatgtttattt gcatctg	pD_S1rev; pD_M1mut	NF54/PKAc cOE S1/PDK1_wt; NF54/PKAc cOE M1/PDK1_mut
hr1KD_F	CGTTGGCCGATTCATTAATGtagtgacatgtacc gttcc	pD_pdk1-gfpdd	NF54/PDK1 cKD
hr1KD_R	GTTCCCTGGTATCTCTCAAGccacttacttgcttctt ccatttc	pD_pdk1-gfpdd	NF54/PDK1 cKD
gfpdd_F	CTTGAGAGATACCAGGGAACtagtggatccagtg gaatgagtaaag	pD_pdk1-gfpdd	NF54/PDK1 cKD
gfpdd_R	CTATCATTCTAATTTTAGAAGCTCCACac	pD_pdk1-gfpdd	NF54/PDK1 cKD
hr2KD_F	TGGAGCTTCTAAAATTAGAATGATAGaatata acatatataaataaaaacaatttcttttac	pD_pdk1-gfpdd	NF54/PDK1 cKD
hr2KD_R	CCTCTTCGCTATTACGCCAGgtgtttcacaagaa cttaagg	pD_pdk1-gfpdd	NF54/PDK1 cKD
sgRNA_S1rev_F	TATT*gaatttcagtgatgtgttta*	pHF_gC_S1rev	NF54/PKAc cOE S1/PDK1_wt
sgRNA_S1rev_R	AAAC*taaacacatcactgaaattc*	pHF_gC_S1rev	NF54/PKAc cOE S1/PDK1_wt
sgRNA_M1mut_F	TATT*gaatttcagtgatgtgttta*	pHF_gC_M1mut	NF54/PKAc cOE M1/PDK1_mut
sgRNA_M1mut_R	AAAC*taaacacatcactgaaattc*	pHF_gC_M1mut	NF54/PKAc cOE M1/PDK1_mut
sgRNA_pdk1_F	TATT*aaatggttagaacgatatca*	pHF_gC_pdk1-gfpdd	NF54/PDK1 cKD
sgRNA_pdk1_R	AAAC*tgatatcgttctaaccattt*	pHF_gC_pdk1-gfpdd	NF54/PDK1 cKD

Supplementary Table 2. Primers used for diagnostic PCRs on gDNA of transgenic parasite lines. Names and sequences of primers and transgenic cell lines are indicated.

Primer name	**Sequence 5' → 3'**	**Cell line**
1_F	atgcagtttattaaaaatttgc	NF54/AP2-G-mScarlet/PKAc cKD
1_R	gtgtgagttatagttgtattcc	NF54/AP2-G-mScarlet/PKAc cKD
2_F	gcgaggaagcggaagagc	NF54/AP2-G-mScarlet/PKAc cKD
2_R	cattatcaaaacaggcaattg	NF54/AP2-G-mScarlet/PKAc cKD
3_F	ggatcattcaaagatgactc	NF54/AP2-G-mScarlet/PKAc cKD
3_R	gtatgtgaaaacaactaaaacatg	NF54/AP2-G-mScarlet/PKAc cKD
4_F	attatgggaaaataatccttac	NF54/PKAc cOE M1; NF54/PKAc cOE M2 NF54/PKAcT189V cOE
4_R	gctcagagattgcatgcaag	NF54/PKAc cOE M1; NF54/PKAc cOE M2 NF54/PKAcT189V cOE
5_F	ctttaattttattttggtcatg	NF54/PKAc cOE M1; NF54/PKAc cOE M2 NF54/PKAcT189V cOE
5_R	cttttacaatatgaacataaagtac	NF54/PKAc cOE M1; NF54/PKAc cOE M2 NF54/PKAcT189V cOE
6_F	gttcatgctcctcaacaaag	NF54/PKAc cOE M1; NF54/PKAc cOE M2 NF54/PKAcT189V cOE
6_R	gaacaaatacataagagcgc	NF54/PKAc cOE M1; NF54/PKAc cOE M2 NF54/PKAcT189V cOE
7_F	aaaccaggacatgcaaatgttatt	NF54/PDK1 cKD
7_R	tctaatgaattgtccatcatgc	NF54/PDK1 cKD
8_F	ggttatgtacaggaaagaac	NF54/PDK1 cKD
8_R	attcgccattcaggctgc	NF54/PDK1 cKD
9_F	gatcgaaccaagcttatattaac	NF54/PDK1 cKD
10_F	gcgaggaagcggaagagc	NF54/PDK1 cKD

Supplementary Dataset 1. Multiple nucleotide sequence alignment of Pf3D7_1121900/*pfpdk1* sequences of unselected NF54/PKAc cOE clones and the PfPKAc OE-tolerant survivor populations. The PfPDK1 coding sequence of the unselected M1 and M2 clones are identical to the Pf3D7_1121900 reference sequence retrieved from PlasmoDB (www.plasmodb.org) (top row). Sequences of the survivor populations (S1-S6) are shown and deviations from the reference sequence are highlighted in green. Survivor S6 consists of two subpopulations with one carrying the c.252A>T mutation and the other one carrying the c.491A>G mutation (as verified by inspection of the sequencing read-pairs).

References

1 Brancucci, N. M. B. *et al.* Lysophosphatidylcholine Regulates Sexual Stage Differentiation in the Human Malaria Parasite Plasmodium falciparum. *Cell* **171**, 1532-1544.e1515, doi:10.1016/j.cell.2017.10.020 (2017).

2 Fivelman, Q. L. *et al.* Improved synchronous production of Plasmodium falciparum gametocytes in vitro. *Mol Biochem Parasitol* **154**, 119-123, doi:10.1016/j.molbiopara.2007.04.008 (2007).

3 Lavazec, C. *et al.* Microsphiltration: a microsphere matrix to explore erythrocyte deformability. *Methods in molecular biology (Clifton, N.J.)* **923**, 291-297, doi:10.1007/978-1-62703-026-7_20 (2013).

4 Madeira, F. *et al.* The EMBL-EBI search and sequence analysis tools APIs in 2019. *Nucleic Acids Res* **47**, W636-w641, doi:10.1093/nar/gkz268 (2019).

5 Biondi, R. M. *et al.* Identification of a pocket in the PDK1 kinase domain that interacts with PIF and the C-terminal residues of PKA. *The EMBO journal* **19**, 979-988, doi:10.1093/emboj/19.5.979 (2000).

Chapter 6

General Discussion

Chapter 6
General Discussion

Cellular signalling is essential in all domains of life and kinases play an extremely important role in a variety of signalling pathways. Several *P. falciparum* kinases have been investigated and functionally characterized. However, our knowledge on signalling pathways in the malaria parasite and especially on the function of kinases in sexual commitment and development is still extremely scarce.

Brancucci and colleagues have revealed the importance of the host lipid LysoPC in sexual commitment signalling of malaria parasites [8]. In case the LysoPC level in the environment of *P. falciparum* parasites is high, this host lipid is taken up by the parasite and metabolized via the Kennedy pathway. In general, this metabolic pathway results in the generation of phosphatidylcholine (PC) [73], an essential and abundant membrane component of the malaria parasite [74]. Interestingly, once LysoPC levels and consequently PC levels drop, an alternative route of the Kennedy pathway seems to be activated in the malaria parasite, thus still ensuring the production of sufficient PC [8]. However, how the drop in LysoPC finally results in the expression of PfAP2-G in the parasite nucleus remains unknown [8].

In this work, we hypothesized that kinases are essential components of the signalling pathway acting upstream of PfAP2-G and hence trigger its expression. We therefore investigated the involvement of nine *P. falciparum* protein kinases in this putative signalling pathway. We selected these nine kinases based on their function in *Plasmodium* parasites or other eukaryotes. However, we found no conclusive experimental evidence for an involvement of any of the nine investigated kinases in the putative signalling pathway triggering expression of PfAP2-G (Chapter 2). Nevertheless, preliminary data suggest a potential involvement of PfMRK in sexual commitment signalling (Chapter 2), and additional experiments are planned to confirm these data (PhD project, Matthias Wyss).

Kinase inhibitor screens performed by Nicolas Brancucci in the lab of Till Voss revealed several additional candidate kinases potentially involved in this signalling pathway (Brancucci et al, manuscript in preparation). Today, we are still committed to our hypothesis that sexual commitment is dependent on kinase signalling. Ongoing and future work performed in the laboratories of Till Voss and now also Nicolas Brancucci will hopefully identify one or several kinases as well as other pathway components involved in the upstream pathway triggering expression of PfAP2-G.

Having generated a variety of different transgenic cell lines, we decided to investigate these further to identify potential phenotypes resulting from changes in kinase expression levels on asexual parasite development. In addition, the ability to produce large amounts of gametocytes using –SerM medium [8] (up to 50% sexual commitment and 3-5% gametocytaemia) did not only allow me to study sexual commitment but also to investigate intraerythrocytic sexual development and male gametogenesis.

I demonstrated that the atypical MAPK PfMAP-2 is dispensable for asexual development and show that, similar to the *P. berghei* orthologue PbMAP-2 [75-77], this kinase is important for male gametogenesis. For the first time, I was able to show on a single cell level that PfMAP-2 expression is specific to male gametocytes. Furthermore, the capability to generate the MAPK double KO parasite line revealed the dispensability of both *P. falciparum* MAPK, PfMAP-1 and PfMAP-2, for asexual and sexual intraerythrocytic development. In addition, I concluded that the two *P. falciparum* MAPKs have distinct roles in the parasite, since the function of PfMAP-2 cannot be compensated by PfMAP-1 (and *vice versa*) (Chapter 3).

Studying the catalytic subunit of the *P. falciparum* CK2 kinase, PfCK2α, we confirmed its constitutive expression in both the parasite nucleus and cytoplasm and its importance in RBC invasion by merozoites. We further showed that PfCK2α likely has an essential function in asexual development besides its role in erythrocyte invasion. Finally, we revealed that PfCK2α is required for sexual stage maturation and proposed a direct or indirect role for PfCK2α in the generation or dynamics of the inner membrane complex, or the underlying microtubulin and actin network in gametocytes (Chapter 4).

My investigation of the catalytic subunit of the *P. falciparum* PKA kinase, PfPKAc, confirmed its essential role in merozoite invasion and hence its indispensability for the proliferation of asexual blood stage parasites. Furthermore, depletion of PfPKAc resulted in increased deformability of erythrocyte-infected gametocytes. I also report the lethality of overexpressing PfPKAc and the successful selection of OE survivors. Whole genome sequencing of six OE survivors revealed mutations in the putative serine/threonine kinase Pf3D7_1121900, which we identified as PfPDK1, an orthologue of the PDK1 kinase known to activate PKA in model eukaryotes. Lastly, I present evidence that this activation likely takes place via phosphorylation of T189 on PfPKAc (Chapter 5).

Although open questions on the exact functions and substrates of PfMAP-2, PfCK2α and PfPKAc remain, the present work revealed previously unreported roles and interactions of these kinases in *P. falciparum*. The essentiality of PfPKAc and PfCK2α for asexual parasite development was previously reported [60,61,78]. However, in the scope of this work, I revealed that PfMAP-2 (and both *P. falciparum* MAPKs) is dispensable for asexual parasite development. Being able to study sexual commitment and development in a

large number of parasites further allowed me to identify important functions for all three kinases at different stages of intraerythrocytic sexual parasite development.

Whereas the impact of PfMAP-2 and PfCK2α deletion (and conditional depletion) on sexual stage transmission to mosquitoes is likely very drastic, the consequences of PfPKAc depletion on transmission are less clear. Knocking down PfPKAc expression led to an increased deformability of stage III and stage V gametocyte-infected erythrocytes. However, parasite morphology and male gametocyte exflagellation were not affected by PfPKAc kinase depletion. Hence, the decrease of PfPKAc expression might only slightly (or not at all) affect the transmission of *in vitro* cultivated gametocytes to a mosquito vector and their subsequent development. However, studying sexual development in PfPKAc DiCre-inducible KO parasites [60,61] might still identify an important role for PfPKAc in gametocytogenesis and/or gametogenesis. To date, we know that the rigidity of immature gametocytes is important in the human host allowing parasites to sequester in tissues such as the bone marrow. In contrast, the increased deformability of stage V gametocytes allows them to leave their site of sequestration and re-enter the blood stream from where they can be picked up by a mosquito vector [79-81]. Hence, increased gametocyte deformability upon PfPKAc depletion would likely affect gametocyte maturation and survival of sexual parasite stages in the human host. In addition, complete PfPKAc deletion might even result in a stronger effect. A recent study has further reported the importance of cAMP/PfPKA signalling in the activity of new permeability pathways (NPP) in gametocytes and hence its role in regulating the differential susceptibility to solute uptake between immature and mature sexual stages [82]. For instance, re-activation of NPPs in stage V gametocytes was inducible by cAMP and this led to an increased uptake of Artemisinin in these mature sexual stages [82]. In conclusion, PfPKAc is important during several stages and processes of asexual and sexual parasite development and decreased kinase activity would likely have a profound effect on parasite survival in the human host. In addition, to conclusively identify a potential role for PfPDK1 in gametocytogenesis and/or gametogenesis, the generation of a PfPDK1 DiCre-inducible KO parasite line would be the way to go.

I conclude from my work that decreasing PfCK2α expression had the strongest impact on the development and survival of asexual and sexual intraerythrocytic parasite stages. Hence, the lack or a strong decrease of PfCK2 activity would likely prevent parasite development in both the human host and mosquito vector. This broad impact range is likely based on the pleiotropic activity of PfCK2, which was previously reported for CK2 in model eukaryotes [83-86]. The putative pleiotropic activity of PfCK2 in asexual and sexual intraerythrocytic development and hence the prospect to generate a dual-active drug combining asexual parasite clearance with transmission-blocking activity render PfCK2α

an attractive drug target. Future studies are needed to determine whether the generation of a cell-permeable compound specifically targeting parasite PfCK2α is achievable.

In this work, we aimed at identifying a kinase involved in the putative upstream signalling pathway triggering expression of PfAP2-G and consequently sexual commitment. Although we failed to identify such a kinase, a new PfAP2-G reporter cell line was generated and an experimental pipeline to study sexual commitment and commitment signalling candidates was co-developed within the scope of this work (Chapter 2; Brancucci et al., manuscript in preparation). In addition, this PhD project has revealed previously unreported functions of three *P. falciparum* kinases and with PfPDK1 also identified an additional essential component of cAMP signalling in the parasite. I hope that present work will inspire future studies on kinase function in asexual and sexual parasite development as well as in sexual commitment and ideally help promote antimalarial drug development.

References
General Introduction and Discussion

1 Singh, B. & Daneshvar, C. Human infections and detection of Plasmodium knowlesi. *Clinical microbiology reviews* **26**, 165-184, doi:10.1128/cmr.00079-12 (2013).

2 Sutherland, C. J. *et al.* Two nonrecombining sympatric forms of the human malaria parasite Plasmodium ovale occur globally. *The Journal of infectious diseases* **201**, 1544-1550, doi:10.1086/652240 (2010).

3 WHO. World Malaria Report 2019. (2019).

4 Dalrymple, U., Mappin, B. & Gething, P. W. Malaria mapping: understanding the global endemicity of falciparum and vivax malaria. *BMC Medicine* **13**, 140, doi:10.1186/s12916-015-0372-x (2015).

5 Cowman, A. F., Healer, J., Marapana, D. & Marsh, K. Malaria: Biology and Disease. *Cell* **167**, 610-624, doi:https://doi.org/10.1016/j.cell.2016.07.055 (2016).

6 Baker, D. A. Malaria gametocytogenesis. *Mol Biochem Parasitol* **172**, 57-65, doi:10.1016/j.molbiopara.2010.03.019 (2010).

7 Josling, G. A. & Llinas, M. Sexual development in Plasmodium parasites: knowing when it's time to commit. *Nat Rev Microbiol* **13**, 573-587, doi:10.1038/nrmicro3519 (2015).

8 Brancucci, N. M. B. *et al.* Lysophosphatidylcholine Regulates Sexual Stage Differentiation in the Human Malaria Parasite Plasmodium falciparum. *Cell* **171**, 1532-1544.e1515, doi:10.1016/j.cell.2017.10.020 (2017).

9 Bruce, M. C., Alano, P., Duthie, S. & Carter, R. Commitment of the malaria parasite Plasmodium falciparum to sexual and asexual development. *Parasitology* **100 Pt 2**, 191-200, doi:10.1017/s0031182000061199 (1990).

10 Bancells, C. *et al.* Revisiting the initial steps of sexual development in the malaria parasite Plasmodium falciparum. *Nature microbiology* **4**, 144-154, doi:10.1038/s41564-018-0291-7 (2019).

11 Ono, T., Ohnishi, Y., Nagamune, K. & Kano, M. Gametocytogenesis Induction by Berenil in Cultured Plasmodium falciparum. *Experimental Parasitology* **77**, 74-78, doi:https://doi.org/10.1006/expr.1993.1062 (1993).

12 Buckling, A. G., Taylor, L. H., Carlton, J. M. & Read, A. F. Adaptive changes in Plasmodium transmission strategies following chloroquine chemotherapy. *Proc Biol Sci* **264**, 553-559, doi:10.1098/rspb.1997.0079 (1997).

13 Williams, J. L. Stimulation of Plasmodium falciparum gametocytogenesis by conditioned medium from parasite cultures. *The American journal of tropical medicine and hygiene* **60**, 7-13, doi:10.4269/ajtmh.1999.60.7 (1999).

14 Lingnau, A., Margos, G., Maier, W. A. & Seitz, H. M. The effects of hormones on the gametocytogenesis of Plasmodium falciparum in vitro. *Applied parasitology* **34**, 153-160 (1993).

15 Kaushal, D. C., Carter, R., Miller, L. H. & Krishna, G. Gametocytogenesis by malaria parasites in continuous culture. *Nature* **286**, 490-492, doi:10.1038/286490a0 (1980).

16 Read, L. K. & Mikkelsen, R. B. Comparison of adenylate cyclase and cAMP-dependent protein kinase in gametocytogenic and nongametocytogenic clones of Plasmodium falciparum. *The Journal of parasitology* **77**, 346-352 (1991).

17 Usui, M. *et al.* Plasmodium falciparum sexual differentiation in malaria patients is associated with host factors and GDV1-dependent genes. *Nature Communications* **10**, 2140, doi:10.1038/s41467-019-10172-6 (2019).

18 Balaji, S., Babu, M. M., Iyer, L. M. & Aravind, L. Discovery of the principal specific transcription factors of Apicomplexa and their implication for the evolution of the

AP2-integrase DNA binding domains. *Nucleic Acids Res* **33**, 3994-4006, doi:10.1093/nar/gki709 (2005).
19 Painter, H. J., Campbell, T. L. & Llinas, M. The Apicomplexan AP2 family: integral factors regulating Plasmodium development. *Mol Biochem Parasitol* **176**, 1-7, doi:10.1016/j.molbiopara.2010.11.014 (2011).
20 Kafsack, B. F. *et al.* A transcriptional switch underlies commitment to sexual development in malaria parasites. *Nature* **507**, 248-252, doi:10.1038/nature12920 (2014).
21 Sinha, A. *et al.* A cascade of DNA-binding proteins for sexual commitment and development in Plasmodium. *Nature* **507**, 253-257, doi:10.1038/nature12970 (2014).
22 Alano, P. *et al.* COS cell expression cloning of Pfg377, a Plasmodium falciparum gametocyte antigen associated with osmiophilic bodies. *Mol Biochem Parasitol* **74**, 143-156, doi:10.1016/0166-6851(95)02491-3 (1995).
23 Lopez-Rubio, J. J., Mancio-Silva, L. & Scherf, A. Genome-wide analysis of heterochromatin associates clonally variant gene regulation with perinuclear repressive centers in malaria parasites. *Cell Host Microbe* **5**, 179-190, doi:10.1016/j.chom.2008.12.012 (2009).
24 Salcedo-Amaya, A. M. *et al.* Dynamic histone H3 epigenome marking during the intraerythrocytic cycle of Plasmodium falciparum. *Proc Natl Acad Sci U S A* **106**, 9655-9660, doi:10.1073/pnas.0902515106 (2009).
25 Grewal, S. I. & Jia, S. Heterochromatin revisited. *Nat Rev Genet* **8**, 35-46, doi:10.1038/nrg2008 (2007).
26 Maison, C. & Almouzni, G. HP1 and the dynamics of heterochromatin maintenance. *Nat Rev Mol Cell Biol* **5**, 296-304, doi:10.1038/nrm1355 (2004).
27 Zeng, W., Ball, A. R., Jr. & Yokomori, K. HP1: heterochromatin binding proteins working the genome. *Epigenetics* **5**, 287-292, doi:10.4161/epi.5.4.11683 (2010).
28 Flueck, C. *et al.* Plasmodium falciparum heterochromatin protein 1 marks genomic loci linked to phenotypic variation of exported virulence factors. *PLoS Pathog* **5**, e1000569, doi:10.1371/journal.ppat.1000569 (2009).
29 Brancucci, N. M. B. *et al.* Heterochromatin protein 1 secures survival and transmission of malaria parasites. *Cell Host Microbe* **16**, 165-176, doi:10.1016/j.chom.2014.07.004 (2014).
30 Filarsky, M. *et al.* GDV1 induces sexual commitment of malaria parasites by antagonizing HP1-dependent gene silencing. *Science (New York, N.Y.)* **359**, 1259-1263, doi:10.1126/science.aan6042 (2018).
31 Josling, G. A., Williamson, K. C. & Llinás, M. Regulation of Sexual Commitment and Gametocytogenesis in Malaria Parasites. **72**, 501-519, doi:10.1146/annurev-micro-090817-062712 (2018).
32 Josling, G. A. *et al.* Dissecting the role of PfAP2-G in malaria gametocytogenesis. *Nature Communications* **11**, 1503, doi:10.1038/s41467-020-15026-0 (2020).
33 de Nadal, E., Ammerer, G. & Posas, F. Controlling gene expression in response to stress. *Nat Rev Genet* **12**, 833-845, doi:10.1038/nrg3055 (2011).
34 Cooper, G. M. *The Cell: A Molecular Approach. 2nd edition. Pathways of Intracellular Signal Transduction.*, Vol. 2 (Sunderland (MA): Sinauer Associates, 2000).
35 Manning, G., Plowman, G. D., Hunter, T. & Sudarsanam, S. Evolution of protein kinase signaling from yeast to man. *Trends Biochem Sci* **27**, 514-520, doi:10.1016/s0968-0004(02)02179-5 (2002).
36 Hunter, T. Signaling--2000 and beyond. *Cell* **100**, 113-127, doi:10.1016/s0092-8674(00)81688-8 (2000).
37 Purvis, J. E. & Lahav, G. Encoding and decoding cellular information through signaling dynamics. *Cell* **152**, 945-956, doi:10.1016/j.cell.2013.02.005 (2013).
38 Conrad, M. *et al.* Nutrient sensing and signaling in the yeast Saccharomyces cerevisiae. *FEMS Microbiol Rev* **38**, 254-299, doi:10.1111/1574-6976.12065 (2014).

39 Dunand-Sauthier, I. *et al.* Stress-activated protein kinase pathway functions to support protein synthesis and translational adaptation in response to environmental stress in fission yeast. *Eukaryot Cell* **4**, 1785-1793, doi:10.1128/EC.4.11.1785-1793.2005 (2005).
40 Schenk, P. W. & Snaar-Jagalska, B. E. Signal perception and transduction: the role of protein kinases. *Biochimica et Biophysica Acta (BBA) - Molecular Cell Research* **1449**, 1-24, doi:https://doi.org/10.1016/S0167-4889(98)00178-5 (1999).
41 Cheng, H. C., Qi, R. Z., Paudel, H. & Zhu, H. J. Regulation and function of protein kinases and phosphatases. *Enzyme Res* **2011**, 794089, doi:10.4061/2011/794089 (2011).
42 Hanks, S. K. & Hunter, T. Protein kinases 6. The eukaryotic protein kinase superfamily: kinase (catalytic) domain structure and classification. *FASEB journal : official publication of the Federation of American Societies for Experimental Biology* **9**, 576-596 (1995).
43 Hanks, S. K. Genomic analysis of the eukaryotic protein kinase superfamily: a perspective. *Genome Biol* **4**, 111, doi:10.1186/gb-2003-4-5-111 (2003).
44 Johnson, L. N. & Barford, D. The effects of phosphorylation on the structure and function of proteins. *Annual review of biophysics and biomolecular structure* **22**, 199-232, doi:10.1146/annurev.bb.22.060193.001215 (1993).
45 Kim, E. K. & Choi, E. J. Pathological roles of MAPK signaling pathways in human diseases. *Biochim Biophys Acta* **1802**, 396-405, doi:10.1016/j.bbadis.2009.12.009 (2010).
46 Gustin, M. C., Albertyn, J., Alexander, M. & Davenport, K. MAP kinase pathways in the yeast Saccharomyces cerevisiae. *Microbiology and molecular biology reviews : MMBR* **62**, 1264-1300 (1998).
47 Bardwell, L. A walk-through of the yeast mating pheromone response pathway. *Peptides* **25**, 1465-1476, doi:10.1016/j.peptides.2003.10.022 (2004).
48 Solyakov, L. *et al.* Global kinomic and phospho-proteomic analyses of the human malaria parasite Plasmodium falciparum. *Nat Commun* **2**, 565, doi:10.1038/ncomms1558 (2011).
49 Doerig, C. *et al.* Protein kinases of malaria parasites: an update. *Trends Parasitol* **24**, 570-577, doi:10.1016/j.pt.2008.08.007 (2008).
50 Baker, D. A. *et al.* Cyclic nucleotide signalling in malaria parasites. *Open Biol* **7**, doi:10.1098/rsob.170213 (2017).
51 Brochet, M. & Billker, O. Calcium signalling in malaria parasites. **100**, 397-408, doi:10.1111/mmi.13324 (2016).
52 Talevich, E., Tobin, A. B., Kannan, N. & Doerig, C. An evolutionary perspective on the kinome of malaria parasites. *Philos Trans R Soc Lond B Biol Sci* **367**, 2607-2618, doi:10.1098/rstb.2012.0014 (2012).
53 Ward, P., Equinet, L., Packer, J. & Doerig, C. Protein kinases of the human malaria parasite Plasmodium falciparum: the kinome of a divergent eukaryote. *BMC Genomics* **5**, 79, doi:10.1186/1471-2164-5-79 (2004).
54 Anamika, Srinivasan, N. & Krupa, A. A genomic perspective of protein kinases in Plasmodium falciparum. *Proteins* **58**, 180-189, doi:10.1002/prot.20278 (2005).
55 Talevich, E., Mirza, A. & Kannan, N. Structural and evolutionary divergence of eukaryotic protein kinases in Apicomplexa. *BMC evolutionary biology* **11**, 321, doi:10.1186/1471-2148-11-321 (2011).
56 Doerig, C. & Grevelding, C. G. Targeting kinases in Plasmodium and Schistosoma: Same goals, different challenges. *Biochim Biophys Acta* **1854**, 1637-1643, doi:10.1016/j.bbapap.2015.03.002 (2015).
57 Ferguson, F. M. & Gray, N. S. Kinase inhibitors: the road ahead. *Nature reviews. Drug discovery* **17**, 353-377, doi:10.1038/nrd.2018.21 (2018).
58 Gross, S., Rahal, R., Stransky, N., Lengauer, C. & Hoeflich, K. P. Targeting cancer with kinase inhibitors. *The Journal of clinical investigation* **125**, 1780-1789, doi:10.1172/jci76094 (2015).

59 Littler, D. R. *et al.* Disrupting the Allosteric Interaction between thePlasmodium falciparumcAMP-dependent Kinase and Its Regulatory Subunit. *Journal of Biological Chemistry* **291**, 25375-25386, doi:10.1074/jbc.M116.750174 (2016).
60 Patel, A. *et al.* Cyclic AMP signalling controls key components of malaria parasite host cell invasion machinery. *PLOS Biology* **17**, e3000264, doi:10.1371/journal.pbio.3000264 (2019).
61 Wilde, M.-L. *et al.* Protein Kinase A Is Essential for Invasion of Plasmodium falciparum into Human Erythrocytes. **10**, e01972-01919, doi:10.1128/mBio.01972-19 %J mBio (2019).
62 Leykauf, K. *et al.* Protein kinase a dependent phosphorylation of apical membrane antigen 1 plays an important role in erythrocyte invasion by the malaria parasite. *PLoS Pathog* **6**, e1000941, doi:10.1371/journal.ppat.1000941 (2010).
63 Dastidar, E. G. *et al.* Involvement of Plasmodium falciparum protein kinase CK2 in the chromatin assembly pathway. *BMC biology* **10**, 5, doi:10.1186/1741-7007-10-5 (2012).
64 Graciotti, M. *et al.* Malaria protein kinase CK2 (PfCK2) shows novel mechanisms of regulation. *PLoS One* **9**, e85391, doi:10.1371/journal.pone.0085391 (2014).
65 Ruiz-Carrillo, D. *et al.* The protein kinase CK2 catalytic domain from Plasmodium falciparum: crystal structure, tyrosine kinase activity and inhibition. *Sci Rep* **8**, 7365, doi:10.1038/s41598-018-25738-5 (2018).
66 Holland, Z., Prudent, R., Reiser, J. B., Cochet, C. & Doerig, C. Functional analysis of protein kinase CK2 of the human malaria parasite Plasmodium falciparum. *Eukaryot Cell* **8**, 388-397, doi:10.1128/EC.00334-08 (2009).
67 Doerig, C. & Meijer, L. Antimalarial drug discovery: targeting protein kinases. *Expert opinion on therapeutic targets* **11**, 279-290, doi:10.1517/14728222.11.3.279 (2007).
68 Klein, E. Y. Antimalarial drug resistance: a review of the biology and strategies to delay emergence and spread. *International journal of antimicrobial agents* **41**, 311-317, doi:10.1016/j.ijantimicag.2012.12.007 (2013).
69 Talman, A. M., Clain, J., Duval, R., Ménard, R. & Ariey, F. Artemisinin Bioactivity and Resistance in Malaria Parasites. *Trends in Parasitology* **35**, 953-963, doi:https://doi.org/10.1016/j.pt.2019.09.005 (2019).
70 Blagborough, A. M. *et al.* Transmission-blocking interventions eliminate malaria from laboratory populations. *Nature Communications* **4**, 1812, doi:10.1038/ncomms2840 (2013).
71 Tiburcio, M. *et al.* A Novel Tool for the Generation of Conditional Knockouts To Study Gene Function across the Plasmodium falciparum Life Cycle. *MBio* **10**, doi:10.1128/mBio.01170-19 (2019).
72 Fivelman, Q. L. *et al.* Improved synchronous production of Plasmodium falciparum gametocytes in vitro. *Mol. Biochem. Parasitol* **154**, 119-123 (2007).
73 Gibellini, F. & Smith, T. K. The Kennedy pathway--De novo synthesis of phosphatidylethanolamine and phosphatidylcholine. *IUBMB life* **62**, 414-428, doi:10.1002/iub.337 (2010).
74 Gulati, S. *et al.* Profiling the Essential Nature of Lipid Metabolism in Asexual Blood and Gametocyte Stages of Plasmodium falciparum. *Cell Host Microbe* **18**, 371-381, doi:10.1016/j.chom.2015.08.003 (2015).
75 Tewari, R., Dorin, D., Moon, R., Doerig, C. & Billker, O. An atypical mitogen-activated protein kinase controls cytokinesis and flagellar motility during male gamete formation in a malaria parasite. *Mol Microbiol* **58**, 1253-1263, doi:10.1111/j.1365-2958.2005.04793.x (2005).
76 Khan, S. M. *et al.* Proteome analysis of separated male and female gametocytes reveals novel sex-specific Plasmodium biology. *Cell* **121**, 675-687, doi:10.1016/j.cell.2005.03.027 (2005).

77 Rangarajan, R. *et al.* A mitogen-activated protein kinase regulates male gametogenesis and transmission of the malaria parasite Plasmodium berghei. *EMBO Rep* **6**, 464-469, doi:10.1038/sj.embor.7400404 (2005).
78 Tham, W. H. *et al.* Plasmodium falciparum Adhesins Play an Essential Role in Signalling and Activation of Invasion into Human Erythrocytes. *PLoS Pathog* **11**, e1005343, doi:10.1371/journal.ppat.1005343 (2015).
79 Tiburcio, M. *et al.* A switch in infected erythrocyte deformability at the maturation and blood circulation of Plasmodium falciparum transmission stages. *Blood* **119**, e172-180, doi:10.1182/blood-2012-03-414557 (2012).
80 Aingaran, M. *et al.* Host cell deformability is linked to transmission in the human malaria parasite Plasmodium falciparum. *Cell Microbiol* **14**, 983-993, doi:10.1111/j.1462-5822.2012.01786.x (2012).
81 Joice, R. *et al.* Plasmodium falciparum transmission stages accumulate in the human bone marrow. *Science translational medicine* **6**, 244re245, doi:10.1126/scitranslmed.3008882 (2014).
82 Bouyer, G. *et al.* Plasmodium falciparum sexual parasites regulate infected erythrocyte permeability. *bioRxiv*, 2020.2005.2018.101576, doi:10.1101/2020.05.18.101576 (2020).
83 Bian, Y. *et al.* Global screening of CK2 kinase substrates by an integrated phosphoproteomics workflow. *Scientific reports* **3**, 3460, doi:10.1038/srep03460 (2013).
84 Franchin, C. *et al.* Re-evaluation of protein kinase CK2 pleiotropy: new insights provided by a phosphoproteomics analysis of CK2 knockout cells. *Cellular and Molecular Life Sciences* **75**, 2011-2026, doi:10.1007/s00018-017-2705-8 (2018).
85 Meggio, F. & Pinna, L. A. One-thousand-and-one substrates of protein kinase CK2? *FASEB journal : official publication of the Federation of American Societies for Experimental Biology* **17**, 349-368, doi:10.1096/fj.02-0473rev (2003).
86 Jung, S.-I. *et al.* Yeast casein kinase 2 governs morphology, biofilm formation, cell wall integrity, and host cell damage of Candida albicans. *PLOS ONE* **12**, e0187721, doi:10.1371/journal.pone.0187721 (2017).

Curriculum Vitae

Eva Hitz

Sägestrasse 55	077 411 22 62
5600 Lenzburg	eva.hitz@swisstph.ch
Born:	27.01.1991
Nationality:	Swiss

Education

06/2016 – 09/2020	Ph.D. in Cell Biology Swiss TPH; University of Basel Focus: Kinases and sexual commitment in *Plasmodium falciparum* Supervisor: Prof. Till Vos Graduation: 18.09.2020, summa cum laude
8/2014 - 2/2016	Master of Science in Infection Biology Swiss TPH; University of Basel Focus: Exported proteins in malaria parasites/*Plasmodium falciparum* Supervisor: Prof. Hans-Peter Beck Final grade: 5.7
8/2011 - 7/2014	Bachelor of Science in Biology University of Basel Major: Animal and Plant Sciences Final grade: 5.7
08/2007 - 07/2011	Gymnasium at “Neue Kantonsschule Aarau” Major subject: French Minor subject: Biology Final grade: 5.5
08/2006 - 06/2007	Au pair in Geneva; language school (DIDAC Sprachschulen AG)
1996 - 2006	Basic education in Switzerland

Languages

German	Native language
English	Fluent (Cambridge English: C1 Advanced (CAE))
French	Fluent (B2/gymnasium)
Italian	Intermediate (B1/gymnasium)

Courses and Conferences

2020

- Transferable Skills Course: Good Scientific Practice
  Location: University of Basel, CH
- MAM conference 2020: Molecular Approaches to Malaria
  Location: Lorne, AUS
- Good Clinical Practice Course
  Location: Clinical Trial Center Zurich (online-based course)

2019

- EMBL conference: BioMalPar XV: Biology and Pathology of the Malaria Parasite (poster presentation)
  Location: EMBL Heidelberg, DE

2018

- Bioinformatics Summer School 2018
  (20/08/2018 - 24/08/2018; poster presentation)
  Location: University of Glasgow, UK
- EMBL conference: BioMalPar XIV: Biology and Pathology of the Malaria Parasite (poster presentation)
  Location: EMBL Heidelberg, DE

2017

- EMBL conference: BioMalPar XIII: Biology and Pathology of the Malaria Parasite
  Location: EMBL Heidelberg, DE
- SSTMP student meeting 2017
  (02/11/2016-03/11/2016; oral presentation)
  Location: Schwarzenberg, CH

2016

- EMBO Practical Course: High throughput microscopy for systems biology
  (17/10/2016 – 23/10/2016; poster presentation)
  Location: EMBL Heidelberg, DE
- Writing to Be Published for the Natural Sciences
  Location: Sprachenzentrum der Universität Basel, CH
- Introduction to R/Bioconductor
  Location: University of Basel, CH

- SSTMP student meeting 2016
  (24/11/2016-25/11/2016; oral presentation)
  Location: Grindelwald, CH

Teaching

Supervision of Master students (MSc in Infection Biology)

02/2017-02/2018	Sarah Höhn
02/2018-02/2019	Olivia Grüninger
02/2019-02/2020	Lito Zambounis and Basil Thommen

Publications

- Brancucci, N., Gerdt, J., Wang, C., De Niz, M., Philip, N., Adapa, S., Zhang, M., Hitz, E., Niederwieser I., Boltryk, S. et al. (2017). Lysophosphatidylcholine Regulates Sexual Stage Differentiation in the Human Malaria Parasite *Plasmodium falciparum*. *Cell* 171, 1532-1544.

- Hitz, E., Balestra, A., Brochet, M., Voss, T. S. (2020). PfMAP2 is essential for male gametogenesis in the malaria parasite *Plasmodium falciparum*. *Scientific Reports* 10, 11930.

- Hitz, E., Grüninger, O., Passecker, A., Scheurer, C., Brancucci, N., Wittlin, S., Beck, H.-P., Voss, T. S. (2021) The catalytic subunit of *Plasmodium falciparum* casein kinase 2 is essential for gametocytogenesis. *Communications Biology* 4, 336 (2021).

- Hitz, E., Wiedemar, N., Brancucci, N., Passecker, A., Vakonakis, I., Mäser, P., Voss, T. S. A 3-phosphoinositide-dependent protein kinase-1 homologue is essential for activation of protein kinase A in malaria parasites. Manuscript in preparation, publication planed 2021.

Professional memberships

06/2016 – now	Swiss Society of Tropical Medicine and Parasitology (SSTMP)